A study into alternative bone remodelling under tension and compression in the proximal femur after one year of hopping exercises using quantitative computerised tomography and finite element simulation

By

Matthew Taylor

Submitted in partial fulfilment for the Degree of PhD in Biomedical Engineering

2020

Centre for Biomedical Engineering

Department of Mechanical Engineering Sciences

University of Surrey

Abstract

Bone remodelling is an important process with numerous clinical implications. It is generally assumed that the bone will experience the same bone remodelling response to the stimulus under tension and compression. However, laboratory studies suggest that the bone could exhibit alternative bone remodelling under tension and compression as the result of different bone remodelling mechanisms; where alternative bone remodelling is defined as two or more different/alternative bone remodelling responses in relation to the same stimulus. Here, tension and compression are assumed to be the same stimulus, where the absolute value of the strain stimulus is used. Very little research has been conducted into this phenomenon and if it occurs under physiologically applied loading conditions. Therefore, it is unclear how prevalent alternative bone remodelling is under physiological loading conditions.

To investigate if the bone does exhibit alternative bone remodelling under tension and compression under physiological loading conditions, this study examined the bone remodelling behaviour of the proximal femur of 11 male subjects (mean age ± SD: 70.91 ± 2.78) taking part in a one-year hopping clinical exercise trial. This was achieved by comparing the change in density of each subject, measured by quantitative computerised tomography, against the mechanical stimulus, determined by subject specific finite element simulations. Here the stimulus was determined to be the principal strain experienced in hopping minus the principal strain experienced during everyday activities which were either walking or stair climbing. The stimulus-remodelling relationships were determined by comparing the change in density and stimulus using a previously published bone remodelling algorithm.

This study managed to demonstrate consistent differences in the bone remodelling observed under tension and compression. Where it was observed that at lower stimuli the compressive regions experience a higher change in density in relation to the stimulus in comparison to the tensile regions, until a cross-over point where tension experiences a higher change in density in comparison to compression ($p < 0.01$). This cross over point occurs at a stimulus of approximately 670 με which corresponds to a change in density of approximately 3.5%, which is higher than the typical change in density experienced in the cortical bone during exercise. This cross over between the two stimulus-remodelling relationships is thought to be the result of the Hueter-Volkmann law.

It was also observed that the bone remodelling under compression has a higher variance in the change in density in relation to the stimulus, in comparison to tension ($p < 0.01$), which is thought to the be result of linear microdamage formation and subsequent remodelling initiation under compression. This high variance in the change in density under compression causes for the stimulus-remodelling relationships under tension and compression to merge somewhat at lower stimuli, which can give the impression of a single stimulus-remodelling relationship. Furthermore, differences in the residual regression biases under tension and compression was observed, where the bone remodelling under tension demonstrated significantly lower regression biases in comparison to the bone remodelling under compression ($p = 0.141$).

Evidence from this study also suggests that the tensile and compressive stimulus-remodelling relationships are independent of each other, but correlations of varying strength were made between the observed characteristics and the subjects' age and BMI, with the correlations being typically stronger under tension. However further research is warranted into these correlations due to the small sample size and population demographic used in this study.

Note of Thanks

I would like to thank my family and friends who have remained continually supportive during the process of my research. In particular I would like to thank my partner Fiona Clements and my mother Alison Taylor who have been a constant source of support.

I would also like to thank members of the University of Surrey for their support and guidance during my research. Specifically, I would like to thank Dr Wei Xu for all his support, along with Dr Serge Cirovic, Dr Sarah Allison and Professor Andy Crocombe, whose advice and support have been invaluable.

Contributions

I would like to acknowledge and thank Dr Sarah Allison, and all the research members of the clinical exercise trial, for allowing me to use their data in my thesis.

Statement of Authenticity

I declare that this thesis and the work herein are the results of my own effort. Any ideas, data, images or text resulting from the work of others (whether published or unpublished) are fully identified and attributed to their originator. This thesis has not been submitted in whole or in part for any other academic degree or professional qualification. I agree that the university has the right to submit my work to the plagiarism detection services for originality checks. Whether or not drafts have been so-assessed the university reserves the right to require an electronic version of the final document (as submitted) for assessment as above.

Matthew Taylor

Contents

Figures

Tables

Equations

Nomenclature

2D	Two Dimensional
3D	Three Dimensional
b	Power law constant, used in the bone remodelling algorithm
BMI	Body mass index
c	Remodelling constant, y-axis intercept
cm	Centimetre
CL	Control Leg
CT	Computerised Tomography
D, d	Distance
e	Mathematical constant ≈ 2.71828
E	Elastic Modulus
EL	Exercise Leg
EMG	Electromyography
f	Loading frequency
F, fn	Function
F_{AB}	Abductor muscle force (applied to the greater trochanter)
F_{HC}	Hip contact force
F_x	Force in the x-axis

F_y	Force in the y-axis
F_z	Force in the z-axis
FE	Finite Element
FD	Forward Dynamics
g	Grams
HCF	Hip contact force
H-S	Hop-Stair loading scenario (see Definitions)
HU	Hounsfield units
H-W	Hop-Walk loading scenario (see Definitions)
ISB	International Society of Biomechanics
JCF	Joint contact force
k	Rate constant, used in the bone remodelling algorithm
LμCr	Linear Microdamage
m	Meter
MES	Minimally effective strain
n	Number of different loading conditions
N	Newtons
N_i	Number of loading cycles

P(x,t)	Osteoblast recruitment stimulus at the surface location x, as a function of time, t
p, p(x,t)	Percentage probability of an area/region/element initiating bone remodelling due to microdamage
p	p-value
qCT	Quantitative Computerised Tomography
r_{oc}	Relative amount of bone mineral absorbed by osteoclasts
R_{SED}	SED rate
RsSp	Resorption Space
RMSE	Root Mean Square Error
S	Bone remodelling stimulus
S_+	Positive bone remodelling stimulus threshold
S_{max}	Maximum strain stimulus
SD	Standard deviation
SED	Strain Energy Density
SO	Static optimisation
SPSS	Statistical Package for the Social Sciences
SR_{true}	The stimulus-remodelling relationship experienced by the areas of the bone undergoing remodelling
SR_0	Representing areas of bone not experiencing any bone remodelling and therefore no stimulus-remodelling relationship

STP	Standard temperature and pressure
t	Time
T	Temperature, Tunnelling
T_o	Thermostat set point
V	Volume proportion of the bone experiencing bone remodelling
ε	Strain
ε_{hop}	Strain due to hopping
ε_o	Pre-set remodelling strain threshold
ε_r	Reference strain
ε_{stair}	Strain due to stair climbing
ε_{walk}	Strain due to walking
∂	Change in
ρ_{ash}	Bone ash density
μ	Micro (10^{-6})
μ_a	Linear attention coefficient
μ_i	Mechanosensitivity of the osteocyte
θ	Angle
ρ	Bone density

ρ_i	New bone density
ρ_o	Original bone density
τ	Time constant, representing time required for osteocytes to accommodate to the new loads
ω	Accumulated microdamage (does not differentiate between linear microdamage and diffuse damage)
ω_r	Reference level of accumulated microdamage (does not differentiate between linear microdamage and diffuse damage)

Definitions

Within this thesis the following definitions are used to define bone remodelling, its characteristics and any subsequent observations:

Alternative Bone Remodelling: This is the term used to describe two or more different bone remodelling behaviours, in relation to the same stimulus. The term ‘alternative’ was used as it infers a continual difference in the bone remodelling behaviour which can be observed and quantified; however, it also infers that no two subjects have the same bone remodelling behaviour or difference.

Alternative Bone Remodelling Mechanism: Any bone remodelling mechanism, which affects one or more stages in the bone remodelling cycle, to cause alternative bone remodelling behaviour.

Atypical Stimulus-Remodelling Relationship: The atypical stimulus-remodelling relationship, is a stimulus-remodelling relationship which has a power law constant less than 1, observed when using a nonlinear remodelling algorithm, resulting in the relationship shown in Figure P-1-1. This relationship is explored throughout the study and is not a sign of abnormality. It is called “atypical” because it shows a stimulus-remodelling relationship which is not typically associated with bone remodelling.

Figure P-1-1: The atypical stimulus-remodelling relationship

b value: Through conducting this study, it was found that using the power law constant from the remodelling, denoted by the letter 'b,' shown in equation P-1, was the most useful comparison tool for exploring the differences in the tensile and compressive bone remodelling behaviour. This power law constant, was thus denoted the b value.

$$\frac{\partial \rho}{\partial t} = k(\varepsilon - \varepsilon_0)^b \qquad P\text{-}1$$

Bone Remodelling: Bone remodelling is the continuous, lifelong cellular process of removing and depositing bone, where any change in bone density or properties as a result of this process is in response to an external stimulus, of lack thereof, be it mechanical or hormonal.

Bone Remodelling Behaviour: This is an all-encompassing term which describes any behaviour or characteristics of the bone which involves the change in bone density in response to a stimulus. This term is generally used in circumstances where a difference in bone remodelling between two regions is known/observed, however differences in bone remodelling can involve multiple different behaviours.

Hop-Stair Loading Scenario: The Hop-Stair loading scenario describes the strain stimulus produced by subtracting the strains caused by applying stair climbing loads from the strains produced by applying hopping loads.

Hop-Walk Loading Scenario: The Hop-Walk loading scenario describes the strain stimulus produced by subtracting the strains caused by applying walking loads from the strains produced by applying hopping loads.

k value: The k value is the name given to refer to the rate constant used in bone remodelling algorithms, which are denoted by the letter 'k.'

Negative Bone Remodelling: Bone remodelling where the bone density decreases, which is typically in response to a lack of a stimulus or alternative bone remodelling mechanism.

Physiological Loading Conditions: This describes any loading applied to bone which can be expected to be applied under everyday conditions and has not been externally manipulated. Examples of this is loading applied during activities such as walking and exercise.

Positive Bone Remodelling: Bone remodelling where the bone density increases.

Stimulus: The stimulus is what drives and causes bone remodelling. In this study, following the literature, the stimulus is mechanically based strain stimulus and is defined by subtracting the old 'target' strain from the new strain, as described in Chapter 2.

Stimulus-Remodelling Relationship: This describes the mathematical relationship which best defines the change in density (plotted in the y-axis) in relation to the stimulus (plotted in the x-axis). Therefore, the stimulus-remodelling relationship is best defined using a bone remodelling algorithm. Bone remodelling algorithms are explored in Chapter 2 and the stimulus-remodelling relationship in the areas of the bone under tension and compression are explored in Chapter 4.

Stimulus-Remodelling Plots: Plotting the raw data for each subject used in this study, where the change in density (y-axis) is plotted against the mechanical stimulus (x-axis) on a single graph.

Strain Environment: Any area in which the bone is experiencing strain.

Strain Data Set: Three strain data sets in the proximal femur are explored in this study, the general (the whole proximal femur), the tensile (only the part of the bone where tension is the dominant principal strain) and the compressive (only the part of the bone where compression is the dominant principal strain). The general data set comprises of both the tensile and compressive strain data sets and does not describe nor include any other data set or area in addition to the tensile and compressive.

Typical Stimulus-Remodelling Relationship: The typical stimulus-remodelling relationship, is a stimulus-remodelling relationship which has a power law constant more than or equal to 1, observed when using a power law bone remodelling algorithm, resulting in the relationship shown

in Figure P-1-2. This relationship is explored throughout the study and is called “typical” because it shows a stimulus-remodelling relationship which is typically associated with bone remodelling.

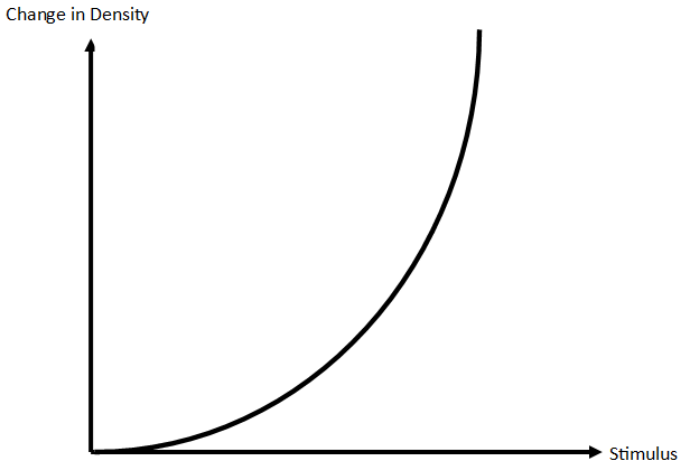

Figure P-1-2: The typical stimulus-remodelling relationship

Chapter 1. Introduction

The skeletal system is critical for locomotion and load bearing, and as a result, a substantial amount of research has been conducted into its mechanical strength and adaptation to mechanical loading. The concept that the bone adapts its mechanical properties to the loads which it experiences stems from the observations of Julius Wolff (1896), and as so is often referred to as "Wolff's law." This adaptation is achieved through bone remodelling, which is the lifelong, continuous, change of the bone through cellular processes (Robling and Turner 2009). It is currently assumed that the bone experiences the same bone remodelling behaviour under tensile and compressive loads, an assumption which is inherently used by bone remodelling algorithms, which are used to predict future bone remodelling.

Alternative bone remodelling behaviour can be described as two or more different/alternative bone remodelling responses to the same stimulus, a phenomenon which has been identified in laboratory (Rubinacci, Black et al. 1988, Stokes 2002, Herman, Cardoso et al. 2010) and pathological conditions (Lin 2010). An ageing population has seen a rise in demand for orthopaedic implants (Morrison, N Kashlan et al. 2015, Wong 2016), research into orthopaedic fractures (Keyak 2001) and methods to increase bone density (Kukuljan, Nowson et al. 2011, Allison, Folland et al. 2013, Christen, Ito et al. 2014, Troy, Mancuso et al. 2018). With this, bone remodelling algorithms are becoming increasingly relied upon to determine future bone remodelling in response to implants, exercise, or lack thereof. Numerous bone remodelling algorithms are based on the biological mechanisms which have been demonstrated to cause alternative bone remodelling behaviour under tension and compression (Frost 1987, McNamara and Prendergast 2007, Fernández, García-Aznar et al. 2012). However, to the author's knowledge, no study has been conducted to determine if alternative bone remodelling behaviour under tension and compression occurs under physiological loading conditions and in the absence of disease. It is therefore unclear how prevalent tensile and compressive alternative bone remodelling is under physiological loading conditions, and what, if any, impact it may have on bone remodelling algorithms.

Tensile and compressive loads are currently considered to be the same stimulus in bone remodelling, coming under the categorisation of mechanical stimuli. Furthermore, the bone under both tension and compression are considered to have the same mechanical properties and stress-strain response under these loads as shown in Figure 1-1. Therefore, any difference in bone remodelling behaviour observed between tension and compression is currently considered to be alternative bone remodelling. This can lead to confusion depending on which article is being cited and the aim of the study. Tensile and compressive loads are considered to be the same stimulus because generally, they have the same effect on the bone remodelling processes and mechanotransducive signalling described in Chapter 2. As shown in Chapter 2, assuming the same bone remodelling behaviour under tension and compression has resulted in accurate stimulus-remodelling relationships and simulations. As a consequence, often any difference between tension and compression, mechanically or otherwise is not acknowledged in bone remodelling studies, where only the "stimulus" as a singular entity is mentioned.

In mechanics, as shown in Figure 1-1, tensile stress/strain is often modelled as positive, and compressive stress/strain is modelled as negative. This mechanical difference between tension and compression is overcome in bone remodelling studies by assuming the stimulus is an absolute value, and therefore both tensile and compressive stimuli are always considered positive values. These assumptions are present in both engineering simulation studies which typically focus on mathematical algorithms, and in laboratory studies which typically focus on *in vivo* and *ex vivo* observations. However, it is often subtle differences in the bone remodelling processes and mechanotransducive signalling which result alternative bone remodelling behaviour (Rubinacci, Black et al. 1988, Stokes 2002, Herman, Cardoso et al. 2010). In the case of this study, subtle differences in bone remodelling behaviour, in different bone remodelling stages under tension and compression, are what result in alternative bone remodelling. But the studies which have observed alternative bone remodelling, generally only focus on specific scenarios and/or a single stage in the bone remodelling cycle, making it difficult to apply them to the whole bone remodelling process, and as such are often overlooked.

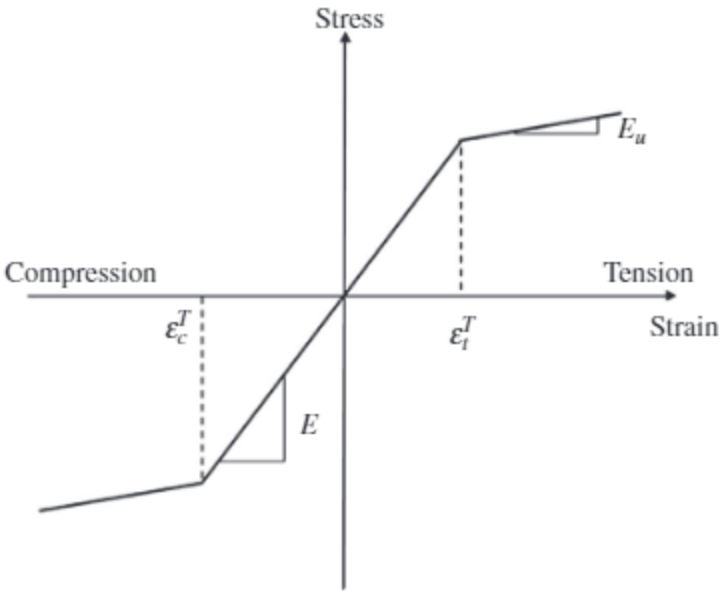

Figure 1-1: Representation of the tensile and compressive stress/strain experienced by the bone, where the bone follows the same stress/strain gradient under tension and compression. Here ε_c^T and ε_t^T are the compressive and tensile yield strains and E_u is the post yield modulus (Gong, Wang et al. 2020).

This study set out to conduct an initial investigation into if alternative bone remodelling in tension and compression can be observed under physiological loading conditions. To achieve this, an observational-based study was conducted utilising data from the Allison, Folland et al. (2013) clinical exercise trial, where thirty-four healthy men, mean ± SD age of 69 ± 4.0 years, hopped 50 times a day, every day for a year. The clinical exercise trial achieved an average increase in cortical bone density of 2.7% which is similar to that achieved by other exercise studies. Of the subjects from the Allison, Folland et al. (2013) clinical exercise trial, 11 passed an inclusion criteria to be used in this study. For these 11 subjects, the subject specific change in density in different locations along the proximal femur was measured from the pre and post exercise quantitative CT (qCT) scans, using *Materialise Mimics Research version 19.0* software. This was compared against the mechanical stimulus, calculated using subject specific finite element simulations run in *Simulia Abaqus/CAE 2017*. The tensile and compressive stimulus-remodelling relationships were then determined using regression analysis against a previously established remodelling algorithm $\left(\frac{\partial \rho}{\partial t} = k(\varepsilon - \varepsilon_o)^b\right)$, and compared against each other. The results were then compared against different anthropometric, physiological and experimental parameters to determine if there were any external, measurable influences on the results of this study.

1.1 Overview of Findings

At the onset of this study, with no previous similar studies, the researcher was unsure of what results they would obtain, and what, if any, difference in the bone remodelling between tension and compression would be observed. Previous studies into pathological conditions and laboratory experiments have revealed that alternative bone remodelling between tension and compression occurs. However, there are wide gaps between observations and no direct studies which apply alternative bone remodelling to physiological loading. Nonetheless, using 11 subjects from the Allison, Folland et al. (2013) clinical exercise trial, which passed an inclusion criteria, differences in bone remodelling behaviour under tension and compression in the cortical bone were observed. These differences were characterised by consistent observations, being: 1. Using the equation $\frac{\partial \rho}{\partial t} = k(\varepsilon - \varepsilon_o)^b$, tension was observed to consistently have a higher b value than compression (p = 0.054), with the k value calculable by the b value for both tension and compression ($p < 0.01$); 2. Differences in the RMSE and R^2 values, where tension has a lower RMSE (p = 0.164) and higher R^2 value ($p < 0.01$), and, 3. Differences in the observed regression biases, where tension has a significantly lower regression bias (p = 0.141).

The results of this study suggest that the stimulus-remodelling relationships under tension and compression are independent of each other; however, correlations of varying strength were observed between the aforementioned alternative bone remodelling characteristics and the subjects age and BMI, with stronger correlations typically being observed under tension. Due to the small sample size and limited population demographic further research is required to better understand these correlations. A further notable observation was that, beyond a cross-over point, the difference in stimulus-remodelling relationships cause for increasing deviation in the change in density under tension and compression in response to the stimulus. Before this cross-over point, the tensile and compressive stimulus-remodelling relationships are harder to differentiate. This cross-over point occurs at a stimulus and a change in density which is higher than the typical change in density experienced by the cortical bone during exercise, suggesting that alternative bone remodelling becomes more of an issue in very high loading conditions.

Whilst this study cannot directly observe any bone remodelling mechanisms, the results of this study were compared against known characteristics of previously identified bone remodelling

mechanisms which are known to cause alternative bone remodelling. Through this comparison, it was postulated that the high RMSE, low R^2, and significant regression biases observed in compression in relation to tension could be the result of different microdamage production and subsequent bone remodelling initiation experienced under tension and compression. It was thought that the random production and random initiation of bone remodelling as a result of linear microdamage caused random variations in the volume of the bone experiencing remodelling, effecting the measured change in density under compression. It was further postulated that the age of the subjects could be a factor, particularly in the high R^2 value observed under compression, due to the increase in residual linear microdamage which is associated with age. Furthermore, it was postulated that the Heuter-Volkmann law could be a contributor to the difference in the tensile and compressive b values, where it suppresses the change in density under compression as the stimulus increases.

1.2 Thesis Structure

This thesis is split into six chapters and two appendices.

Chapter 1. Introduction. This chapter introduces the rationale behind the study and its method, along with providing overviews of the study findings and structure.

Chapter 2. Literature Review. In this chapter, the current literature regarding bone remodelling and its quantification is examined along with any observations and/or evidence towards alternative bone remodelling being experienced under tensile and compressive loads. It examines the musculoskeletal models of the proximal femur and continues to introduce bone remodelling data of the proximal femur from the Allison, Folland et al. (2013) clinical exercise study. The chapter finishes with a study aim and objectives.

Chapter 3. Finite Element Model and Simulated Strains. Finite element simulation is a key factor in this study, where it allows the determination of the strain stimulus experienced by the proximal femur, without the use of any invasive strain gauges. This chapter introduces the subjects used in the Allison, Folland et al. (2013) clinical exercise study and, how the subject specific finite element models were set up. This chapter continues to examine the simulated strain experienced

by each of the subjects and compares the results against previously *in vivo* measured and simulated strains during similar activities.

Chapter 4. Bone Remodelling Observations. This chapter carries out the aim of this study and investigates, details and summarises the bone remodelling observations made in the tensile and compressive strain data sets of the 11 subjects used from the Allison, Folland et al. (2013) clinical data.

Chapter 5. Discussion. This chapter compares the observations of this study against identified bone remodelling mechanisms known to cause alternative bone remodelling behaviour in an attempt to derive which mechanisms may have had an influence on the observed results. It continues to discuss the potential effect of any parameters and limitations of the study.

Chapter 6. Conclusion. This chapter concludes the findings of this study, examines their impact, makes reference to the limitations of this study and introduces any required future work.

Appendix A. Statistical Tests. Here, the statistical tests used in this study are introduced and explained.

Appendix B. Material Transfer Agreement. This appendix displays the material transfer agreement signed with Allison, Folland et al. (2013) to allow this study to use its data.

Chapter 2. Literature Review

2.1 Introduction

Whilst it is accepted that a variety of factors can cause the bone remodelling to be different in different people (Parfitt 2004), bone remodelling is generally considered to follow the same behaviour. Previous studies have provided evidence towards alternative bone remodelling behaviour under tension and compression as a result of different biological mechanisms within the bone in laboratory and pathological conditions (Rubinacci, Black et al. 1988, Bentolila, Boyce et al. 1998, Stokes 2002, Herman, Cardoso et al. 2010): Where alternative bone remodelling can be defined as the differential bone remodelling response to the same mechanical stimulus. If alternative bone remodelling behaviour under tension and compression occurs under physiological loading conditions, this could introduce problems to remodelling algorithms under the assumption that the bone remodelling is the same. The aim of this chapter is to explore the literature regarding bone remodelling, alternative bone remodelling, finite element simulation, musculoskeletal models, bone remodelling study methods and introduce the Allison, Folland et al. (2013) clinical exercise trial.

2.2 Skeletal Adaptation to Mechanical Loading

Bone is classified into two types, which are defined by its molecular structure, these are cortical (compact) and trabecular (cancellous/spongy) bone, as shown in Figure 2-1. The mechanical properties and histology of the two types of bone are different (Rhoa, Kuhn-Spearingb et al. 1998); where cortical bone is much more densely packed than trabecular bone and is generally found in areas of high stress. Both types of bone adapt and change in response to the mechanical environment, in a process called bone remodelling. In the bone remodelling response to a mechanical stimulus, trabecular bone experiences change in microarchitecture and density (Huiskes, Ruimerman et al. 2000, Adachi, Kameo et al. 2010) whilst cortical bone only experiences a change in density (Rhoa, Kuhn-Spearingb et al. 1998, Turner 1998, Nobel, Peet et

al. 2003, Hansen, Zioupos et al. 2008). However, both cortical and trabecular bone undergo the same cellular remodelling process (Schindeler, McDonald et al. 2008, Eriksen 2010, Qin 2013).

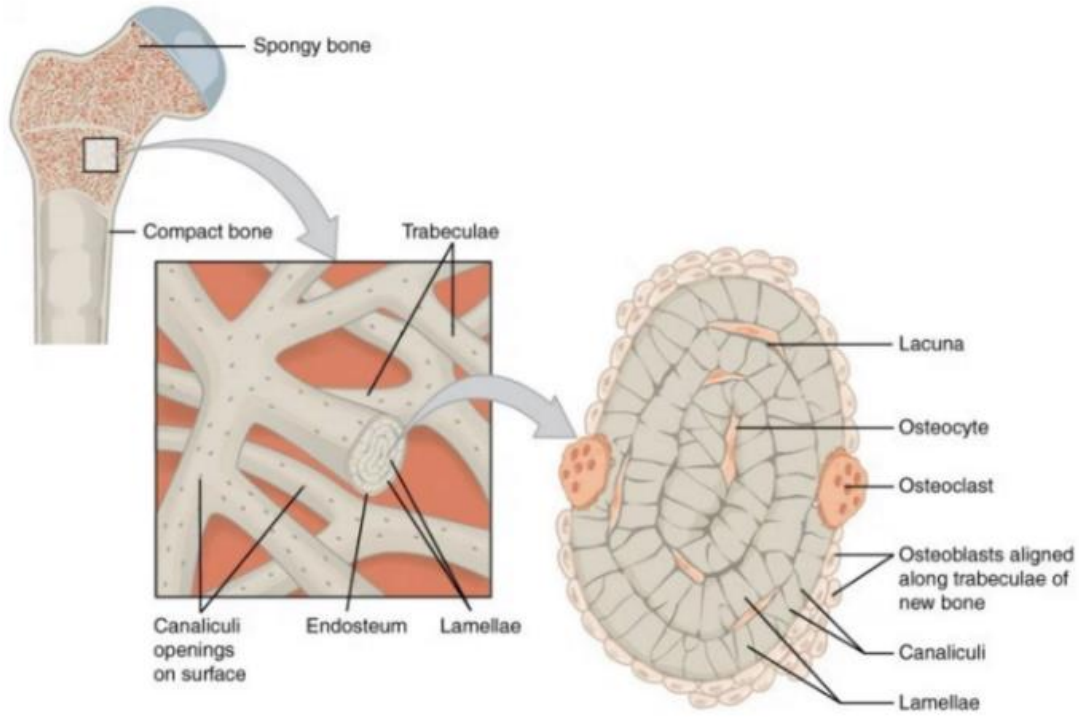

Figure 2-1: Structure of cortical and trabecular bone (BoneAndSpine.com 2018)

The bone remodelling process, also known as the bone remodelling cycle, has four clear cellular stages: activation, resorption, reversal and formation (Eriksen 2010, Drevelle and Faucheux 2013, Qin 2013) as shown in Figure 2-2. These stages can only occur in this order and no two stages can occur in the same location simultaneously (Robling and Turner 2009). Once the remodelling process has been initiated (activation), the full cycle will occur, with each stage signalling for the next. During the resorption stage, the osteocyte and the surrounding extracellular matrix are removed by osteoclasts (Schindeler, McDonald et al. 2008, Robling and Turner 2009). Following reversal, new bone is deposited by osteoblasts in formation. The result of this process can be either an increase (positive remodelling) or a decrease (negative remodelling) in the in bone's mechanical strength. This is characterised by a change in density which can be internal (intrinsic remodelling) or on the surface of the bone resulting in a change in the cross-sectional area (extrinsic remodelling). The cellular process which carries out bone remodelling is the same for both positive and negative remodelling (Eriksen 2010).

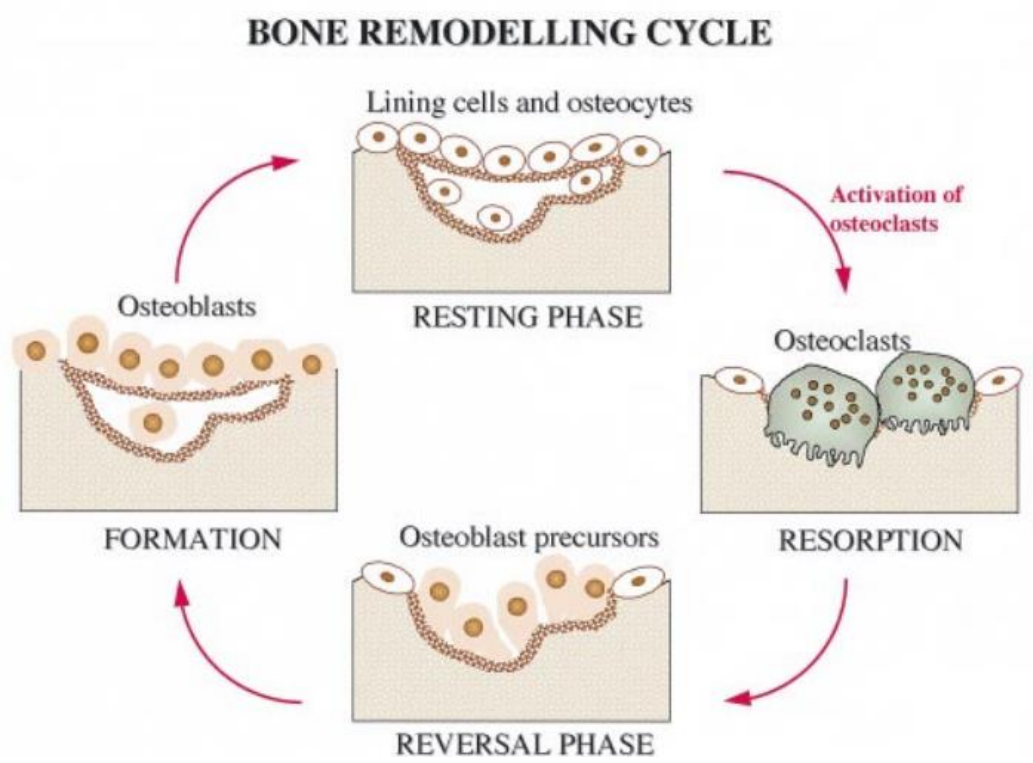

Figure 2-2: Image of the bone remodelling cycle from Hill (1998)

2.2.1 Mechanotransduction

Mechanotransduction is the process in which the mechanical energy applied to the bone is transferred into cellular biochemical signals which control the different stages of bone remodelling. This is an essential process, without which the bone would not be able to adapt to its mechanical environment. It is usually referred to as an all-encompassing process for the whole of the bone remodelling cycle. However, each stage of bone remodelling has its own independent biological signals, despite in many cases the mechanotransductive process being incredibly alike (Robling and Turner 2009, Webster, Schulte et al. 2015).

Numerous mechanotransductive outputs, such as the change in density or resorption area, have been correlated with mechanical inputs to a high degree of accuracy, yet little is still known about the biochemical signals. This is partly due to high complexity of the mechanotransductive process where numerous biochemicals are involved, and the inability to isolate and study the effect of these biochemicals individually (Ruimerman, van Rietbergen et al. 2005, Robling and Turner 2009, Shahi, Peymani et al. 2017). Furthermore, difficulties arise in studying individual bone

remodelling stages. For example, studying the effects of mechanical loads on stages such as resorption in humans is much more difficult than studying the effect they have on formation. To observe a bone remodelling stage, the bone has to be harvested from a host at the correct time. Therefore, the majority of studies investigating the effects of mechanical loading on the bone use rodents, which mainly due to their size, can experience different remodelling processes than humans (Robling and Turner 2009). There has been substantial progress using *in vitro* methods to study individual bone remodelling processes and the influence of different biochemicals (Plotkin, Mathov et al. 2005, Plotkin 2014). However, these are often criticised, including by the experimenter themselves, as the experimental setup may not accurately represent *in vivo* environments, both mechanically and biochemically (Plotkin, Mathov et al. 2005, Robling and Turner 2009, Kotiya and Silva 2013).

2.2.2 Shear Flow Hypothesis

The current leading mechanotransductive theory is the shear flow hypothesis. This theory postulates that shear forces applied via interstitial fluid flow in the medullary canal are detected by mechanoreceptors on the osteocyte surface, as shown by Figure 2-3. This then activates genes which in turn, control different stages of bone remodelling, as shown by Figure 2-4 (Turner 1998, Burr, Robling et al. 2002, McGarry, Klein-Nulend et al. 2005, Plotkin, Mathov et al. 2005, Robling and Turner 2009, Adachi, Kameo et al. 2010, Eriksen 2010, Li, Jacox et al. 2018). It is thought that the flow of the interstitial fluid is not caused by shear stresses/strains in the bone, but is induced by differential pressure gradients in the interstitial fluid, caused by the deformation of the bone due to mechanical loads, where the interstitial fluid flows from regions of compression (high pressure) to regions of tension (low pressure) as demonstrated in Figure 2-5 (Burr, Robling et al. 2002).

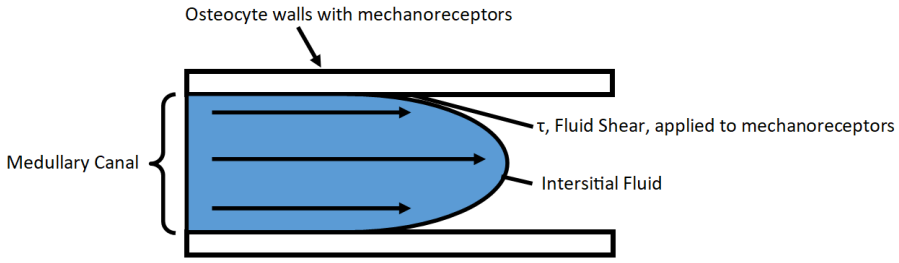

Figure 2-3: Application of shear forces to the mechanoreceptors by the interstitial fluid in the medullary canal

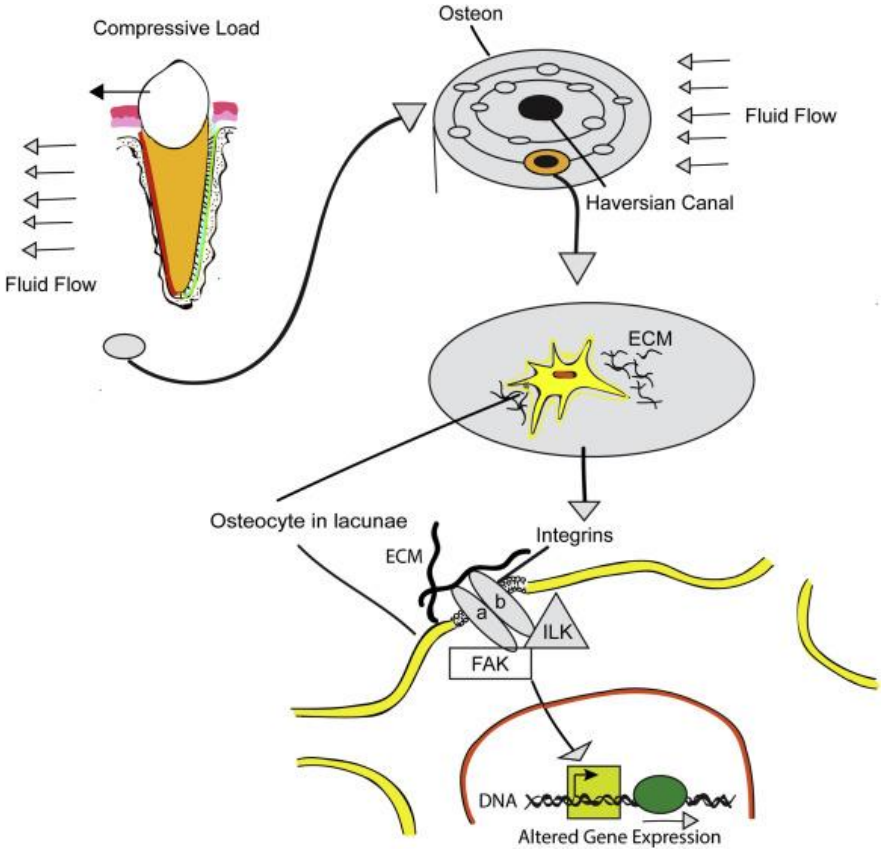

Figure 2-4: Image from Li, Jacox et al. (2018), demonstrating the shear flow hypothesis mechanotransductive process in dentistry, with the tooth pushing on the mandible bone, where fluid flow of the interstitial fluid around osteocytes causes shear strain on mechanoreceptors, resulting in altered gene expression. Where the ECM is the extra cellular matrix, DNA is Deoxyribonucleic acid, integrins are receptors, and FAK and ILK and biochemical signals. NOTE: The shear flow mechanotransductive process is the same throughout the bone, in both density and general orthopaedics.

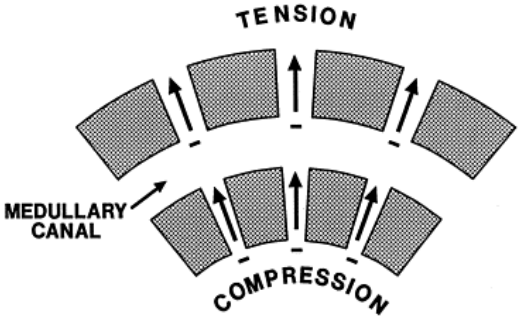

Figure 2-5: The deformation of the bone causing fluid flow through the canalicular channels from regions of compression to regions of tension, applying shear stress against the osteocyte lying within the lacunae (Burr, Robling et al. 2002).

There is strong experimental evidence supporting the shear flow hypothesis, with strong correlations between the pressure gradient and bone remodelling (Turner, Forwood et al. 1994, Knothe Tate and Knothe 2000, Qin, Kaplan et al. 2003). The mapping and measurement of pressure gradients is complicated due to the number of variables which affect the interstitial fluid pressure (Ciani, Doty et al. 2005). Nonetheless, evidence suggests that the influence of the pressure gradient on the fluid flow has an effective diameter of a few millimetres (Qin, Kaplan et al. 2003), suggesting that the bone remodelling mechanotransductive signalling through the shear flow hypothesis is highly localised. Furthermore, during bone deformation the overall volume of the bone is assumed to remain constant, therefore the sum of the change in interstitial fluid pressures also remains constant. If at any point the change in deformation stops, the interstitial pressure will quickly equalise and experience relaxation, returning back to its original value (Papathanasopoulou, Fotiadis et al. 2004). This means that the mechanical deformation must be continuously applied in a dynamic manner to have any bone remodelling response. This is particularly true for mechanotransduction of signals for bone formation, where the bone does not experience positive remodelling under static loading (Lanyon and Rubin 1984, Rubin and Lanyon 1984).

As discussed later in this chapter, bone remodelling algorithms typically use local strain as a stimulus to determine bone remodelling, as strain can more easily be calculated and measured, and has far fewer variables. This substitution of interstitial fluid pressure gradients for strain is suitable since the local strain environment has been strongly correlated to the local pressure gradient (Pollack, Korostoff et al. 1977, Owan, Burr et al. 1997, Mak and Zhang 2001) enabling a high bone remodelling prediction ability using the strain.

2.2.3 Additional Factors to Bone Remodelling

Numerous hormonal/systemic stimuli have been demonstrated to affect each stage of the bone remodelling process (Murrills, Stein et al. 1990, Kalervo Väänänen and Härkönen 1996). Systemic remodelling factors affect the whole skeletal system and in some cases can have a profound effect on the bone, causing degenerative diseases such as osteoporosis, especially in females (Seeman 2003); where hormones such as estrogens, androgens and parathyroid hormone have been

demonstrated to attenuate osteocyte, osteoclast and osteoblast apoptosis (Murrills, Stein et al. 1990, Jilka, Weinstein et al. 1999, Jilka, Noble et al. 2013, Plotkin 2014).

Being reliant on cellular processes, the overall health of an individual is known to influence the bone remodelling process, with some evidence suggesting that the body mass index (BMI) and bone remodelling can be interrelated, where the BMI has been correlated to different bone remodelling processes (Cao 2011). However, this assertion comes with numerous caveats; where it is postulated that BMI cannot be directly correlated to bone remodelling but is simply representative, or a result of other factors which are also influencing bone remodelling. Furthermore, there are inconsistencies in the correlation of the BMI with the factors which are thought to influence bone remodelling, for example, the use of the BMI as an indicator of a subject's overall health which has been demonstrated to have flaws (Bell, Carslake et al. 2018, NHS 2019). As such the relationship between the BMI (and/or its contributing factors, e.g body fat mass) and bone remodelling is highly complex (Hou, He et al. 2020), and any correlations and/or connections between the two continues to be researched (Mosca, Goldberg et al. 2017, Hou, He et al. 2020). Nonetheless, the BMI continues to be a good general indicator of how the overall bone remodelling metabolic processes should be responding, and therefore is still measured and correlated against results in studies examining the overall bone remodelling process (Allison, Poole et al. 2015, Mosca, Goldberg et al. 2017, Hou, He et al. 2020).

Non-naturally occurring factors have also been demonstrated to influence bone remodelling, with two common factors being smoking and alcohol. Smoking is known to be detrimental to bone remodelling, where tobacco has been demonstrated to increase bone resorption, particularly in men (Supervia, Nogues et al. 2006). Alternatively, alcohol has been demonstrated to have mixed effects. Whilst its influence on younger individuals is still uncertain, light alcohol consumption has been demonstrated to have beneficial effects on older individuals, whereby slowing the bone remodelling process, it slows the loss of bone density with age. Alternatively, heavy alcohol consumption is associated with decreased bone density and increased fracture risk (Gaddini, Turner et al. 2016).

2.3 Alternative Bone Remodelling

It is generally thought that bone remodelling follows the same remodelling response in relation to the stimulus throughout the bone. Whilst it is accepted that different people can experience different bone remodelling rates (Parfitt 2002, Parfitt 2004), it is generally considered that the bone will experience the same stimulus-remodelling relationship. An assumption which is carried forward into bone remodelling algorithms.

Alternative bone remodelling can be defined as two or more different bone remodelling responses to the same stimulus, resulting in two or more different changes in density in response to the same stimulus. There are numerous cellular mechanisms which influence each stage of the bone remodelling process. The majority of these act systemically effecting the whole skeletal system equally: However alternative bone remodelling mechanisms, cause alternative bone remodelling behaviour by differently affecting one or more of the bone remodelling stages, either by influencing mechanotransduction or through other processes, in one or more locations. There are two essential ways in which alternative bone remodelling mechanisms achieve this: 1) Amplification, where one or more stages of the bone remodelling cycle is aided, increased, supported or helped in some way. 2) Suppression, where one or more stages of the bone remodelling cycle is prevented, slowed down or restrained in some way.

Alternative bone remodelling under tension and compression is not a new or novel concept. Different independent mechanisms have been demonstrated or suggested to cause alternative remodelling in tension and compression (Rubinacci, Black et al. 1988, Bentolila, Boyce et al. 1998, Stokes 2002). However, the studies which have identified alternative bone remodelling behaviour have all been in laboratory or pathological (e.g. scoliosis) conditions. There has been no study into alternative bone remodelling behaviour under physiological loading conditions. This makes it difficult to determine what, if any, effect alternative bone remodelling has under physiological loading conditions. Furthermore, whilst numerous remodelling algorithms are based on mechanisms which have been demonstrated to cause alternative remodelling behaviour (Frost 2003, Taylor and Lee 2003, McNamara and Prendergast 2007, Vahdati and Rouhi 2009, Fernández, García-Aznar et al. 2012, Cerrolaza, Duarte et al. 2017), the effect of alternative bone remodelling behaviour on remodelling algorithms has not been investigated.

Here, for this study, a distinction needs to be made between bone remodelling pathological conditions and physiological loading conditions. With a focus on alternative bone remodelling, the stimulus-remodelling relationships under tension and compression need to be examined. The physiological loading conditions are the loads applied to the bone *in vivo*, in normal conditions, without any additional external influence. Pathological conditions which effect bone remodelling can come in a wide variety, and can affect both the biomechanical and metabolic/cellular processes essential to bone remodelling. In fact, many pathological conditions can occur under physiological loading conditions (Stokes 2002). However, bone remodelling pathological conditions result in abnormal bone remodelling behaviour, and thus effect the stimulus-remodelling relationship. It is these abnormalities in the bone remodelling behaviour which are studied and quantified, often without reference to the initial stimulus-remodelling relationship which would have been present without the pathological condition. Therefore, the stimulus-remodelling relationships observed in pathological conditions cannot be applied to the bone remodelling experienced under physiological loading in normal conditions. Nonetheless, it should be noted that the bone remodelling mechanisms which are identified in pathological conditions which contribute to alternative bone remodelling, may also be present in normal conditions, but less have less of an effect, and therefore still need to be acknowledged when examining alternative bone remodelling under physiological loading in normal conditions.

In the literature, the researcher has identified three bone remodelling mechanisms which have been attributed to causing alternative bone remodelling in tension and compression. These are microdamage production, the piezoelectric effect and the Hueter-Volkmann law, all of which are explored in detail in this section and are summarised in Table 2-1. A comparison of these identified mechanisms against the results of this study is made in Chapter 5. The alternative bone remodelling experienced as a result of these mechanisms is different and independent to each mechanism. The mechanisms themselves are also independent of each other, and therefore all may be acting at the same time (Cerrolaza, Duarte et al. 2017). This is in addition to other bone remodelling processes, acting systemically, which also may be occurring at the same, where the resultant bone remodelling and stimulus-remodelling relationships is a superposition of the influence of all mechanisms and processes.

Table 2-1: Individual characteristics of alternative bone remodelling mechanism on the stimulus-remodelling relationship based on the literature review

Mechanism	Observations		Stage of Bone Remodelling
	Tension	Compression	
Microdamage	No effect	Initiates remodelling	Initiation
Piezoelectric	Electropositive potential signals for resorption	Electronegative potential signals for formation	Resorption and Formation
Hueter-Volkman	Increase in bone remodelling	Retards bone growth by up to 40%	Resorption and Formation

2.3.1 Microdamage

Skeletal microdamage or micro-fractures are microscopic fractures within the bones' extracellular matrix. Fractures are commonly only thought of as complete fractures that require medical intervention; however, at any point in time, the human bone can contain thousands of microscopic fractures. These microscopic fractures follow the laws of fracture mechanics and fatigue and therefore are often referred to as microscopic fatigue damage (O'Brien, Taylor et al. 2003, Taylor and Lee 2003, Seref-Ferlengez, Kennedy et al. 2015). Several theories state that microdamage initiates bone remodelling through processes such as: The microdamage removal theory where the cellular process of removing microdamage initiates remodelling (Turner 1998, Turner and Akhter 1999, Huiskes, Ruimerman et al. 2000, Burr, Robling et al. 2002, Frost 2003, Burr 2014); and the microdamage criticality theory where remodelling is initiated when the amount of microdamage reaches a critical value (Prendergast and Taylor 1994, Vahdati and Rouhi 2009).

Until recently, it was thought that there was only one type of microdamage in the bone. However, developments in microdamage detection techniques and technology have enabled a closer look into the bone and have revealed that there are two types of microdamage, which have been called: 1) Linear microdamage, and 2) Diffuse damage (Herman, Cardoso et al. 2010). The two types of microdamage are initially distinguished and subsequently named by their geometry. Linear microdamage is a sharply defined crack/cracks which form on the lamella level and are typically 30 – 100 μm in length before its growth is halted, most likely due to anatomical features (Burr and Martin 1993, Boyce, Fyhrie et al. 1998, Seref-Ferlengez, Basta-Pljakic et al. 2014). It can form either longitudinally or transversely against the grain structure (O'Brien, Taylor et al. 2003). Alternatively diffuse damage is a cluster or "diffuse" of cracks on the sub-lamellar level which are

typically no longer than 1 µm (Herman, Cardoso et al. 2010). It is characterised as being practically out of control, separating mineral aggregates from each other and the surrounding organic matrix.

Linear microdamage can only be produced under dynamic, continually changing, compressive loading (Boyce, Fyhrie et al. 1998, Taylor and Lee 2003, Karim and Vashishth 2013) while diffuse damage can be produced under any tensile load (Karim and Vashishth 2013). For diffuse damage, the tensile loading can be applied via time-dependent creep like loading and/or cycle-dependant fatigue like loading (Bentolila, Boyce et al. 1998). However, creep appears to be the dominant stimulus (Seref-Ferlengez, Basta-Pljakic et al. 2014). This causes compartmentalisation of the two types of microdamage, which has been demonstrated to be true to p-values between <0.001 and <0.03 (Bentolila, Boyce et al. 1998, Boyce, Fyhrie et al. 1998, Herman, Cardoso et al. 2010, Karim and Vashishth 2013, Seref-Ferlengez, Basta-Pljakic et al. 2014). Nonetheless, some studies have demonstrated a small amount of cross-production, where linear microdamage is formed under the tensile dominant region and diffuse damage is produced under compressive dominant region, as shown in Figure 2-6 (Karim and Vashishth 2013).

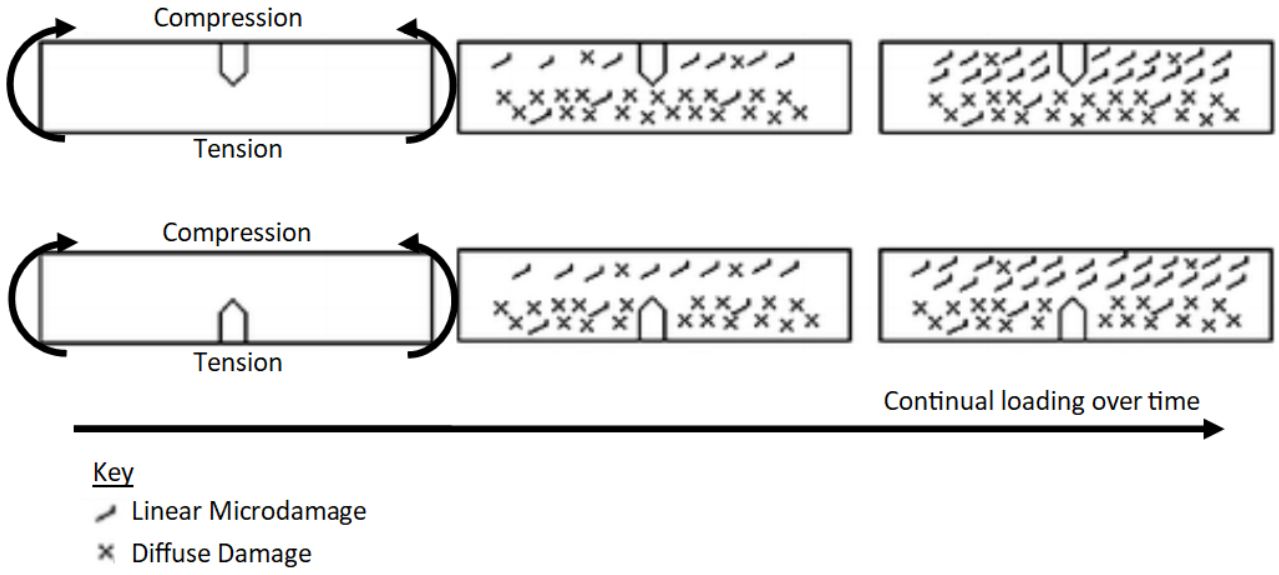

Figure 2-6: Production and compartmentalisation of diffuse damage and linear microdamage under tension and compression. Image adapted from Karim and Vashishth (2013)

The compartmentalisation of the two types of microdamage is further assisted by the bone's fracture toughness properties in response to microdamage production. Linear microdamage lowers the fracture toughness of the bone (Burr, Turner et al. 1998, Karim and Vashishth 2013) while diffuse damage increases the bone's fracture toughness (Parsamian and Norman 2001). Fracture toughness is the amount of energy an object can absorb per volume before fracture and is independent of elastic modulus, stiffness and other strength parameters. Microdamage accumulation has been demonstrated to have a larger effect on fracture toughness than bone strength (Currey, Brear et al. 1996). It has been proposed that the presence of diffuse damage does not suppress the initiation of linear microcracks, but does suppress their propagation (Karim and Vashishth 2013). Parsamian and Norman (2001) demonstrated an almost linear correlation between fracture toughness and diffuse damage up to a 60% increase in fracture toughness at a volume of approximately 0.05 mm^2/mm^2 diffuse damage.

Both diffuse damage and linear microdamage are the result of dissipation of the built up elastic strain energy through the production of new surface cracks (Wang 2013). Therefore, both types of microdamage occur at yield, which takes place locally in the bone (Biewener 1993, Schaffler, Pitchford et al. 1994, Wang 2013). Due to the different yield strains of the bone under tension and compression, diffuse damage is always produced before linear microdamage (Karim and Vashishth 2013). In the cortical bone, tensile yield strain has been measured to be between 4000 and 7000 με (Currey 2004, Wang and Nyman 2007) and compressive yield strain has been measured to be between 6000 and11000 με (Biewener 1993, Niebur, Feldstein et al. 2000, Nyman, Ni et al. 2008, Zioupos, Hansen et al. 2008, Leng, Dong et al. 2009) as shown in Table 2-2.

Table 2-2: Measured human cortical tensile and compression yield strains in literature.

Location	Tensile Yield Strain (με)	Compressive Yield Strain (με)	References
Femoral	6000 – 7000	-	(Currey 2004)
Femoral	4000 – 7000	-	(Wang and Nyman 2007)
Femoral	-	6000 – 11,000	(Biewener 1993, Niebur, Feldstein et al. 2000)
Femoral	-	7000 – 8000	(Nyman, Ni et al. 2008, Leng, Dong et al. 2009)
Femoral	-	~7500	(Zioupos, Hansen et al. 2008)

The measured yield strain of bone differs depending on testing method (Wang 2013) sample size, testing orientation (Hansen, Zioupos et al. 2008) wetness (Sasaki and Enyo 1995, Yanashita, Li et al. 2002), potential resorption cavities (Hernandez, Gupta et al. 2006), and potential prior microdamage (Burr, Turner et al. 1998). Age appears to have very little or no effect on the yield strain of either cortical or trabecular bone (Kopperdahl and Keaveny 1998, Wang 2013).

2.3.1.1 Apoptosis

As shown by Figure 2-7 and Table 2-3, by inducing microdamage production and observing the subsequent remodelling, *in vivo* studies have shown an alternative bone remodelling response in compression and tension as a result of microdamage production. A remodelling response is observed under compression due to linear microdamage (Bentolila, Boyce et al. 1998, Herman, Cardoso et al. 2010). Alternatively, absolutely no remodelling response was observed under tension as a result of diffuse damage production (Bentolila, Boyce et al. 1998, Herman, Cardoso et al. 2010, Seref-Ferlengez, Basta-Pljakic et al. 2014, Seref-Ferlengez, Kennedy et al. 2015). In these studies, this caused a change in density under compression, but not under tension.

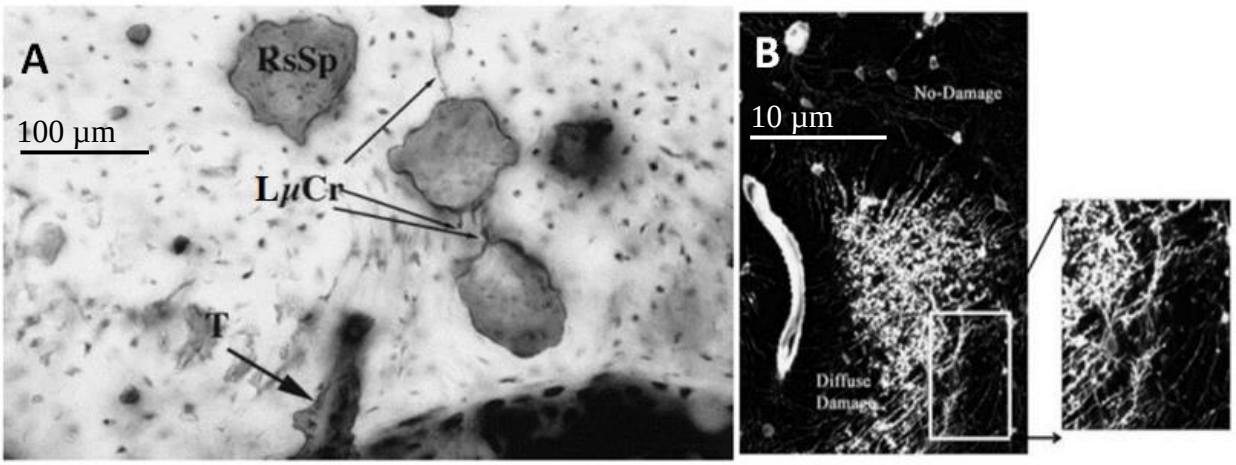

Figure 2-7: (A) Cross section of a rat unlar after fatigue loading. Showing resorption spaces (RsSp) in association with linear microdamage (LµCr) and osteoclastic tunnelling (T) from the periosteal surface (Bentolila, Boyce et al. 1998). (B) Diffuse Damage in the bone with no remodelling initiation (Seref-Ferlengez, Kennedy et al. 2015)

Table 2-3: Summary of in vivo differential bone remodelling responses to linear microdamage and diffuse damage observed in the literature

Stimulus	Observation	Reference
3800 ± 500 με	Linear microdamage initiates remodelling. Diffuse damage does not initiate remodelling.	(Herman, Cardoso et al. 2010)
16.1 ± 1 N applied until 15% stiffness loss	Diffuse damage does not initiate remodelling. Bone repairs itself back to the original state in an unknown process.	(Seref-Ferlengez, Basta-Pljakic et al. 2014)
4000 ± 495 με	Linear microdamage removed by osteoclasts. No remodelling activity due to Diffuse damage.	(Bentolila, Boyce et al. 1998)

The cause for the alternative remodelling response to linear microdamage and diffuse damage is the initiation of bone remodelling through apoptosis, which initiates the bone remodelling process by signalling for osteoclasts through the apoptosis signalling pathway (Robling and Turner 2009, Jilka, Noble et al. 2013, Burr 2014, Plotkin 2014). Of the two types of microdamage, only the compressive formed linear microdamage causes osteocyte apoptosis, which it achieves through either: damaging the osteocyte, removing the osteocyte from the extracellular matrix or damaging the extracellular matrix disrupting the essential fluid flow for osteocyte survival (Plotkin, Mathov et al. 2005, Jilka, Noble et al. 2013, Plotkin 2014). All of these linear microdamage processes disrupt the essential delivery of oxygen causing the effected osteocytes to become hypoxic (Plotkin, Mathov et al. 2005) which results in apoptosis (Dodd, Raleigh et al. 1999). An osteocyte takes approximately 24 hours to become hypoxic (Plotkin, Mathov et al. 2005); however, osteocyte hypoxia has multiple factors, such as the distance from the Harversian canal.

Diffuse damage alternatively does not alter osteocyte integrity, remove the osteocyte from the extracellular matrix or damage the extracellular matrix disrupting the essential fluid flow (Seref-Ferlengez, Basta-Pljakic et al. 2014, Seref-Ferlengez, Kennedy et al. 2015). Therefore, diffuse damage does not cause osteocyte apoptosis and cannot trigger bone remodelling (Bentolila, Boyce et al. 1998, Herman, Cardoso et al. 2010, Seref-Ferlengez, Basta-Pljakic et al. 2014, Seref-Ferlengez, Kennedy et al. 2015).

Both Burr and Martin (1993) and Taylor and Lee (2003) attempted to quantify and predict where linear microdamage would be produced and initiate bone remodelling. Both studies found it difficult to determine this due to the number of unmeasurable factors; such as crack growth halting

due to cement lines and other microdamage being present. Therefore, linear microdamage production and bone remodelling initiation are considered almost 'random.' It should also be noted, that neither linear microdamage nor diffuse damage have been demonstrated to have any effect on any other stage of bone remodelling, the difference in microdamage only causes alternative bone remodelling through the initiation stage.

2.3.2 Piezoelectric

It has long been reported that the bone has piezoelectric properties where electrical potentials are generated under both compressive and tensile loads (Andrew A. Marino 1971). It is thought that the piezoelectric effect is a major source of bioelectrical activity within the bone (Cerrolaza, Duarte et al. 2017). When the bone undergoes mechanical deformation, it experiences electrical polarization from two mechanisms: 1.) Piezoelectric collagen; where the collagen molecules have a high crystallinity and are highly oriented (Fukada and Yasuda 1957). And 2.) Fluid in the calcified matrix which is forced to move from areas of compression to tension, causing a stream of potentials in the same direction (Eriksson 1974). The piezoelectric properties occur throughout the bone; as the bone walls are full of multiple fine fibrous sheets where collagen molecules are unidirectionally oriented with crystals of hexagonal symmetry (Martin 1979).

The piezoelectric effect is not a mechanotransductive mechanism, but instead a marker of mechanical loads and fluid flow, a known mechanotransductive process (Gusmão and Belangero 2015). With the high complexity in mechanotransduction and some processes not being fully understood, the potential role of piezoelectricity is nonetheless debated by some authors (Stroe, Crolet et al. 2011). Mathematical models calculating the piezoelectric signals have been demonstrated to accurately determine the resorption and formation sites within the bone (Fernández, García-Aznar et al. 2012, Cerrolaza, Duarte et al. 2017). It worth considering that the accuracy achieved in these remodelling calculations may be the result of the piezoelectricity being a marker of the mechanical loads, not bone remodelling being a result of piezoelectricity.

Nonetheless, piezoelectric properties have been demonstrated to assist in fracture healing (Kuzyk and Schemitsch 2009) and as a result they are utilised in orthopaedic growth therapy, as a method to aid in fracture repair (Orthofix Holdings 2019). Currently, piezoelectric material is being

investigated as a viable third generation orthopaedic implant scaffold to stimulate bone growth aiding osseointegration (Navarro, Michiardi et al. 2008, Tandon, Blaker et al. 2018). It is thought that the piezoelectric potentials could be “hijacking” different stages of mechanotransduction, impacting on cellular ion channels within the fluid flow (Gusmão and Belangero 2015).

Piezoelectricity of the bone has not been directly linked with causing alternative remodelling between tension and compression. However, tensile and compressive loads have been linked to alternative electrical potentials; where compression generates electronegative potentials and tension generates electropositive (Becker, Bassett et al. 1964, Kuzyk and Schemitsch 2009). It has been demonstrated that bone formation is signalled for under electronegative potentials while resorption is signalled for under electropositive potentials (Rubinacci, Black et al. 1988). It is thought that this could cause a higher amount of formation under compression and a higher amount of resorption under tension. However, there is a severe lack of evidence into this effect and further research is required before any conclusions can be made.

2.3.3 Hueter-Volkmann Law

The Hueter-Volkmann law is a mechanism which effects the resorption and formation stages of the bone remodelling cycle, causing bone growth retardation under compression and bone growth acceleration under tension (Stokes 2002, Villemure, Aubin et al. 2004, Kim, Kim et al. 2010). As demonstrated by Figure 2-8 it can cause severe deformation and curvature of the spine. It has also been linked with clinical conditions such as scoliosis, Blount's disease, club foot, Scheuermann's kyphosis, compensatory growth associated with fractures, spondylolisthesis and slipped capital femoral epiphysis (Stokes 2002, Kim, Kim et al. 2010).

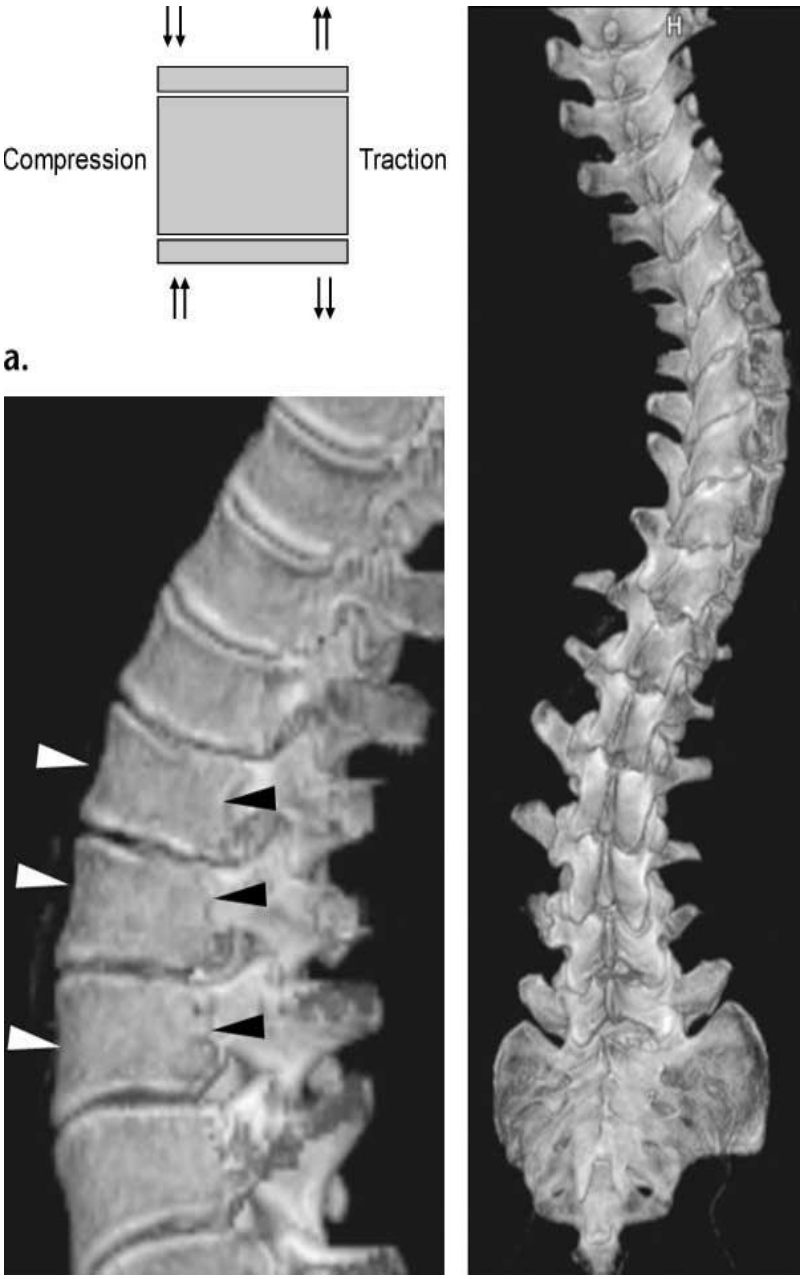

Figure 2-8: Image of scoliosis of the spine used to train physicians of the potential effect of the Hueter-Volkmann law where the bone has been demonstrated to experienced retarded growth under compression and higher amounts of growth under tension (Kim, Kim et al. 2010),

The Hueter-Volkmann law is typically associated with continual static loading (Stokes 2002, Stokes, Gwadera et al. 2005); however, it has been demonstrated to occur under everyday dynamic conditions, and as a consequence it is often described as idiopathic (Villemure, Aubin et al. 2004, Lin 2010). A possible explanation for the ability of the Hueter-Volmann law to occur under dynamic loading could be found via the strain shift; where the mean strain can drift away from

zero in dynamic loading, as shown in Figure 2-9. Here, assuming that the loading pattern is sinusoidal, the mean strain experienced by the bone is that shown in equation 2-1.

$$\varepsilon_{mean} = \frac{\varepsilon_{max} - \varepsilon_{min}}{2} \qquad 2\text{-}1$$

Where ε_{mean} is the mean strain, ε_{max} is the maximum strain and ε_{min} is the minimum strain. Therefore, if the sinusoidal strain is not around zero, the mean strain experienced by the bone during loading shifts. This would suggest that as the bone experiences sinusoidal compressive strain, it will also experience a mean compressive strain, possibly inducing the Hueter-Volkmann effects.

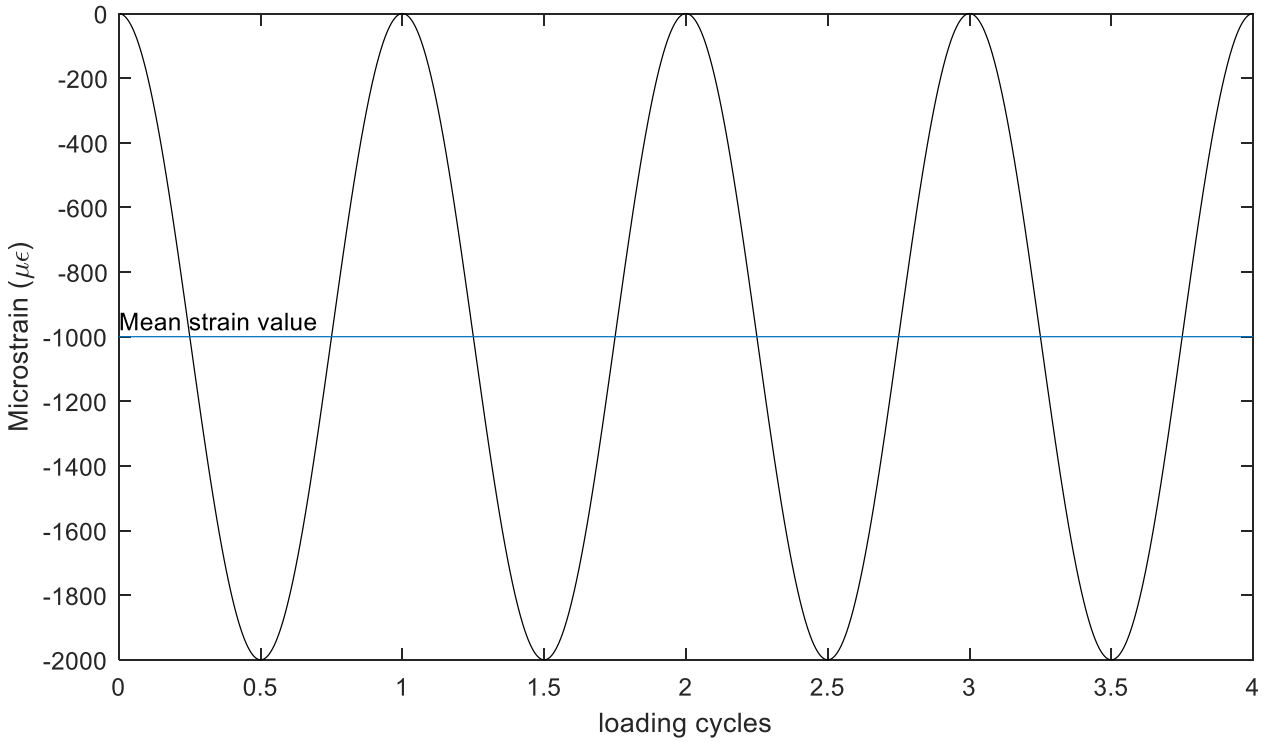

Figure 2-9: Strain shift in a sinusoidal compressive loading wave of 2000 με

There is substantial *in vivo* and clinical research into the Hueter-Volkmann law due to the potential clinical severity of the deformation (Stokes and Laible 1990, Stokes 2002, Villemure, Aubin et al. 2004, Stokes, Gwadera et al. 2005). These studies have indicated that the Hueter-Volkmann law appears to have a much more significant effect on the bone under compression, than it does on the bone under than tension: Where, a sustained static compressive load of a physiological magnitude

has been demonstrated to retard bone growth by up to 40% (Stokes, Gwadera et al. 2005). The bone growth acceleration rate under tension appears to be significantly less (Stokes 2002). Furthermore, it must be noted that the influence of the Hueter-Volkmann law under compression can occur under any loading (static or dynamic) due to its idiopathic nature, however, the influence the Hueter-Volkmann law under tension can only occur under dynamic loading. This is due to bone formation only occurring under dynamic loading (Lanyon and Rubin 1984, Rubin and Lanyon 1984).

There is currently no generally accepted theory for the cause of the Hueter-Volkmann law, although many authors have proposed ideas (Villemure, Aubin et al. 2004) and it is possible that more than one aetiology exists. With this in mind, most theories for the Heuter-Volkmann law are medically based, focusing on pathological pathways (one pathological condition leading to another) for conditions such as scoliosis, usually theorising that it initiates with an initial abnormality or instability (Villemure, Aubin et al. 2004).

A mechanically based theory of how the Hueter-Volkmann law is caused is the flow restriction theory which is originated in density/orthodontics (Li, Jacox et al. 2018). The theory states that the compressive loads restrict the blood flow causing regional mild hypoxia, which in-turn causes hypoxia-inducible factor-1 to stimulate cell proliferation and angiogenesis (Niklas, Proff et al.). This theory states that the tensile and compressive loads effect the shear flow mechanotransduction of the bone (see 2.2.2 Shear Flow Hypothesis), where compression is thought to increase the signals for resorption whilst tension is thought to decrease the signals for resorption and increase signals for formation through different cellular biochemical processes (Li, Jacox et al. 2018). In dentistry and orthodontics this allows for the tooth to move towards the compressive side, a phenomenon utilised by orthodontic braces. It also compliments observations made in the study of the Hueter-Volkmann law in general bone remodelling (Stokes, Gwadera et al. 2005).

2.4 Bone Remodelling Investigations

There are numerous different methods in which bone remodelling is studied, each have their own advantages and disadvantages. The typically employed methods of bone remodelling investigation can be split into self-design simulations and observational, both of which are explored here.

2.4.1 Self-Design Simulations

Self-design simulations are a commonly used, finite element-based method to study bone remodelling in certain conditions/environments (Beaupré, Orr et al. 1990, Bitsakos, Kerner et al. 2005, Turner, Gillies et al. 2005, van der Meulen and Hernandez 2013). Here, a finite element mesh model is set up, which is typically 'blank' (a homogenously applied single density, single mechanical property distribution) such as that shown in Figure 2-10. Each element is assigned a bone remodelling algorithm, such as those discussed in 2.5 Bone Remodelling Algorithms, where following the application of musculoskeletal loads, the model is left to produce its own internal density distribution over a number of iterations, until an equilibrium is reached and the density in the elements stops changing. Depending on the model, 10's to 100's and in some cases 1000's of iterations may be required to reach an equilibrium. In some cases if the data is available, the output density distribution of the self-design simulation is qualitatively compared to clinical data to validate the model and its inputs (Turner, Gillies et al. 2005).

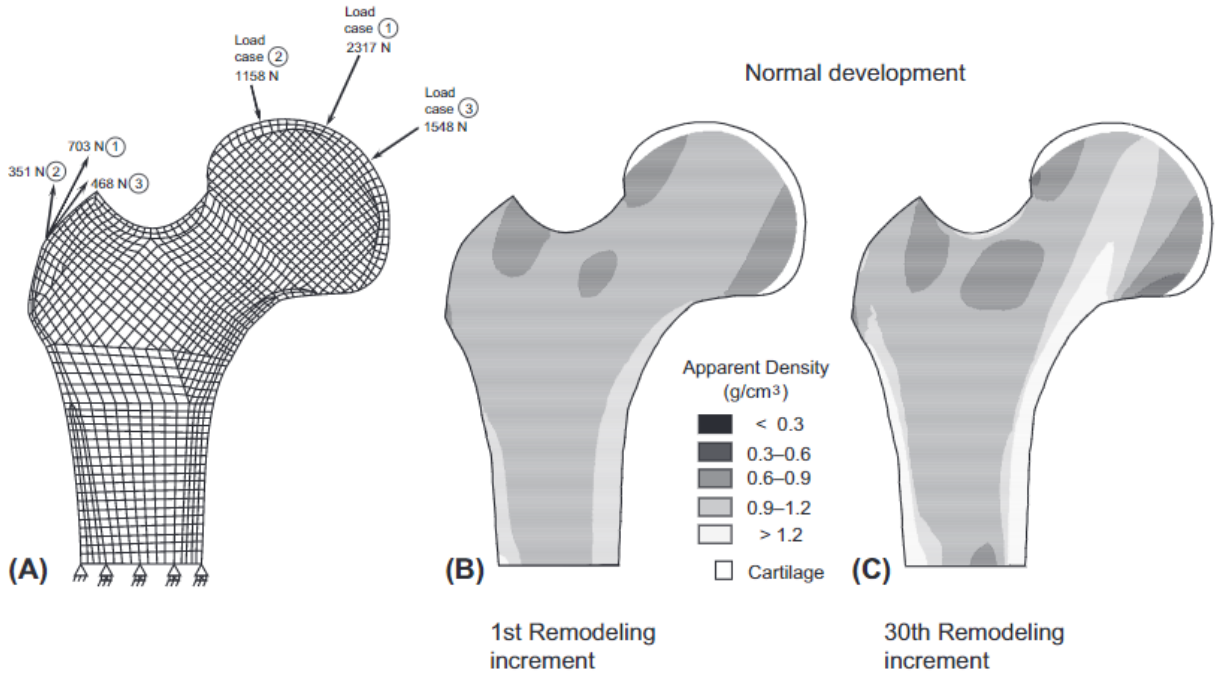

Figure 2-10: Self-design simulation example, with (A) the finite element mesh and the results from one iteration (B) and 30 iterations (C) (van der Meulen and Hernandez 2013)

The use of the self-design simulation has numerous advantages over other bone remodelling investigations, namely that numerous factors can be isolated and investigated quickly, safely and independently, without the need to operate on, or manipulate, the bone of any animal or human subjects. As a result, the self-design method has proven to be a useful tool in determining the change in density around orthopaedic implants (Bitsakos, Kerner et al. 2005, Turner, Gillies et al. 2005). However, the downside of self-design simulations is that they are completely reliant on the initial bone remodelling algorithms and other assumptions used in the simulation being correct.

2.4.2 Observational Studies

Observational studies can be split into laboratory and clinically based, which involve the direct measurement of an output in relation to different stimuli and/or variables. For laboratory-based observational studies, these can be split into further two categories of *in vitro* and *in vivo. In vitro* experimentation offers a "sterile" investigatory platform, where parameters can be controlled. Therefore typically, *in vitro* studies are used to investigate functions of specific stimuli or variables on induvial live cells which cannot be otherwise observed *in vivo* (Plotkin, Mathov et al. 2005, Plotkin 2014). However, whilst *in vitro* studies have allowed insight into numerous bio-chemical pathways, it has been criticised for not accurately representing the *in vivo* environment. Alternatively, *in vivo* laboratory and clinically based studies perfectly represent the true environment; but, with this comes intersubjectivity and numerous uncontrollable biological variables, which affect the results and cannot be eliminated. These uncontrollable variables can also themselves be intersubjective and are typically based on individual circumstances. For bone remodelling these typically include age, sex, overall health and lifestyle including activeness, the presence of medication and/or other substances and the presence of any pathology (Hou, He et al. 2020). As a result, the variables, for example can include things such as endocrinal and haemopoietic factors, the effectiveness of the osteoblasts, osteoclasts and intermediary cells along with any and all signalling processes and the metabolic speed (rate of remodelling) of the individual cells. For example, a subject with low calcium concentration in the blood will experience a higher resorption rate in bone remodelling than usual (Kukuljan, Nowson et al. 2011). Nonetheless, these uncontrollable biological variables, whilst can influence the observed result, typically do not render the results unusable. A good example of this is osteoporosis. The

progression of this degenerative disease in an individual can be effected by numerous factors, however it still follows a predictable path (Seeman 2003).

In vivo laboratory-based studies are typically carried out on small animals and usually involve the external application of mechanical loads and the removal of the bone from the host (Bentolila, Boyce et al. 1998, Kotiya and Silva 2013). Whilst this is highly informative, there are differences between the orthopaedic physiology of the small animal and the human, which makes the results not always completely transferable (Robling and Turner 2009). Clinical-based studies carried out on humans cannot observe the individual bone remodelling processes with current technology, so can only measure the output density using non-invasive measurement techniques (Allison, Folland et al. 2013, Troy, Mancuso et al. 2018) and measure the chemicals in the blood known to be associated with bone remodelling (Eriksen 2010). Furthermore, clinical studies in humans require the participation of numerous subjects, which requires stringent screening, recruitment and ethics, and the outcome is not guaranteed. Furthermore, in human-based studies, participants can drop out of the study and circumstances can change, such as additional pathologies becoming a factor, all of which can impact the output of the results.

Due to the large number of variables which can influence observational studies and the time and money it takes to set up and conduct an observational study, self-design simulations are becoming an increasingly more popular method to investigate bone remodelling output in different conditions in replace of observational studies. However, as previously mentioned, self-design simulations rely on the bone remodelling algorithms being correct. These remodelling algorithms, although in some cases are based on theory, the fundamental basics need to be based on observations. Therefore, observational studies are essential for the correct running of self-design simulations.

2.4.3 Change in Density Over Time

Bone remodelling is a relatively slow process, where in humans, depending on the location, the remodelling cycle can take 120-150 days (Eriksen 2010). This period is highly affected by endocrine and other systemic factors, for example in situations such as Myxedema and during bisphosphonate treatments, the bone remodelling cycle can take exceed 1,000 days (Eriksen 1986).

Furthermore, there are intervals of approximately 2.5 years for successive bone remodelling events in the same location (Hart, Newton et al. 2020). This causes the time for the bone to respond and adapt to a stimulus to go into the period of years (Zehnder, Risi et al. 2004, Cheung, Tile et al. 2008, Bergmann, Body et al. 2011).

Bone remodelling algorithms which are used to quantify the change in density in response to a stimulus, such as those shown in 2.5 Bone Remodelling Algorithms, can be summarised as equation 2-2.

$$\frac{\partial \rho}{\partial t} = kS \qquad 2\text{-}2$$

Where S is the stimulus of the particular remodelling algorithm, k is a remodelling constant, ∂t represents the time of a single iteration/cycle, $\partial \rho$ is the change in bone density, and $\frac{\partial \rho}{\partial t}$ represents the change in density over that one iteration/cycle. Using the self-design method, the $\frac{\partial \rho}{\partial t}$ output of the bone remodelling algorithm changes as the iterations progress, with the typical change in density output from the self-design iterations being shown in Figure 2-11. These demonstrate a period of rapid change in density until the equilibrium is reached. However, with the need for some self-design simulations to use hundreds of iterations, the $\frac{\partial \rho}{\partial t}$ is arbitrary and not representative of a true bone remodelling cycle.

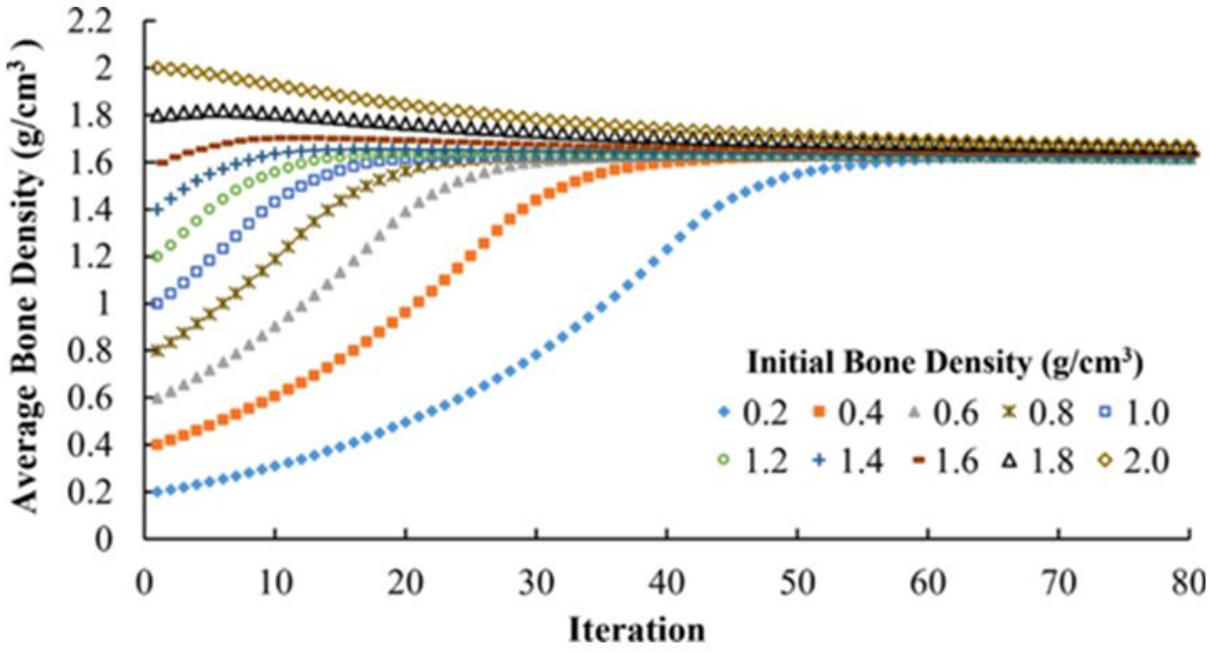

Figure 2-11: Outputs from a self-design simulation using different initial bone densities (Su, Yuan et al. 2019).

Observational-based clinical trials demonstrate a measured, and therefore true, change in density over time in response to stimuli (Zehnder, Risi et al. 2004, Cheung, Tile et al. 2008, Bergmann, Body et al. 2011). This shows a change in density over time which is much slower than those predicted by most self-design simulations, with examples of clinical observations shown by Figure 2-12. The same bone remodelling algorithms used in self-design simulations, such as those shown in 2.5 Bone Remodelling Algorithms, can also be used in observational-based studies to compare the change in density against different stimuli. However, based on the steady change in bone density over time, the ∂t for a single iteration of bone remodelling algorithms used in observational-based clinical trials, to represent the rate of bone remodelling $\left(\frac{\partial \rho}{\partial t}\right)$, can be 6, 12, 24 or 36 months.

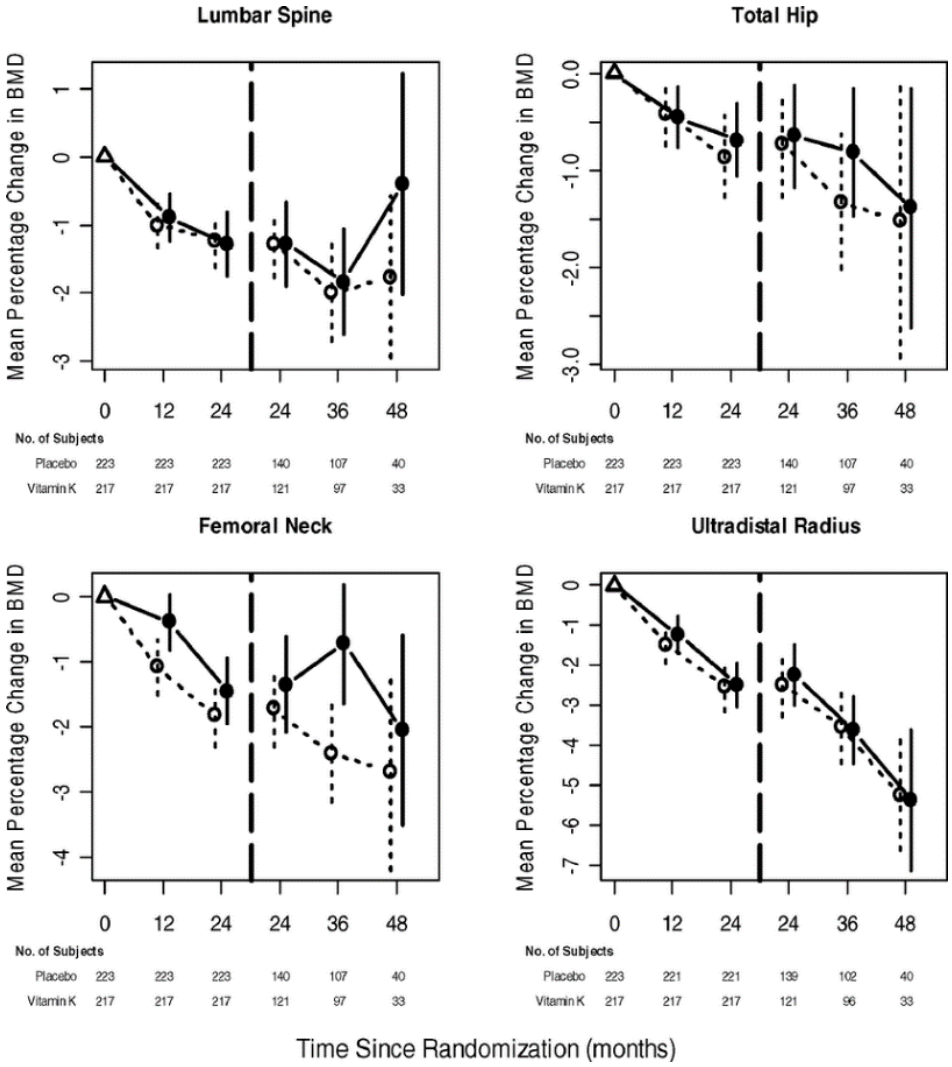

Figure 2-12: Change in bone density over time from a clinical trial in response to endocrinal and mechanical stimuli, where BMD is the bone mineral density (Cheung, Tile et al. 2008)

2.4.4 Use of CT Scans for Bone Remodelling Investigation

The main output measured in bone remodelling studies is the bone density as this is the main factor which determines the bone strength. Currently, the two main methods for measuring the bone density are *ex vivo* examination and non-invasive image-based techniques (Bentolila, Boyce et al. 1998, Stokes, Gwadera et al. 2005, Herman, Cardoso et al. 2010, Seref-Ferlengez, Basta-Pljakic et al. 2014, Seref-Ferlengez, Kennedy et al. 2015). The *ex vivo* method requires the removal of the bone from the living (or recently euthanised) host, and inspection using microscopy, which renders it impossible for re-implantation. For obvious reasons, this method is therefore unsuitable for a

study into human bone remodelling. Hence, most studies use non-invasive image-based techniques for clinical studies.

Computerized tomography (CT) scans are a non-invasive imaging technique that uses high energy electromagnetic waves to produce an accurate image of the 3D density distribution. The ability to provide a 3D image offers distinct advantages over density-based imaging techniques such as x-rays which can only provide 2D images. The 3D image allows for detailed anatomical and physiological observations and as such are often used in clinical studies. Due to the high radiation introduced in CT scans, their use is carefully selected. Imaging techniques such as Magnetic Resonance Imaging (MRI) provide a much safer form of internal imaging, with no exposure to dangerous high energy electromagnetic waves. However, unlike CT scans which produce a picture based on the density of the tissue, MRI's use the magnetic characteristics of Hydrogen atoms. With much less water in bone than other tissues, bones are displayed as an almost single shade of black. If special conditions are met, MRIs can provide quantitative data on bone density and cross-sectional geometric properties; but this requires a complex set up and therefore is not-often used (Hong, Hipp et al. 1999).

The accuracy of the CT scan in determining bone density and different bone functions depends on three different factors: 1. The required spatial resolution to determine the bone density and/or remodelling functions. 2. The spatial resolution capability of the CT device. 3. The calculation of the density from the CT output. For the required spatial resolution to determine the bone density and/or remodelling functions, guidelines have been produced for the resolution required for the assessment of different features in the bone (Bouxsein, Boyd et al. 2010). The spatial resolution ability depends on the CT device, where medical CT devices currently have an approximate spatial resolution of 0.5×0.5×0.5 mm (Lin and Alessio 2009) which is more than adequate to measure bone remodelling. Micro-CTs have a spatial resolution of approximately $0.1 \times 0.1 \times 0.1$ μm (0.001×0.001×0.001 mm) (Rueckel, Stockmar et al. 2014) which allows the examination of the microarchitecture of the bone in much more detail. It should be noted that for live human-based *in vivo* trials, micro-CTs cannot be used, as they can only be used on samples no larger than a couple of centimetres, and as such would require the sample to be removed from the human host. This is demonstrated in Figure 2-13, which shows the difference between medical and micro-CT devices.

Figure 2-13: Comparison between a medical CT device (A)(Canon) and a micro CT device (B)(AZO 2020),, demonstrating that a micro CT device cannot be applied to a large sample.

CT machines do not measure density directly, alternatively the most common output of CTs to is the Hounsfield Units (HU), which measures the linear attenuation coefficient, μ_a, and compares it to that of water at standard temperature and pressure (STP) ($HU_{(WATER)} = 0$, at STP), as shown by equation 2-3 (Helgason, Taddei et al. 2008).

$$HU = 1000 \times \frac{\mu_{a\,(MEASURED)} - \mu_{a\,(WATER)}}{\mu_{a\,(WATER)} - \mu_{a\,(AIR)}} \qquad 2\text{-}3$$

Like any other device, each CT machine is different from each other and works within certain tolerances, where measurement variability can be experienced (Mackin, Fave et al. 2015). Therefore, each CT scan may give a different density reading for the same sample. Quantitative

CT (qCT) scans offer a further advantage in that they provide calibration phantoms to ensure that the density measurement remains consistent. This allows for an accurate comparison of changes in density in clinical studies. CT imaging can be combined with finite element simulations, which can provide results which can be used in both self-design and observational-based studies. In an observational-based study, if more than one CT is taken, the change in 3D density can be compared against calculated stimuli using finite element simulation (Troy, Mancuso et al. 2018) or used to assess the overall effect of a certain exercise (Allison, Folland et al. 2013) or chemical/drug. In a self-design simulation, the predicted density output of the simulation can be compared or based on the CT image.

2.4.5 What is Bone Density

Bone density is a relatively simple, yet complex, concept to define. Simply put, it is the amount of bone within a set area/volume, which is measured as mass per area/volume. However, being a mixture of cells and calcified features such as the extra cellular matrix, what is defined as 'bone' in the calculation of the bone density changes. A summary of different definitions is given in Table 2-4.

In biomechanics and bone remodelling studies the calculation of the bone density is important for two features: 1. The calculation of the change in density, and 2. The calculation of the elastic modulus. For the calculation of the change in density, regardless of which density calculation method is used, so long as the same one is used throughout then the same percentage change in density should be obtained. Alternatively, for the calculation of the elastic modulus, the density calculation could have an impact on the output. The elastic modulus is calculated using the bone density via a density-elasticity equation, as discussed in sections 2.8.1.2 Density-Elasticity Equation, and 3.3.3 Mechanical Properties. As discussed in these sections, there are numerous different density-elasticity equations, which have been developed through comparison of different samples (Helgason, Perilli et al. 2008). Differences in these samples, which could range in anything from differences in age to collection site, result in different density-elasticity equations. Studies obtain the best results when using density-elasticity equations which have been derived from samples which best match their test population. For cortical and trabecular bone, in the femur of men aged approximately 40-90, the ash density has proven reliable (Keller 1994, Eberle,

Gottlinger et al. 2013). This density can be obtained non-invasively using the Hounsfield units of qCTs through equation 2-4.

$$\rho_{ash} = 0.0361 + (0.000731311 \cdot HU) \qquad 2\text{-}4$$

Where HU is the Hounsfield units (Eberle, Gottlinger et al. 2013).

Table 2-4: Definition of bone density from different articles.

Density Name	Density Definition	Reference
Real density	$\rho_{real}(g/cm^3) = \frac{hydrated\ tissue\ mass}{bone\ tissue\ volume}$	(Galante, Rostoker et al. 1970)
Apparent density	$\rho_{app}(g/cm^3) = \frac{hydrated\ tissue\ mass}{total\ specimen\ volume}$	(Galante, Rostoker et al. 1970)
Apparent wet density	$\rho_{wet}(g/cm^3) = \frac{hydrated\ tissue\ mass}{total\ specimen\ volume}$	(Keyak, Lee et al. 1994)
Apparent dry density	$\rho_{dry}(g/cm^3) = \frac{dry\ tissue\ mass}{total\ specimen\ volume}$	(Keller 1994, Keyak, Lee et al. 1994)
Ash density	$\rho_{ash}(g/cm^3) = \frac{Ash\ mass}{total\ specimen\ volume}$	(Galante, Rostoker et al. 1970, Keyak and Falkinstein 2003)
Actual density	$\rho_{actual}(g/cm^3) = \frac{hydrated\ tissue\ mass}{total\ specimen\ volume}$	(Sharp, Tanner et al. 1990)
Porosity	$1 - \frac{apparent\ density}{real\ density}$	(Sharp, Tanner et al. 1990)
Bone volume fraction	$\frac{BV}{TV} = \frac{Bone\ tissue\ volume}{Total\ specimen\ volume} = \frac{apparent\ density}{real\ density}$	(Gibson 1985)

Total specimen mass: The specimen mass including marrow.

Hydrated tissue mass or wet tissue mass: The specimen mass weighted in air after defatting, rehydration and centrifuging on a blotting paper.

Dry tissue mass: The specimen mass weighted in air after defatting and drying at moderate temperatures.

Ash mass: The mineral in bone, which is mostly made up of calcium, which can be obtained as the specimen weight after defatting and heating in a furnace at a temperature of 500℃ or mor for approximately 24 hours.

Bone tissue volume: Volume of bone excluding pores.

2.5 Bone Remodelling Algorithms

Bone remodelling algorithms are used to quantify the change in bone density in relation to a stimulus. Bone remodelling algorithms are typically evaluated and developed through empirical observations, using either human participants or animals, using the methods described in 2.4 Bone Remodelling Investigations. In the case of animals, a more structured study can be set out, where external loading of different magnitudes can be applied manually and the change in density can be carefully monitored using high resolution CTs. Alternatively, in human-based studies the method must be less invasive, therefore in this case, bone remodelling algorithms are applied using calculated mechanical stimuli and non-invasive imagery (Christen, Ito et al. 2014, Troy, Mancuso et al. 2018). This section explores different strain-based bone remodelling algorithms and critically evaluates them.

2.5.1 Frost's Mechanostat

A popular remodelling algorithm is the mechanostat theory, proposed by Frost (1983, 1987, 2001, 2003). Frost determined that there must be a biological mechanosensory feedback mechanism controlling the bone remodelling process, a theory which is universally accepted. Modelled on a basic thermostat equation, Frost proposed that change in density as a result of bone remodelling can be calculated using a strain-based stimulus, as shown in equation 2-5.

$$\frac{\partial \rho}{\partial t} = k(\varepsilon - MES) \qquad 2\text{-}5$$

Where $\frac{\partial \rho}{\partial t}$ is the change in density over a period of time, ε is the new absolute, peak, principal strain ($|\varepsilon_{peak}|$), *MES* is the minimum effective strain for remodelling to occur and *k* is a rate constant. Frost proposed that both positive and negative remodelling will occur either side of MES remodelling thresholds, where in the middle, no bone remodelling would occur, in an area dubbed the "lazy-zone" as shown in Figure 2-14.

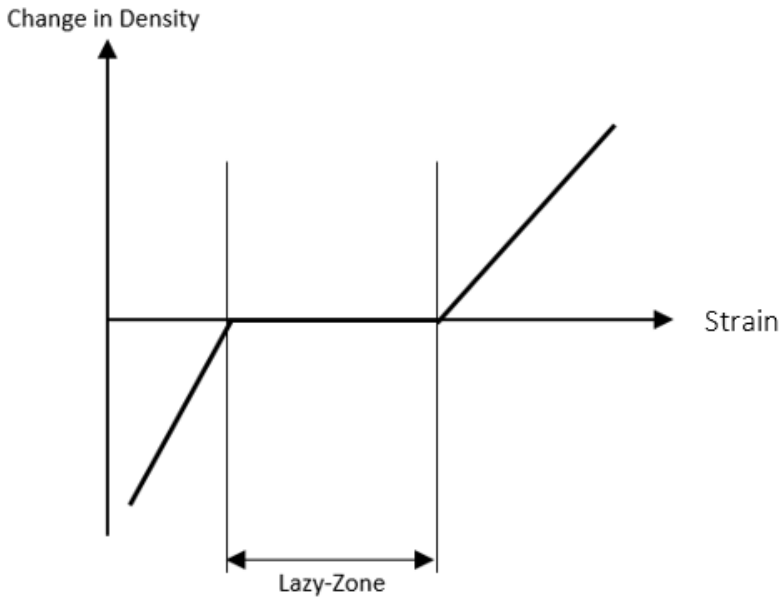

Figure 2-14: Strain feedback graph based on Frost (1987)'s mechanostat, where the lazy-zone is between the positive and negative bone remodelling MES thresholds.

Based on the idea that microdamage produced in the bone under load initiates positive bone remodelling and disuse initiates negative bone remodelling, Frost proposed MES remodelling thresholds of < |50| to |200| με for negative remodelling and > ~|4000| με for positive remodelling based on observations made mostly in small animals. As such equation 2-5 becomes equation 2-6 which produces the graph shape shown in Figure 2-14.

$$\frac{\partial \rho}{\partial t} = \begin{cases} k_{+}(\varepsilon - 4000) & for\ \varepsilon \geq 4000\ \mu\varepsilon \\ 0 & for\ 200 < \varepsilon < 4000\ \mu\varepsilon \\ -k_{-}(\varepsilon - 200) & for\ \varepsilon \leq 200\ \mu\varepsilon \end{cases} \qquad 2\text{-}6$$

Where k_+ is the rate constant for positive remodelling and k_- is the rate constant for negative remodelling. It should be noted that Frost (1983, 1987, 2001, 2003) does not differentiate between the two types of microdamage formed in the bone (described in 2.3.1 Microdamage). Nonetheless, despite not accounting for the different types of microdamage, the use of the mechanostat equation to describe bone remodelling in humans has proven highly successful. Similar bone remodelling algorithms to the mechanostat equation have been proposed, with slight variations, such as Cowin and Hegedus (1976) remodelling algorithm, shown in equation 2-7 which has been used successfully in self design simulations (Frehill 2010).

$$\frac{\partial \rho}{\partial t} = k(\varepsilon - \varepsilon_T)^b \qquad 2\text{-}7$$

Where ε_T is a pre-set strain threshold and b is a power law constant.

2.5.2 Cellular Accommodation

A downfall of equation 2-5 and 2-7 is that they predict if a bone was to suddenly receive little or no stimulus, it would undergo continuous negative remodelling and simply resorb away, which is contrary to reality (Paker, Bugdayci et al. 2009). This therefore presented a paradox named the "disuse fallacy" (Turner 1999). In response to the disuse fallacy, cellular accommodation was proposed (Turner 1999, Schriefer, Warden et al. 2005, Vahdati and Rouhi 2009); a theoretical mechanism, based on the idea that since bones are poorly innervated and therefore cannot rely on the central nervous system, osteocytes must be able to accommodate themselves locally to the mechanical stimulus (Turner 1999). This would be achieved through either cytoskeletal reorganisation or changing the extracellular microenvironment (Turner 1998, Turner 1999, Schriefer, Warden et al. 2005).

To incorporate cellular accommodation into remodelling algorithms, Turner (1999) proposed two different equations. The first equation for the response of the bone to mechanical loading is shown in equation 2-8.

$$\frac{\partial \rho}{\partial t} = k(\varepsilon - F(\varepsilon, t)) \qquad 2\text{-}8$$

Where $\frac{\partial \rho}{\partial t}$ is the change in density over time, ε is the new peak absolute principal strain, k is a rate constant, and $F(\varepsilon, t)$ is the cellular accommodation function, given by equation 2-9.

$$F(\varepsilon, t) = \varepsilon_o + (\varepsilon - \varepsilon_o)\left(1 - e^{-t/\tau}\right) \qquad 2\text{-}9$$

Where t is the time between the new and original strains, ε_o is the original peak absolute principal strain and τ is a constant for the time taken for osteocytes to accommodate (Turner 1999). The second equation for disuse conditions is shown in equation 2-10.

$$\frac{\partial \rho}{\partial t} = -k\varepsilon_o e^{-t/\tau} \qquad 2\text{-}10$$

Where $\frac{\partial \rho}{\partial t}$ is the change in density over time, *k* is a rate constant, *t* is the time between the new and original strains, ε_o is the original peak absolute principal strain and τ is a constant for the time taken for osteocytes to accommodate (Turner 1999). The use of cellular accommodation in remodelling algorithms have been proven accurate when compared to clinical and experimental data (Vahdati and Rouhi 2009).

The rate constant used by Turner (1999) in the case of mechanical loading has since been further expanded by Schriefer, Warden et al. (2005) to become a function of the specific surface area of the bone, as shown in equation 2-11.

$$\frac{\partial \rho}{\partial t} = k(\rho)(\varepsilon - F(\varepsilon, t)) \qquad 2\text{-}11$$

Where ρ is the bone density, which is related to the specific surface area of the bone using the density-area function from Martin (1984). Recently more accurate algorithms relating density and surface area have emerged, which suggest that the correlation between bone surface area and density is subject-specific (Lerebours, Thomas et al. 2015). However, these algorithms have been shown to require micro-CTs, which are not always available.

2.5.3 Atypical Bone Remodelling

Based on the principle of cellular accommodation, Turner (1999) describes how the relationship between the change in density and the stimulus can be dependent on the sequence of preceding mechanical loading. This can cause the stimulus-remodelling relationship to deviate from the norm and form relationships which would otherwise be called atypical. However, this is not a sign of abnormality. Turner (1999) gives the example of his equation for bone remodelling, which assumes a linear stimulus-remodelling relationship. The actual relationship can be anything but linear, and therefore Turner added a power law constant to his equation, b, which can have any value, as shown by equation 2-12.

$$\frac{\partial \rho}{\partial t} = k(\varepsilon - F(\varepsilon, t))^b \qquad 2\text{-}12$$

Turner uses two examples, one where the change in density is more highly influenced by higher stimuli and b = 3, and another where the change in density is more highly influenced by lower stimuli and b = 1/3, as demonstrated in Figure 2-15.

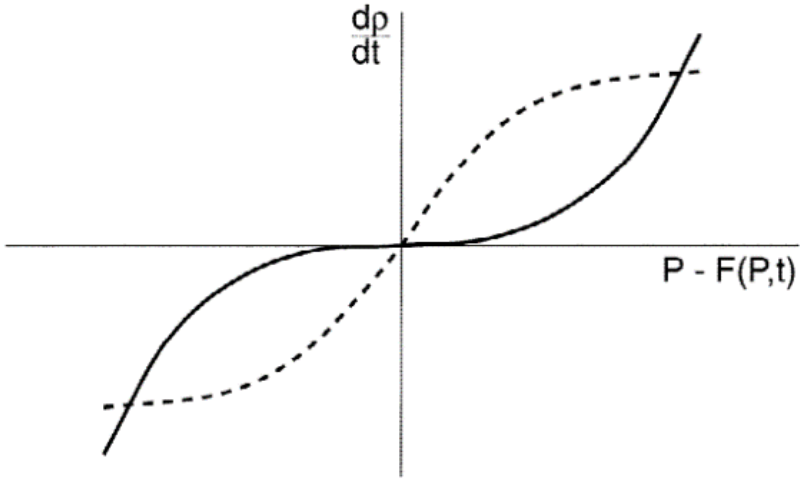

Figure 2-15: Two different stimulus-remodelling relationships proposed by Turner (1999) due to cellular accommodation, where P-F(P,t) is the connotation used by Turner to describe the change in density in relation to the stimulus $(\varepsilon_i - F(\varepsilon, t))$.

2.5.4 Continual Remodelling

The existence of remodelling thresholds and the lazy-zone in response to mechanical stimuli has been questioned, with clinical evidence suggesting that that bone is continually remodelling and the lazy zone does not exist (Christen, Ito et al. 2014). Nonlinear relationships between the bone remodelling response and the mechanical stimulus without the presence of a lazy-zone have been proposed (Carter 1982, van der Meulen and Hernandez 2013); where the bone is continually remodelling around a single reference stimulus, as shown in Figure 2-16. Here, one could argue that the lazy-zone is simply representative of a range of stimuli, where the change in density is minutely small and therefore considered to be nil, as shown by Figure 2-17.

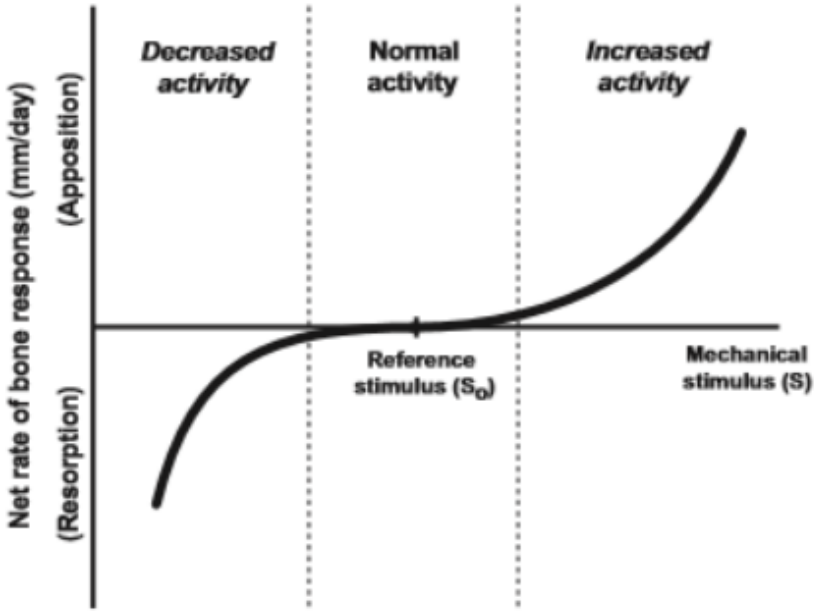

Figure 2-16: Nonlinear relationship between the bone remodelling response and the mechanical stimulus from van der Meulen and Hernandez (2013)

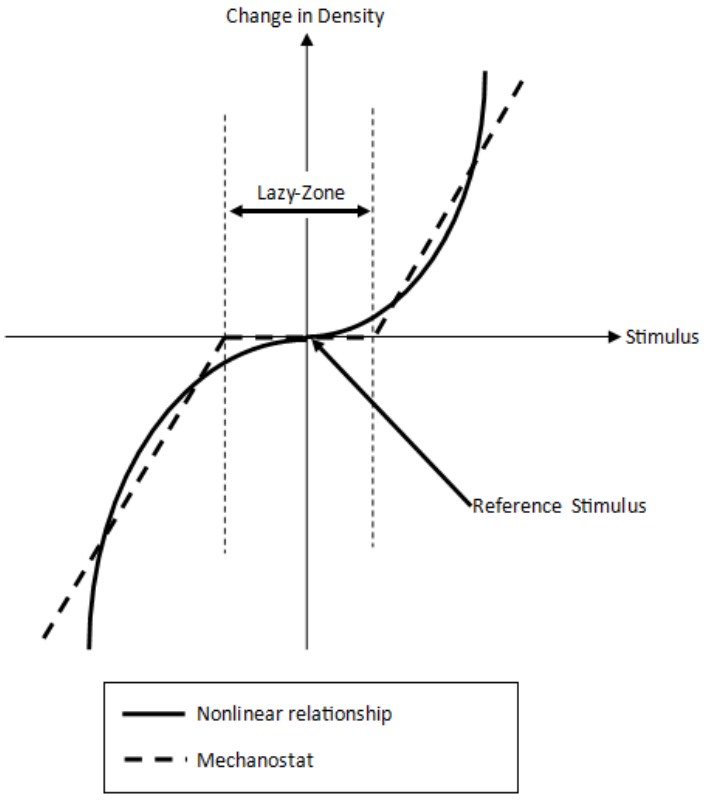

Figure 2-17: Comparison between the continual remodelling theory and the mechanostat stimulus-remodelling relationships to demonstrate that the lazy-zone is simply minutely small remodelling and therefore considered nil.

Adapting the continual remodelling approach to a strain-based stimulus (van der Meulen and Hernandez 2013), a remodelling equation for the nonlinear stimulus-remodelling relationship can be expressed, as shown in equation 2-13.

$$\frac{\partial \rho}{\partial t} = k(\varepsilon - \varepsilon_r)^b \qquad 2\text{-}13$$

Where $\frac{\partial \rho}{\partial t}$ is the change in density over time, ε is the new peak absolute principal strain, ε_r is the reference strain/stimulus, *k* is the rate constant and *b* is a power law constant. The reference strain in equation 2-13 is location specific. With different areas of the bone experiencing different strains, the reference strain is different across the entire skeleton. This allows for areas of the skeletal system which do not typically experience load (e.g. the skull) to not be predicted to be in disuse.

The remodelling algorithms which use thresholds in the stimulus such as the Frost (1987) algorithm (equation 2-5) base their thresholds on features such as microdamage production initiating remodelling. Microdamage is only produced after a certain strain is reached (Wang 2013), which gives the thresholds their value. But there are numerous bone remodelling initiation pathways (Robling and Turner 2009, Eriksen 2010), for example, the natural apoptosis of osteocytes over time, which occurs to approximately 2% of osteocytes per year in normal homeostasis (Parfitt 2004). This gives the opportunity for bone remodelling to occur without the need for the stimulus to overcome an initial threshold, allowing for any strain value to be used as a reference value.

The use of a reference strain can be aligned with the optimal remodelling theory, which states that the bone follows an optimal self-design process, where the bone microarchitecture and density distribution are arranged to provide the most optimal strain distribution for the loads being experienced (Harrigan and Hamilton 1994, Colloca 2009, Jang, Kim et al. 2009, Andrade-Campos, Ramos et al. 2012). Simulations of both cortical and trabecular bone using structural engineering topology optimisation equations have been demonstrated to provide strong resemblance to observed layouts in the bone. If the bone is considered to be optimally adjusted before bone remodelling initiation, the reference strain in equation 2-13 could be considered to be the optimal strain.

2.5.5 Circulation Strain

A physiological reason for the bone wanting to maintain a single optimal strain comes from the circulation strain, which describes the strain required for the bone to remain alive. Much like every other cell in the body, osteocytes need to import oxygen and nutrients and export waste to survive (Plotkin, Mathov et al. 2005). In most cases, this is achieved through diffusion exchange with blood vessels in the periosteum and Haversian canal. In small, well vascularized bones such as the skull, all the osteocytes are close enough to blood vessels to exchange oxygen, nutrients and waste without any assistance. However, in larger load-bearing bones, being well vascularized would mean that there is less bone (as more area is taken up by the vascularization) and they would not be strong enough to sustain the applied loads. Therefore, these larger bones are less vascularized and as a result, some osteocytes are too far away from the blood vessels to receive the nutrients via diffusion alone. For these larger bones, the exchange of oxygen, nutrients and waste to and from the osteocytes is assisted by the movement of the interstitial fluid (Knothe Tate and Knothe 2000, Plotkin, Mathov et al. 2005) which is achieved through bending/deforming the bone through the application of external loads (Knothe Tate and Knothe 2000, Burr, Robling et al. 2002). In disuse, the bone does not undergo this deformation, starving the osteocytes of the essential oxygen causing them to become hypoxic (Dodd, Raleigh et al. 1999). This in turn causes them to undergo apoptosis within 24 hours (Dodd, Raleigh et al. 1999), which signals for the initiation of the remodelling cellular process (Robling and Turner 2009, Jilka, Noble et al. 2013, Burr 2014, Plotkin 2014). The same lack of deformation which starved the osteocytes of oxygen, also does not provide a shear flow of interstitial fluid for the mechanotransduction during formation and therefore, the bone experiences a decrease in density (Dodd, Raleigh et al. 1999, Nobel, Peet et al. 2003, Plotkin, Mathov et al. 2005, Plotkin 2014).

The further the osteocyte is away from the centre of the Harversian system, the more the bone has to deform to provide an adequate amount of interstitial fluid flow to prevent apoptosis. The amount of deformation needed to assist interstitial fluid flow so that every osteocyte can survive is the circulation strain. Nobel, Peet et al. (2003) produced an apoptotic-strain relationship by applying different levels of strain to live rats and measuring the number of apoptotic osteocytes. This relationship found a near negative exponential relationship between the surface strain and the number of apoptotic osteocytes, which reached an asymptote at approximately 2000 με. This

apoptotic-strain relationship, can be applied to the Harversian layout, to show the amount of strain required to enable fluid flow throughout the entire canal, as shown in Figure 2-18.

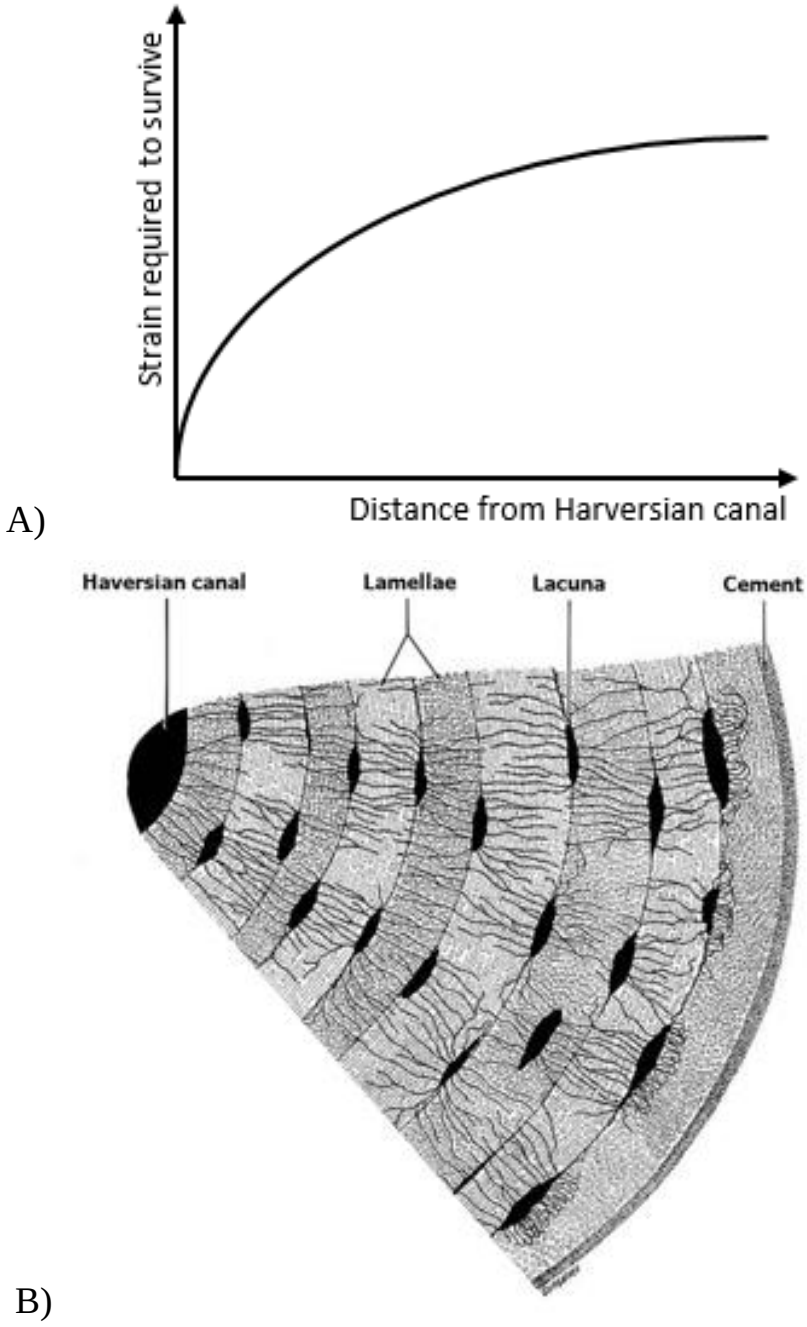

Figure 2-18: Diagram demonstrating the requirement of deformation for osteocyte survival with A) strain required for an osteocyte to survive based on the Nobel, Peet et al. (2003) apoptotic-strain curve plotted against B) a Harversian system (BiologyOnline 2001)

Whilst there are some osteon size differences between animals and humans (Jowsey 1966); the 2000 με value is congruent with the approximate centre of the lazy-zone in remodelling algorithms (Frost 1987, Frost 2003). This phenomenon is also more associated with strain than stress (Dodd, Raleigh et al. 1999, McGarry, Klein-Nulend et al. 2005, Plotkin, Mathov et al. 2005). This is because in a high stress but minimal strain scenario, which could be expected under high loads in a highly dense bone would result in minimal movement of the interstitial fluid and therefore is more likely to result in minimal bone formation.

2.5.6 Strain Rate

In vitro studies into bone remodelling have shown that the strain rate of the mechanical loading has an impact on bone formation (O'Connor, Laynon et al. 1982, Turner, Owan et al. 1995). With the peak strain rate being proportional to the loading frequency and strain magnitude in a sinusoidal loading wave, Turner (1998) proposed that the mechanical stimulus can be expressed as equation 2-14.

$$S = k \sum \varepsilon f \qquad 2\text{-}14$$

Where *S* is mechanical stimulus, *k* is remodelling constant, ε is the peak-to-peak strain magnitude, and *f* is the loading frequency in cycles per second. This equation can be applied to any periodic loading, using the Fourier method, which expresses periodic loading as a series of different sine waves at different frequencies and amplitudes. This equation has been used in bone remodelling investigations on its own without a preceding or reference stimulus (Troy, Mancuso et al. 2018), such as equation 2-15, or alternatively it can be substituted into another remodelling equation where it replaces the strain magnitude, such as equation 2-16.

$$\frac{\partial \rho}{\partial t} = k \sum \varepsilon f \qquad 2\text{-}15$$

$$\frac{\partial \rho}{\partial t} = k \sum (\varepsilon f - \varepsilon_o f_o) \qquad 2\text{-}16$$

This equation has had a strong correlation with bone formation in applied loading conditions and *in vitro* studies and has implications in bone healing methods such as externally applied, low

magnitude, high frequency stimuli for bone repair (Goodship, Lawes et al. 2009). However, it is impractical for physiological loading conditions, as it is only applicable for loading environments (Warden and Turner 2004) which are not representative of those achieved in physiological loading (Lanyon and Rubin 1984, Burr, Milgrom et al. 1996).

2.5.7 Heterogeneous Bone Remodelling

One issue with most bone remodelling algorithms is that they assume homogenous bone remodelling. This inherently assumes that initiation, resorption and formation occur homogeneously across the bone. Bone remodelling does not occur homogeneously, rather it occurs heterogeneously under both tension and compression. As demonstrated by Figure 2-19 a single linear microdamage crack can cause numerous areas of bone remodelling, but outside of these areas, anti-apoptotic proteins are generated preventing further bone remodelling (Jilka, Noble et al. 2013).

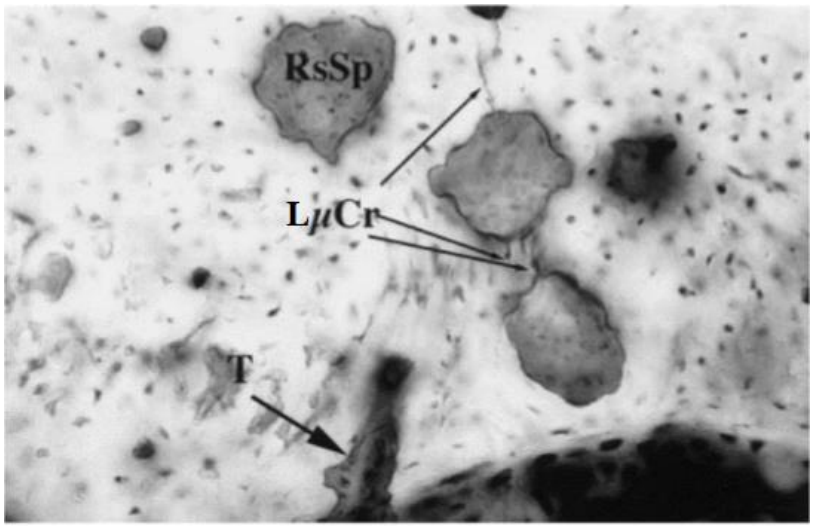

Figure 2-19: The heterogeneity of bone remodelling in a rat (Bentolila, Boyce et al. 1998) under compression showing resorption spaces (RsSp) in association with linear microdamage (LμCr) and osteoclastic tunnelling (T) from the periosteal surface (Bentolila, Boyce et al. 1998).

This can cause problems when using bone remodelling algorithms to determine the response to a mechanical stimulus in small areas. One method of increasing the determination ability of bone remodelling algorithms is to increase the area being examined: Where in comparing the effect of sampling volume on the remodelling results, weak correlations have been observed between the

change in density and the mechanical environment on the microscale but strong correlations have been observed on the macroscale (Kim, Takai et al. 2003, Webster, Wirth et al. 2012). It was postulated, that small sample areas/volumes may miss bone remodelling areas causing a high variance in the change in density when compared to the stimulus, as shown in Figure 2-20. Alternatively, larger sample areas/volumes encapsulate an even distribution of remodelling areas and non-remodelling areas, providing less variance.

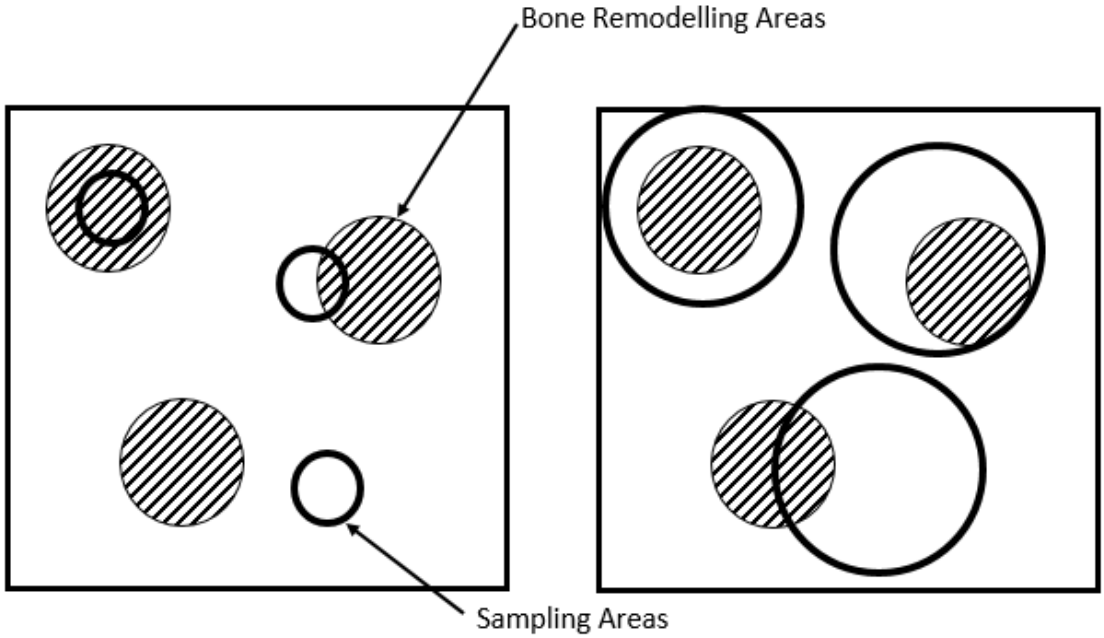

Figure 2-20: Simple comparison of large and small remodelling sampling areas in the same location, where the smaller sample area will experience a higher variance in the change in density than the larger sampler area.

The area required to provide a stable relationship between the mechanical stimulus and the bone remodelling response depends on numerous factors, including anatomical location, bone biomechanics and species; where, in the human proximal femur sample areas/volumes with diameters of approximately 5 to 10 mm are often used to examine the clinical data for bone remodelling (Turner, Anne et al. 1997, Bitsakos, Kerner et al. 2005).

2.5.8 Mechanistic Models

Mechanistic approaches model cellular biology, which can be used in an attempt to account for the heterogeneity of bone remodelling response to mechanical stimuli. Many factors contribute to the mechanobiology in the transfer of mechanical load to biological signals (Robling and Turner

2009, van der Meulen and Hernandez 2013) and the cellular mechanisms involved in the repose to mechanical load are highly complicated (Ruimerman, van Rietbergen et al. 2005). Nonetheless, different theoretical models describing the cellular response to mechanical load have been developed (Huiskes, Ruimerman et al. 2000) and are constantly being reviewed and updated (Ruimerman, van Rietbergen et al. 2005, Vahdati and Rouhi 2009, Gong, Wang et al. 2020).

A commonly used theory, with different adaptions, was developed by Huiskes, Ruimerman et al. (2000) who stated that the bone tissues contain a finite number of osteocytes per area. Huiskes proposed that these osteocytes are sensitive to the maximum mechanical signal in a certain area, applied in recent loading, a theory which is supported by *in vivo* experimentation (Rubin and Lanyon 1984, Turner 1998, Burr, Robling et al. 2002). It was proposed by Huiskes, Ruimerman et al. (2000) that once bone remodelling was initiated, osteocytes signal for osteoclast through the sum of the osteocyte signals and a constant reference signal. Using this theory, Huiskes, Ruimerman et al. (2000) proposed that the local change in bone density can be determined by equation 2-17.

$$\frac{\partial \rho}{\partial t} = k\{P(x,t) - S_T\} - r_{oc} \qquad for \quad P(x,t) > S_T \tag{2-17}$$

Where $\frac{\partial \rho}{\partial t}$ is the change in density over time, *k* is a proportionality constant, S_T is a threshold level for bone remodelling to occur, similar to the MES used in equation 2-5, r_{oc} is the relative amount of bone mineral resorbed by osteoclasts per day in the sample volume, and $P(x,t)$ is the osteoblast recruitment stimulus at the surface location *x*, as a function of time, *t*, given by equation 2-18,

$$P(x,t) = \sum_{1}^{N} f_i(x)\mu_i R_{SED,i}(t) \tag{2-18}$$

Where, μ_i is the mechanosensitivity of the osteocyte, *i*, $R_{SED,i}(t)$ is the SED rate in the location of the osteocyte, *i*, and $f_i(x)$ is the function for the influence of the osteocyte on recruiting osteoblasts. Whilst Huiskes, Ruimerman et al. (2000) assumed the mechanical load to be the strain energy density, other stimuli have been used such as strain magnitude (McNamara and Prendergast 2007). It was assumed that the signal from the osteocyte decreases exponentially with distance, and therefore $f_i(x)$ is given by equation 2-19.

$$f_i(x) = e^{-d_i(x)/D} \qquad 2\text{-}19$$

Where, $d_i(x)$ is the distance between the osteocyte, *i*, and the location, *x*, and *D* represents the distance from an osteocyte at which the effect of the recruitment has reduced to a certain level (Mullender and Huiskes 1995).

Huiskes, Ruimerman et al. (2000) accommodated for heterogeneity of bone remodelling by including a probability of bone remodelling activation; where the probability of activation was considered to be spatially random. A probability of bone remodelling initiation of 10% was assigned for this spatially random initiation, as shown by equation 2-20.

$$\text{Hypothesis I: } p(x,t) = 10\% \qquad 2\text{-}20$$

Where *p(x,t)* is the percentage change of bone remodelling initiation per iteration. In the disuse scenario Huiskes, Ruimerman et al. (2000) set a strain dependant equation, as shown by equation 2-21.

$$\text{Hypothesis II: } p(x,t) = c[a - P(x,t)], \quad if \quad P < a \qquad 2\text{-}21$$

Where, *c* and *a* are constants.

Due to the increased computer power required by mechanistic models, they are usually only applied over small areas, where they are typically used to determine trabecular bone architecture and density distribution, as shown by Figure 2-21. Mechanistic models are often used as self-design simulations, where the model is run over multiple iterations until an equilibrium (called homeostasis in Figure 2-21) is reached. Again, much like the self-design simulations used in larger models, 100's to 1000's of iterations are required to reach an equilibrium. As such, the $\frac{\partial \rho}{\partial t}$ function of the mechanistic models is arbitrary and does not represent a true bone remodelling cycle.

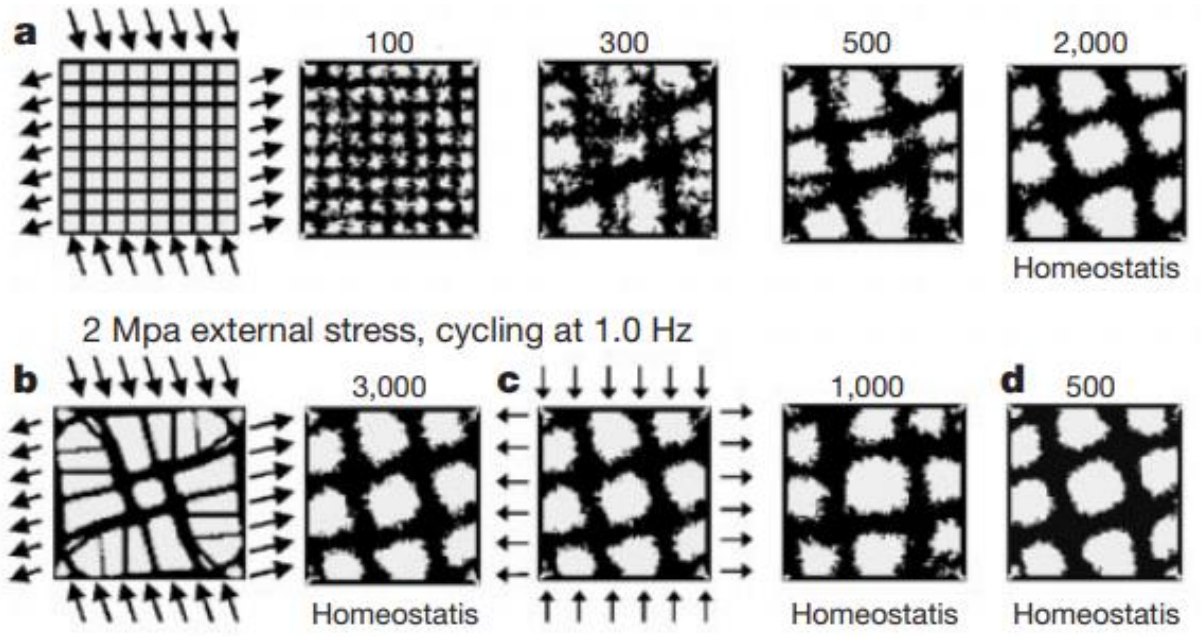

Figure 2-21: A mechanistic model self-design simulation, examining the simulated architectural and density distribution in trabecular bone after a different number of iterations using a blank finite element simulation mesh (shown in a), with different loads applied in a-d (Huiskes, Ruimerman et al. 2000)

2.5.9 Critical Evaluation of Bone Remodelling Algorithms

Six different bone remodelling algorithms where strain, or strain energy density, is used as the stimulus, have been reviewed in this section. These being the Frost (1987) mechanostat, Cowin and Hegedus (1976)'s remodelling algorithm, Turner (1999)'s theory on cellular accommodation, the continual remodelling theory (van der Meulen and Hernandez 2013, Christen, Ito et al. 2014), the strain rate theory (Turner 1998), and the Huiskes, Ruimerman et al. (2000)'s mechanistic model. With the exception of the strain rate theory, all of the remodelling algorithms are applicable for physiological loading. The strain rate theory, much like all the other bone remodelling algorithms reviewed in this study, was developed and validated through experimental/clinical observations (Turner, Owan et al. 1995). However as discussed in section 2.5.6 Strain Rate, the processes which are required to take place for this remodelling algorithm to become accurate only occur in loading scenarios which are not achieved in physiological loading. It is nonetheless useful, as it gives a good insight into bone remodelling processes and provides pathways for non-invasive orthopaedic healing treatments, such as low magnitude, high frequency stimuli.

In the application of the strain rate bone remodelling algorithm, some researchers apply the equation without reference to either a threshold or an initial reference strain, such as that shown in equation 2-15. In a single loading application, such as the application of non-invasive, low magnitude, high frequency stimuli to the upper limb to encourage positive bone remodelling, equation 2-15 yielded a basic correlation to the results due to its own correlation with the bone remodelling mechanisms, such as that observed in Troy, Mancuso et al. (2018). However, equation 2-15, with no reference strain or threshold, predicts that the bone will continually remodel with no end point, which is false. As such, this highlights the requirement for a threshold or reference strain within bone remodelling algorithms.

With the exception of the Huiskes, Ruimerman et al. (2000) mechanistic model and Turner's (1999) theory on cellular accommodation, all the remodelling algorithms reviewed in this study correlate the initial input (mechanical loads) to the output (change in density) without accounting for different cellular processes that occur in bone remodelling. This inherently assumes that the numerous stages in the bone remodelling cycle follow the same stimulus. Even here, the Huiskes, Ruimerman et al. (2000) mechanistic model and Turner's (1999) theory on cellular accommodation use statistical probability and assumptions to incorporate some of the cellular processes. Therefore, all bone remodelling algorithms follow a single a large assumption, that all cellular processes in bone remodelling will follow the singular stimulus input, in this case the strain. Nonetheless, this assumption is valid and possible because it is the mechanical loading stimuli experienced by the bone which controls and influences the majority of the bone remodelling stages, including the final stage of bone remodelling, as shown in Figure 2-22; where the final density of the new bone is determined. This makes it possible to predict and quantify bone remodelling using a single stimulus, without the need for numerous measurements which in many cases would defeat the point of the prediction (e.g. prediction of the bone remodelling around a custom designed 3D-printed implant for validation and verification purposes).

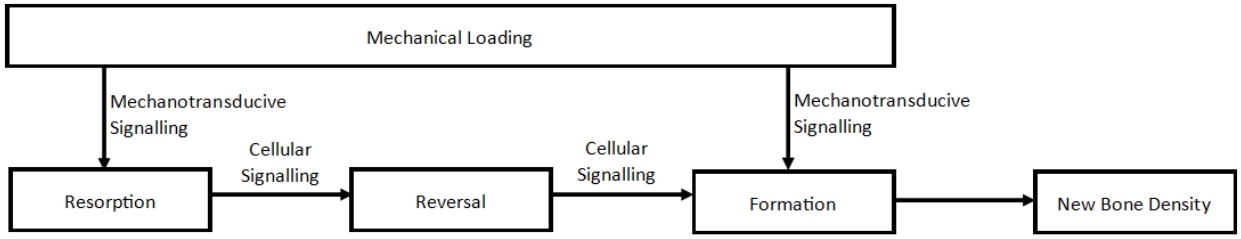

Figure 2-22: Basic overview of the bone remodelling process, showing the basic stages and where the mechanical loading influences the cellular processes

Very little has been done to review and compare different bone remodelling algorithms. As such there is no standardised remodelling algorithm to be used in research and/or industry. Often the bone remodelling algorithm used in a simulation appears to be at the preferred discretion of the one running the simulation. Whilst this allows for constant development and improvement of remodelling algorithms, it leaves 3D-printed implant manufacturers in uncertainty of what remodelling algorithm to use if they should want to use simulation as a validation and verification technique (Morrison, N Kashlan et al. 2015). The evaluation of the remodelling algorithm is therefore left to the researcher themselves, where virtually all published algorithms report good correlation to a combination of clinical and/or experimental data. As such no bone remodelling stands out as more accurate than the others.

Nonetheless, as research progresses, researchers do criticise other remodelling algorithms, where there are reports that some remodelling algorithms, such as Frost (1987)'s mechanostat does not conform well with certain experimental observations (Turner 1999). Even further criticism of bone remodelling algorithms which utilise the lazy-zone, which comes from their requirement to use thresholds to determine the lazy-zone. As discussed in section 2.5.1 Frost's Mechanostat, Frost (1987) used a single set of standardised thresholds, which he based off observations. The use of standardised thresholds is a typical practice when applying bone remodelling algorithms to a large area, for example the femur (Cowin and Hegedus 1976, Frehill, Crocombe et al. 2009). However, a simple examination of the strains experienced by the femur alone, as shown in Figure 2-23, shows that a range of different strains are experienced in different parts of the femur on a daily basis, where no two parts of the femur can be said to experience the same strain as the other. Therefore, appling Frost (1987)'s threshold values to the strains experienced by the femur suggests that different areas would constantly be in remodelling. This criticism of Frost's mechanostat was

identified by Turner (1999), who as discussed in section 2.5.2 Cellular Accommodation, identified that Frost's mechanostat predicts that areas of the skeletal system which do not experience loading on a typical basis (e.g. the skull) would experience constant resorption. Turner (1999) called this the disuse fallacy. As a result Turner (1999) incorporated thresholds that accommodate to the typical loading experienced by the local area in which the remodelling algorithm is being applied. This therefore allows for the remodelling algorithm to adjust/accommodate to induvial environments. However, it should be noted that Turner (1999)'s cellular accommodation equation is not all-applicable. The accommodation feature, shown in equation 2-10 relies on several assumptions and measurements (such as the time taken for osteocytes to accommodate in an individual) which are not always known and difficult to obtain without further measurements and therefore can be impractical.

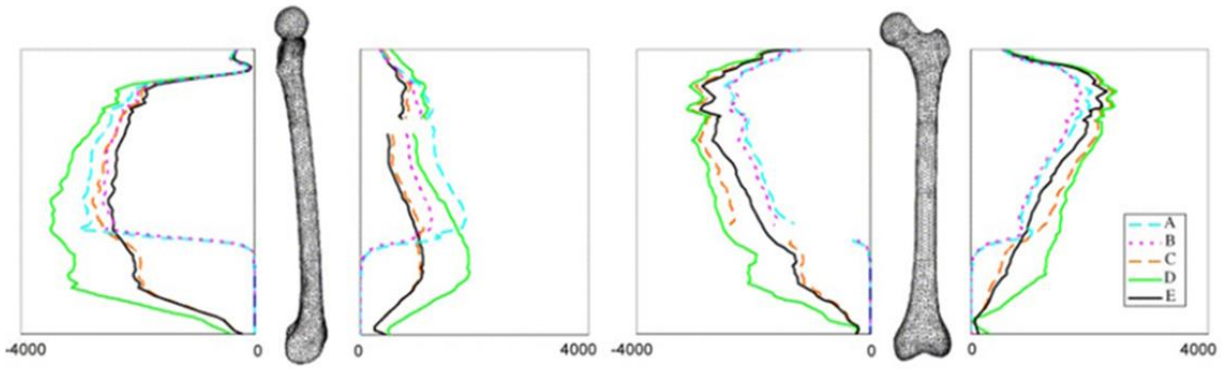

Figure 2-23: Femoral micro-strain results for walking using different loading models shown in section 2.8.2 Standard Femoral Model, from Speirs, Heller et al. (2007)

There is further criticism of any remodelling algorithm that uses the lazy-zone and therefore thresholds, where clinical evidence in human-based studies has suggested that the lazy-zone does not exist (Christen, Ito et al. 2014). As discussed in section 2.5.4 Continual Remodelling and shown in Figure 2-15, the presence of the lazy-zone could have been an interpretation of a range of stimuli where there is very little amount of bone remodelling response. This could also have been influenced by the technology of the day, where earlier X-ray machines, on which Frost (1987)'s mechanostat and other lazy-zone based remodelling algorithms were established may not have picked up on smaller changes of density as easily as todays qCT scans. Bone remodelling theories such as the continual remodelling theory, as discussed in 2.5.4 Continual Remodelling, use a reference strain which is location specific and also use non-linear stimulus-remodelling

relationships in replace of a lazy-zone with thresholds, like that shown in Figure 2-16. The use of a reference strain assumes that the bone remodelling will cease once the strain experienced by the bone reaches its original value (the reference strain). This theory is similar to Turner (1999)'s cellular accommodation, where both remodelling algorithms are location specific, and is also supported by the optimal remodelling theory (Andrade-Campos, Ramos et al. 2012) and physiological features such as the circulation strain, as discussed in section 2.5.5 Circulation Strain.

In reference to the circulation strain, the continual remodelling theory and Turner (1999)'s cellular accommodation, and all other bone remodelling algorithms, neglect to take into account extreme changes in loads and the location of the area/volume being examined in the bone/skeletal system. As discussed in section 2.5.5 Circulation Strain, areas of the femur close to the periosteum or any vascular canal do not require bone deformation to assist in the circulation of nutrients and waste. Therefore, in extreme sudden disuse cases (e.g. sudden coma) the continual remodelling theory predicts that the change in density would continue until the original strain is achieved and cellular accommodation predicts that the change in density would cease throughout the entire bone/skeletal system after a period of time. Both of these are incorrect. Due to the osteocytes requirement for nutrients and removal of waste (Plotkin, Mathov et al. 2005), osteocytes which are too far from a vascular canal to circulate the nutrients and waste via diffusion alone, cannot simply accommodate to the new loads in the case of sudden extreme disuse, as cellular accommodation would predict. Additionally, with no loading, the bone would not simply resorb away into nothing, as continually remodelling would predict. Instead, the resorption would be based on the location of the bone, where osteocytes which are close enough to vascular canals (mainly those close to the periosteum) would survive, whilst those which are too far from a vascular canal would die and result in negative remodelling.

In conclusion of the review of bone remodelling algorithms, there is no all-encompassing, perfect, all-applicable bone remodelling algorithm. As research continues, and technologies improve, more can be incorporated into bone remodelling algorithms which may allow for better prediction of individual remodelling stages. However, with this often comes the requirement for more measurements, which often introduce impracticality. With this it should be noted that the simpler remodelling algorithms, which account for biological process, such as the continual remodelling

theory do not appear to introduce any additional error when compared to bone remodelling algorithms which incorporate numerous factors. As such, it appears that the best bone remodelling algorithm to be used in a particular study, is the one which best suits the setup, requirements and applicable data. With this it should also be noted, that in their application, all bone remodelling algorithms and application methods bring with them inherited assumptions and limitations.

2.6 Mechanosensory Saturation

In a single loading session, the effect of the mechotransductive stimulus on bone formation rate will diminish logarithmically with each load due to a phenomenon known as mechanosensory saturation (Rubin and Lanyon 1984, Umemura, Ishiko et al. 1997, Turner 1998, Burr, Robling et al. 2002). This phenomenon is independent of the deformation and circulatory strain required to keep large load bearing bones alive (see 2.5.5 Circulation Strain). After losing its response to mechanical stimulus the bone will eventually regain full sensitivity again through mechanosensory recovery. The recovery period takes approximately 8 hours for a full recovery; however, some mechanosensory recovery occurs within 0.5 – 7 seconds, and after 14 seconds the bone was demonstrated to increase formation rate by 50%. It is believed that the recovery period length is not proportional to the length of the prior loading (Burr, Robling et al. 2002).

The effect of mechanosensory saturation has been demonstrated to follow a logarithmic pattern, described by equation 2-22.

$$\frac{\partial \rho}{\partial t} \propto \sum_{i=1}^{n} log(1 + N_i) S_i \qquad 2\text{-}22$$

Where; $\frac{\partial \rho}{\partial t}$ is the change in density over time, *n* is the number of different daily loading conditions, *N* is the number of loading cycles for each loading condition and S_i is the applied bone formation stimulus (Turner 1998). Experimental evidence of mechanosensory saturation has been observed by Rubin and Lanyon (1984) and Umemura, Ishiko et al. (1997) on turkey unlae and rat tibiae, as shown in Figure 2-24. From this evidence, it is suggested that any loading beyond 50 cycles in a single bout is largely ineffective in stimulating any further bone remodelling response (Burr, Robling et al. 2002). A secondary side effect of mechanosensory saturation is that the bone will respond to the highest magnitude stimulus, even with far fewer loading cycles than a lower load

with far more loading cycles, as demonstrated by Figure 2-24. As a result, short intense bouts of exercise have a larger impact on the bone than long low intensity activity.

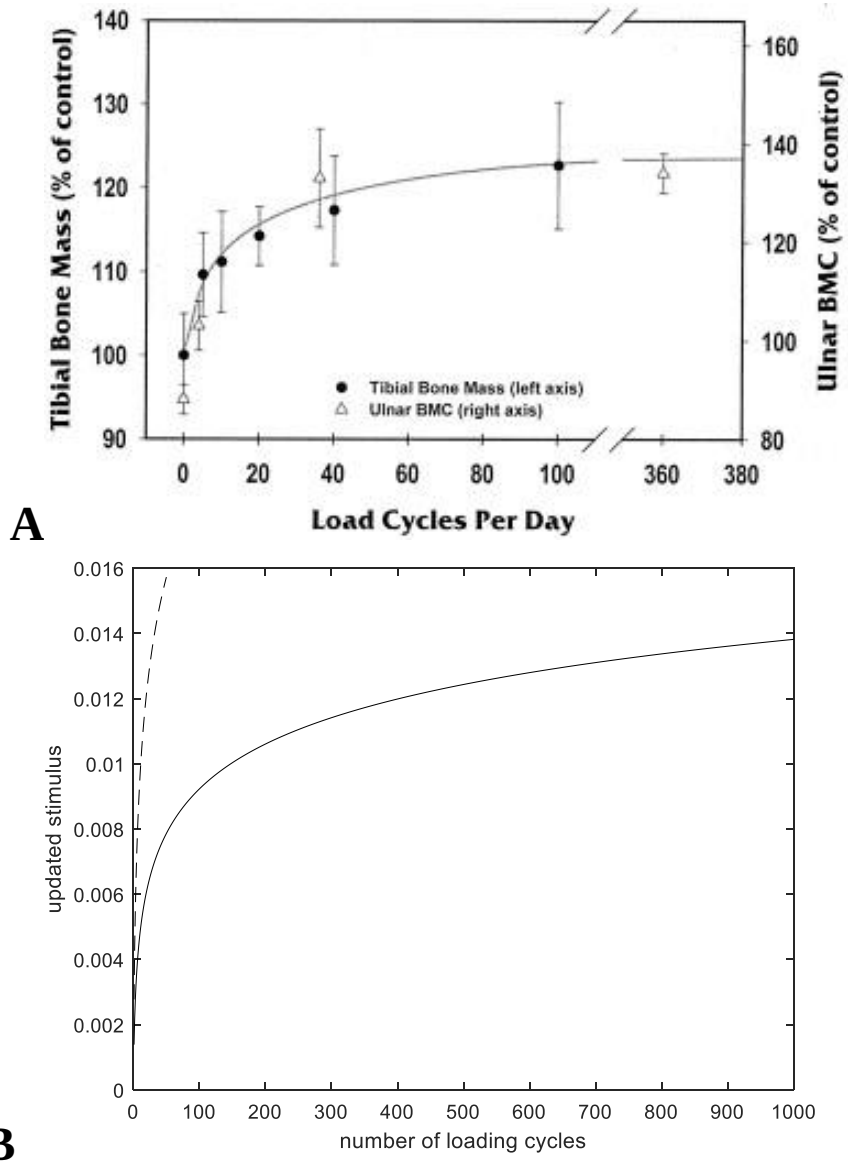

Figure 2-24: A) Results from Rubin and Lanyon (1984) and Umemura, Ishiko et al. (1997), as presented in Burr, Robling et al. (2002) showing the effect of diminishing returns on the change in bone density after a different number of loading cycles per day on turkey unlae (Δ) and rat tibiae (•). B) Effect of mechanosensory saturation, comparing the effect of 50 cycles of 4000 με (dashed line) against 1000 cycles of 2000 με (solid line) on the mechanical stimulus.

2.7 Orthopaedic Pathogenesis with Ageing

Orthopaedic conditions such as osteoporosis are directly associated with age (Seeman 2003) where the bone substantially decreases in density which subsequently increases the risk of fracture in

multiple locations of the body (van Staa, Dennison et al. 2001). As a result, with an ageing population, in 2008 it was estimated that orthopaedic degenerative and inflammatory problems account for half of all chronic conditions in developed countries (Navarro, Michiardi et al. 2008). Typically, orthopaedic implants are used to correct or solve these problems, however the demand is outgrowing the supply. In 2018 the national joint registry had recorded over 2.1 million total hip, shoulder, ankle and knee arthroplasties which had been implanted in the UK alone over a 14 year period (NJR 2018). Furthermore, aside from the risk of the surgery, debris from the implants can introduce pathologies such as pseudotumors, granulomas, osteolysis, neuropathy, neoplasia and many more (Langkamer, Case et al. 1992).

Another method used to treat osteoporosis is with drugs such as bisphosphonates which inhibit the resorption stage of bone remodelling (Drake, Clarke et al. 2008). However, it is becoming increasingly clear that the use of drugs is only delaying the degenerative problem and in many cases can create other problems. Resorption is required to remove linear microdamage from the bone and formation cannot occur without resorption occurring first. As a result, bisphosphonates result in a skeletal system which experiences a build-up of linear microdamage and cannot increase in density, even with an increased stimulus (Mashiba and Burr 2001, Drake, Clarke et al. 2008, Papapoulos 2008, Seraphim, Al-Hadithy et al. 2012).

Exercise is becoming an increasingly popular “prescribed” method/treatment to act as prevention for orthopaedic degenerative diseases and therefore prevent the need for drugs and implants (Milgrom, Finestone et al. 2000, Milgrom, Miligram et al. 2001, Du, Silberschmidt et al. 2018). The majority of what we know about bone remodelling is based on the observations of young animals and young humans. With this, age is typically associated with negative connotations in bone mechanoresponsiveness. This is most likely due to the prevalence of degenerative conditions such as osteoporosis, however it is unclear if older bones are less mechanoresponsive than younger bones as there is evidence both for and against this view (Kotiya and Silva 2013). It is considered that any potential change in bones mechanoresponsive with age is a complicated combination of biochemical processes, causing a mixture of different results. Nonetheless, evidence has shown that aged bones are adequately mechanoresponsive, providing that the bones receive a suitable stimulus (Kotiya and Silva 2013).

2.7.1 Allison et al. Clinical Exercise Trial

With exercise "prescriptions" becoming an increasingly popular method to combat degrative diseases, it is important to know which exercises have the best effect. High impact exercises are known to cause higher bone densities than exercises with low impact, where runners have a significantly higher bone density than swimmers (Scofield and Hecht 2012). However, there is limited research into the use of impact exercises as an osteoporosis prevention tool. In response to there being little research into the influence of high impact exercises on the change in bone density, particularly in older men, Allison, Folland et al. (2013) conducted a clinical exercise trial into the use of hopping for men with a mean ± SD age of 69 ± 4.0 years. In this study thirty-four healthy human men hopped 50 times a day, every day for one year on a randomly assigned leg, with an example shown in Figure 2-25. All subjects in this study were of European origin, with no diseases known to influence bone, neuromuscular function or the ability to perform exercises. Before the study, anthropometric, lifestyle, physical activity and dietary characteristics were collected and assessed, with the mean results shown in Table 2-5.

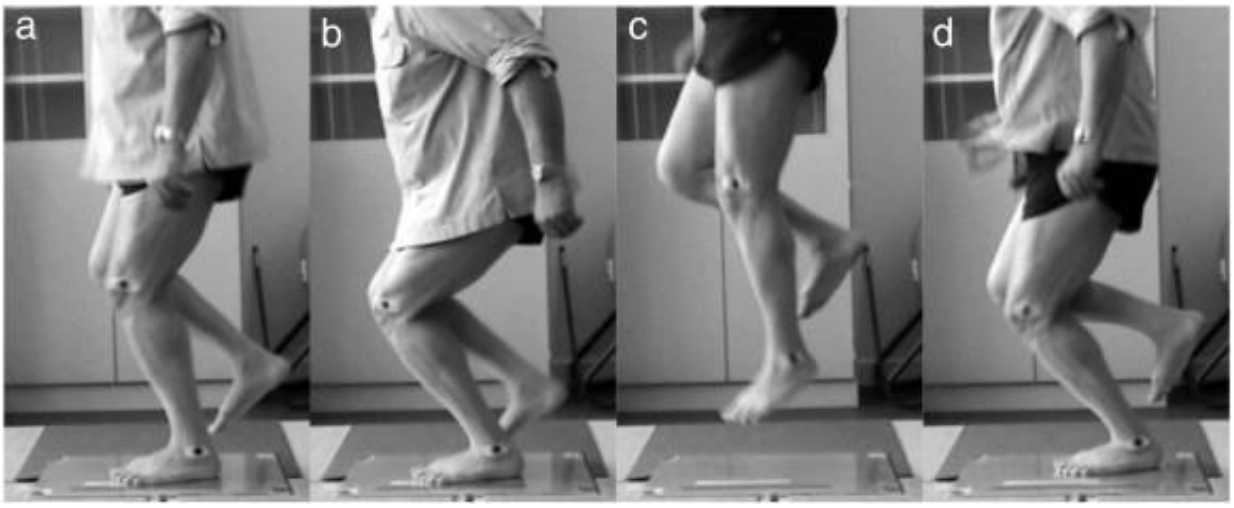

Figure 2-25: Demonstrative pictures of the hopping exercise being undertaken by one of the subjects from the hopping clinical trial, showing: (a) the start position, (b) countermovement initial to take off, (c) flight of hop, (d) landing on the exercise leg. Taken from Allison, Folland et al. (2013).

Table 2-5: Mean anthropometric, lifestyle, physical activity and dietary characteristics of participants from the Allison, Folland et al. (2013) clinical trial

Parameter	**Mean**	**±**	**SD**
Age (years)	69.9	±	4.0
Height (m)	1.753	±	0.063
Weight (kg)	80.4	±	8.4
BMI (kg/m^2)	26.2	±	2.3
Total body fat (%)	26.9	±	4.9
Proportion of men with previous fractures (%)	48.6		
Current physical activity (hrs/wk)	1.8	±	2.0
Baecke physical activity questionnaire score:			
- Work index score	2.7	±	0.5
- Sport index score	2.8	±	1.0
- Leisure index score	2.6	±	0.5
- Total index score	8.2	±	1.5
Energy Intake (MJ/day)	9.8	±	2.1
Total Fat (% energy)	34.2	±	7.9
CHO (% energy)	46.6	±	6.7
Protein (% energy)	14.5	±	2.6
Alcohol (% energy)	4.6	±	4.7
Calcium intake (mg/day)	1068.2	±	259.6
Vitamin D intake (µg/day)	3.3	±	1.8

The density of the proximal femur before and after the one-year trial was measured using quantitative CT scans, with a resolution of 0.75 × 0.75 mm in the transverse plane and 2 mm axially, which is more than adequate to determine the change in density for bone remodelling studies (Gong, Wang et al. 2020). Before the study and in between the hopping exercises the subjects from the Allison, Folland et al. (2013) clinical trial were physically active undertaking their typical daily activities, but did not include exercise (strength, power, or weight-bearing endurance). The clinical study demonstrated an increase in bone density across the proximal femur as a result of hopping, with the cortical bone experiencing an average increase in bone density of 2.7% ($p < 0.001$) (Allison, Folland et al. 2013, Allison, Poole et al. 2015), with the distribution shown in Figure 2-26 and Figure 2-27. The percentage change in density achieved in this exercise trial is similar to that achieved in other exercise studies (1.8% and 2.1%) (Kukuljan, Nowson et al. 2009, Kukuljan, Nowson et al. 2011). Thus the Allison, Folland et al. (2013) clinical trial has made an important contribution in demonstrating that hopping is just as an effective tool in preventing osteoporosis in the hip as other exercises.

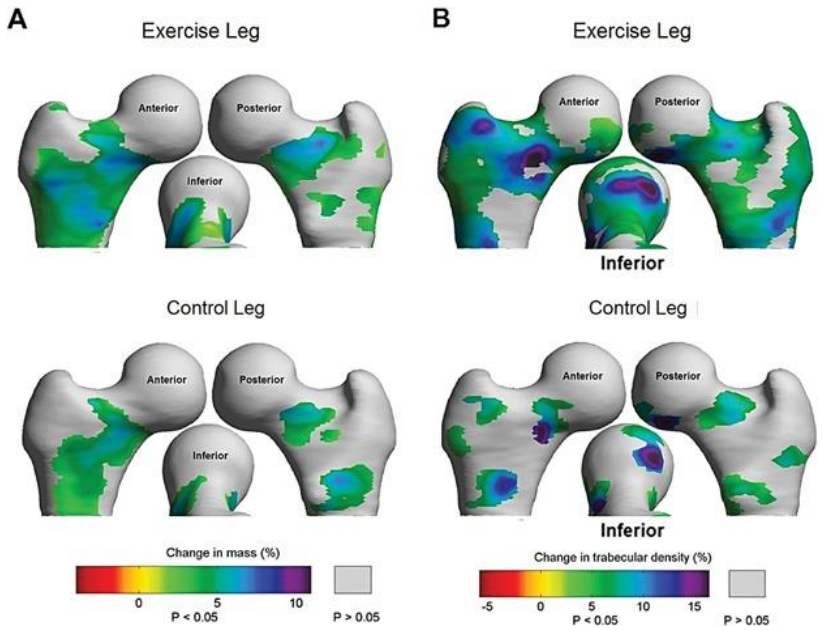

Figure 2-26: Bone density increase as a result of hopping in the exercise (hopping) and control legs, in (A) the cortical surface mass density, and (B) the endocortical trabecular density (Allison, Poole et al. 2015).

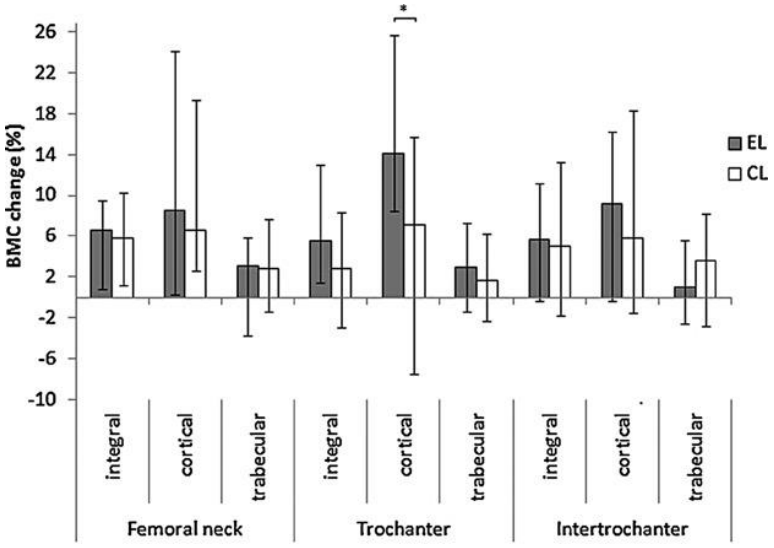

Figure 2-27: Increase in density in different areas of the proximal femur, observed in the clinical exercise trial (Allison, Poole et al. 2015), where; EL is the exercise leg and CL is the control leg.

The age and sex demographic of the Allison, Folland et al. (2013) subjects are at a point where changes in the bone physiology begin more resorption than formation (Seeman 2003) however the decrease in density has not yet been enough to substantially increase the fracture risk (van Staa, Dennison et al. 2001), with a location specific incidence of fracture with age, shown in Figure 2-28. This makes the age and sex demographic an ideal time to start preventative exercises.

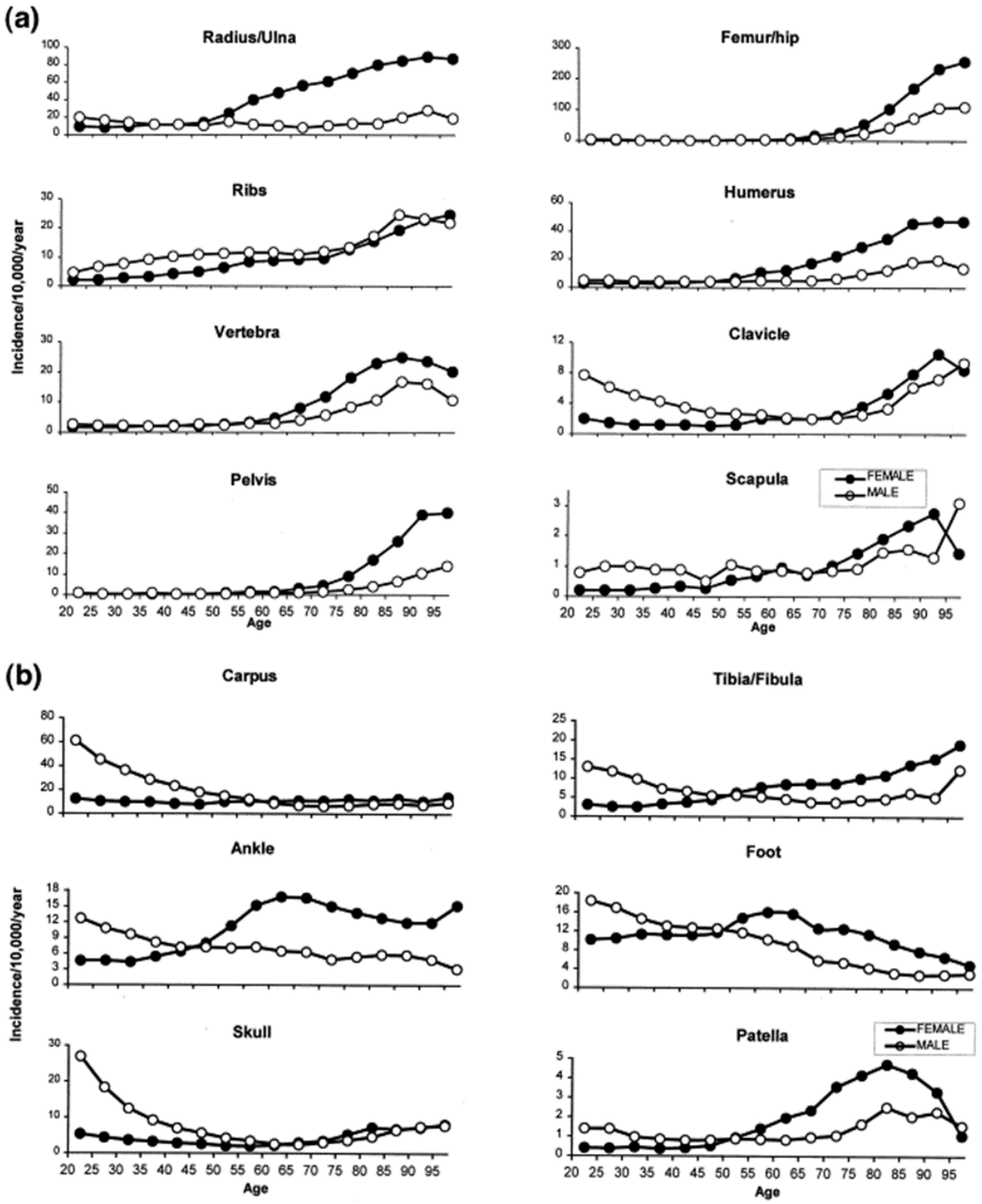

Figure 2-28: Age and gender specific incidence of fractures among a population of 5 million as registered in the General Research Database 1988-1998, showing: (a) Fractures in locations where risk increases with age. (b) Fractures in locations where risk does not increase with age (van Staa, Dennison et al. 2001).

2.7.2 Crosstalk

The concept of crosstalk is a well excepted and observed phenomenon in biological signal transduction pathways, which has numerous definitions due to its complex nature. One such definition is that crosstalk is where the components of one or more signal transduction pathways affects one or more other similar or related systems, causing a biological response of some kind (Vert and Chory 2011). A simple example of biomechanical crosstalk is where increased muscle tone, results in increased loading on the bone and therefore a bone remodelling response. A more complex form of crosstalk was observed in the Allison, Poole et al. (2015) data, where as shown in Figure 2-27, the control leg also experienced an increase in bone density, despite not experiencing an increase in mechanical loading. This type of crosstalk is well documented in exercise, however it is yet unclear which endocrinal, biomechanical, or combination of crosstalk pathways is responsible for this observed crosstalk (He, He et al. 2020). Nonetheless, in the case of investigations examining the influence of loading on bone remodelling where hopping is involved, such as that in Allison, Poole et al. (2015), crosstalk does not interfere with the research focusing on the exercise limb. It does however introduce interesting research opportunities to observe how crosstalk has influenced the control limb.

New observations into crosstalk have also introduced possible new treatment pathways where research is beginning to reveal that endocrinal and biomechanical orthopaedic crosstalk mechanisms result in bone-to-muscle and muscle-to-bone crosstalk mechanisms (Maurel, Jähn et al. 2017). These bone and muscle crosstalk mechanisms have introduced exciting new potential therapeutic approaches for treating degenerative conditions such as sarcopenia and osteoporosis (Maurel, Jähn et al. 2017, He, He et al. 2020).

2.8 Finite Element Simulation of the Femur

In the case of the femur, due to the complexity of the anatomy, the number of vital arteries, and high amount of soft tissue, the direct *in vivo* measurement of experienced strain is extremely invasive and as such is rarely conducted. In studying the effects of mechanical stresses and strains on the bone, some animal studies apply loads via an external mechanism (Bentolila, Boyce et al. 1998, O'Brien, Taylor et al. 2003, Karim and Vashishth 2013, Seref-Ferlengez, Basta-Pljakic et al. 2014, Seref-Ferlengez, Kennedy et al. 2015). Though, this is not suitable for humans, and in

particular the femur, as a result, finite element simulation is the typically used method to determine the physiological strain (Ramos and Simoes 2006, Speirs, Heller et al. 2007). Finite element simulation is a commonly used tool in biomedical engineering, where its accuracy in determining stresses and strains experienced by both soft and hard biological tissues along with manufactured objects has seen it become an increasingly accepted verification and validation method for the development of medical devices, including orthopaedic implants (Morrison, N Kashlan et al. 2015, Morrison, Pathmanathan et al. 2018). Finite element simulation offers further advantages in that it can be conducted at any time, and individual parameters can be isolated and examined.

For biological materials, finite element simulation can be split into that of soft tissue (Oomens, Maenhout et al. 2003) and hard tissue (bone) (Ramos and Simoes 2006, Speirs, Heller et al. 2007). In simulating stresses and strains experienced by the bone, the loads applied by the soft tissue (muscles) are needed, however, dependant on the study aim, the physical inclusion of the soft tissues is not necessarily required. In the case of determining the strains experienced in the femur during different activities, such as walking, stair climbing and hopping, the physical inclusion of the soft tissue is not required.

2.8.1 Bone Mechanical Properties

In order to determine the stress/strains experienced by any object, mechanical properties need to be applied. Both the cortical and trabecular bone are orthotropic materials. For the accurate assignment of the orthotropic materials, nine independent elastic constants and the spatial orientation of the principal axes of the orthotropy are required. Baca, Horak et al. (2008) conducted a comparison between the influence of orthotropic and isotropic material assignment of the bone, where they found that for an accurate determination of bone stress and strain, orthotropic materials are only required for small scale simulations (e.g. $1 \times 1 \times 1$ mm cubes), whilst on a larger scale the use of isotropic material distribution provides perfectly accurate results. This assertion is supported by numerous studies using isotropic material assignment in the finite element simulation of the bone and achieving accurate results (Ramos and Simoes 2006, Speirs, Heller et al. 2007, Taddei, Schileo et al. 2007).

2.8.1.1 Bone as a Linear Elastic Material

Both cortical and trabecular bone are well documented as being viscoelastic with their properties being affected by the strain rate (Rhoa, Kuhn-Spearingb et al. 1998). As the strain rate increases, the elastic modulus increases and the yield strain decreases (Hansen, Zioupos et al. 2008). The largest effect is under the tensile loads where a ductile to brittle transition in moderate to high strain rates have been reported (Hansen, Zioupos et al. 2008). However, this viscoelastic nature for human cortical and trabecular bone is only apparent once the strain rate has exceeded approximately 2 s^{-1} (Hansen, Zioupos et al. 2008, Zioupos, Hansen et al. 2008). As shown in Table 2-6, physiological strain rates experienced by humans have been measured to be between 0.013 – 0.05 s^{-1} which is similar to those experienced by other animals. The highest measured strain rate in humans of 0.05 s^{-1} was obtained using temporarily implanted strain gauges placed on the tibia of a healthy "athletic" participant during "vigorous activities" such as running (Burr, Milgrom et al. 1996). Due to the difference in the strain rate required to induce the viscoelastic properties of bone and the physiologically applied strain rates, the human bone has been demonstrated to act linearly elastic under physiological loading conditions (Juszczyk, Cristofolini et al. 2011).

Table 2-6: In vivo measured physiological strain rates of the skeletal system, measured in humans, horses and dogs.

Strain Rate (s^{-1})	**Method**	**Species**	**Source(s)**
0.005-0.05	Implant	Equine, Canine	Rubin and Lanyon (1982)
0.013	Implant	Human	Lanyon, Hampson et al. (1975)
0.05	Implant	Human	Burr, Milgrom et al. (1996)

2.8.1.2 Density-Elasticity Equation

Consisting of two different types of bone (cortical and trabecular) and with bone remodelling adjusting the local mechanical properties, the bone as a whole global model (e.g. the femur) is a heterogeneous structure. Numerous studies apply a homogenous distribution of the material properties by using singular elastic modulus values for both cortical and trabecular bone. Whilst this method has been demonstrated to provide accurate results (Ramos and Simoes 2006, Speirs, Heller et al. 2007) local strain distributions are better determined using a heterogeneous material distribution as they better account for the local deviations in elastic modulus and density (Helgason, Taddei et al. 2008). A subject specific heterogeneous material determination can be

determined using the density of the bone, where a density-elasticity equation is used to calculate the elastic modulus.

There are numerous density-elasticity equations which are typically developed through comparison of the bone density against mechanical testing of bone harvested from donors. With most donors being elderly, there is a gap in literature where the effect of age on the density-elasticity equation has not been adequately studied. Numerous studies use two different density-elasticity equations for cortical and trabecular bone (Helgason, Perilli et al. 2008), where currently there are two methods used in assigning the material properties/equations to different areas of the bone; automatic and manual. Automatic assignment of the material properties is achieved by using the density of the bone, where a threshold density is assigned to separate between cortical and trabecular bone. However, the automatic assignment of cortical and trabecular density-elasticity equations has been demonstrated to produce poor stress/strain distributions through incorrect assignment (Helgason, Taddei et al. 2008). Manual assignment of the material properties/equations essentially works in the same way as the automatic assignment, however in replace of using a density threshold to differentiate between cortical and trabecular bone, it requires a manual user input. This therefore relies on the user determining what is cortical and trabecular bone and leaves significant room for error. Furthermore, it not uncommon in using the manual method to have gaps where no material assignment has been made. With the density-elasticity equations and single inputs for cortical and trabecular bone being significantly different (Helgason, Perilli et al. 2008), the incorrect assignment of the material properties can have a significant detrimental effect on the stress/strain distribution. The risk of incorrect assignment is furthered by the fact the only way to truly determine between cortical and trabecular bone is a histological study (Rhoa, Kuhn-Spearingb et al. 1998) which requires removal of the bone from the host. Alternatively, the use of a single density-elasticity equation which encompasses both cortical and trabecular bone eliminates incorrect assignment, inconsistencies and does not leave gaps between the bone assignment. Using 23 human femur samples, from 14 fresh donors aged 61.5 ± 9.5 years (mean ± S.D, full range 48 – 90), with 10 being male and 4 being female, Eberle, Gottlinger et al. (2013) investigated if a single density-elasticity relationship can be used. They found that a single density-elasticity equation can be applied accurately and used in a finite element simulation.

2.8.1.3 Partial Volume Effect

With different bespoke and purchasable software's, numerous techniques exist in transferring a CT scan of a bone to a finite element mesh with subject specific properties such as the elastic modulus based on physiological density. Using the software of *Materialise Mimics Research version 19.0, Materialise 3-matic Research version 18.0* for segmentation and *Simulia Abaqus/CAE 2017* for finite element analysis, two different meshes must be created. The first mesh to be created is the three-dimensional CT voxel mesh, comprised of pixels. This is the layout of the density distribution as measured by the CT scan, which is comparable to a photograph from a digital camera. The second mesh is the finite element mesh, which is derived from the CT voxel mesh. The partial volume effect is where a pixel of the CT voxel mesh covers two mediums which results in the pixel assuming the weighted mean density of the two mediums. As a result this introduces a potential issue in the density and width determination measurement of the bone, where the bone is surrounded by a lower density soft tissue and the voxel mesh pixels on the outer edge of the bone can partially cover soft tissue which can cause blurring (Hangartner 2007). The partial volume effect has been demonstrated to have an increasing influence as the cross-sectional width of the higher density material (bone) decreases. As such it has a larger influence on trabecular bone than cortical bone (Hangartner 2007).

As CT imaging technology progresses, with voxel pixels getting smaller and imaging resolutions improving, the influence of the partial volume effect on modern imaging is reducing. In addition, most CT imaging software's offer both CT voxel mesh and finite element mesh generation, with inbuilt proprietary programmes to tackle the partial volume effect which. These could be based on a combination of numerous mathematical techniques (Treece and Gee 2015). The full details of these techniques are often kept secret to protect intellectual property, nonetheless a popular technique in which software programmes can be based on is the thresholding technique (Buie, Campbell et al. 2007, Hangartner 2007). This technique uses a set HU value threshold, of which everything below will be excluded, to determine the correct thickness (Hangartner 2007, Treece and Gee 2015). A consideration with the thresholding technique is that for smaller cross-sectional widths, it can become unreliable (Treece and Gee 2015). Furthermore, the thresholding technique alone does not adjust the density of the pixels on the outer edge which have been affected by the partial volume effect despite the thresholding. A method for accounting for possible incorrect

density on the outer is the edge nodal interpolation method, which is applied to the finite element mesh (Helgason, Taddei et al. 2008). This method redefines any elastic modulus and density of any surface element or node if the internal node/element has a higher elastic modulus/density.

2.8.2 Standard Femoral Model

The proximal femur has been a focus of bone remodelling, ever since the concept was first introduced by Wolff (1896) who noticed that the trabecular distribution of the proximal femur is similar to that of stress patterns of a curved crane, as shown by Figure 2-29.

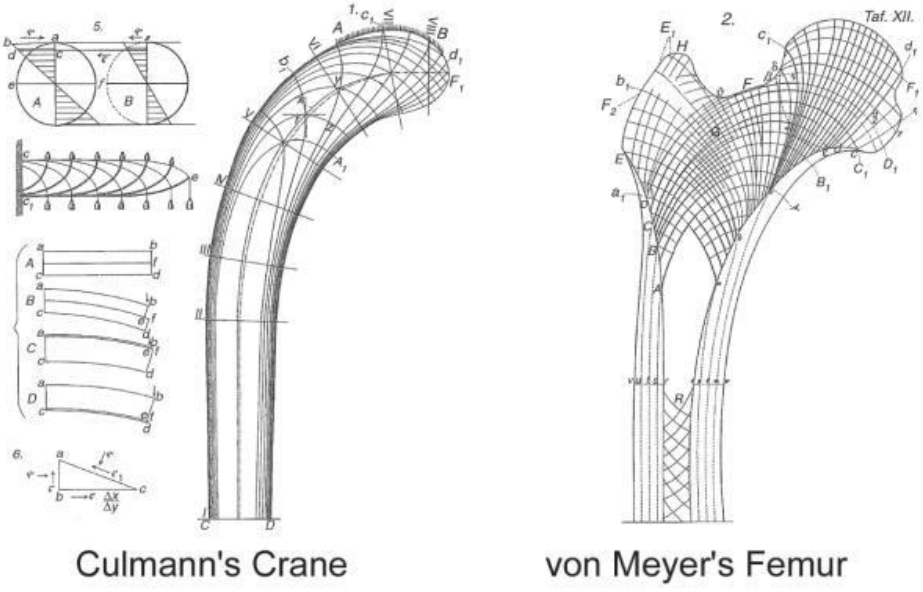

Figure 2-29: Comparison of stress patterns of the curved crane by an engineer Culmann, and von Meyer's femur, showing the trabecular distribution of the proximal femur (Robling and Turner 2009).

The femoral musculoskeletal system is a complex, dense system of muscles surrounding the largest bone in the body. The femur is held in place by a ball and socket synovial joint at the femoral head, which fits inside the acetabulum of the pelvis. Excluding whole body movement, the femur is capable of three degrees of freedom, which are controlled by different muscles. These muscles can be split down into four groups: Adductors (pull the thigh toward the body centre line in the frontal plane), abductors (pull the thigh away from the body centre line in the frontal plane), flexors (pull the thigh away from the body centre line in the sagittal plane) and extenders (pull the thigh towards the body centre line in the sagittal plane), with the planes shown in Figure 2-30. The femur is also capable of rotation around its axis, which is controlled by several of the muscles.

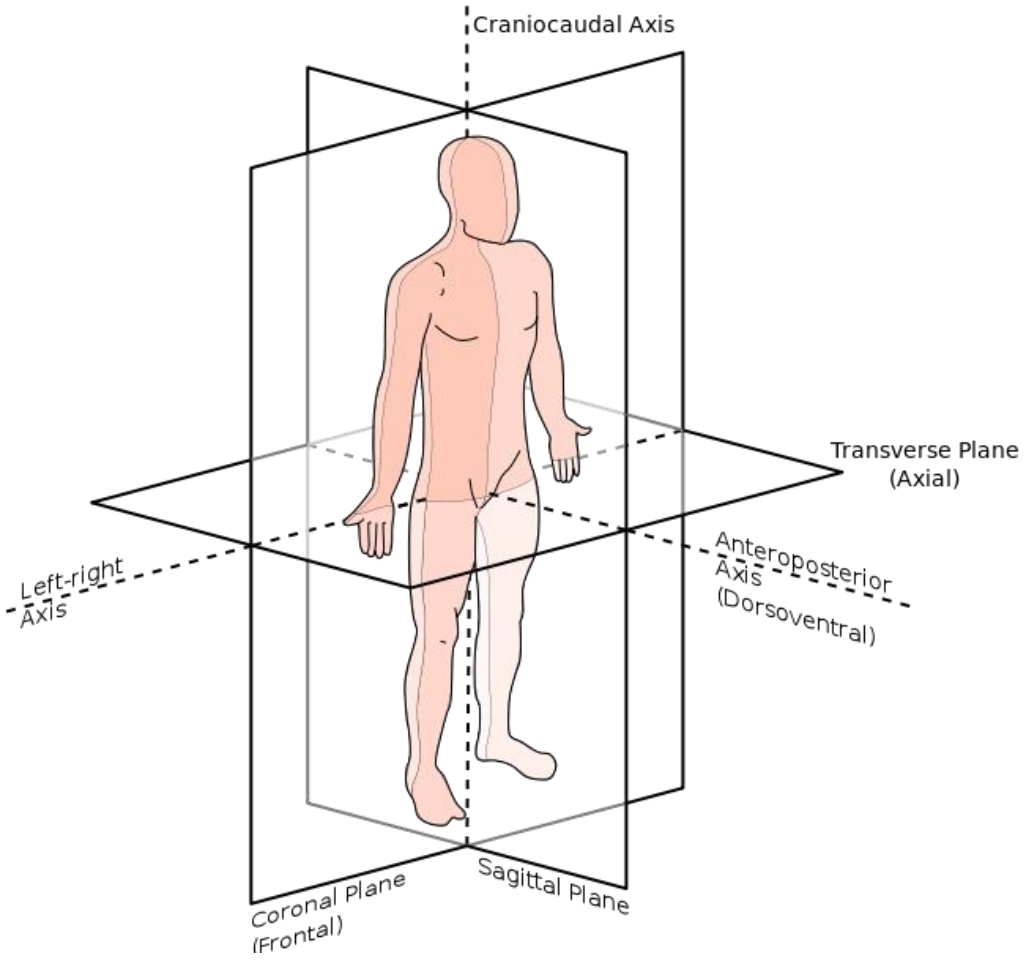

Figure 2-30: Anatomical planes of the human body (NIH 2000)

Despite the complexity of the femur and its muscles, the standard model of the femur and pelvis used in finite element simulation and bone remodelling determination, for both 2D and 3D simulations is very simple. It consists of the proximal femur which has been truncated and constrained at some-point along the femoral shaft, with the hip joint contact force and the gluteal abductor muscle forces which are attached to the greater trochanter as shown in Figure 2-31 (Turner, Anne et al. 1997, Bitsakos, Kerner et al. 2005, Ramos and Simoes 2006, Speirs, Heller et al. 2007, Baca, Horak et al. 2008). The gluteal abductors are generally classed as the gluteus medius and gluteus minimus, however some studies expand the gluteal abductor muscles to include all gluteal muscles (Heller, Bergmann et al. 2005, Speirs, Heller et al. 2007).

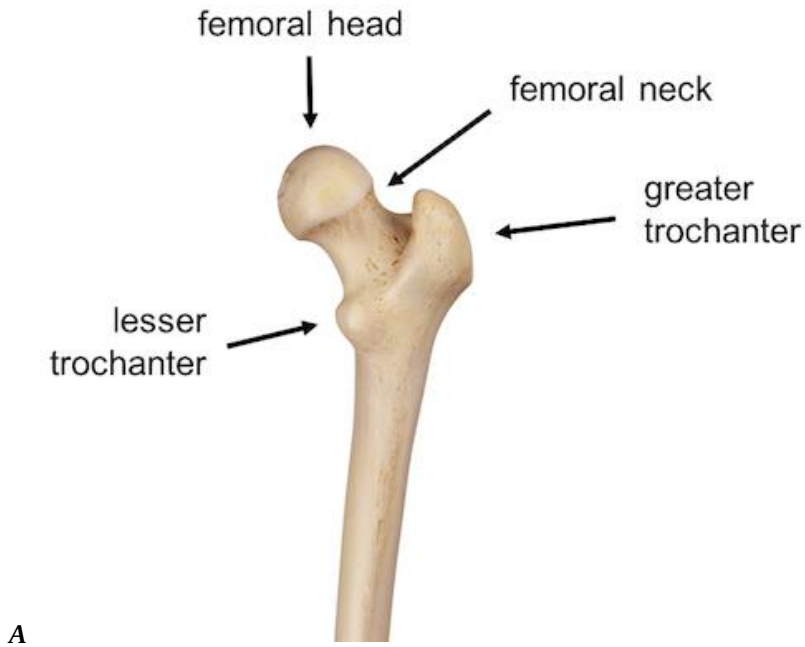

A

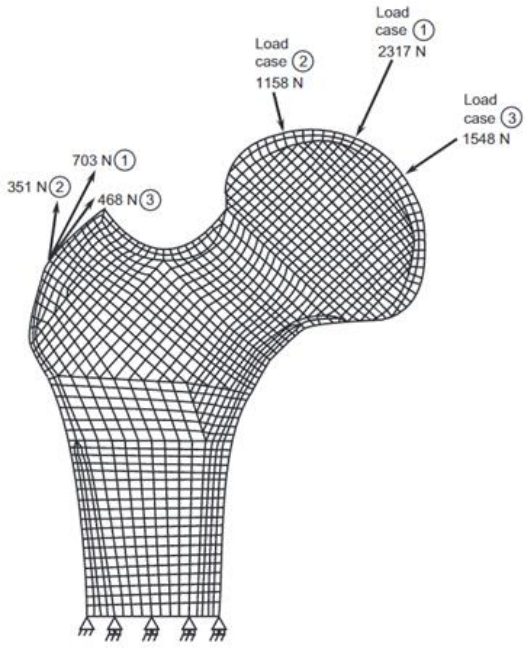

B

Figure 2-31: A) Basic femoral anatomy. B) Finite element simulation to determine the strain distribution for a bone remodelling study utilising the standard femoral hip model (van der Meulen and Hernandez 2013)

In a static environment, the standard femoral model is also often used in biomechanical load analysis to determine the hip contact load and abductor muscle forces, where the femoral head is treated as the fulcrum, the hip joint contact and gluteal abductor muscle forces are calculated in relation to the body weight force (Warrener 2017, Sangeux 2019) as shown in Figure 2-32. But

the standard model cannot be used to accurately determine the musculoskeletal forces in a dynamic (movement of the femur during ambulation) environment, due to the requirement to include additional muscles and the inability of the standard model to account for balance in the sagittal and frontal planes. For this a more complex musculoskeletal model is required, as explored in 2.9 Dynamic Musculoskeletal Loads.

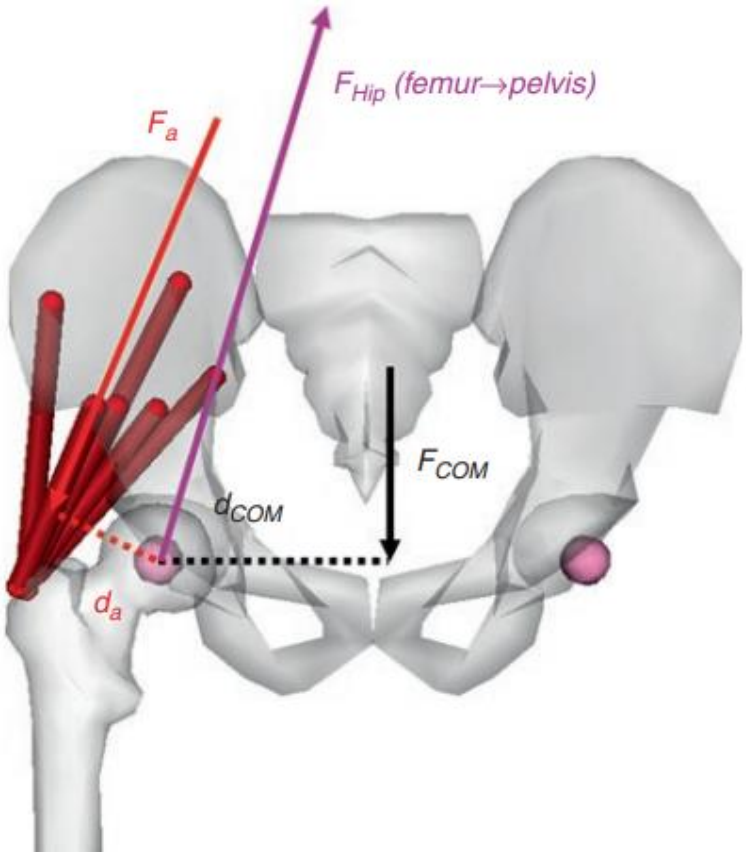

Figure 2-32: Standard model of the femur and pelvis for biomechanical calculations showing a computer simulation, including the hop contact force (F_{Hip}), the abductor muscle forces (F_a), and the body weight force (F_{com}), where d_a and d_{com} represent the distances/lengths of the moment arms (Sangeux 2019).

Nonetheless, biomechanically once the musculoskeletal loads are known, the simplification of the pelvis and femur musculature and loads to the standard model in dynamic environments to evaluate the effect of loads on the hip is acceptable. This is because other muscles than the gluteal muscles have been demonstrated to have little influence on the peak hip joint contact forces in gait (Correa, Crossley et al. 2010), with the influence of each muscle shown in Table 2-7. As such, testing of orthopaedic hip implants is often designed around the standard femur model (Basu 2017). Other muscles in addition to the gluteus muscles, notably the iliopsoas, have been demonstrated to have

some notable impact on the hip contact impulse (integral of the hip contact force over time) and such are included in some finite element simulations (Speirs, Heller et al. 2007). It should be noted though that the hip contact impulse is not important for bone remodelling in the hip joint, as due to mechanosensory saturation, bone remodelling only responds to the highest peak loads (Burr, Robling et al. 2002).

Table 2-7: Contributions of key muscle forces and other loading sources on the peak hip contact force and the hip contact impulse (integral of the hip contact force over time) on the anterior, superior and medial regions of the femoral head during gate (Correa, Crossley et al. 2010)

	Contributions to peak hip contact force (force/BW) Components			**Contributions to hip contact impulse [(force/BW)*time] Components**		
	Anterior	**Superior**	**Medial**	**Anterior**	**Superior**	**Medial**
Key hip-spanning muscles						
Gluteus medius	1.10	1.87	0.89	19.71	77.45	33.46
Gluteus maximus	−0.30	1.27	0.39	−6.87	21.16	6.28
Hamstrings	−0.02	0.27	0.01	−1.04	11.74	0.22
Iliopsoas	0.03	0.02	< 0.01	24.85	14.68	1.81
Rectus femoris	< 0.01	0.04	< 0.01	0.67	7.73	−0.10
Piriformis	−0.03	0.06	0.07	−3.72	4.67	7.68
Adductors	−0.01	0.06	0.03	−0.04	9.67	5.35
Subtotal	0.77	3.58	1.39	33.56	147.50	54.72
Key non-hip-spanning muscles						
Vasti	0.18	0.32	0.09	3.24	4.77	0.51
Soleus	0.01	0.01	< 0.01	0.15	4.83	1.10
Gastrocnemius	< 0.01	< 0.01	< 0.01	−1.11	1.57	0.82
Subtotal	0.18	0.32	0.09	2.28	11.17	2.43
Gravitational forces	< 0.01	0.09	0.04	0.03	5.41	0.06
Others	0.10	−0.05	−0.03	−1.15	−3.29	−0.06
Total	**1.06**	**3.94**	**1.48**	**34.72**	**160.38**	**57.15**

Speirs, Heller et al. (2007) conducted numerous finite element simulations examining the influence of different constraint locations and the inclusion of different femoral muscles on the strain experienced by the femur during walking and stair climbing, with the constraints and muscles described in Table 2-8 and shown in Figure 2-33, where the muscle and joint contact loads were taken from Heller, Bergmann et al. (2005). Speirs, Heller et al. (2007) found that the different simulations, including the standard model produced highly comparable strain distributions and magnitudes, particularly in the proximal femur as shown in Figure 2-34.

Table 2-8: Different loading conditions from Speirs, Heller et al. (2007) where the loads were taken from Heller, Bergmann et al. (2005)

Case	Loads	Constraints
A	Simplified: HCF + abductor	Diaphysis
B	Simplified: HCF + abductor + vasti	Diaphysis
C	Complex: JCFs + all muscles	Diaphysis
D	Complex: JCFs + all muscles	Condyles
E	Complex: JCFs + all muscles	Joint

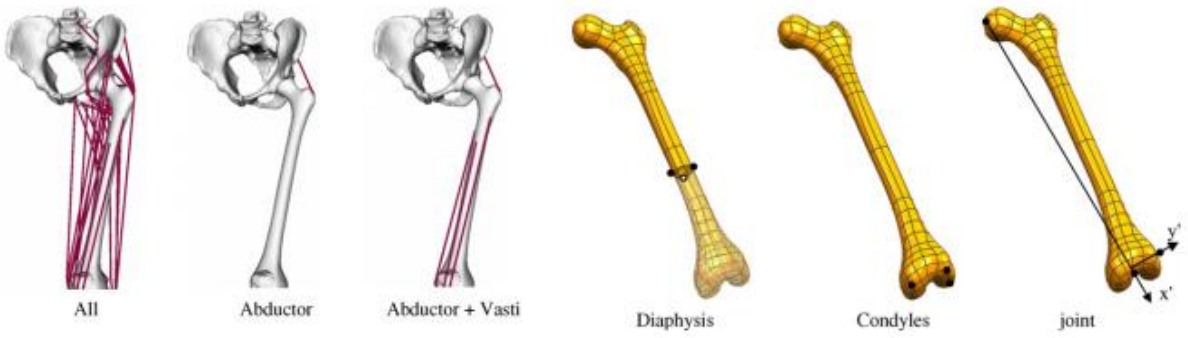

Figure 2-33: Boundary conditions used from the Speirs, Heller et al. (2007) where the finite element model is made up based on a standardised femur, using tetrahedral elements with cortical and trabecular bone regions with the assigned elastic moduli of 17 and 1 GPa respectively.

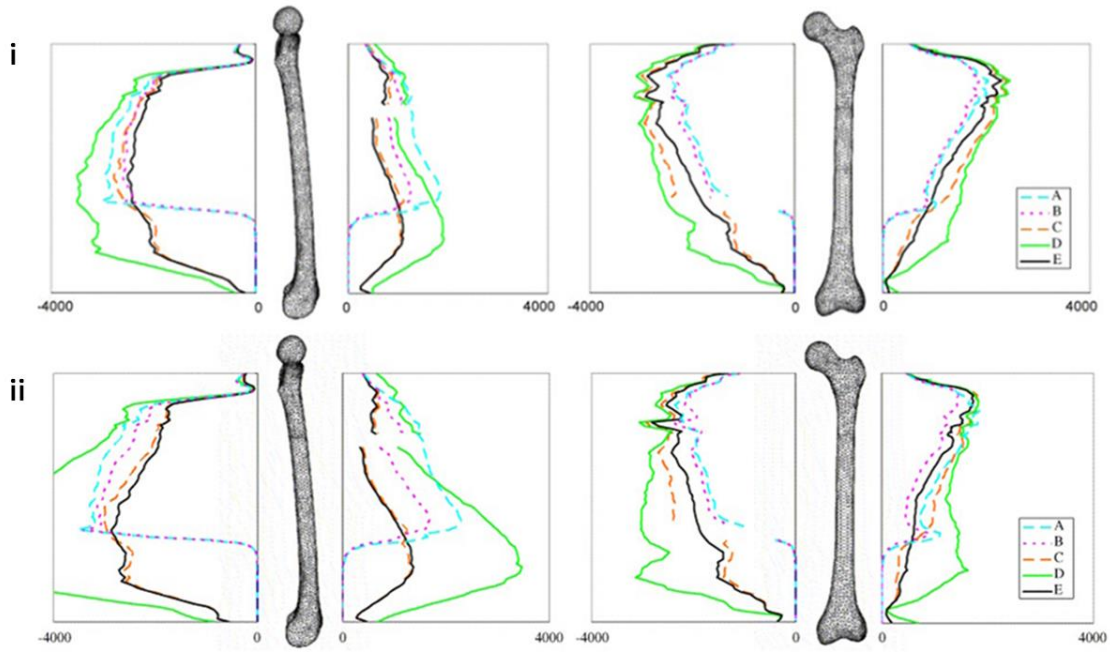

Figure 2-34: Femoral micro-strain results for walking (i) and stair climbing (ii) from Speirs, Heller et al. (2007)

Some studies suggest that a wider inclusion of muscles is required for a more stable strain distribution in the distal femur (Duda, Heller et al. 1998), an observation backed by Speirs, Heller et al. (2007). However, the inclusion of more muscles introduces errors as numerous muscles attached to the femoral shaft are hard to accurately position (Duda, Brand et al. 1996) and there is discretion in the exact muscle forces. Furthermore, it has been suggested that the attachment sites of the muscles introduce strain artefacts in the local vicinity (Modenese, Phillips et al. 2011). Nonetheless, the basic strain distribution for the proximal femur appears to remain the same regardless of the model (Duda, Heller et al. 1998, Rudman, Aspen et al. 2006, Speirs, Heller et al. 2007).

2.9 Dynamic Musculoskeletal Loads

Musculoskeletal loads are important in determining bone remodelling and fracture risk (Stansfield, Nicol et al. 2003, Bitsakos, Kerner et al. 2005, Frehill, Crocombe et al. 2009, Halldin, Jimbo et al. 2011). The complexity in calculating musculoskeletal forces has resulted in there being two types of study: 1) Those which calculate the musculoskeletal forces, and 2) Those which use the pre-calculated muscular forces from previous studies, where bone remodelling studies usually fall into the second category. Those studies which calculate the musculoskeletal forces produce models which can be used by those needing to incorporate musculoskeletal forces for other investigations. This is usually a singular maximum loading condition, representative of the particular movement being studied (Turner, Anne et al. 1997, Bergmann, Deuretzbacher et al. 2001, Heller, Bergmann et al. 2005, Cleather, Goodwin et al. 2011, Anderson and Madigan 2013).

Whilst the standard femoral model can be used to determine the femoral strain and bone remodelling outcome, it cannot be used to determine musculoskeletal forces acting in a dynamic situation (where the limb is moving). As such a more complex model is required, which includes a larger number of muscles. Muscles have multiple roles in the movement of the limb, where it is generally accepted that muscles not only apply loads to the bone for movement and stabilisation, through agonistic muscle contractions, but they also dampen external forces. This is achieved through synergistic and antagonistic muscle contraction and by controlling the angle of the bone when the external load is applied (Andreas Hölzera 2013, Helwig, Hindenlang et al. 2013). Without numerous invasive implants, which would require multiple surgeries, musculoskeletal

loads cannot be directly measured *in vivo*. This makes invasive measurements of the musculoskeletal loads in humans impractical, especially for the proximal femur, where a large amount of soft tissue increases the surgical complexity. As a result a substantial amount of research has been conducted into computerised musculoskeletal models to calculate the internal loads during movement (Erdemir, McLean et al. 2007).

In these simulations, muscles can be modelled as either passive or active. Passive models describe the muscles using a series of non-active mechanical components, such as springs and dampers. Examples of these are the Maxwell model, Voigt model and Kelvin model (Romero and Alonso 2016), as shown in Figure 2-35. Each model increases in complexity in an attempt to account for the mechanical behaviour of the muscle. An inherent downside of passive muscle models is that they cannot account for both the agonistic and antagonistic muscle forces at the same time. This issue was solved by adding a contractile element to the muscle models in the Hill muscle model (Hill 1938), as shown in Figure 2-35. Today the Hill muscle model is the most commonly used model to determine muscular forces (Erdemir, McLean et al. 2007, Romero and Alonso 2016) and has since been expanded to include features such as tendons and pennation angles (the angle of the axis of the muscle and its fibres) (Erdemir, McLean et al. 2007).

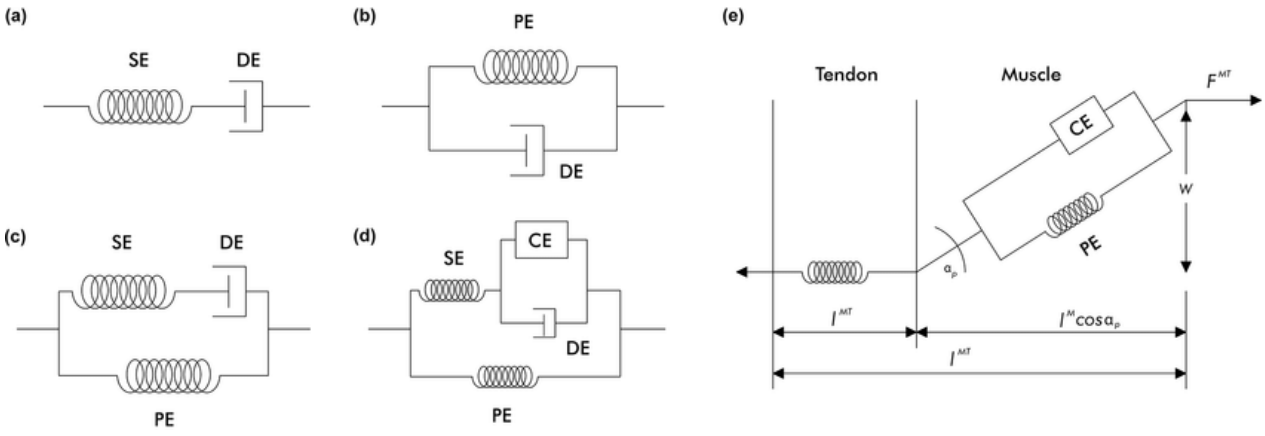

Figure 2-35: Different muscle models (tendon not included a-d) from Romero and Alonso (2016), showing: (a) Maxwell model. (b) Voigt model. (c) Kelvin model. (d) Hill model. (e) Hill muscle model expanded to include tendons. Where: SE is the spring elastic element, DE is the damping element, PE is the parallel elastic element, CE is the contractile element, α_p is the pennation angle, and l is length.

2.9.1 Inverse and Dynamic Optimization

The two methods which are used to simulate the muscular forces acting on the bone are inverse static optimisation and forward dynamic optimisation. Inverse optimisation-based simulations are a commonly used tool to estimate muscle forces in lower extremity movement (Erdemir, McLean et al. 2007, Cleather, Goodwin et al. 2011). In an inverse optimisation simulation, the joint torque forces are calculated using kinematic and reaction force data for a single point in time/the movement, as shown in Figure 2-36. Then using this the muscle forces are calculated, where the total muscle force equals the total joint torque force (Erdemir, McLean et al. 2007). Particularly for the femur, the number of muscles introduces a load sharing problem, where the system is statically indeterminate as the amount of force applied by each independent muscle is unknown. This can be solved by minimising an objective function, typically the total muscle force, subject to constraints of mechanical equilibrium at the joints and physiological limits of the biological tissues (Erdemir, McLean et al. 2007, Modenese, Phillips et al. 2011).

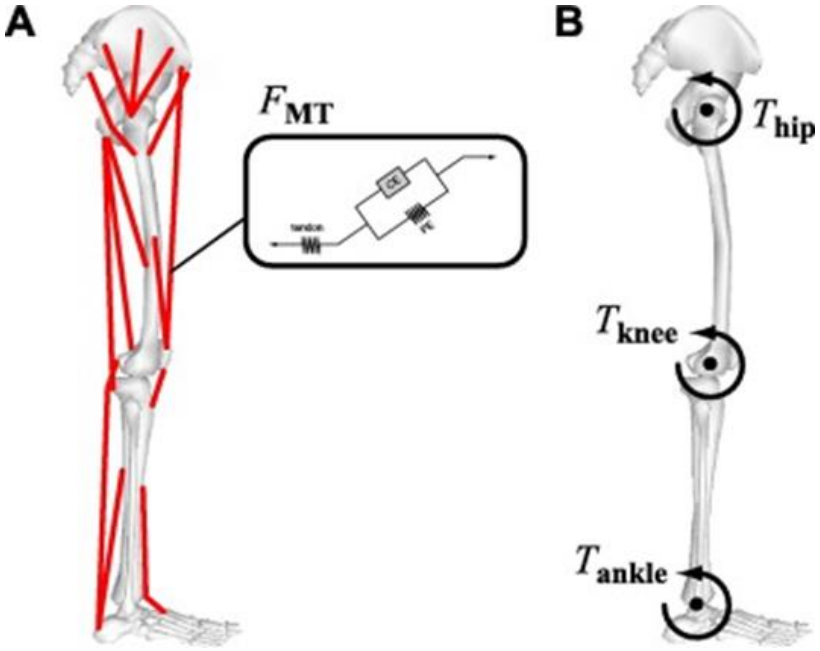

Figure 2-36: Examples of: (A) A musculoskeletal model of the lower extremity used in a forward dynamics solution, where Hill muscle model forces generate the movement of the hip, knee and ankle joints (Erdemir, McLean et al. 2007). (B) An example of an inverse optimisation model, simplified to the just the joint torque angles (Erdemir, McLean et al. 2007).

There are different methods of inverse optimisation which assign their own parameters and can use different equations (Cleather, Goodwin et al. 2011). However, all inverse optimisation models are limited by the same constraints; it relies on the accuracy of the kinematic data, where measurement errors could be present (Holden, Orsini et al. 1997), it is often based on approximations of anthropometric and dynamic force data, and foremost, it cannot differentiate between muscles, where different muscles can produce the same movement. Furthermore, kinematic data and subsequent kinetic data does not account for the antagonistic muscle contractions. The exclusion of antagonistic muscle forces is not as important in 'typical' ambulation, but is significant in patients suffering from conditions such as neuromuscular deterioration (Kostka, Niwald et al. 2019).

In an attempt to aid the determination of which muscles are being used and when, the comparison of musculoskeletal models against electromyography (EMG) in the determination of the femoral loads is becoming more common (Duda, Schneider et al. 1997, Duda, Heller et al. 1998, Erdemir, McLean et al. 2007, Horsman, Koopman et al. 2007, Modenese, Phillips et al. 2011, Helwig, Hindenlang et al. 2013). This has enabled the incorporation of factors such as co-muscle contraction (Erdemir, McLean et al. 2007). Whilst EMG is a useful tool to determine which muscles are contracting and when, the magnitudes of the detected electrical neuro signals are not proportional to muscle contraction force. Furthermore, inaccuracies caused by factors such as muscle overlap can produce confusing and often contradicting data (Modenese, Phillips et al. 2011).

In a forward dynamic optimisation simulation, the model (see Figure 2-36) is compared against kinematic data, where numerous muscle contraction combinations are tested, over numerous iterations, until the model produces a best fit to the clinical kinematic data. This process requires a significant amount of computing processing power and therefore is not always practical. Furthermore, this method produces a theoretical output based on the input parameters and is known to produce more than one output for the same kinematic data set (Erdemir, McLean et al. 2007).

Within both the inverse and forward dynamic simulations/calculations the joint is generally assumed to be frictionless and the bone is usually modelled as a rigid body. This is because the inclusion of bone strain in estimating muscle forces requires the use of complex finite element

simulations, which can require thousands or millions of iterations within numerous routines, where each iteration can take hours (Erdemir, McLean et al. 2007, Edwards, Miller et al. 2016). Because the strain of the bone is several orders of magnitude lower than that of the musculotendonous strain, it is assumed that the strain of the bone has negligible influence on the whole body motion and as such can be simulated as a rigid body in muscle force determination (Edwards, Miller et al. 2016).

2.9.2 Effect of Age on Muscle and Hip Contact Forces

It is well documented that muscles deteriorate in quality and strength with age (Lindle, Metter et al. 1997). However, this appears to have less of a detrimental effect on the loads experienced by the femur as would be expected. Anderson and Madigan (2013) conducted a study examining the loads applied to the femur during gait for walking by subjects across a wide age range. Here the muscle loads were calculated using inverse optimisation in *OpenSim* against kinematic and ground reaction force data. The subjects were split into two categories of younger (aged 25.0 ± 4.3 years old) and older (aged 79.4 ± 4.6 years old), each of which contained 5 subjects. The results from this study demonstrated that subjects of the two age groups experienced similar muscle and joint contact forces, in magnitude and pattern. This suggests that while the muscles are detreating with age, they are still capable of applying the loads required to achieve ambulation.

2.9.3 Published and Open Source Muscle Force Models

Several researchers have made publicly available musculoskeletal models and published musculoskeletal loads for different activities. This allows for other studies to accelerate their research without the complication of setting up an accurate musculoskeletal model, or having to calculate the musculoskeletal loads for the activities of interest. Some of these models and activities are explored here.

2.9.3.1 London Lower Limb Model

A commonly used commercially available inverse optimisation-based model is the London Lower Limb Model, a modifiable lower limb musculoskeletal model, shown in Figure 2-37, available on *OpenSim* software. Based on the anatomical models proposed by Delp and Loan (1995) and Horsman, Koopman et al. (2007) with the applied criterion of mechanical equivalence proposed

by van der Helm and Veenbaas (1991), the London Lower Limb model is considered a particularly suitable and accurate musculoskeletal model which can be used for investigation into different movements (Modenese, Phillips et al. 2011). With all muscles included, the model is comprised of 163 actuators to represent 38 muscles for six bodies (pelvis, femur, patella, tibia, hindfoot, midfoot plus phalanxes) with four hinges (patella-femoral joint, tibiofemoral joint, talocrural joint and subtalar joint). The model has a total of 12 degrees of freedom with the pelvis having all 6 degrees of freedom relative to the ground and uses a Hill muscle model type system where it assumes a limit of muscle forces between zero and maximum muscle isometric force (Modenese, Phillips et al. 2011). Much like any model of the lower limb musculature, a large number of actuators are required to accommodate for the curvature and overlap of several muscles, particularly the gluteus maximus, which results in an ever-changing muscle moment during movement (Modenese, Phillips et al. 2011).

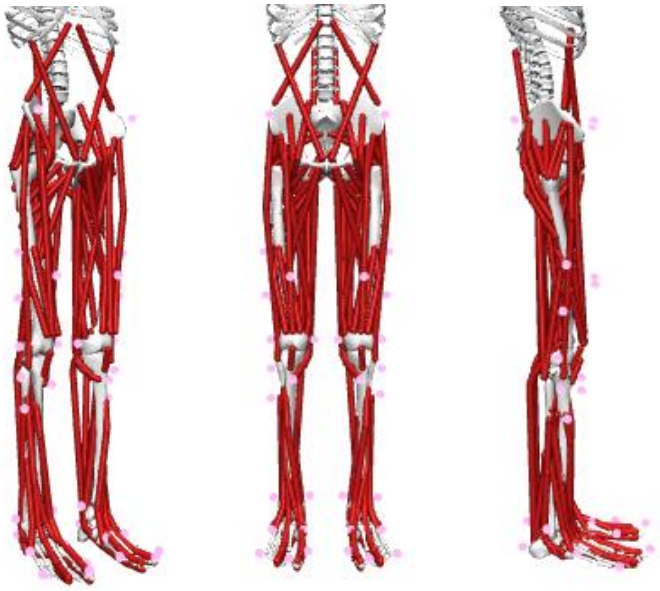

Figure 2-37: Snapshots of the London Lower Limb Model taken in OpenSim 4.0

Typically, two forms of validation are carried out in musculoskeletal models: 1) Comparison against the direct measurement of joint contact forces, and 2) comparison against ECG data. Both of these validation studies were carried out for the London Lower Limb model (Koopman and Horsman 2008, Modenese, Phillips et al. 2011) where the studies concluded the London Lower Limb model to be capable of producing appropriately balanced sets of muscle and joint contact forces that can be used in a wide range of applications requiring accurate quantification.

2.9.3.2 General Activities

A general activity is any activity which is typically undertaken by an able-bodied person, on a daily basis. These are typically considered to be walking and stair climbing as they are the most common everyday routine movements undertaken, particularly in older people who do not partake in exercise (Heller, Bergmann et al. 2005). They are favoured as rehabilitative and osteoporosis prevention exercises as they are the two routine activities which apply the highest musculoskeletal loads to the hip (Bergmann, Deuretzbacher et al. 2001) and as such aid with bone remodelling stimulation. As a result, the musculoskeletal mechanics for walking and stair climbing are two of the most highly studied movements (Duda, Schneider et al. 1997, Bergmann, Deuretzbacher et al. 2001, Heller, Bergmann et al. 2001, Taylor, Heller et al. 2004, Heller, Bergmann et al. 2005, Speirs, Heller et al. 2007, Modenese, Phillips et al. 2011).

A commonly used model to calculate the musculoskeletal forces during general activities is the model from Heller, Bergmann et al. (2001). The model utilises a simplified version of the London Lower Limb Model (Modenese, Phillips et al. 2011), produced by grouping several of the muscles together, as shown in Figure 2-38 and summarised in Table 2-9. The musculoskeletal loads were determined using inverse static optimisation against kinematic and ground reaction force data from four subjects, aged 51 to 76 years old, with a body weight range of 703 to 972 N, sex not disclosed. From this, a model for a "typical" subject was produced, where typical hip contact and muscle force loads were determined, correlated against the subjects' body weight. This offers a widely applicable model, which can be utilised by other studies so long as the body weight is known (Ramos and Simoes 2006, Scheerlinck and Casteleyn 2006).

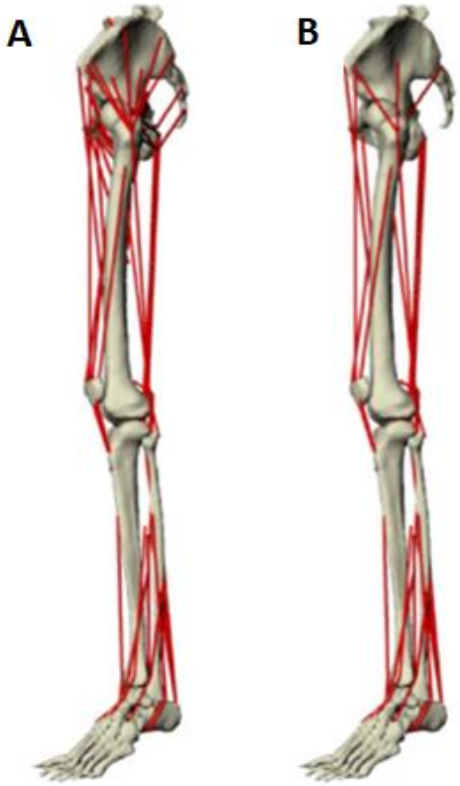

Figure 2-38: Comparison of the London Lower Limb Model (A) and the simplified model from Heller, Bergmann et al. (2001) which is reproduced in Heller, Bergmann et al. (2005) (B)

Table 2-9: Summary of the simplification of the London lower limb model used in (Heller, Bergmann et al. 2001, Heller, Bergmann et al. 2005), showing the muscles used in the London lower limb model (A) and the pooling (B), where '-' signifies that the muscles were not used.

London Lower Limb Model	Simplified model
Gluteus medius, gluteus minimus, gluteus maximus	Abductor
Adductor magnus, adductor longus, adductor brevis	Adductor
Iliopsoas major, pectineus gemellus inferior, superior obturator externus, internus piriformis	-

2.9.3.3 Hopping and Jumping

Hopping and jumping are two exercises considered to be the same musculoskeletal mechanism, which have a high prevalence in sport (Milgrom, Finestone et al. 2000, Augustsson, Thomee et al. 2006, Cleather and Bull 2010). Athletes who partake in high impact sports, such as those which involve running and jumping have been demonstrated to have significantly higher bone density in

comparison to those who undertake sports such as swimming (Scofield and Hecht 2012). Because of this, alongside its natural application, and ability to be conducted at home unsupervised, studies are being conducted into its potential as a osteoporosis prevention exercise (Allison, Folland et al. 2013, Allison, Poole et al. 2015). It is for these reasons that multiple studies have been conducted into its musculoskeletal mechanics (Spägele, Kistner et al. 1999, van der Harst, Gokeler et al. 2007, Cleather and Bull 2010, Cleather, Goodwin et al. 2011, Cleather, Goodwin et al. 2013), which have demonstrated hopping and jumping to be a reliable (Augustsson, Thomee et al. 2006) and easily reproducible (Veilleux and Rauch 2010) exercise in musculoskeletal analysis.

Cleather, Goodwin et al. (2011) compared different calculation techniques for vertical jumping, using inverse static optimisation of kinematic and ground reaction force data of twelve males, aged 27.1 ± 4.3 years, with a mean mass of 83.7 ± 9.9 kg. Subject specific scaling of the London Lower Limb model was created by comparing anthropometric measurements against a cadaveric model (Horsman, Koopman et al. 2007), from which Cleather, Goodwin et al. (2011) generalised the muscle and joint contact forces experienced by a subject based on their specific body mass. From this Cleather, Goodwin et al. (2011) produced a model which can be utilised so long as the body mass/weight is known.

Cleather, Goodwin et al. (2011) found that in all calculation techniques the hip contact force was at its highest during landing, whilst the hip muscles forces overall were at their maximum during vertical take-off, with there being some differences with the individual muscles. Due to the spring-like nature of the leg which bends during landing, the maximum hip joint contact force coincides with the maximum ground reaction force which occurs approximately 200 – 300 milliseconds after initial contact of the ground (van der Harst, Gokeler et al. 2007, Cleather, Goodwin et al. 2011, Cleather, Goodwin et al. 2013) where the femur is at an average of 25 degrees flexion and 0 degrees adduction (van der Harst, Gokeler et al. 2007, Sinsurin, Vachalathit et al. 2013, Myer, Bates et al. 2015, Hebert-Losier, Schelin et al. 2018).

2.10 Study Aim

Bone remodelling is currently assumed to follow the same general stimulus-remodelling relationship throughout the entire bone/skeletal system under physiological loading conditions.

Conversely, there is evidence that alternative bone remodelling behaviour can occur between tension and compression as the result of alternative bone remodelling mechanisms identified in this chapter.

Numerous bone remodelling algorithms are based on the mechanisms which have been demonstrated to, or are thought to, cause alternative bone remodelling behaviour (Frost 1987, Taylor and Lee 2003, McNamara and Prendergast 2007, Vahdati and Rouhi 2009, Fernández, García-Aznar et al. 2012). Yet, the studies which have examined alternative bone remodelling responses under tension and compression have thus far been under laboratory conditions which apply extrinsic loading to the bone (Bentolila, Boyce et al. 1998, Stokes 2002, Stokes, Gwadera et al. 2005, Karim and Vashishth 2013, Seref-Ferlengez, Basta-Pljakic et al. 2014, Seref-Ferlengez, Kennedy et al. 2015) or in pathological conditions (Lin 2010). No study has been conducted into if alternative bone remodelling behaviour in tension and compression occurs under physiological loading conditions in the absence of disease. Therefore, it is unclear how prevalent alternative bone remodelling is under physiological loading conditions.

The aim of this study was to take the first step into investigating the presence of alternative bone remodelling behaviour in tension and compression under physiological loading conditions. For this an observational-based clinical study is required, where a measured change in density needs to be compared against a mechanical stimulus. Externally applied loads are not applicable for this study as they may cause a deviation in the loads from those experienced in physiological conditions. As a result, the study requires the use of finite element simulation to determine the mechanical stimulus.

2.10.1 Objectives

To meet the aim of this study and its investigational requirements, the researcher secured clinical data from the Allison, Folland et al. (2013) exercise trial under a material transfer agreement, shown in Appendix B. Using the data from the Allison, Folland et al. (2013) exercise trial the objectives were as follows.

The first objective was to set up and create an accurate data set in which to examine the stimulus and change in density experienced by the subjects of the Allison, Folland et al. (2013) exercise

trial. This consisted of first conducting an inclusion process, examining the clinical data for any parameters which may influence the results of this study. Following this, accurate subject specific finite element meshes for each selected subject were to be set up and accurate musculoskeletal loads applied. Once this was complete, the study needed to develop a reliable way to measure the change in density in regions of compression and tension, using the finite element simulation results to determine which regions to use.

The second objective of this study, once the finite element models had been created, was to compare the change in density against the stimuli, to determine and compare the stimulus-remodelling relationships. The objective was to do this for the general (combined, entire proximal femur), tensile and compressive strain data set regions, to investigate if there is any difference between the tensile and compressive stimulus-remodelling relationships and how they compare to the general stimulus-remodelling relationship.

Following the identification of the tensile and compressive stimulus-remodelling relationships and the bone remodelling behaviour, the third objective of the study was to compare the results against biological and physiological variables to determine, what, if any, influence they may have.

The fourth objective of this study was to compare the observations of the stimulus-remodelling relationships against identified alternative bone remodelling studies to postulate which mechanisms may have had an influence.

Chapter 3. Femoral Finite Element Model and Simulated Strains

3.1 Introduction

Chapter 2 describes how finite element simulation is combined with musculoskeletal loads to determine femoral strains which can be used in bone remodelling studies. The data from the Allison, Folland et al. (2013) clinical trial provided qCT scans which allowed for accurate measurements in the change in density, however did not detail the strain experienced by the femur. Therefore, accurate, subject specific finite element models of the Allison, Folland et al. (2013) clinical trial subjects needs to be produced to determine the femoral strains to enable an investigation into bone remodelling. The aim of this chapter is to detail the inclusion criteria used in this study, development of the subject specific finite element models, the application of musculoskeletal loads and evaluate the simulated strains which will be used to determine the stimulus-remodelling relationships.

3.2 Clinical Dataset

Under a material transfer agreement (see Appendix B) clinical data consisting of the qCT scans of the proximal femur, along with subject data such as height, mass, BMI and body fat measurements for thirty-four subjects were secured from the Allison, Folland et al. (2013) clinical exercise trial, which was introduced in Chapter 2. From the qCT scans, the bone density was considered to be measurable to the closest 0.001 g/cm^2 (Allison, Folland et al. 2013, Allison, Poole et al. 2015). This was considered to be able to comfortably measure a 0.1 % change in density across the entire observed density range.

3.2.1 Inclusion Criteria

The data from the Allison, Folland et al. (2013) clinical trial was put through an inclusion criteria to ensure the highest quality results. The initial inclusion criteria was to exclude any subjects which did not have the full anatomy of the proximal femur present in the qCT scan. Some scans were not wide enough and did not include the greater trochanter, which was required to allow for adequate muscle attachments, without which accurate simulations to determine the strain could not be carried out. The second inclusion criteria was that the bone must exhibit a large enough change in bone density to allow for a difference in bone remodelling in tension and compression to be observed. A figure displaying the subjects which passed and failed this criteria is shown in Figure 3-1. It was reasoned that if no remodelling occurred, such as in the lazy zone, no difference between the remodelling behaviour in tension and compression would be observed. Across the entire subject range, the clinical trial demonstrated an average increase in cortical bone density of 2.7% ($p < 0.001$) across the entire proximal femur as a result of hopping, however some specific regions experienced a higher change in density of > 6% (Allison, Folland et al. 2013, Allison, Poole et al. 2015). Other studies into the influence of exercise on the bone density observed similar changes in density (1.8% and 2.1% (Kukuljan, Nowson et al. 2009, Kukuljan, Nowson et al. 2011)). Therefore, it was postulated that if alternative bone remodelling was to occur in physiological loading conditions, it would be within this percentage change in density. Therefore, to maximise the chances of observing alternative bone remodelling, only subjects who had achieved a 2% change in density in at least one location was considered for this study. As shown in Table 3-1, out of the original 34 subjects used in the Allison, Folland et al. (2013) study, 11 (32%) passed the inclusion criteria to be used in this study. No statistical correlation or difference was found between the subjects which did or did not pass the inclusion criteria and the other subject data recorded by Allison, Folland et al. (2013).

Table 3-1: Table showing how many subjects from the Allison, Folland et al. (2013) clinical data passed and failed the inclusion criteria in this study.

Criteria	Passed	Failed
Criteria 1	30	4
Criteria 2*	11	19
Total	11	23

*Only those subjects which passed criteria 1 were considered in criteria 2

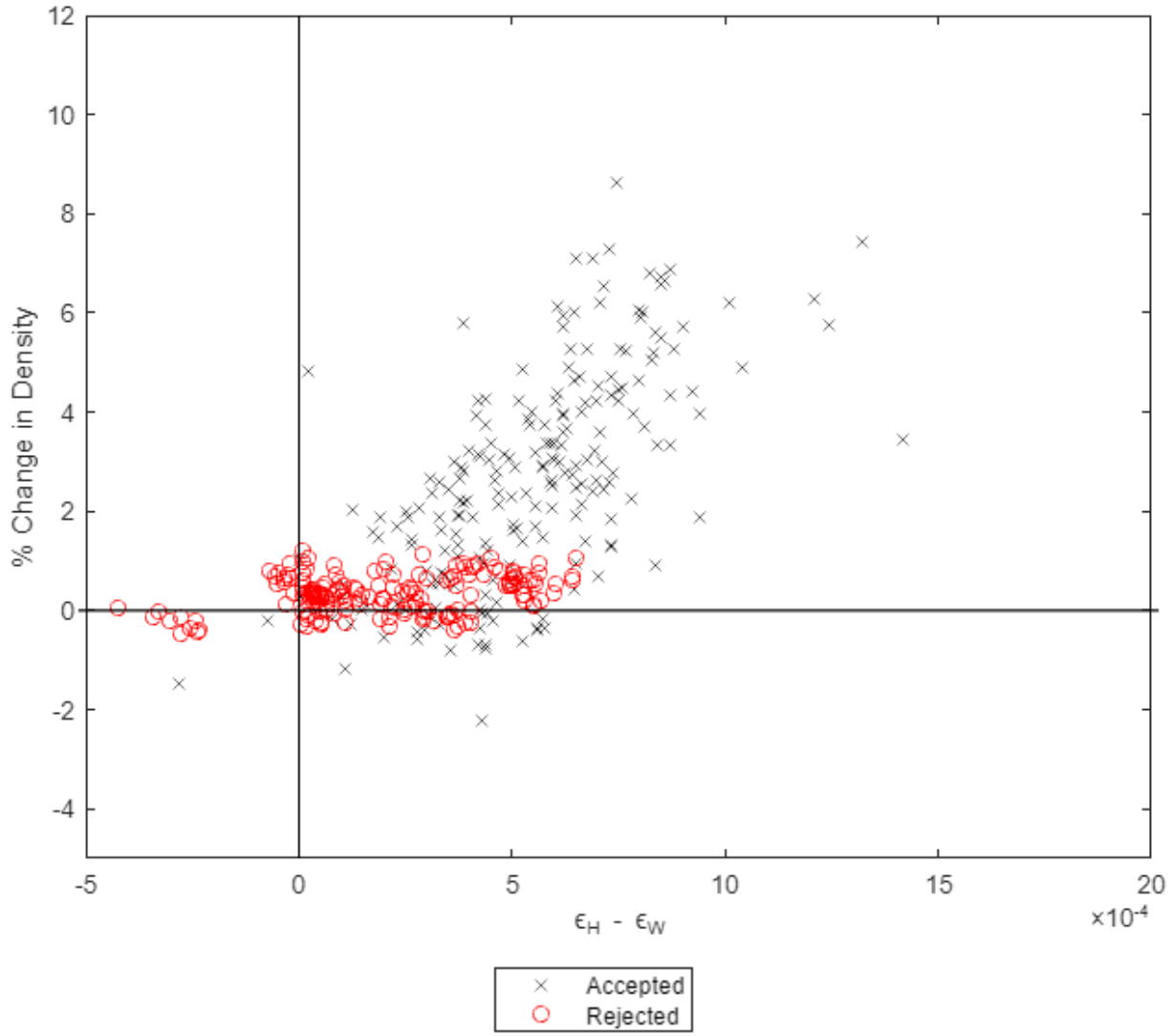

Figure 3-1: Figure displaying subjects which passed (x) and were rejected (o) following criteria 2 of the inclusion criteria, with the percentage change of density plotted against the Hop-Walk stimulus ($\varepsilon_H - \varepsilon_W$), as described in section 4.2 Methodology.

Using 3-Dimensional comparisons of the qCT scans of the 11 subjects which passed the inclusion criteria, no structural change was observed in any of the femurs as a response to the exercise trial, meaning that the only response to the hopping trial by the 11 subjects used in this study was a change in density. The subject-specific data consisting of the maximum change in density and anthropometric data of the 11 subjects used in this study who had passed the inclusion criteria is shown in Table 3-2.

Table 3-2: Subject specific data for the subjects used in the study, collected by the Allison, Folland et al. (2013) clinical trial.

Subject	Exercise Leg	Age at trial start (years)	Height (m)	Mass (kg)	BMI (kg/m^2)	Max. Change in Density (%)
1	Right	67	181.20	89.50	27.26	6.9
2	Right	69	175.70	71.40	23.13	3.0
3	Right	73	187.00	82.60	23.62	4.9
4	Left	70	169.20	87.10	30.42	7.1
5	Left	70	177.00	80.30	25.63	8.6
6	Right	70	178.00	80.30	25.34	6.0
7	Right	70	171.70	72.20	24.49	2.4
8	Right	78	170.10	76.30	26.37	6.6
9	Right	73	165.40	81.50	29.79	4.8
10	Left	71	186.80	81.20	23.27	7.4
11	Left	69	180.40	77.40	23.78	6.3
Mean	-	70.91	176.59	79.98	25.74	5.8
SD	-	2.78	6.72	5.28	2.41	1.9
Min.	-	67.00	165.40	71.40	23.13	2.4
Max.	-	78.00	187.00	89.50	30.42	8.7

NOTE: The maximum change in density is the maximum change in density measured at one point in the proximal femur, it is not representative of the change in density across the entire proximal femur.

3.2.2 Calibration Phantoms

Quantitative CT scans are equipped with calibration phantoms to ensure that the density measurement remains consistent. These consist of five rods of different pre-set densities, which run along the bottom of the CT table, so that they are captured in the scan, as shown in Figure 3-2. For each subject which passed the inclusion criteria, the Hounsfield unit of the calibration rods was recorded, with the comparison shown in Table 3-3. With the low standard deviation between each of the subjects, the calibration phantoms, and therefore the qCT scans were considered acceptable for this trial.

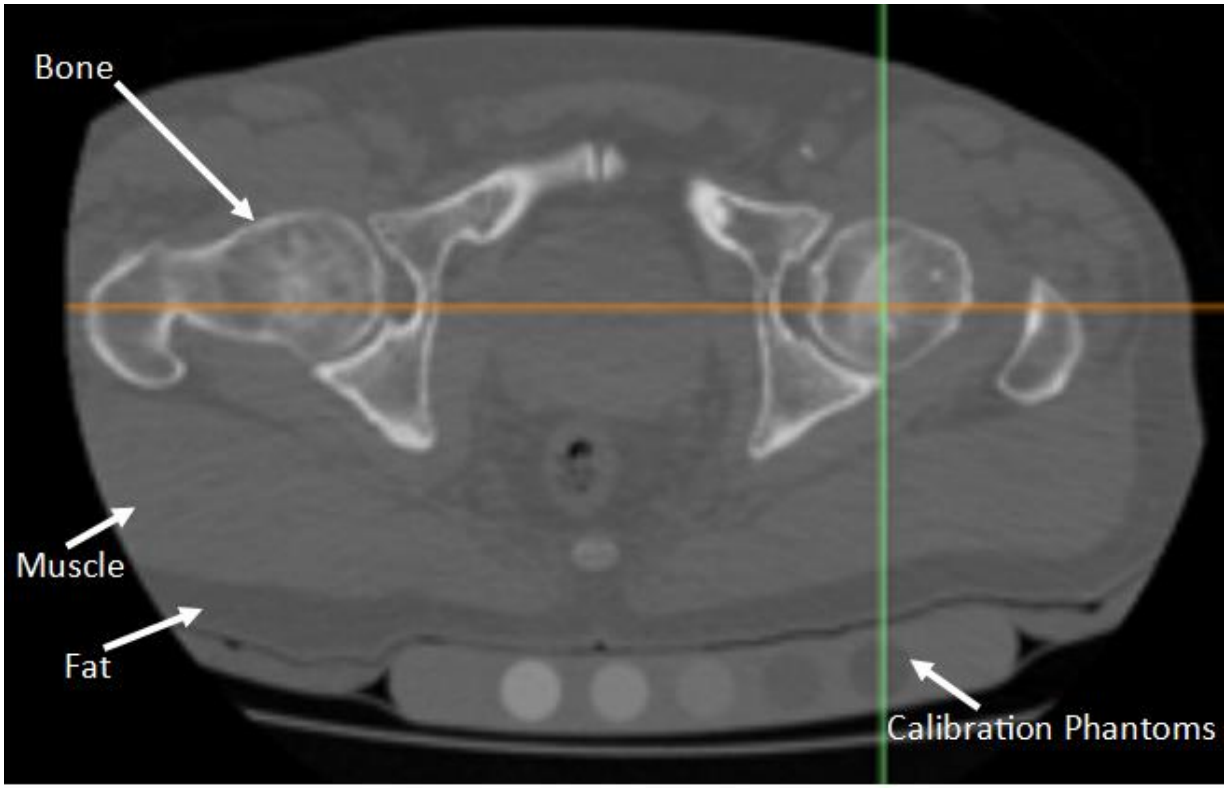

Figure 3-2: Calibration phantoms in one of the qCT scans taken by Allison, Folland et al. (2013) clinical trial, as observed in Materialise Mimics Research version 19.0, with a pixel resolution of 0.75 x 0.75 mm in the observed plane.

Table 3-3: Calibration phantom values for the subjects from the Allison, Folland et al. (2013) clinical trial used in this study, where HU is the Hounsfield unit.

Rod	**1**	**2**	**3**	**4**	**5**
Mean HU value	491.00	364.60	198.80	-28.20	-66.40
S.D (every subject)	1.33	1.08	1.55	1.54	0.84

3.3 Finite Element Model Development

To determine the mechanical strain experienced by each of the subjects which passed the inclusion criteria, subject specific finite element simulations were used. The qCT scans of each subject from the Allison, Folland et al. (2013) clinical data set which passed the inclusion criteria were imported into *Materialise Mimics Research version 19.0* software, shown in Figure 3-3, where the exercise bone was segmented.

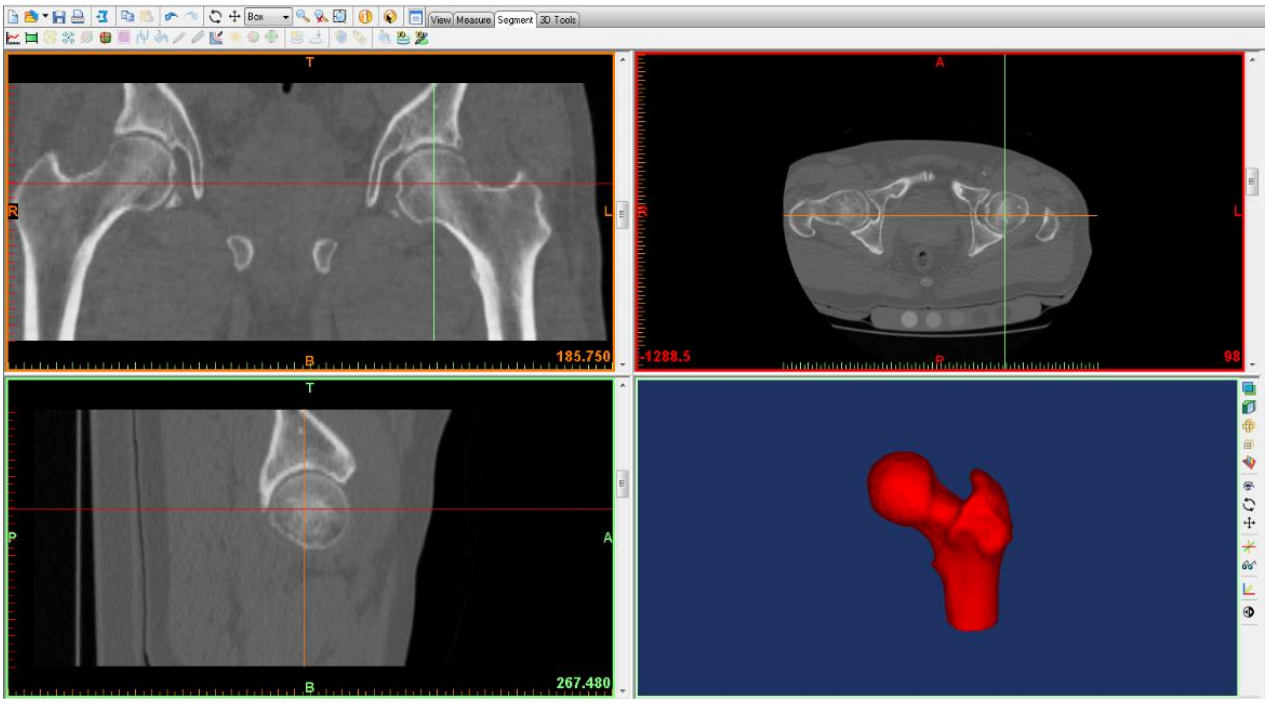

Figure 3-3: Femoral segmentation in Materialise Mimics Research version 19.0, with a pixel resolution of 0.7 x 0.75 mm in the axial plane, and 0.75 x 2 mm in the coronal and sagittal planes.

3.3.1 Element Mesh

The segmented femurs were then exported into *Materialise 3-matic research version 18.0*; where a universal mesh was applied throughout the model using four node tetrahedral elements (C3D4), as shown in Figure 3-4. Care was taken to ensure that the element size was as equal as possible throughout the model, including both on the surface and internally. Aspect ratios were kept to a minimum at all times to ensure the highest quality mesh.

In setting up a FE mesh, the simulating engineer has a choice of numerous different types of elements, all of which have their own pros and cons. For this study, the C3D4 element was chosen for numerous reasons. In particular the tetrahedral shape of the C3D4 element has been demonstrated to be the most efficient element shape for FE simulation of the bone (Wang, Nelson et al. 2004, Ramos and Simoes 2006). Additionally, in complex shapes such as the proximal femur, without extra shape functions, hexahedral elements can experience phenomenon such as shear locking (Wang, Nelson et al. 2004) and hour-glassing (Burkhart, Andrews et al. 2013), which have negative effects on the strain output. The C3D4 element has 4 nodes which are used to calculate the strain. A higher number of nodes, which are available in other elements, can provide a higher

amount of accuracy through increased strain resolution. However, this increased accuracy depends on individual case-by-case models, and therefore is not guaranteed. Furthermore, increasing the number of nodes significantly increases the computational time. The C3D4 was determined to be suitable for this study, through its proven track record in simulations of the proximal femur (Ramos and Simoes 2006), and was confirmed through convergence investigations, as discussed in section 3.3.2 Optimum Mesh Density.

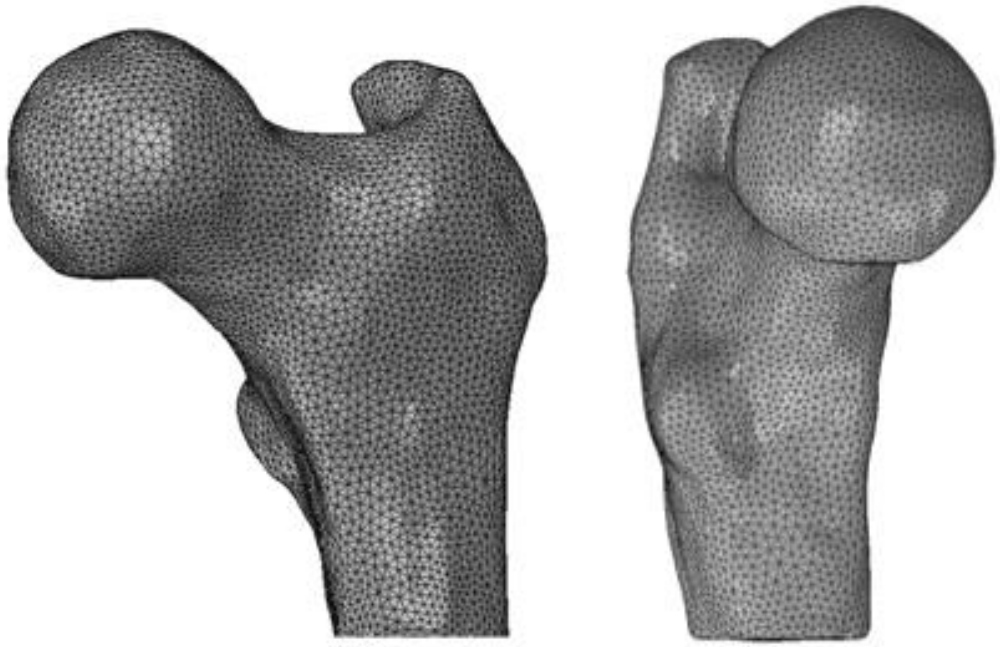

Figure 3-4: Finite element mesh of a selected subject in this study, showing the C3D4 tetrahedral elements generated in Materialise 3-matic research version 18.0.

3.3.2 Optimum Mesh Density

To determine the optimum mesh density, a displacement convergence study was carried out on the subject femurs with a heterogeneous mesh with isotropic linear elastic material properties assigned using the density-elasticity equation shown in 3.3.3 Mechanical Properties. The number of elements was systematically increased until the cumulative sum of the strain energy density (SED) converged to a 1% agreeance (Zannoni, Mantovani et al. 1998, Burkhart, Andrews et al. 2013). Using this method an optimum maximum element length of 2 mm was determined and applied to all the models, with the averaged convergence study result shown in Figure 3-5. This was

considered an appropriate size of element for examination for the regions of interest, which would be approximately 5-10 mm^2 in size (Turner, Anne et al. 1997, Bitsakos, Kerner et al. 2005).

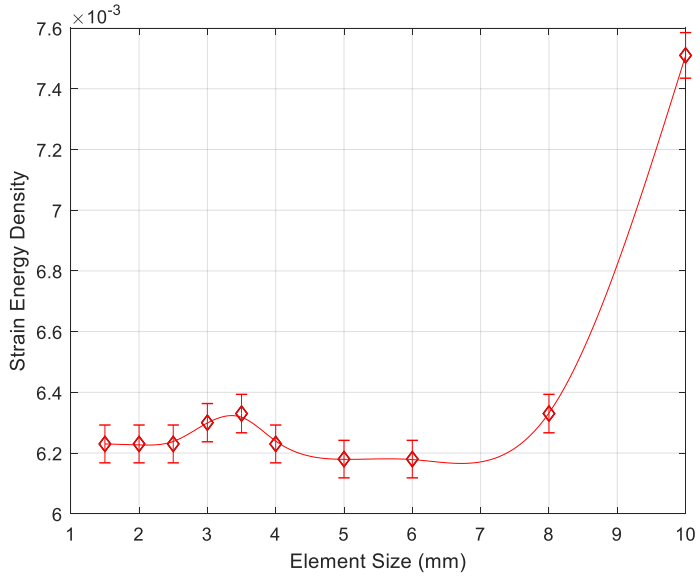

Figure 3-5: Results from the averaged mesh density (element size) convergence study with error bars displaying 1% agreeance in the whole model total strain energy density

The convergence testing method used in this study examines the entire proximal femur, however for examining bone remodelling, this study is interested in the local principal strain for regions of approximately 5-10 mm^2 in size (Turner, Anne et al. 1997, Bitsakos, Kerner et al. 2005). Whilst the convergence method used was developed for similar investigations which also focused on local strain (Zannoni, Mantovani et al. 1998, Burkhart, Andrews et al. 2013), examining the entire proximal femur in the convergence study leaves room for error where the local strain has not been specifically examined. However, convergence focusing on the local strain is often avoided as results can be misleading, in particular because local convergence of one area does not ensure convergence of the rest of the model.

3.3.3 Mechanical Properties

Following the research into the mechanical properties of the bone described in Chapter 2, this study opted for a single density-elasticity equation incorporating both the cortical and trabecular bone. Again, following the research described in Chapter 2, this study applied heterogeneous, isotropic, linear elastic properties to the finite element mesh using the material assignment options in *Materialise 3-matic research version 18.0.* To achieve this, each individual element was

assigned its own elastic modulus using a density-elasticity equation, from Keller (1994), as shown in equation 3-1.

$$E = 10.5\rho_{ash}^{2.29} \qquad 3\text{-}1$$

where E is the elastic modulus and ρ_{ash} is the ash density (g/cm^3), which was calculated using equation 2-4. The Poisson's ratio was set at 0.3 (Helgason, Perilli et al. 2008, Helgason, Taddei et al. 2008).

To further validate the use of Keller (1994) single density-elasticity equation, it was compared against typically used density-elasticity equations for cortical (Lotz, Gerhart et al. 1991) and trabecular bone (Lotz, Gerhart et al. 1990) and typically used single value inputs for the two types of bone (Keller 1994), as shown in Figure 3-6. It was found that the single density-elasticity equation had a high convergence with the two independent equations.

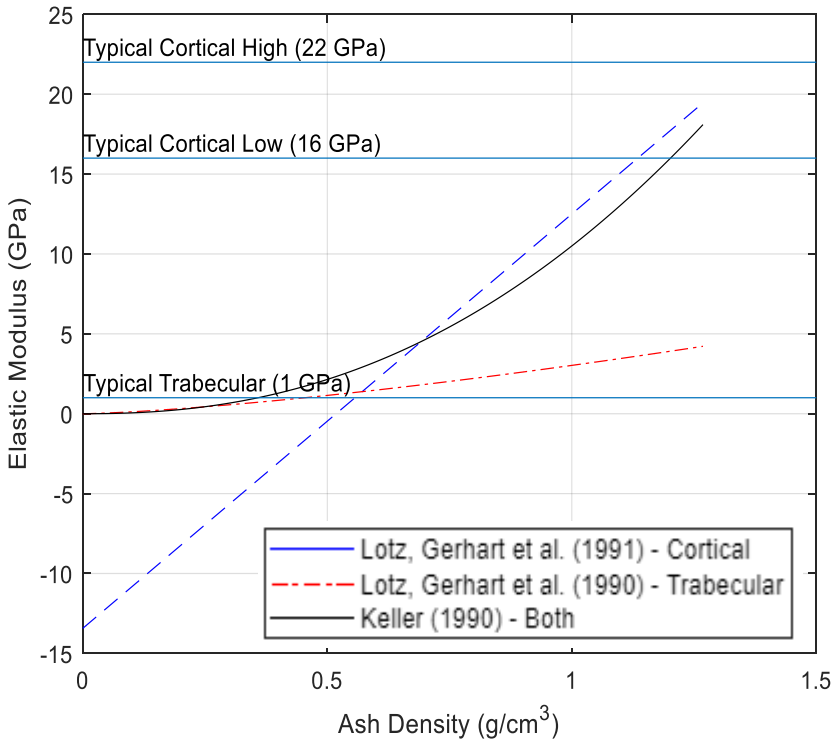

Figure 3-6: Comparison of the Lotz, Gerhart et al. (1991) density-elasticity equation for cortical bone, Lotz, Gerhart et al. (1990) density-elasticity equation for trabecular bone and the Keller (1994) density-elasticity equation for both cortical and trabecular bone, incorporating typical single elastic modulus values for cortical and trabecular bone reported in Keller (1994).

3.3.4 Femoral Loads

The role of the femoral loads in this study was to be applied to the subject specific finite element meshes to provide accurate mechanical stimuli to be compared against the change in density to assess the stimulus-remodelling relationships. To allow for accurate application of the loads, subject specific coordinate systems were applied based on the International Society of Biomechanics (ISB) recommendations (Wu, Siegler et al. 2002). For this, the femoral head, femoral neck, greater trochanter, lesser trochanter and femoral shaft were used as land marks (Unlu, Kesmezacar et al. 2011). The origin was set as the femoral head, the x axis was posterior to anterior, the y axis was caudal to cranial (distal to proximal) and the z axis was medial to lateral as shown in Figure 3-7. The zero hip angle was assumed to be with the subject lying supine, and positive rotation was assumed to be abduction and flexion. The mechanical axis from the centre of the condyles to the femoral head was assumed to be parallel to the femoral y-axis, at 6 degrees from the shaft axis and 3 degrees from the central body vertical axis (Tria 2020) .

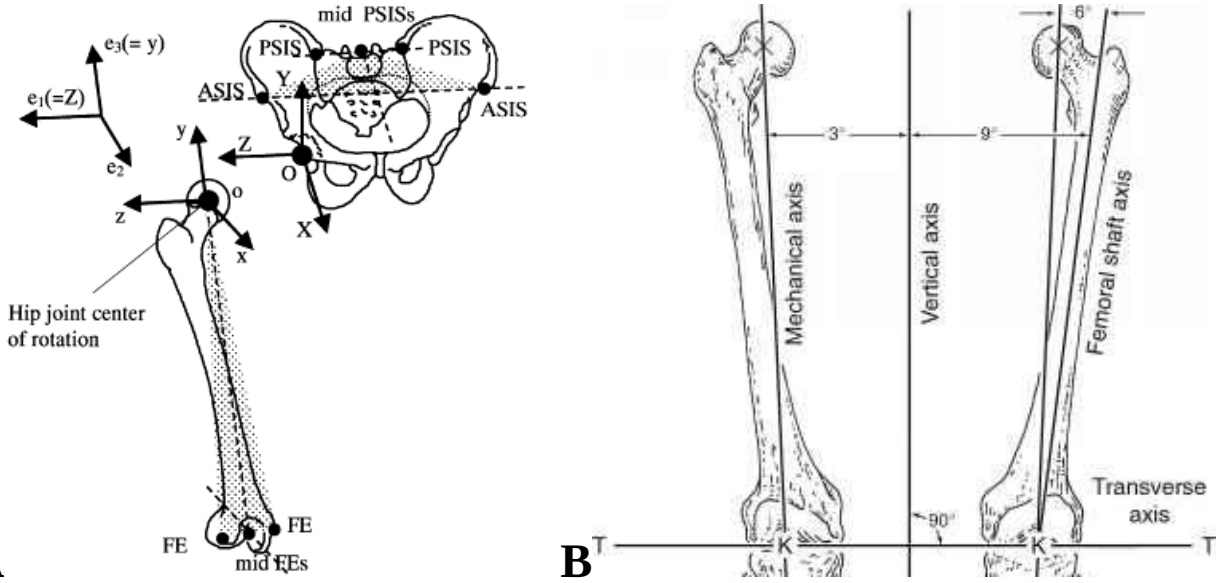

Figure 3-7: A) Hip and femur coordinate system based on the International Society of Biomechanics recommendations, where the femoral head and acetabulum are considered the origins (Wu, Siegler et al. 2002). B) Location of the femoral mechanical axis in relation to the femoral shaft and central body vertical axis (Tria 2020).

In the Allison, Folland et al. (2013) clinical exercise study, the subjects hopped 50 times a day, every day for a year. Before the clinical exercise study, the subjects were described to be active and undertaking 'general activities' but not partaking in sports. As described in Chapter 2, general loads are considered to be walking and stair climbing. As a result, to most accurately simulate the loads experienced by the femurs of the subjects used in this study, three simulations were carried out on each femur, utilising loads from previous musculoskeletal studies: 1) The maximum walking loads taken from Heller, Bergmann et al. (2005); 2) The maximum stair climbing loads taken from Heller, Bergmann et al. (2005); and 3) The maximum hop/jump loads taken from Cleather, Goodwin et al. (2011) using the traditional method for inverse calculation. To avoid the introduction of strain artefacts (Modenese, Phillips et al. 2011) through the use of too many muscles, the decision to use the standard femoral model as described in 2.8.2 Standard Femoral Model was made in this study, utilising only the hip contact and abductor muscles forces. The application of the loads and the running of the simulations were conducted using *Simulia Abaqus/CAE 2017* where the hip contact and muscle forces were applied evenly across the surfaces of the femoral head (F_{HC}) and greater trochanter (F_{AB}), with the bottom face being fully constrained with a Encastré boundary condition as shown in Figure 3-8 and the magnitude of the loads applied in this study being shown in Table 3-4.

.

Figure 3-8: Finite element simulation mesh and applied musculoskeletal loads on a selected subject in this study, demonstrating the application of the hip contact and abductor muscle loads across the femoral head and lesser trochanter, and the application of the boundary conditions on the femoral shaft. Here the most distal end of the femoral shaft is constrained by an Encastré boundary condition, and the F_{HC} and F_{AB} loads are applied over the areas shown in this figure to best match the anatomical attachment areas.

Table 3-4: Femoral head (Hip Contact Force) and greater trochanter (Abductor Muscle Force) loading magnitudes in body weight (mass) force for both left and right hand femurs

Loading Scenario	Hip Contact Force (F_{HC})	Abductor Muscle Force (F_{AB})
Hopping	5.20	2.30
Stair Climbing	2.51	1.14
Walking	2.38	1.05

Using the subject specific coordinate system, the direction of the hip contact loads was based on previously published data (Bergmann, Deuretzbacher et al. 2001, Heller, Bergmann et al. 2005, Bergmann, Bender et al. 2018, Sangeux 2019) and both the load magnitude and direction was validated by comparison against the open source data on the Orthoload website (https://orthoload.com/database/), made available by Bergmann and colleagues who have been

collecting hip contact force data on implants for more than 30 years. Similarly the muscle force directions were based on previously published data (Heller, Bergmann et al. 2005, Sangeux 2019) and validated by positioning the London Lower Limb model, on *OpenSim 4.0* in the kinematic positions during maximum loading (Heller, Bergmann et al. 2005, van der Harst, Gokeler et al. 2007, Lencioni, Carpinella et al. 2019).

Variations in the ambulatory movements were considered, where it was felt that any significant variations would only likely occur during hopping (e.g. hopping to the side). It was determined that the load magnitudes and directions accommodated for any variations in hopping due to the similarity in the hip contact forces experienced during possible variations of these different movements (Bergmann, Bender et al. 2018) representing minimal changes in the musculoskeletal loading environment, as shown by Figure 3-9.

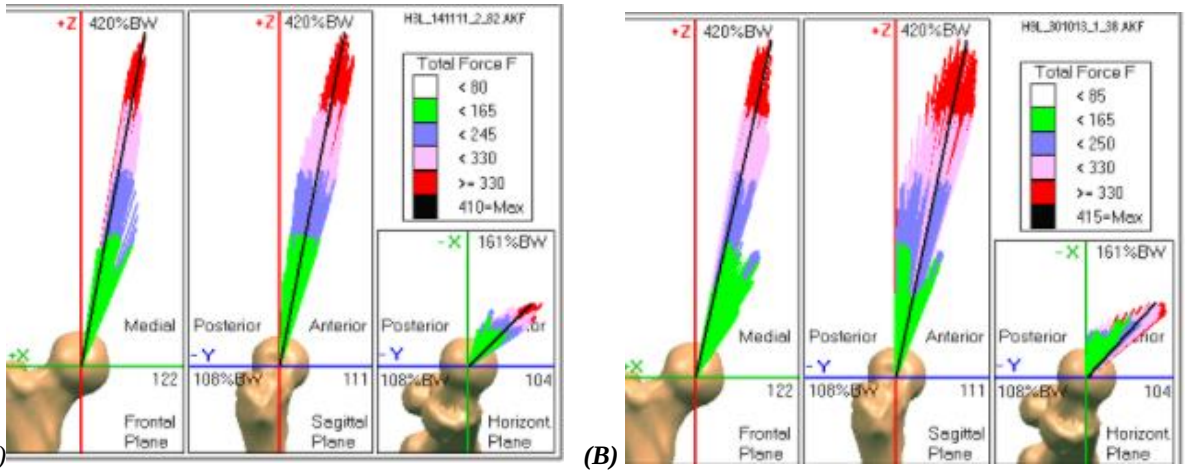

Figure 3-9: In vivo recorded hip contact forces due to jumping in place (A) and jumping side to side (B) (Bergmann, Bender et al. 2018) demonstrating the similarity in the hip contact load vector magnitudes and directions from the two movements.

3.4 Use of Principal Strains

Numerous mechanical outputs can be obtained from a finite element simulation, however for this study, it is important to focus on the principal strain. Whilst the microstructure of the bone is aligned with both the peak principal stress and strain (von Meyer 2011) and some bone remodelling algorithms interchange stress and strain as the stimulus (Turner 1998), mechanical failure in the bone such as yield (Albogha, Kitahara et al. 2015) and bone remodelling processes (Plotkin,

Mathov et al. 2005, Robling and Turner 2009) been demonstrated to be more associated with strain over stress. Whilst the two are directly related, the bone can experience a high stress and low strain in high density (thus high elastic modulus) areas. Since the main mechanotransducive theory is the shear flow hypothesis where signalling for bone formation is caused by bone deformation, not the stress being experienced (McGarry, Klein-Nulend et al. 2005), it follows that bone remodelling is more associated with strain than stress. As such, when it comes to the bone, focusing on the stress can sometimes be misleading.

Using the assumption of continuum mechanics (Lai, Rubin et al. 2009), a well-accepted and utilised mathematical representation of solids in engineering, matter can be regarded as infinitely divisible, so that it can be split into a finite number of infinitesimal elements. If the matter experiences small deformations, in relation to its size, then the stresses and strains can be calculated using the infinitesimal strain theory. Alternatively, if a large deformation is experienced, the assumptions of the infinitesimal strain theory become invalidated. Here, the internal stresses and strains can be calculated by the finite strain theory. In both the infinitesimal strain theory and finite strain theory the elements experience principal strains.

Using the infinitesimal strain theory, which is applicable to the deformation experienced by the bone, principal strains can be explained using the Cauchy Stress Tensor. This is a second-order tensor, σ, that relates a direction vector, n, to a traction vector, $T^{(n)}$, across the surface of the elements used to represent the matter, in the continuum mathematical assumption. This is defined in equation 3-2.

$$T^{(n)} = n.\sigma \qquad 3\text{-}2$$

The tensor itself consists of nine components, which are the stresses experienced by each element, as defined by equation 3-3.

$$\sigma = \begin{bmatrix} \sigma_{11} & \sigma_{12} & \sigma_{13} \\ \sigma_{21} & \sigma_{22} & \sigma_{23} \\ \sigma_{31} & \sigma_{32} & \sigma_{33} \end{bmatrix} \qquad 3\text{-}3$$

Here, being modelled as linear elastic, the stress and strain in the tensor can easily be interchanged by using the elastic modulus, as shown in equation 3-4:

$$E = {}^{\sigma}/_{\varepsilon} \qquad 3\text{-}4$$

Where, E is the elastic modulus, σ is the mechanical stress and ε is the mechanical strain. All strains and shear strains experienced by any location can be placed into a cartesian coordinate system and split into its x, y and z components. Therefore, exchanging stress for strain, and substituting, cartesian x,y,z coordinates into equation 3-3, gives equation 3-5:

$$\varepsilon = \begin{bmatrix} \varepsilon_x & \varepsilon_{xy} & \varepsilon_{xz} \\ \varepsilon_{yx} & \varepsilon_y & \varepsilon_{yz} \\ \varepsilon_{zx} & \varepsilon_{zy} & \varepsilon_z \end{bmatrix} \qquad 3\text{-}5$$

Where, $\varepsilon_x, \varepsilon_y$ and ε_z are the normal strains, and all other strains are shear strains acting parallel to the element face. This is demonstrated in a 2D plane strain environment, as shown Figure 3-10, where all stresses and strains in one direction equal zero (this is the z-direction in the Figure 3-10 example).

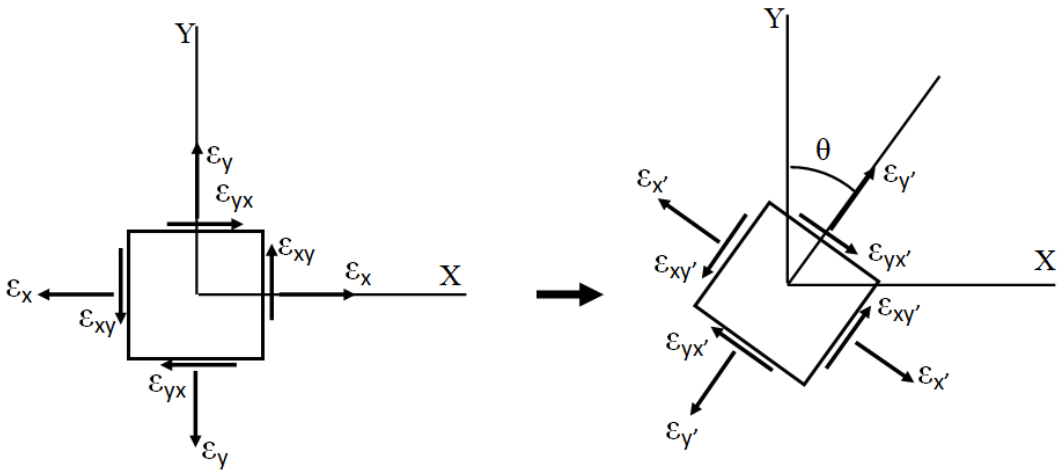

Figure 3-10: Original strain conditions in the x and y coordinate system (left) and principal strain conditions at angle θ from the original coordinate system (right), in plane strain conditions where all strains and shear strains in the z axis is 0, where ε_x and ε_y are strains, and ε_{xy} and ε_{yx} are shear strains.

In every element, there are three planes (two in a plane strain environment), where the shear strains equal 0, and the extremum values of the normal strains are obtained, these are known as the principal strains. This is a characteristic of second order tensors, which have three sets of independent invariant values, where one set of the invariant values are the principal strains. Here, the strains in the tensor are the eigenvalues and the direction vectors are the eigenvectors, also

known as the principal directions. This is often obtained at a different orientation to the original positioning of the tensor and so is assigned the coordinates x', y' and z'. This transformation is displayed in Figure 3-10, and the equation for the principal strain tensor is shown in equation 3-6.

$$\varepsilon' = \begin{bmatrix} \varepsilon_{x'} & 0 & 0 \\ 0 & \varepsilon_{y'} & 0 \\ 0 & 0 & \varepsilon_{z'} \end{bmatrix} \qquad 3\text{-}6$$

Where, ε' is the strain tensor in the principal location, and $\varepsilon_x', \varepsilon_y'$ and ε_z' are the principal (normal) strains. In both 2D and 3D environments, the extremum values are given the names of maximum and minimum principal strains, where typically the maximum principal strain is the highest magnitude tensile strain, often denoted as positive, and the minimum principal strain is the highest magnitude compressive strain, often denoted as negative. For this study, following the bone remodelling and mechanical failure in bone literature, the peak (highest magnitude) extremum principal strain in any location will be used, $\varepsilon_{\text{peak}}$. Therefore, this could be either tension or compression. In the examination of the subject specific strains experienced by each femur, the positive and negative connotation for tension and compression will be kept. However, to allow for these values to be used in the remodelling algorithm without confusion, a note of the orientation will be made and the absolute of the values will be used, $|\varepsilon_{\text{peak}}|$.

3.5 Subject Specific Simulated Strains

The decision was made to focus on the femoral shaft in this study, primarily due to the higher presence of cortical bone, making for a much easier determination of the change in density. Using the subject specific finite element models and musculoskeletal loads described in this chapter, each model was independently simulated for walking, stair climbing and hopping. Then, using 2D paths along the surface, the strain in the anterior, posterior, medial and lateral faces of the femoral shaft were examined, whilst avoiding loading and boundary condition sites to prevent strain artefacts (Gere and Goodno 2009, Modenese, Phillips et al. 2011). The individual and mean, peak magnitude principal strains along the 2D path for each anatomical face for each of the 11 subjects used in this study are shown in Figure 3-11 to Figure 3-14.

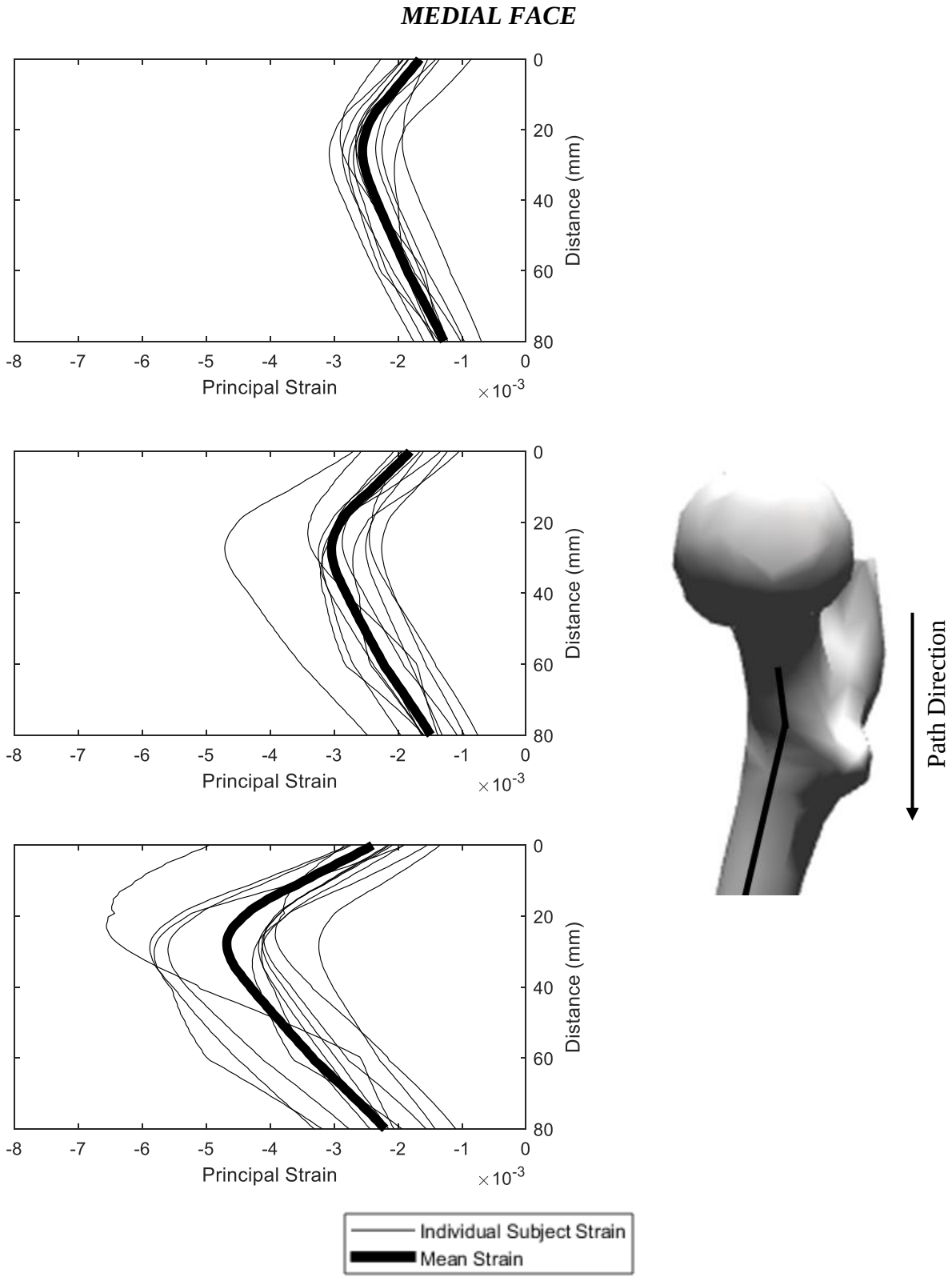

Figure 3-11: Highest magnitude, principal strain (ε_{peak}) on the medial face (shown on the right), for walking (top), stair climbing (middle) and hopping (bottom)

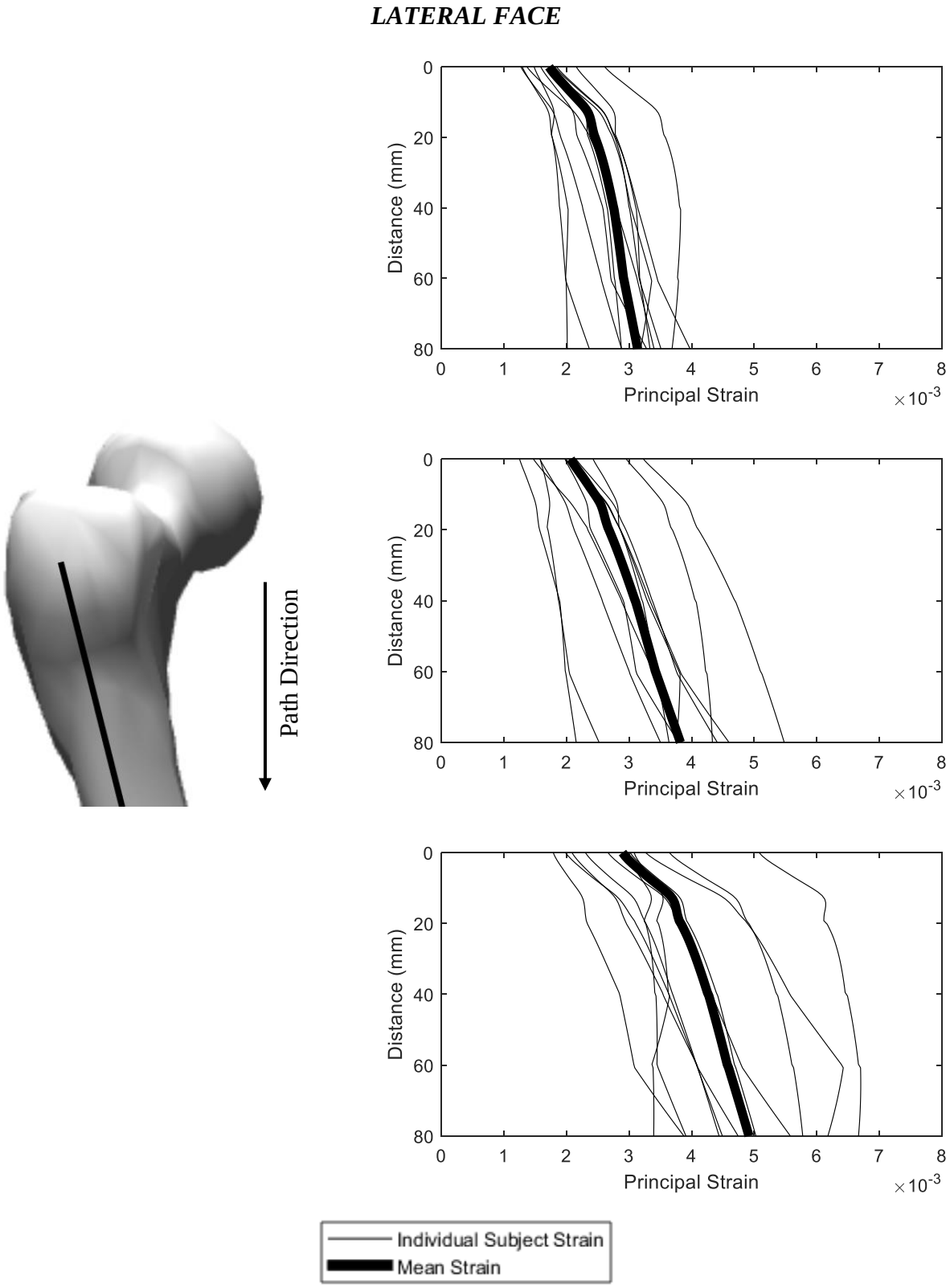

Figure 3-12: Highest magnitude, principal strain (ε_{peak}) on the lateral face (shown on the left), for walking (top), stair climbing (middle) and hopping (bottom)

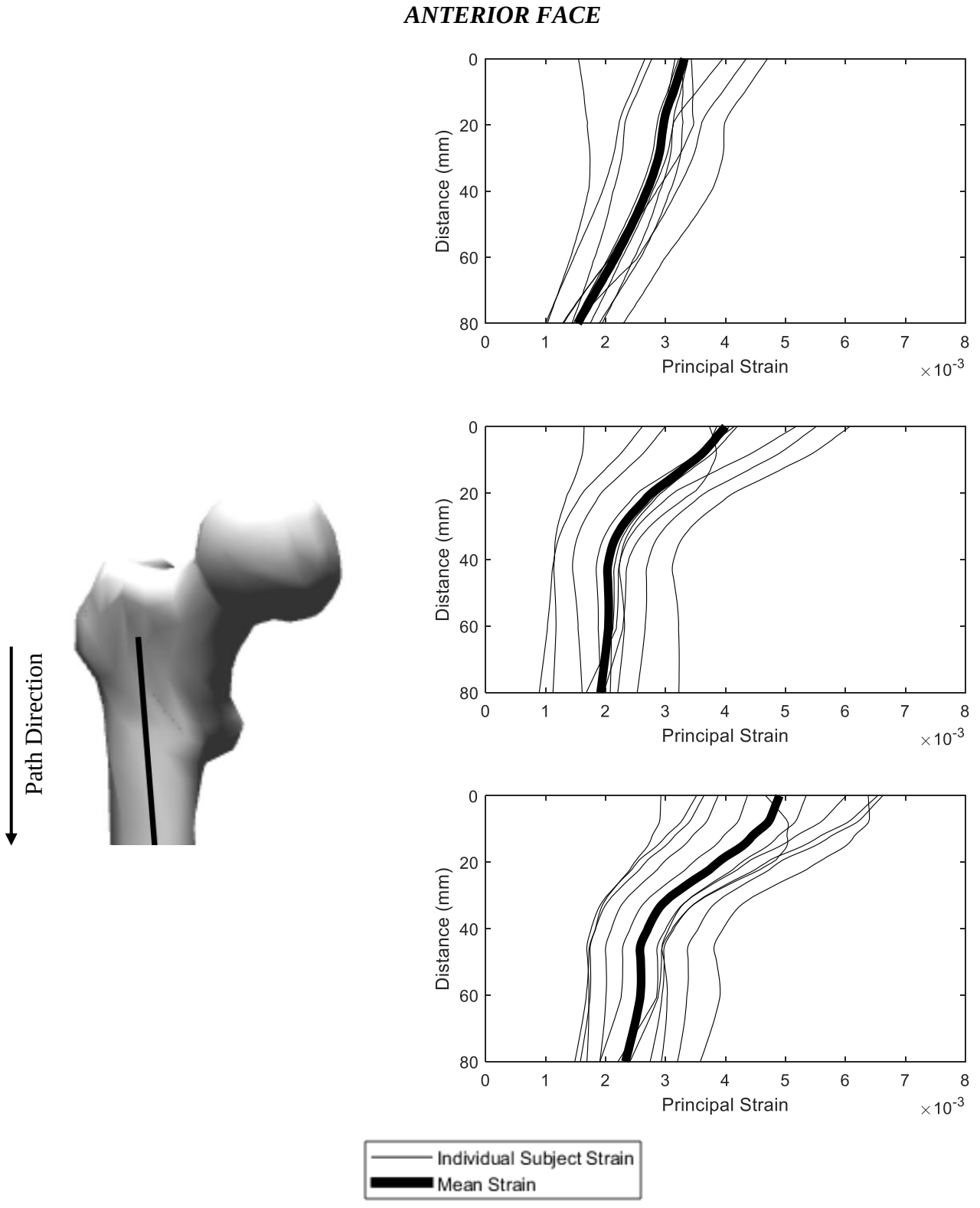

Figure 3-13: Highest magnitude, absolute, principal strain (ε_{peak}) on the anterior face (shown on the left), for walking (top), stair climbing (middle) and hopping (bottom)

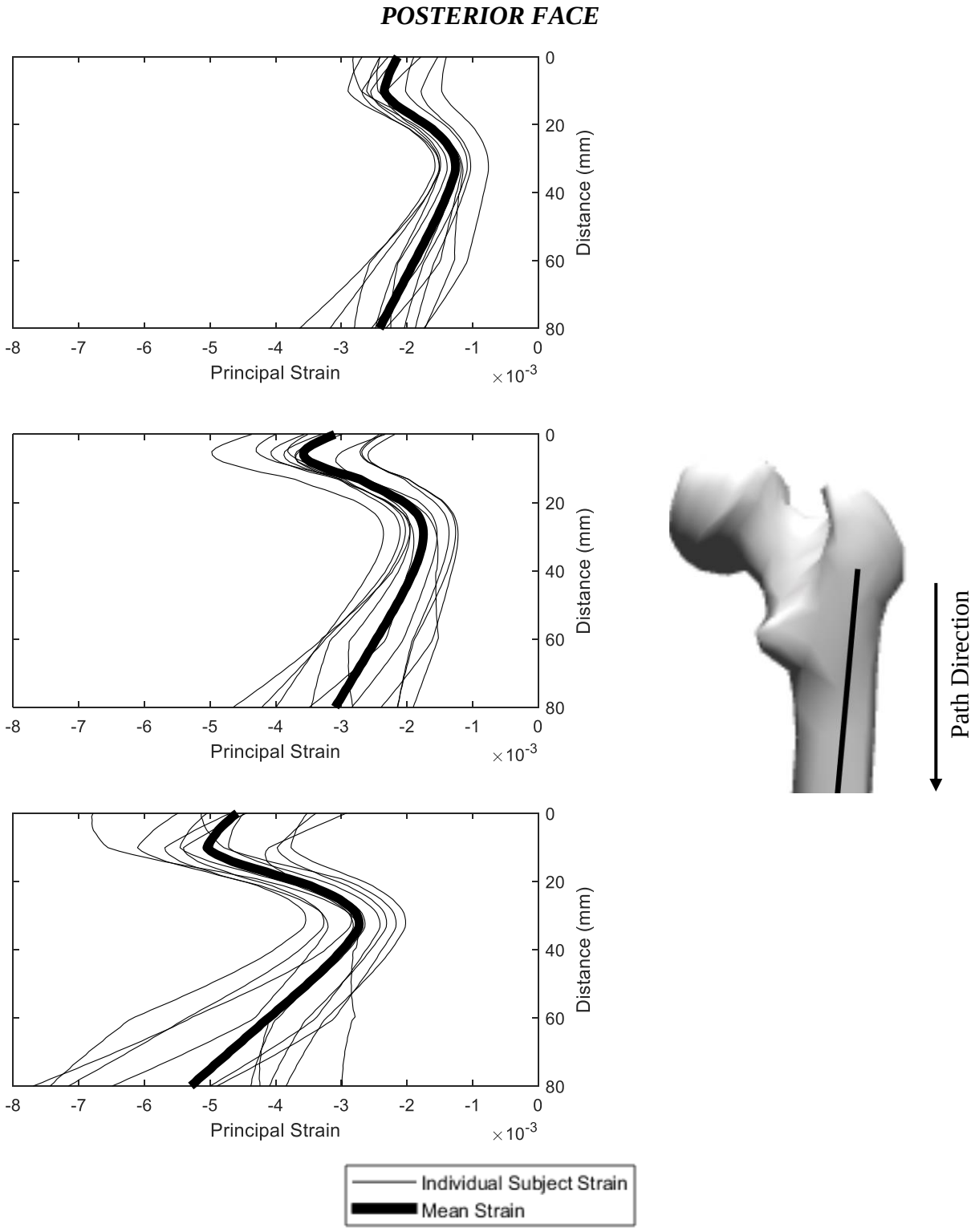

Figure 3-14: Highest magnitude, absolute, principal strain (ε_{peak}) on the posterior face (shown on the right), for walking (top), stair climbing (middle) and hopping (bottom)

3.6 Critical Evaluation of the Finite Element Model and Femoral Strains

This chapter has described the method used, and results obtained in the finite element simulation of eleven, subject specific, human proximal femurs, undergoing walking, stair climbing and hopping, to enable the calculation of the bone remodelling stimulus in Chapter 4. This section critically evaluates the finite element model and the results.

3.6.1 Model and Strain Validation

In comparing the strain distributions simulated in this study between walking, hopping and stair climbing, slight intersubjective differences were observed, which could be the result of differences in subject geometry (Lenaerts, De Groote et al. 2008) and density distribution (Helgason, Taddei et al. 2008). However, overall significant similarities were observed in each face between walking, stair climbing and hopping. In comparing these strain distributions to those of Speirs, Heller et al. (2007), significant similarities were observed on all four faces, for all three activities. This study was unable to directly measure any strains *in vivo* during any of the exercises. Therefore, for the model validation, the simulated strain magnitudes in this study, as shown in Figure 3-11 to Figure 3-14 and Table 3-5, were compared against previously *in vivo* measured and simulated strains, shown in Table 3-6 and Table 3-7. For all four faces, the mean strain simulated in this study for walking and stair climbing approximately correlated with the mean simulated femoral strain for walking and stair climbing from Speirs, Heller et al. (2007) and the theoretical value for the average optimum/reference strain based on the circulation strain (see 2.5.5 Circulation Strain). However, the simulated strains are higher than the *in vivo* measured strains in the femur for both walking and stair climbing by Aamodt, Lund-Larsen et al. (1997). They are also higher than the tibial *in vivo* measured strains by Burr, Milgrom et al. (1996) taken during activities such as running. With this it should be noted that *in vivo* measurement of orthopaedic femoral strains have been shown to be prone to significant errors which can range between 0.01 – 200%, dependant on location, due to factors such as mispositioning and deviations in the direction of the strain gauge in relation to the principal strains experienced by the bone (Cristofolini, McNamara et al. 1997). Furthermore, the subjects in Aamodt, Lund-Larsen et al. (1997) and Burr, Milgrom et al. (1996) are described as athletic and are significantly younger than the subjects used in this study, and

therefore would likely apply higher loads to their lower limbs than the subjects of this study on a regular basis. With the idea that the bone is optimally adjusted to its typical loads and the optimal/reference strain is based on the circulation strain: the subjects of Aamodt, Lund-Larsen et al. (1997) and Burr, Milgrom et al. (1996) would experience similar strains during activities such as running (which would be their typical loads), as the subjects of this study would during walking. As a result, the approximate correlation of the simulated strains in this study with the measured *in vivo* strains of the Aamodt, Lund-Larsen et al. (1997) and Burr, Milgrom et al. (1996) studies is a validation of this study's simulations.

Table 3-5: Mean absolute peak principal micro strain $\left(\left|\mu\overline{\varepsilon_{peak}}\right|\right)$ *for each of the anatomical faces during each activity*

	Anatomical Face				
Activity	**Lateral**	**Anterior**	**Medial**	**Posterior**	**All Combined**
Walk	2657	2565	2058	1833	2278
Stair climbing	3005	2421	2387	2448	2565
Hopping	3990	3046	3464	3973	3618

Table 3-6: In vivo measured strain magnitudes in the human skeletal system during exercise

Strain Range (με)	**Location**	**Activity**	**Subject(s) Age (years)**	**Reference**
1200 – 4200	Tibia	Hopping/jumping	37	(Ingrid, Kjartan et al. 1998)
~ 2000	Tibia	Running	42, 49	(Burr, Milgrom et al. 1996)
~ 1300	Lateral Femur	Walking	24, 49	(Aamodt, Lund-Larsen et al. 1997)
~ 1300	Lateral Femur	Stair climbing	24, 49	(Aamodt, Lund-Larsen et al. 1997)

Table 3-7: In vivo simulated strain magnitudes in the human skeletal system during exercise

Strain Range (με)	**Location**	**Activity**	**Reference**
~ 0 – 3500	Femur	Simulated walking	(Speirs, Heller et al. 2007)
~ 0 – 5000	Femur	Simulated stair climbing	(Speirs, Heller et al. 2007)

No suitable comparison for hopping in the femur could be found for either simulation or *in vivo* measurement: However, the mean simulated strain for hopping over all four faces roughly correlated with the higher end of strain range measured *in vivo* in the tibia in hopping/jumping exercises by Ingrid, Kjartan et al. (1998). In some cases, significantly higher strain magnitudes

were achieved by the subjects of this study under hopping, with the maximum being 7694 με, which was achieved by subject 3 in the posterior face. Whilst high, this was felt to still be a reasonable prediction, as it is within the microdamage production strain range (Wang 2013). Additionally, the subject used in Ingrid, Kjartan et al. (1998) was described as having an active lifestyle and is significantly younger than the subjects of this study. Therefore, it is likely that subject used in Ingrid, Kjartan et al. (1998) would apply higher loads to their femur during everyday use, and therefore would experience lower strains than the subjects of this study during activities such as hopping. Overall, after comparison against the available literature, the strain distributions and magnitudes obtained by the simulations used in this study were considered to be reasonable representations of the strain experienced by the subject specific proximal femurs during the different movements.

3.6.2 Critical Evaluation of the Finite Element Mechanical Properties

As discussed in this chapter, isotropic, heterogeneous, linear elastic properties were applied to the femur in this study, where each element was assigned its own elastic modulus using equation 3-1. However, in reality the bone is orthotropic and viscoelaslastic. Nonetheless, as shown in section 2.8.1.1 Bone as a Linear Elastic Material, the viscoelastic properties of bone only become apparent once the strain rate has exceed 2 s^{-1} before which it is linear elastic (Hansen, Zioupos et al. 2008). Since the strain rate in physiological loading does not exceed approximately 0.05 s^{-1} (Lanyon, Hampson et al. 1975, Burr, Milgrom et al. 1996) the bone can be modelled as linear elastic for this study, without the introduction of any significant error. In regards to the orthotropic nature of the bone, as discussed in section 2.8.1 Bone Mechanical Properties, in comparing finite element simulations against physical testing of the proximal femur, Baca, Horak et al. (2008) demonstrated that for accurate simulations of the bone, the orthotropic properties only need to be accounted for in small scale simulations (approximately 1 mm^3). Any simulation examining the bone on scale larger than approximately 1 mm^3 can be accurately modelled as isotropic. As such it was considered appropriate to simulate the bone ignoring the anisotropic properties without introducing any significant error.

The application of material properties to each element individually applies a level of heterogeneity, which is in line with the true mechanical properties of the bone. However, within each element

there is an inherited material homogeneity which is not in line with the true mechanical properties of the bone. Whilst this method introduces a small discrepancy in the distribution of the material properties from the true distribution; this method of applying material properties to each element individually and accepting a small homogeneity has been thoroughly examined and demonstrated to provide accurate results in strain prediction (Taddei, Schileo et al. 2007, Helgason, Perilli et al. 2008, Helgason, Taddei et al. 2008). Nonetheless, if the elements are too large, too much homogeneity can be applied, which could reduce the accuracy of the simulation. Smaller elements reduce the amount of inherited homogeneity, however increase the computational time. There is a delicate balance between accuracy and computational time, where an optimal mesh density exists which provides the maximum accuracy for the smallest computational time. For this study, the optimum mesh density was calculated using validated methods as discussed in Burkhart, Andrews et al. (2013) and Zannoni, Mantovani et al. (1998), as shown in section 3.3.2 Optimum Mesh Density.

As discussed, the density-elasticity equation 3-1 was used to apply the elastic modulus to each element individually. In determining which density-elasticity equation to use, the age of the subjects was a major consideration, since the bone is well documented to reduce in strength with age (Wang 2013). However, the reduction in bone strength with age appears to be a secondary effect, as a result of anatomical changes such as a reduction in bone density, whilst mechanical properties such as the yield strain and the elastic modulus remain constant with age (Nyman, Roy et al. 2009). Nonetheless, it is unclear if any anatomical changes with age affect the density-elasticity equation. This is primarily due to a lack of research since most density-elasticity equations are determined via mechanical testing of cadavers, which usually come from elderly donors. Previous studies have had success in applying a single density-elasticity equation across a wide age range of subjects (25 to 79 years old) (Anderson and Madigan 2013). Nonetheless, this study used a density-elasticity equation which was obtained using donors of approximately the same age and sex demographic of the subjects in this study.

3.6.3 Critical Evaluation of the Finite Element Musculoskeletal loads

The setup of the finite element models used in this study was based on the standard femoral model as discussed in section 2.8.2 Standard Femoral Model. This is a well utilised model in femoral

biomechanical and bone remodelling investigations (Turner, Anne et al. 1997, Bitsakos, Kerner et al. 2005, Ramos and Simoes 2006, Speirs, Heller et al. 2007, Baca, Horak et al. 2008). However, despite there being numerous muscle attachments on the femur, this model makes the general assumption that additional loading sources, apart from hip contact force and abductor muscle forces do not influence the strain distribution of the proximal femur. As shown in section 2.8.2 Standard Femoral Model, this assumption is supported by Speirs, Heller et al. (2007) and Correa, Crossley et al. (2010), who demonstrated that additional loading sources outside of the standard femoral model have little to no influence on the loads and strains experienced by the proximal femur. As such, the standard femoral model has been accepted by the biomechanical society as an accurate representation of the strains experienced by the proximal femur and as such is used in hip implant design (Basu 2017).

To accurately represent the loads being applied to the subjects' femur in this study, the musculoskeletal loads were taken from studies which specifically investigated loading during walking, stair climbing and hopping/jumping. These are Heller, Bergmann et al. (2005) and Cleather, Goodwin et al. (2011); both of which are based on clinical observations and are calculated using the body mass of each subject and are discussed in 2.9.3 Published and Open Source Muscle Force Models. The use of musculoskeletal loads which incorporated subject specific mass was considered to be more accurate than musculoskeletal loads which give the same single value loads for every subject, such as those from Turner, Anne et al. (1997). Nonetheless, body mass is not a completely intersubjective variable; as there are many factors which contribute to it (e.g. height, muscle mass, fat mass), and as such, there may be some deviation from the actual and simulated loads.

The results obtained from these loads are considered to be reasonably accurate following the strain validation discussed in section 3.6.1 Model and Strain Validation. Nonetheless, this is an area where subject specificness comes at a trade-off with mass-application. To obtain exact femoral loading for an individual, the use of internal strain gauges is needed. However, these are time consuming, dangerous and not directly applicable to multiple subjects. Studies into the mass application of loads, while maintaining subject specificness have found that using subject mass is the most accurate method of quantitative mass-application of subject specific loads, however they have to be accepted with an error margin (Bergmann, Deuretzbacher et al. 2001, Heller, Bergmann

et al. 2001, Heller, Bergmann et al. 2005, Cleather and Bull 2010, Cleather, Goodwin et al. 2011, Modenese, Phillips et al. 2011, Cleather, Goodwin et al. 2013). This being said, with the bone being linear elastic under physiological loads (Hansen, Zioupos et al. 2008, Juszczyk, Cristofolini et al. 2011) and thus modelled as such in this study, any deviation in the calculated loads from the actual loads will not influence the strain distribution and will only have a linear effect on the strain magnitude, which should not affect the stimulus-remodelling relationship results.

3.6.4 Strain Artefacts

Strain artefacts are always a possibility in simulations of the femur, which can be caused by a variety of factors, such as presence of a muscle attachment and high bone density pockets. Studies have produced methods to minimise the likelihood of encountering artefacts in identifying areas of the proximal femur avoid when conducing biomechanical and bone remodelling analysis (Bitsakos, Kerner et al. 2005, Modenese, Phillips et al. 2011). Which as described in section 4.2.1 Change in Density Measurement, are employed in this study. Nonetheless, they can still occur, in many cases unpredictably.

A strain deviation in the form of an artefact was observed in this study, in the medial face of a single subject, as shown in Figure 3-11, and highlighted Figure 3-15. As shown in Figure 3-15, this artefact is more easily noticed in hopping, however a presence is observable in walking and stair climbing. This suggests that the artefact is not the result of an error in the simulation, but likely the result of a physiological anomaly in this subject, which is adversely affecting the simulation. Therefore, this could be representative of a true strain abnormality experienced by the subject, however, one must remain mindful that the simulation may be magnifying this abnormal strain. The same subject also experienced a strain shift of the peak principal strain. It is unclear as to why this has occurred, and whether it is a result of the identified strain artefact or due to individual jumping style, geometry and density distribution, all of which have been demonstrated influence the strain distribution (Helgason, Taddei et al. 2008, Lenaerts, De Groote et al. 2008).

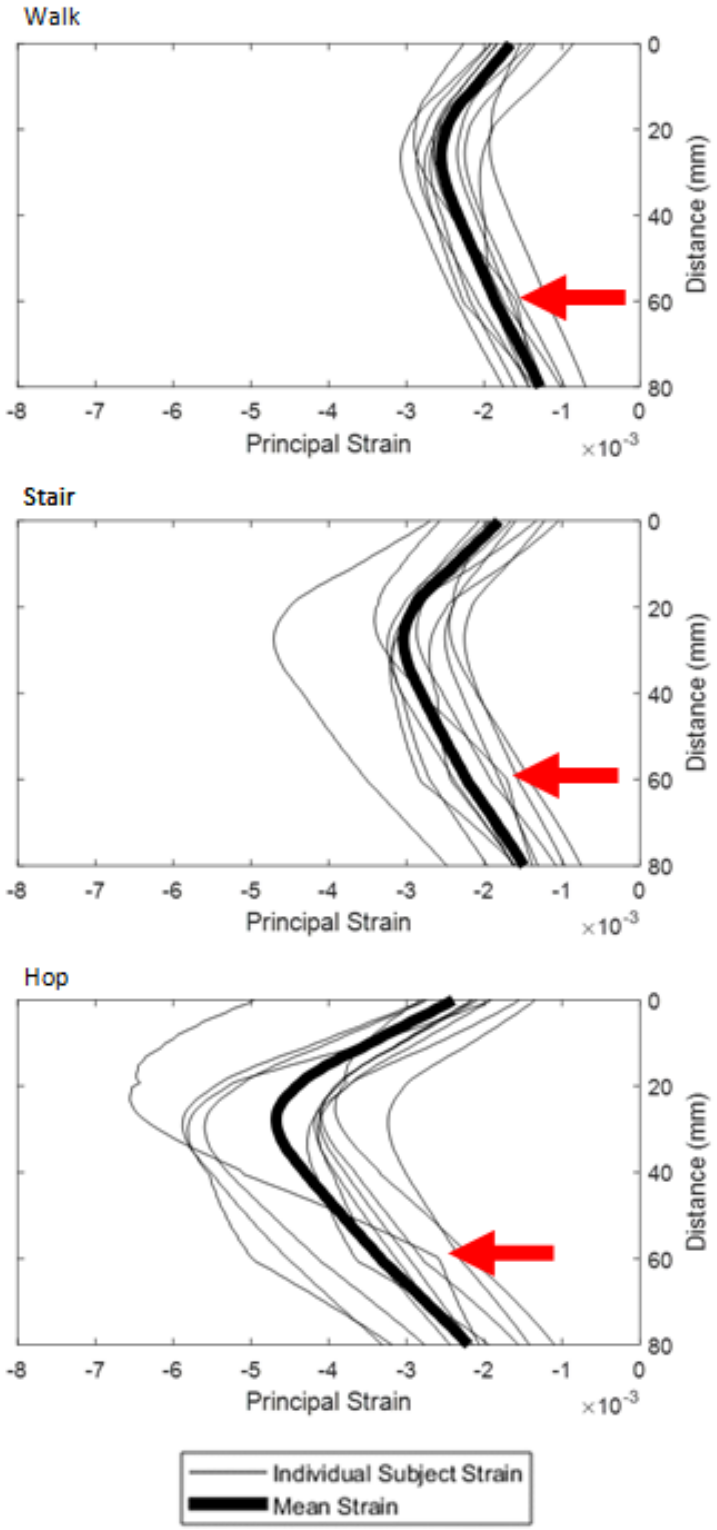

Figure 3-15: Principal strain of each subject on the medical face (shown in Figure 3-11) for walking, stair climbing and hopping, highlighting the strain artefact experienced by a single subject.

3.6.5 Strain Magnitude and Bone Remodelling

Different studies use different definitions of what is included in the bone remodelling stimulus. For this study, using equation 4-1, the bone remodelling stimulus (also called the strain stimulus), S, is the magnitude of the strain being experienced by the bone during the new loading, ε, minus the reference strain, ε_o, as shown by equation 3-7.

$$S = (\varepsilon - \varepsilon_o) \qquad 3\text{-}7$$

Using this definition of the bone remodelling stimulus, and using the two stimuli discussed in section 4.2 Methodology, of hopping minus walking ($\varepsilon_{\text{hop}} - \varepsilon_{\text{walk}}$) and hopping minus stair climbing ($\varepsilon_{\text{hop}} - \varepsilon_{\text{stair}}$), the strain stimuli in this study are in the order of 10^{-4}. Mechanically, this is considered a small, almost infinitesimal, strain magnitude. However, in orthopaedics, this is still a relevant magnitude which obtains bone remodelling responses. Once bone remodelling has been initiated by the mechanical stimulus, the remodelling stimulus only requires a small strain magnitude to elicit a remodelling response (change in density). Numerous different stimuli aside from equation 3-7 have been proposed, as such it can be difficult to quantity the exact bone remodelling response in relation to a particular stimulus value. Furthermore, the remodelling response is dependent on numerous subject specific biological factors, as discussed in Chapter 2. Nonetheless, typically when using strain-based stimuli, the positive bone remodelling response occurs within the stimulus range of 1000-4000 με (10-40 $\times 10^{-4}$ ε), as shown in Figure 3-16 (Hsieh and Turner 2001, Frost 2003, McGarry, Klein-Nulend et al. 2005, Troy, Mancuso et al. 2018).

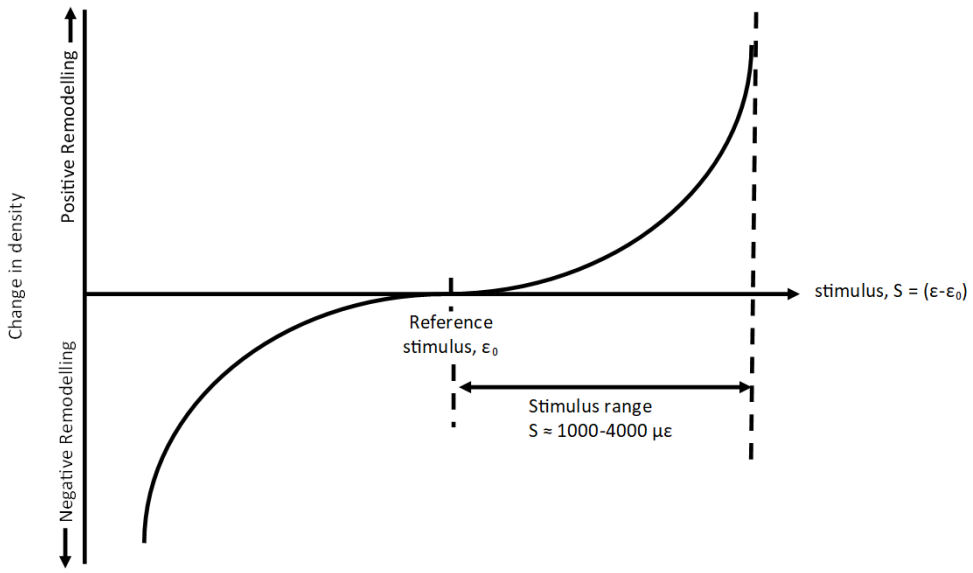

Figure 3-16: The typical bone remodelling response and stimulus range for positive bone remodelling, when using a strain-based stimulus

However, when assessing the bone remodelling response to the strain magnitude, it is important to note that with a lack of a lasy-zone, as stated in the continual remodelling theory, bone remodelling will not occur immediately and automatically in response to any strain above or below the reference strain, as it must first be initiated. For positive bone remodelling, there are numerous bone remodelling initiation processes, where some strain magnitudes are large enough to initiate bone remodelling, such as if they are high enough to create linear microdamage. Alternatively, bone remodelling can be initiated through other processes, such as the random natural apoptosis of osteocytes, which occurs to approximately 2% of the osteocytes in healthy adults per year (Parfitt 2002).

3.6.6 Anatomical Location and Inherited Assumptions

In this study, in order to be able to calculate the bone remodelling in response to the mechanical stimulus, different locations of the proximal femur need to be examined, where different changes in density can be plotted against different mechanical stimuli values. However, in comparing the observations made from different locations of the proximal femur, an inherited assumption is made in this study: that the bone remodelling response to the stimuli is the same and will remodel at the same rate same across the entire proximal femur, with the exception of the tensile and compressive regions. However, following the continual remodelling theory, if different areas of the bone, even

in a local environment, such as the proximal femur, have different reference stimuli, then could different areas of the bone in the same subject have different remodelling rates and behaviours?

The assumption that the same bone remodelling behaviour applies across large areas is commonly made in bone remodelling studies, including those which focus on the proximal femur. Where, in these studies, assuming that bone remodelling rate and behaviour are the same across the proximal femur has yielded accurate results (Turner, Anne et al. 1997, Turner, Gillies et al. 2005, van der Meulen and Hernandez 2013, Hambli 2014). Whilst it is accepted that the anatomical location influences the rate of remodelling (Parfitt 2002), very little comparison has been conducted into examining and quantifying the rate and behaviour of bone remodelling in different areas of the body. This is primarily because a study of this nature is extremely complicated since there are several other factors, including: age (Kotiya and Silva 2013), gender related hormones (Kalervo Väänänen and Härkönen 1996), non-gender related hormones (Murrills, Stein et al. 1990), overall health (Cao 2011), non-medicated drugs (Supervia, Nogues et al. 2006) and medicated drugs (Drake, Clarke et al. 2008). Nonetheless, despite differences in the bone remodelling rate being identified across the body, the same bone remodelling behaviours are usually applied across the entire skeletal system and bone remodelling rates are grouped together and reported within anatomical regions, with the femur being one (Parfitt 2002). As such, the assumption that bone remodelling rate and behaviour is the same across the proximal femur can be considered a safe assumption.

3.6.7 Potential Influence on Results

The critical evaluation of the finite element model has identified different limitations and potential sources of error in the simulated strains and their use in the bone remodelling algorithm to determine bone remodelling behaviour. Whilst none of the identified limitations and potential error sources have been demonstrated to introduce any significant error, they all introduce a slight chance of error. These errors are likely to be unpredictable, and as such, any findings and conclusions made in this study using these strains, need to be made with the knowledge that errors could have been introduced. However, the errors that could be introduced will have different effects on different subjects, and as such, consistency observed within the results indicates a low level of error being introduced.

Chapter 4. Bone Remodelling Observations

4.1 Introduction

Bone remodelling is currently assumed to follow the same general stimulus-remodelling relationship throughout the entire bone/skeletal system under physiological loading conditions, regardless of whether the bone is experiencing tension or compression (Burr 2002, Parfitt 2004, Hadjidakis and Androulakis 2006, Colloca 2009, Bougherara, Klika et al. 2010, Eriksen 2010). Despite this, Chapter 2 has provided evidence that alternative bone remodelling behaviour can occur between tension and compression. The current studies into alternative bone remodelling behaviour are either laboratory-based, where conditions in which alternative bone remodelling behaviours are known to occur are induced (Bentolila, Boyce et al. 1998, Stokes, Gwadera et al. 2005, Herman, Cardoso et al. 2010), or pathologically based; where alternative bone remodelling behaviours are clearly present (Stokes and Laible 1990, Villemure, Aubin et al. 2004, Lin 2010). No study has been conducted into if alternative bone remodelling behaviour under tension and compression is present in 'everyday' loading conditions. The aim of this Chapter, following the aim of this study (see 2.10 Study Aim), is to investigate if alternative bone remodelling behaviour between tension and compression can be observed and quantified in conditions induced by physiological loading.

4.2 Methodology

To determine bone remodelling behaviour of the subjects which had passed the inclusion criteria, quantifiable differences in the bone remodelling response to the stimulus needed to be determined. It was deemed that the best method to achieve this was to use regression analysis against a previously established bone remodelling algorithm. This method was chosen as bone remodelling algorithms have already been demonstrated to be well established in determining stimulus-remodelling relationships and detail what stimuli need to be accounted for.

Multiple different bone remodelling algorithms are used in self-design simulations, which can often include numerous assumptions. However, since this is an observational-based study, it was felt that using a simple bone remodelling algorithm would be best to limit the number of factors, assumptions and unknowns which could influence the results. With clinical evidence that the lazy zone does not exist (Christen, Ito et al. 2014) and that each area of the bone has an independent reference stimulus (van der Meulen and Hernandez 2013): A nonlinear bone remodelling algorithm based on continual remodelling (van der Meulen and Hernandez 2013) was chosen to quantify the bone remodelling response, as shown in equation 4-1.

$$\frac{\partial \rho}{\partial t} = k(\varepsilon - \varepsilon_o)^b \qquad 4\text{-}1$$

Where $\frac{\partial \rho}{\partial t}$ is the percentage change in density over the year period, k is a rate constant, b is a power law constant, ε is the peak magnitude, absolute, principal strain ($|\varepsilon_{\text{peak}}|$) as a result of the new stimulus ('new strain'), and ε_o is the peak magnitude, absolute, principal strain ($|\varepsilon_{\text{peak}}|$) as a result of the old stimulus ('reference strain'). Using the subject specific strain as described in Chapter 3, two stimuli were calculated for each subject individually to meet this stimulus, which best represented the activities of the subjects from the Allison, Folland et al. (2013) clinical trial, these being: 1) Hop-Walk: The absolute peak magnitude principal strain as a result of hopping ($|\varepsilon_{\text{peak}}|_{hop}$) minus the absolute peak magnitude principal strain as a result of walking ($|\varepsilon_{\text{peak}}|_{walk}$), shown in equation 4-2.

$$\text{Hop} - \text{Walk} = (\varepsilon_{\text{hop}} - \varepsilon_{\text{walk}}) \qquad 4\text{-}2$$

2) Hop-Stair: The absolute peak magnitude principal strain as a result of hopping ($|\varepsilon_{\text{peak}}|_{hop}$) minus absolute peak magnitude principal strain as a result of stair climbing ($|\varepsilon_{\text{peak}}|_{stair}$), shown in equation 4-3.

$$\text{Hop} - \text{Stair} = (\varepsilon_{\text{hop}} - \varepsilon_{\text{stair}}) \qquad 4\text{-}3$$

4.2.1 Change in Density Measurement

The subject specific change in density was measured using *Materialise Mimics Research version 19.0*, where the bone density was measured in both the pre- and post-exercise femur. Based on the strain distribution observed by the finite element models in Chapter 3, twenty points in the proximal femur were chosen to investigate bone remodelling behaviour. These comprised of five points on each of the anterior, posterior, medial and lateral faces which remained consistently in either tension or compression; this resulted in ten points in compression and ten points in tension as shown in Figure 4-1. Although the trochanters demonstrated the highest change in density in the clinical exercise trial (Allison, Poole et al. 2015), all muscle attachment areas were avoided as they have been demonstrated to introduce artefacts and can have a negative effect on the results (Bitsakos, Kerner et al. 2005, Modenese, Phillips et al. 2011). Similarly, the bottom face of the truncated femur was also avoided by a minimum of 5 mm to prevent any influence of the constraint.

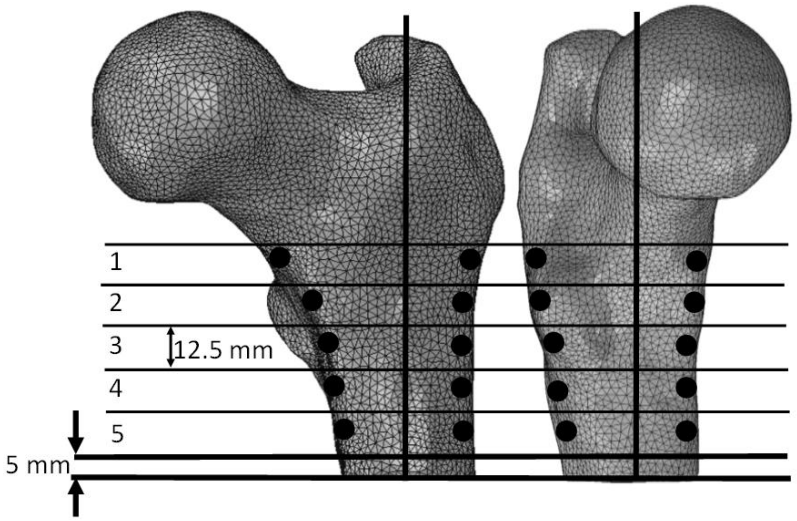

Figure 4-1: Path point positions on the anterior, posterior, medial and lateral faces, used in this study.

To account for heterogeneous bone remodelling as described in 2.5.7 Heterogeneous Bone Remodelling, a convergence study determining the influence of the three dimensional radius on the density measurement around the selected point was conducted. Mechanistic models were considered an inappropriate method to account for heterogenous remodelling in this study, as they are highly complicated and are based on pre-set bone remodelling assumptions which may

interfere with the results. Following methodology for mesh convergence (Zannoni, Mantovani et al. 1998, Burkhart, Andrews et al. 2013) the optimum sample volume was decided by a 1% agreeance, which determined the optimum diameter to be 6 mm, as shown in Figure 4-2. This is similar in size to other sample volumes used in studies comparing clinical data to remodelling algorithms, particularly in the proximal femur (Turner, Anne et al. 1997, Bitsakos, Kerner et al. 2005), as shown in Figure 4-3.

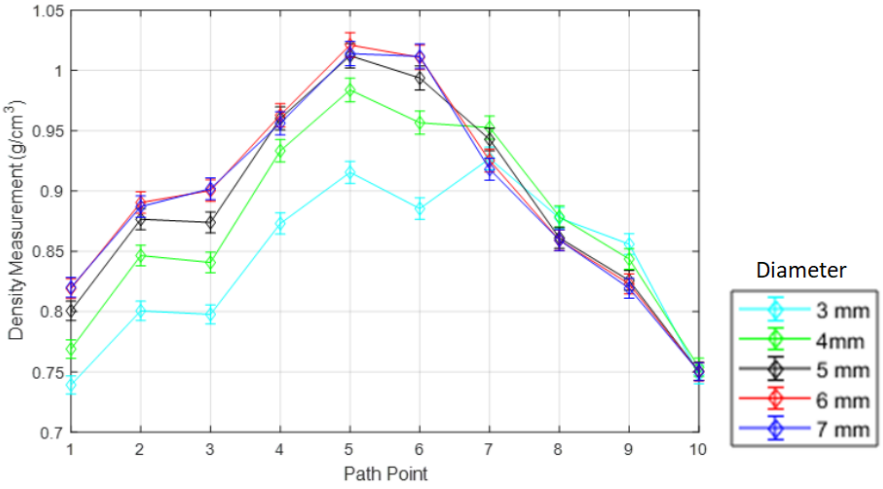

Figure 4-2: Sample size convergence study from different points of one subject with error bars showing 1 % agreeance where points 1-5 are in compression and 6-10 are in tension.

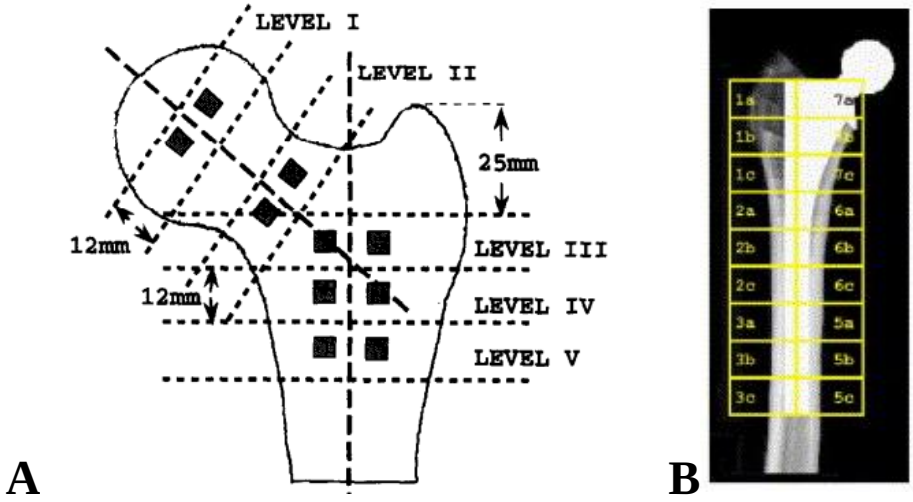

Figure 4-3: Remodelling prediction areas used in Turner, Anne et al. (1997) (A) and Bitsakos, Kerner et al. (2005) (B)

The decision was made to only use cortical bone in this study. This was achieved by placing the sample points within the cortical area of the bone and rejecting any bone with a density value of $0.5\ g/cm^3$ or less which was considered to be trabecular (Treece and Gee 2015). This decision was based on several factors, primarily, on average cortical bone demonstrated a higher change in density than trabecular bone (Allison, Folland et al. 2013, Allison, Poole et al. 2015) increasing the chance of observing alternative bone remodelling. Furthermore in comparison to cortical bone (Speirs, Heller et al. 2007) the strain in the trabecular bone is relatively understudied and remodelling in the trabecular bone can involve architectural changes which are not reflected by a change in density on the macro scale (Vahdati and Rouhi 2009). It was also felt that that the qCT scans did not have a high enough resolution to adequately detail the trabecular change in microarchitecture: where to accurately observe changes in trabecular bone in humans requires micro-qCTs, with a resolution of approximately 20 μm (Depalle, Chapurlat et al. 2013), which was not available in this study

In this study the percentage change in density was used in the remodelling algorithms to give a clearer picture of the proportionate change in density in relation to the stimulus. Due to the strong linear correlation observed between the change in density as a percentage, or grams per centimetre cubed (g/cm^3), as shown by Figure 4-4, the study found the two density measurement methods to be interchangeable with no addition of any errors.

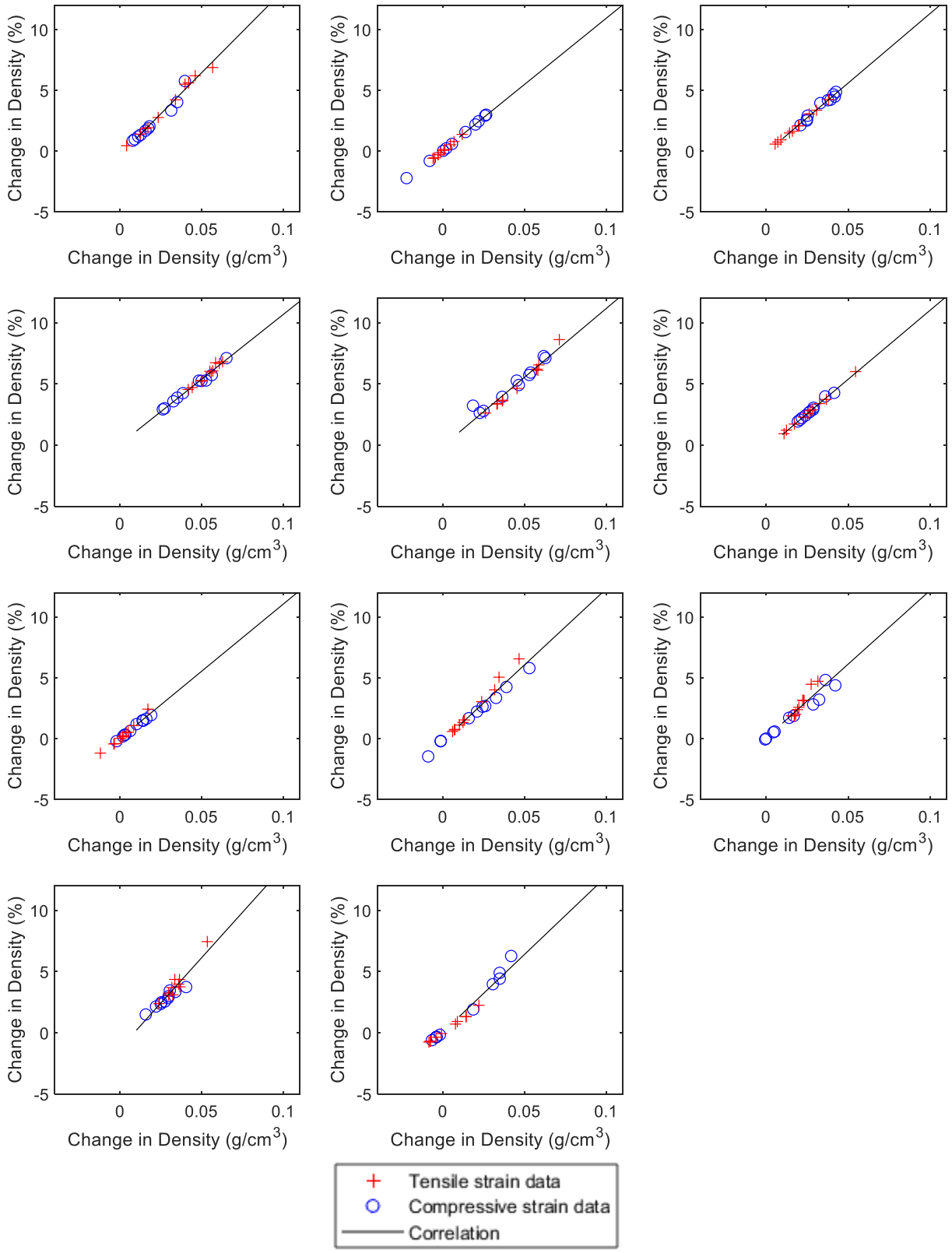

Figure 4-4: Correlation between change in density measurements using g/cm^3 and percentage change in density, for each subject in this study in the tensile and compressive path points shown in Figure 4-1, where subject 1 is top left, with incremental subjects going left to right.

4.3 Preliminary Study

Current bone remodelling theory and algorithms do not differentiate between the tensile and compressive regions and so this study conducted an initial investigation into this method. This was done so, for each subject, without differentiating between tension and compression. The aim of this was to act as a blind study, in an attempt to eliminate any notions or biases and to examine the stimulus-remodelling relationships used by current studies and algorithms. Using the methodology described in 4.2 Methodology, the stimulus-remodelling relationships for the general (whole proximal femur) strain data set were determined for each of the 11 subjects used in this study, with the results shown in Figure 4-5 and Figure 4-6. The individual subjects rate constant (k) and power law (b) values for the general stimulus-remodelling relationship obtained via the regression analysis, for both the Hop-Walk and Hop-Stair loading scenarios are shown in Table 4-1. The goodness of fit of the regression analysis determined stimulus-remodelling relationships to the general strain data set was assessed using the coefficient of determination (R^2) and RMSE statistical tests (as described in A.2 Goodness of Fit Analysis) in *MATLAB version R2017b*, with the results shown in Table 4-2.

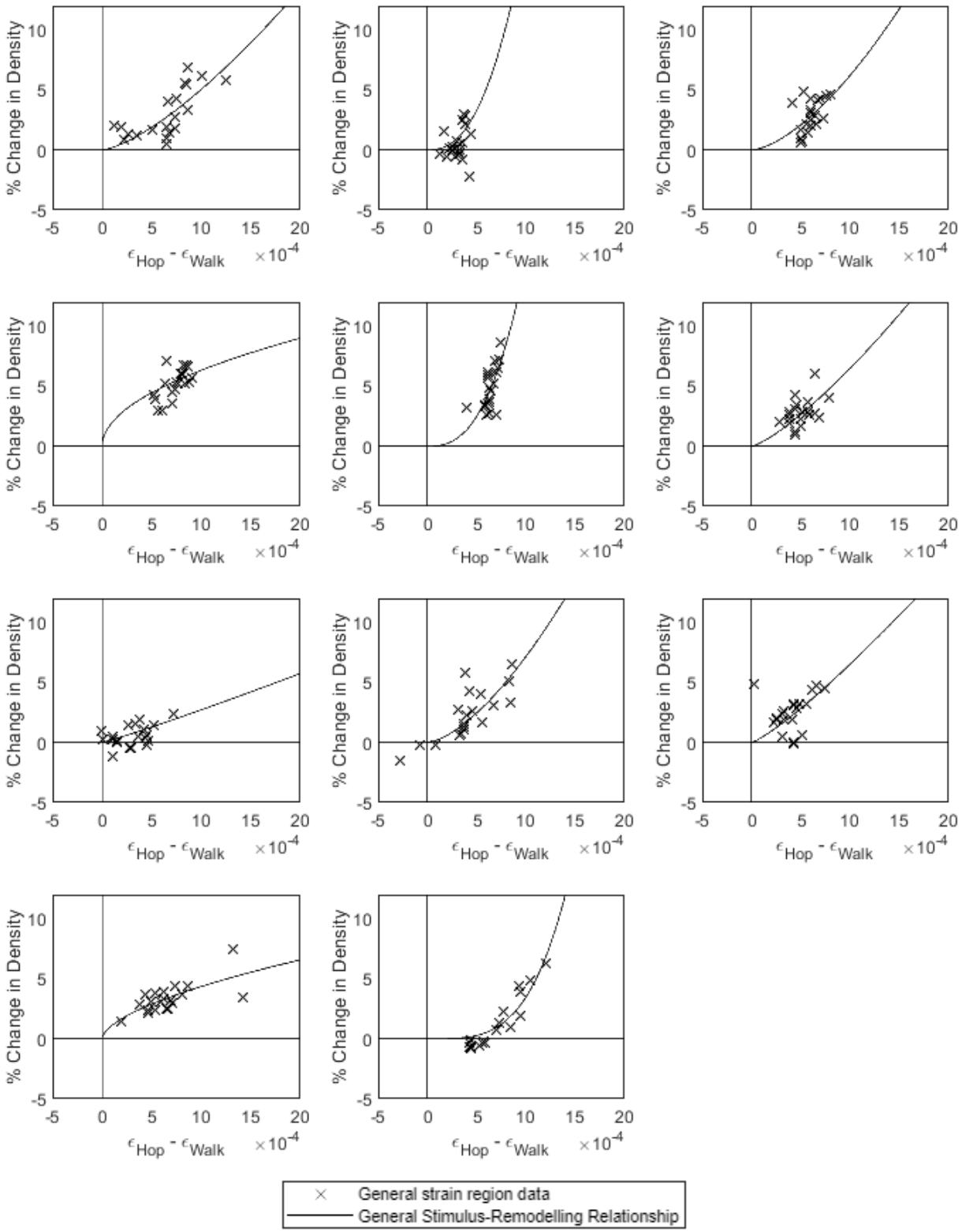

Figure 4-5: All subjects general strain data set stimulus-remodelling plots and relationships for the Hop-Walk loading scenario, where subject 1 is top left, with incremental subjects going left to right.

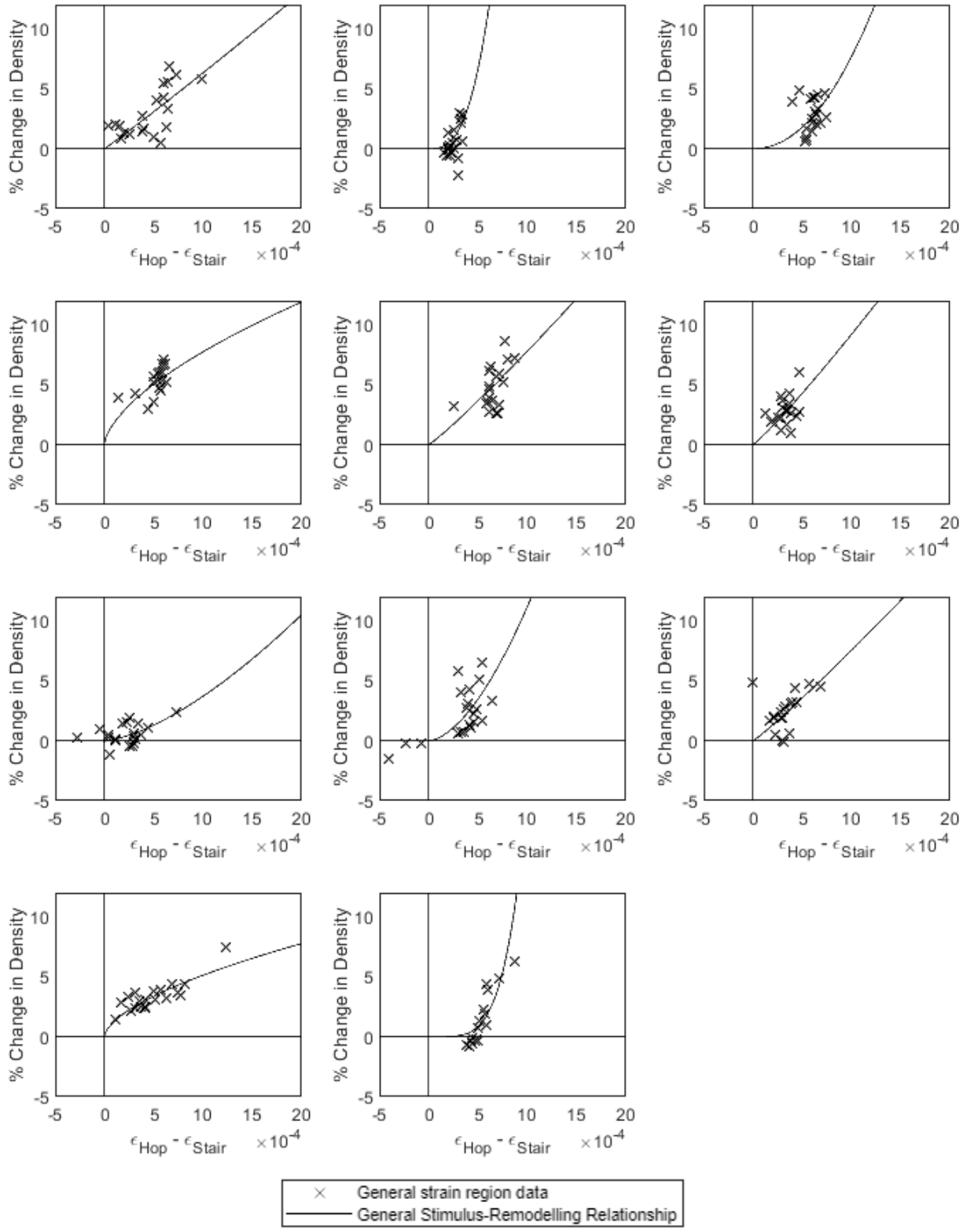

Figure 4-6: All subjects general strain data set stimulus-remodelling plots and relationships for the Hop-Stair loading scenario, where subject 1 is top left, with incremental subjects going left to right.

Table 4-1: Subjects' rate constant (k) and power law constant (b) under the Hop-Walk and Hop-Stair loading scenarios for the general (combined) strain data sets

	Hop-Walk		Hop-Stair	
Subject	**k**	**b**	**k**	**b**
1	9.14×10^{4}	1.42	8.32×10^{3}	1.04
2	3.74×10^{8}	2.44	2.30×10^{10}	2.89
3	3.23×10^{5}	1.57	1.53×10^{7}	2.10
4	2.12×10^{2}	0.51	5.61×10^{2}	0.62
5	1.17×10^{9}	2.63	1.56×10^{4}	1.10
6	5.12×10^{4}	1.30	1.84×10^{4}	1.10
7	4.72×10^{3}	1.08	1.20×10^{5}	1.50
8	3.09×10^{5}	1.55	1.22×10^{6}	1.68
9	2.67×10^{4}	1.20	1.40×10^{4}	1.09
10	2.67×10^{2}	0.60	3.23×10^{2}	0.60
11	3.81×10^{11}	3.68	8.93×10^{14}	4.55
Mean	4.75×10^{21}	1.63	8.91×10^{18}	1.66
Median	3.23×10^{5}	1.42	1.56×10^{4}	1.10
SD	1.57×10^{22}	0.94	2.82×10^{19}	1.11

Table 4-2: R^2 and RMSE values of the stimulus-remodelling relationship for the general strain data set for both the Hop-Walk and Hop-Stair loading scenarios

Subject	**Hop-Walk Scenario**		**Hop-Stair Scenario**	
	R^2	**RMSE**	**R^2**	**RMSE**
1	0.54	1.84	0.44	1.83
2	0.28	1.05	0.46	1.14
3	0.25	1.22	0.01	1.40
4	0.42	0.99	0.34	1.03
5	0.42	1.37	0.23	1.69
6	0.20	1.39	0.10	1.18
7	0.38	0.69	0.37	0.69
8	0.79	1.10	0.38	1.86
9	0.49	1.65	0.61	1.13
10	0.47	0.91	0.66	0.73
11	0.84	0.89	0.70	2.04
Mean	0.46	1.19	0.39	1.34
Median	0.42	1.10	0.38	1.18
SD	0.20	0.35	0.22	0.46

All subjects displayed a positive correlation between the stimulus and the change in density. On average, the Hop-Walk loading scenario achieved a higher R^2 and lower RMSE than the Hop-Stair loading scenario, with a mean R^2 of 0.46 and a mean RMSE of 1.19 suggesting that the Hop-Walk loading scenario may be more closely related to the true stimulus experienced by the subjects used

in this study. Nonetheless, based on previous studies on the influence of mechanical stimuli on the bone density in humans (Troy, Mancuso et al. 2018), the correlations of the change in density with the stimulus from both the Hop-Walk and Hop-Stair loading scenarios were considered to be good.

The power law constant (b value) was considered to be more indicative of the stimulus-remodelling relationship than the rate constant (k), as the b value is typically used to describe the stimulus-remodelling relationship. It was observed that numerous subjects experienced atypical stimulus-remodelling relationships ($b < 1$) in the Hop-Walk and Hop-Stair scenarios, which is explored further in 4.4.2.2 Observed Typical and Atypical Stimulus-Remodelling Relationships. Nonetheless, the mean b value for both the Hop-Walk and Hop-Stair loading scenarios are very similar at 1.63 and 1.66. There are numerous factors which influence bone remodelling (Robling and Turner 2009) so one could easily assume that any variation from the stimulus-remodelling relationship is the result of one of these factors. Interestingly, there were no obvious signs of alternative bone remodelling displayed by any of the subjects, where overall, the stimulus-remodelling plots demonstrated what appeared to be consistent singular stimulus-remodelling relationships. Therefore, the results of this preliminary study would suggest that the same overall stimulus-remodelling relationship is followed throughout the proximal femur, validating the use of a single stimulus-remodelling relationship in bone remodelling simulations.

4.4 Observed Alternative Bone Remodelling

Despite the results of the preliminary study, Chapter 2 describes how alternative bone remodelling has been observed in laboratory and pathological conditions. Using the methodology previously described in 4.2 Methodology, the stimulus-remodelling relationships for the tensile and compressive strain data set were determined for each of the 11 subjects used in this study, with the results shown in Figure 4-7 and Figure 4-8. The individual subjects rate constant (k) and power law (b) values obtained in the regression analysis for the general, tensile and compressive stimulus-remodelling relationships, for both the Hop-Walk and Hop-Stair loading scenarios are shown Table 4-3 and Table 4-4.

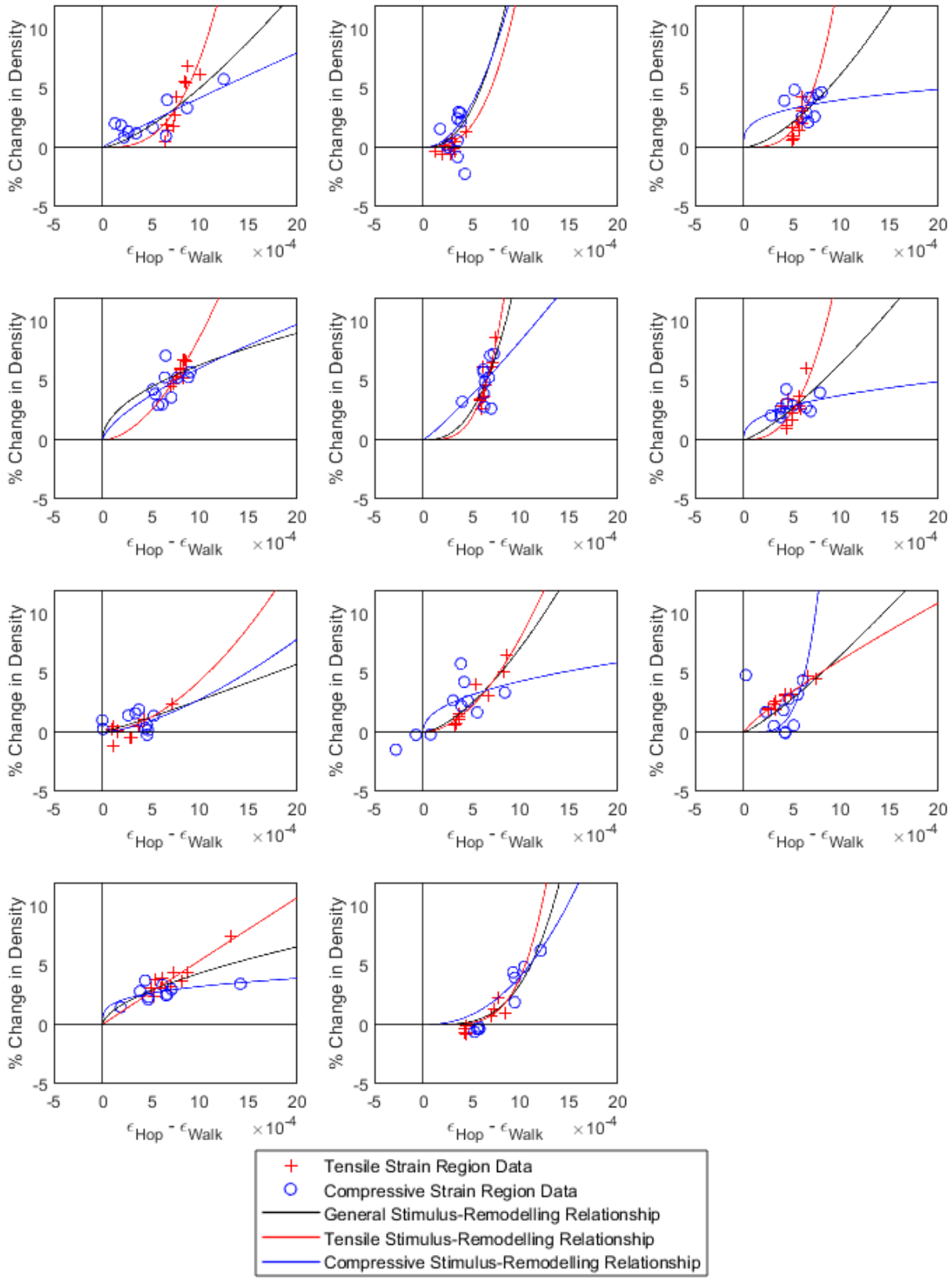

Figure 4-7: All subjects stimulus-remodelling responses in all three strain data sets in the Hop-Walk loading scenario, where subject 1 is top left, with incremental subjects going left to right.

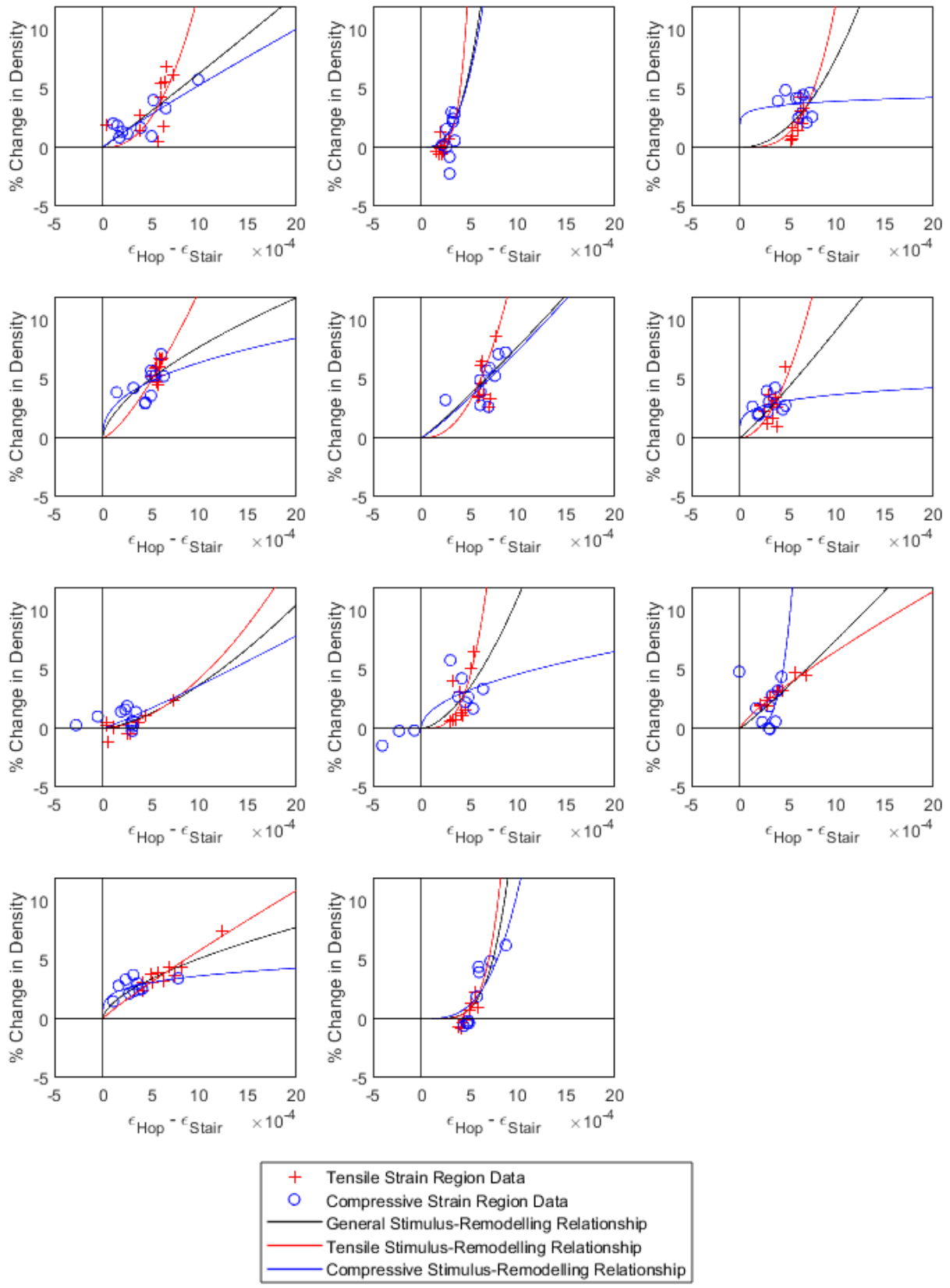

Figure 4-8: All subjects stimulus-remodelling responses in all three strain data sets in the Hop-Stair loading scenario, where subject 1 is top left, with incremental subjects going left to right.

Table 4-3: Subjects' rate constant (k) and power law constant (b) under the Hop-Walk loading scenario for the stimulus-remodelling relationships in the general (combined), tensile and compressive strain data sets.

	General		Tension		Compression	
Subject	**k**	**b**	**k**	**b**	**k**	**b**
1	9.14×10^{4}	1.42	5.35×10^{9}	2.95	2.64×10^{3}	0.93
2	3.74×10^{8}	2.44	7.11×10^{9}	2.90	3.17×10^{7}	2.10
3	3.23×10^{5}	1.57	2.29×10^{11}	3.39	29.75	0.29
4	2.12×10^{2}	0.51	2.29×10^{6}	1.81	690	0.69
5	1.17×10^{9}	2.63	2.10×10^{12}	3.65	2.20×10^{4}	1.14
6	5.12×10^{4}	1.30	1.37×10^{9}	2.65	54.3	0.39
7	4.72×10^{3}	1.08	8.85×10^{5}	1.77	8.79×10^{4}	1.50
8	3.09×10^{5}	1.55	3.19×10^{6}	1.87	96.3	0.45
9	2.67×10^{4}	1.20	2.00×10^{3}	0.84	4.55×10^{14}	4.36
10	2.67×10^{2}	0.60	4.89×10^{3}	0.99	21.7	0.28
11	3.81×10^{11}	3.68	2.93×10^{14}	4.62	2.87×10^{7}	2.28
Mean	3.48×10^{10}	1.63	2.68×10^{13}	2.49	4.13×10^{13}	1.31
Median	3.14×10^{4}	1.42	1.37×10^{9}	2.65	2.64×10^{3}	0.93
SD	1.15×10^{11}	0.94	8.82×10^{13}	1.11	1.37×10^{14}	1.17

Table 4-4: Subjects' rate constant (k) and power law constant (b) under the Hop-Stair loading scenario for the stimulus-remodelling relationships in the general (combined), tensile and compressive strain data sets.

	General		Tension		Compression	
Subject	**k**	**b**	**k**	**b**	**k**	**b**
1	8.32×10^{3}	1.04	2.00×10^{8}	2.39	3.11×10^{3}	0.92
2	2.30×10^{10}	2.89	9.32×10^{18}	5.38	6.87×10^{9}	2.74
3	1.53×10^{7}	2.10	2.22×10^{11}	3.42	8.38	0.11
4	5.61×10^{2}	0.62	1.61×10^{5}	1.37	105	0.40
5	1.56×10^{4}	1.10	2.05×10^{8}	2.37	1.84×10^{4}	1.13
6	1.84×10^{4}	1.10	1.50×10^{7}	1.95	15.8	0.21
7	1.20×10^{5}	1.50	1.13×10^{6}	1.81	7.31×10^{3}	1.10
8	1.22×10^{6}	1.68	5.57×10^{11}	3.36	146	0.50
9	1.40×10^{4}	1.09	1.93×10^{3}	0.82	8.05×10^{15}	4.54
10	3.23×10^{2}	0.60	3.09×10^{3}	0.91	19.23	0.24
11	8.93×10^{14}	4.55	3.15×10^{17}	5.32	3.88×10^{10}	3.18
Mean	8.12×10^{13}	1.66	8.75×10^{17}	2.65	7.35×10^{14}	1.37
Median	1.56×10^{4}	1.10	2.00×10^{8}	2.37	3.11×10^{3}	0.92
SD	2.57×10^{14}	1.11	2.80×10^{18}	1.51	2.31×10^{15}	1.40

As observed in Figure 4-7 and Figure 4-8, both the tensile and compressive stimulus-remodelling relationships demonstrated positive correlations between the stimulus and the change in density for all subjects, much like the general stimulus remodelling relationships, detailed in 4.3 Preliminary Study. Aside from the occasional result which could be classed as abnormal, such as the high change in density at low stimulus in compression in subject 9; no obvious major abnormalities in the stimulus-remodelling relationships were observed in either the tensile or compressive strain regions.

In some subjects, differences in the tensile and compressive stimulus-remodelling relationships were easily and immediately observed. Alternatively, in the majority of subjects the tensile and compressive stimulus-remodelling relationships were quite overlapped, particularly at the lower stimuli, so the differences only became apparent when the stimulus-remodelling relationships were plotted by the regression analysis curves. This similarity at lower strains could have contributed to the lack of any prior observation of alternative bone remodelling in the proximal femur under physiological loading conditions, where any differences in the stimulus-remodelling relationships could easily be attributed to small random variations in the data causing for slight variations in the stimulus-remodelling relationships under tension and compression. However, using the regression analysis curves, differences in the tensile and compressive relationships were observed in all subjects, with the amount of difference in the tensile and compressive stimulus-remodelling relationships varying with each subject. From this, three consistent differences were qualitatively observed in Figure 4-7 and Figure 4-8, suggesting that there is a consistent difference in the tensile and compressive stimulus-remodelling relationships.

The first of these observations was that the tensile and compressive stimulus-remodelling relationships consistently differentiated from each other as the stimulus increased, where the value at which the relationships differentiate from each other is explored further in section 4.4.2.3.1 Cross-Over Point. It is thought that the increasing difference between the stimulus-remodelling relationships could be the increasing effects of the alternative bone remodelling mechanisms with the stimulus, which is explored further in section 5.2 Potential Alternative Bone Remodelling Mechanisms Acting in This Study.

The second observation was that the compressive stimulus-remodelling relationship consistently had a wider variance in the change in density in response to the stimulus in comparison to the tensile stimulus-remodelling relationship. This is explored further in section 4.4.1 Goodness of Fit. The third observation was that the compressive stimulus-remodelling relationship was more likely to be atypical in profile, in comparison to the tensile stimulus-remodelling relationship, which is explored further in section 4.4.2.2 Observed Typical and Atypical Stimulus-Remodelling Relationships.

4.4.1 Goodness of Fit

The goodness of the fit of the regression analysis determined tensile and compressive stimulus-remodelling relationships was assessed using the R^2 and RMSE statistical tests (as described in A.2 Goodness of Fit Analysis) in *MATLAB version R2017b,* with the results shown in Figure 4-9 and the individual subject-specific R^2 and RMSE values for the 11 subjects used in this study shown in Table 4-5 and Table 4-6.

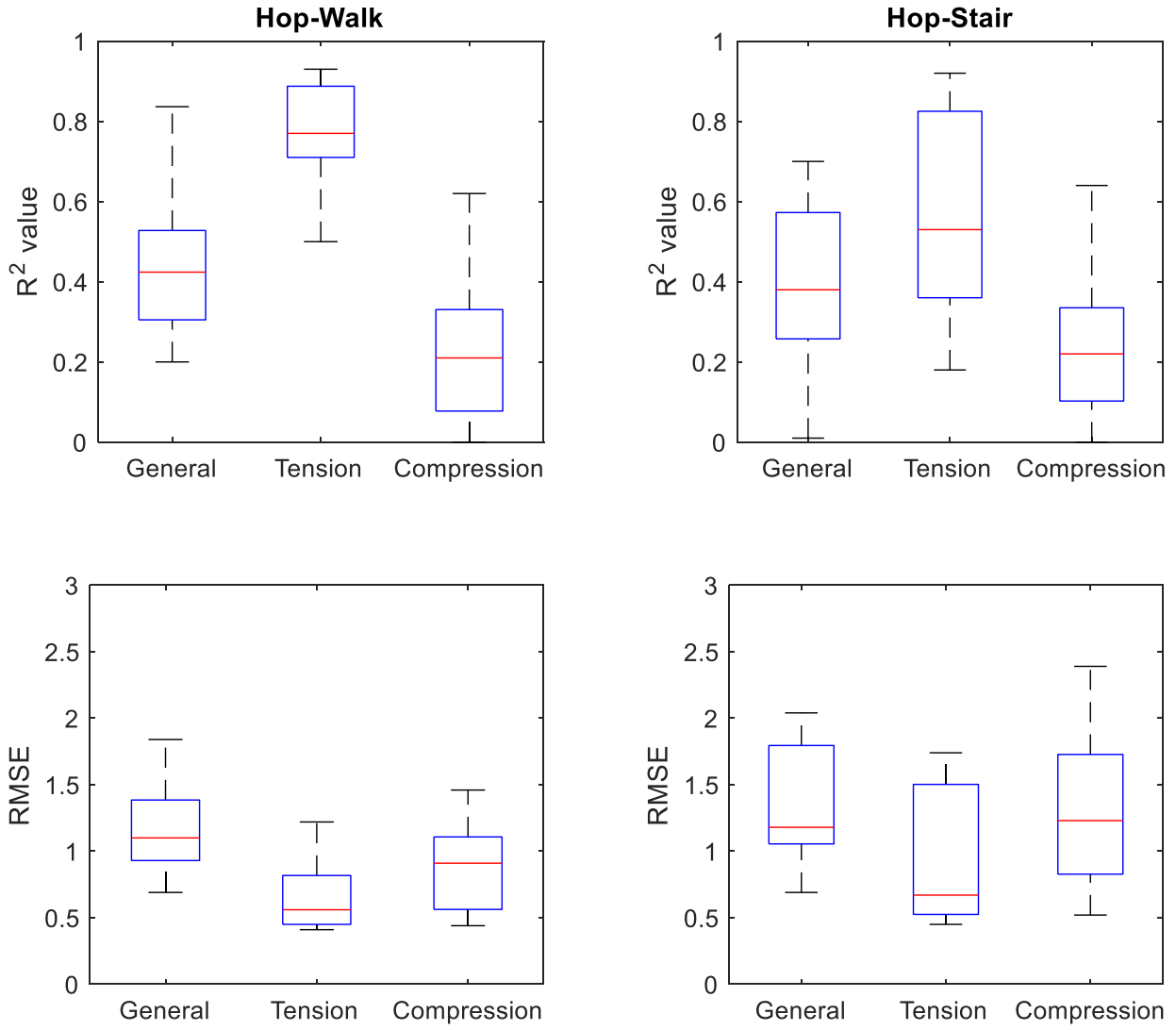

Figure 4-9: Boxplots showing the R^2 and RMSE values of the general, tensile and compressive stimulus-remodelling relationships for all 11 subjects for the Hop-Walk and Hop-Stair loading scenarios, displaying the range (black), standard deviation (blue) and mean (red) values.

Table 4-5: R^2 and RMSE values of the stimulus-remodelling relationship for the Hop-Walk loading scenario for the general, tensile and compressive strain data sets

Subject	General Strain Data Set		Tensile Strain Data Set		Compressive Strain Data Set	
	R^2	RMSE	R^2	RMSE	R^2	RMSE
1	0.54	1.84	0.71	1.22	0.62	0.88
2	0.28	1.05	0.75	0.41	0.00	1.30
3	0.25	1.22	0.77	0.56	0.00	0.95
4	0.42	0.99	0.71	0.42	0.22	1.11
5	0.42	1.37	0.78	0.85	0.20	1.44
6	0.20	1.39	0.50	0.75	0.21	0.66
7	0.38	0.69	0.93	0.53	0.10	0.53
8	0.79	1.10	0.90	0.84	0.07	0.91
9	0.49	1.65	0.93	0.43	0.24	1.46
10	0.47	0.91	0.85	0.51	0.36	0.51
11	0.84	0.89	0.59	0.64	0.59	1.10
Mean	0.46	1.19	0.77	0.65	0.24	0.99
Median	0.42	1.10	0.77	0.56	0.21	0.95
SD	0.20	0.35	0.14	0.25	0.21	0.33

Table 4-6: R^2 and RMSE values of the stimulus-remodelling relationship for the Hop-Stair loading scenario for the general, tensile and compressive strain data sets

Subject	General Strain Data Set		Tensile Strain Data set		Compressive Strain Data set	
	R^2	RMSE	R^2	RSME	R^2	RSME
1	0.44	1.83	0.36	1.70	0.64	0.85
2	0.46	1.14	0.18	0.54	0.00	1.42
3	0.01	1.40	0.72	0.61	0.13	0.89
4	0.34	1.03	0.28	0.67	0.22	1.30
5	0.23	1.69	0.53	1.74	0.42	1.23
6	0.10	1.18	0.36	0.91	0.10	0.82
7	0.37	0.69	0.91	0.52	0.35	0.52
8	0.38	1.86	0.59	1.71	0.05	2.00
9	0.61	1.13	0.92	0.45	0.27	1.83
10	0.66	0.73	0.86	0.48	0.29	0.54
11	0.70	2.04	0.49	0.71	0.68	2.39
Mean	0.39	1.34	0.56	0.91	0.23	1.25
Median	0.38	1.18	0.53	0.67	0.22	1.23
SD	0.22	0.46	0.26	0.53	0.19	0.61

Mimicking the general strain data set results, the Hop-Walk loading scenario achieved on average a higher R^2 and lower RMSE than the Hop-Stair loading scenario, suggesting that walking is more closely aligned with the loads experienced by the femur of the subjects prior to the exercise trial

and the Hop-Walk loading scenario is on average more closely aligned with the true stimulus than the Hop-Stair loading scenario.

A clear difference between the tensile and compressive stimulus-remodelling relationships goodness of fit was observed; where a higher tensile R^2 value was observed in 10 of the 11 subjects in Hop-Walk loading scenario, with one anomaly of subject 11. In the Hop-Stair loading scenario, 9 of the 11 subjects experienced a higher tensile R^2 than compressive, with an additional anomaly of subject 1. It is thought that the subject 1 observation could be the result of the Hop-Walk loading scenario being a closer representation of the true loading than the Hop-Stair loading scenario. A possible factor for the subject 11 observation, where the compressive R^2 is higher or the same as the tensile, could be the subject's age, where the R^2 value under tension was observed to increase with age, whilst the R^2 under compression decreased, as discussed in 4.4.4 Correlation of Results with Physiological Variables. Subject 11 has the second lowest age (69 years old) which suggests that he would have a lower R^2 value under tension and a higher R^2 value under compression than the other subjects. Overall, the mean R^2 value under tension (0.77 and 0.56 in the Hop-Walk and Hop-Stair loading scenarios) is significantly higher than the mean R^2 value under compression (0.24 and 0.23 in the Hop-Walk and Hop-Stair loading scenarios) by an approximate factor of two to three depending on the loading scenario. A lower RMSE in tension was only observed in 6 to 7 subjects depending on the loading scenario, but overall the tensile stimulus-remodelling relationship exhibited a significantly smaller mean RMSE (0.65 and 0.91 in the Hop-Walk and Hop-Stair loading scenarios) than the compressive stimulus-remodelling relationship (0.99 and 1.25 in the Hop-Walk and Hop-Stair loading scenarios) by factors of approximately 1.5 to 1.3.

Using the Wilcoxon signed rank test in *IBM SPSS version 26* (as described in A.1.2 Wilcoxon Signed Rank Test), the difference in the tensile and compressive R^2 value was found to be statistically significant at $p < 0.01$ for the Hop-Walk and Hop-Stair loading scenarios. The statistical difference between the tensile and compressive RMSE values using the Wilcoxon signed rank test was found to be significant to $p = 0.1641$ for the Hop-Walk loading scenario and $p = 0.1934$ for the Hop-Stair loading scenario.

4.4.2 Analysis of the Observed Stimulus-Remodelling Relationships

4.4.2.1 Analysis of b and k Values

As shown in Table 4-3 and Table 4-4 a wide variation in the b and k values was observed in the general, tensile and compressive strain data sets, for both the Hop-Walk and Hop-Stair loading scenarios. There is no consistently published, or agreed upon values for the b and k values. Furthermore, both the b and k values can be highly influenced by numerous factors including age (Kotiya and Silva 2013), gender related hormones (Kalervo Väänänen and Härkönen 1996), non-gender related hormones (Murrills, Stein et al. 1990), overall health (Cao 2011), non-medicated drugs (Supervia, Nogues et al. 2006) and medicated drugs (Drake, Clarke et al. 2008). As a result, very little has been done by previous studies to provide quantitative values for the b and k values. Those studies which do provide quantitative values, typically only provide a b value and leave the k value to the individual researchers digression (Turner 1999, Frehill 2010). The b values observed in this study are within the range of values suggested by other studies, which are typically between 0.3 and 3. Such a wide range in the b value observed in this study was not expected, although this is not a negative observation, and perhaps show how easily the value can change and be affected by different parameters. With no previously published k values there is little to base the results of this study on, however, again such a wide range of values observed in this study was not expected, where depending on the loading scenario and strain region, the difference in k value observed in this study can range between a factor of 10^{15}. However, despite this huge difference in k values, the difference in the stimulus-remodelling relationships does not seem to represent such a large change, where as in shown in Figure 4-7 and Figure 4-8, all of the stimulus-remodelling relationships remain within similar. Nonetheless, such a large difference in the k values is something to be noted and investigated further.

As shown in Figure 4-10, a strong correlation was observed between the b and k values, in the general, tensile and compressive strain data sets for both the Hop-Walk and Hop-Stair loading scenarios. This is a significant observation as it suggests that the k and b values are interlinked and correlated. With most bone remodelling studies which use or investigate bone remodelling algorithms being of a self-design simulation nature, there have been no prior publications, to the author's knowledge, detailing if the b and k values may be correlated. In setting up this study, no

value for b or k was set or chosen as it was unknown what differences in the tensile and compressive stimulus-remodelling relationships would be observed.

Using the Spearman's rank correlation coefficient test (described in A.1.1 Spearman's Rank Correlation Coefficient Test) in *IBM Statistical Package for the Social Sciences (SPSS) version 26*, the strength of the correlation between the b value and k value for all three strain data sets was determined to be statistically significant to $p < 0.01$ in both the Hop-Walk and Hop-Stair loading scenarios, as shown by Table 4-7.

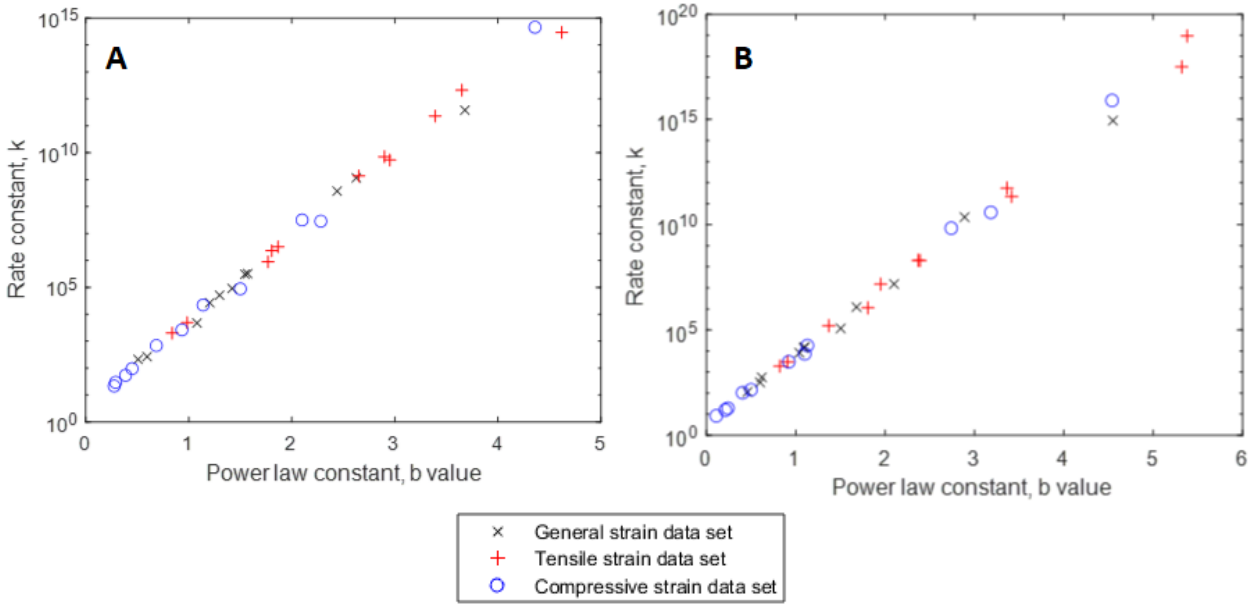

Figure 4-10: Relationship between the b and k values for the general (combined), tensile and compressive strain data sets under both the Hop-Walk (A) and Hop-Stair (B) loading scenarios for the 11 subjects used in this study.

Table 4-7: Spearman's Rho Correlation Coefficients between the b value in the general (combined), tensile and compressive strain data sets for the Hop-Walk and Hop-Stair loading scenarios for the 11 subjects used in this study

	Hop-Walk	**Hop-Stair**
Correlation Coefficient	0.996	0.993
p-value	0.001	0.001

Note: A correlation of |0.1| is considered weak, a correlation of |0.3| is considered moderate and a correlation of |0.5| is considered strong (Field 2018).

The strong correlation also means that one value, in the b and k values, can be calculated by the other. Using regression analysis in *MATLAB version R2017b* the relationships between the b and k values for all three strain data sets were determined to be that shown equation 4-4 for the Hop-Walk loading scenario and equation 4-5 for the Hop-Stair loading scenario.

$$log_{10}(k) = 3.133(b) + 0.5976 \qquad 4\text{-}4$$

$$log_{10}(k) = 3.288(b) + 0.5128 \qquad 4\text{-}5$$

Most bone remodelling studies generalise the stimulus-remodelling relationship over multiple subjects, where typically b values of 0.3 to 3 are used. This is most likely because these values best represent all the data combined over multiple subjects. This is demonstrated in this study, where in combining all the data plots together, for all 11 subjects, for the tensile and compressive strain regions, the mean and median b values, all fit within the range of 0.3 and 3, for both the Hop-Walk and Hop-Stair loading scenarios, as shown in Figure 4-11. Here, the mean and median b values provide a reasonable representation of the overall stimulus-remodelling relationship.

As afore mentioned, neither the b or k value were set in this study, and therefore the regression analysis and the b and k values were determined by Matlab by adjusting both the b and k values to achieve the best fit. It is therefore possible that random variations in the data plots as a result of biological factors and/or errors in the change in density measurement and/or the finite element model could that have contributed to changes in the b and k values, in particular causing the very high range in the k values. However, the consistency of the observations in this study and the strength of the b-k value correlation suggest that they are indicative of observed alternative bone remodelling, and not simply the result of error. Therefore, it is considered that the risk of an error influencing the results of this study is relatively low, and if any error is present in this study, it has had a relatively low influence, and as such it is not likely to considerably effect the findings and conclusions of this study.

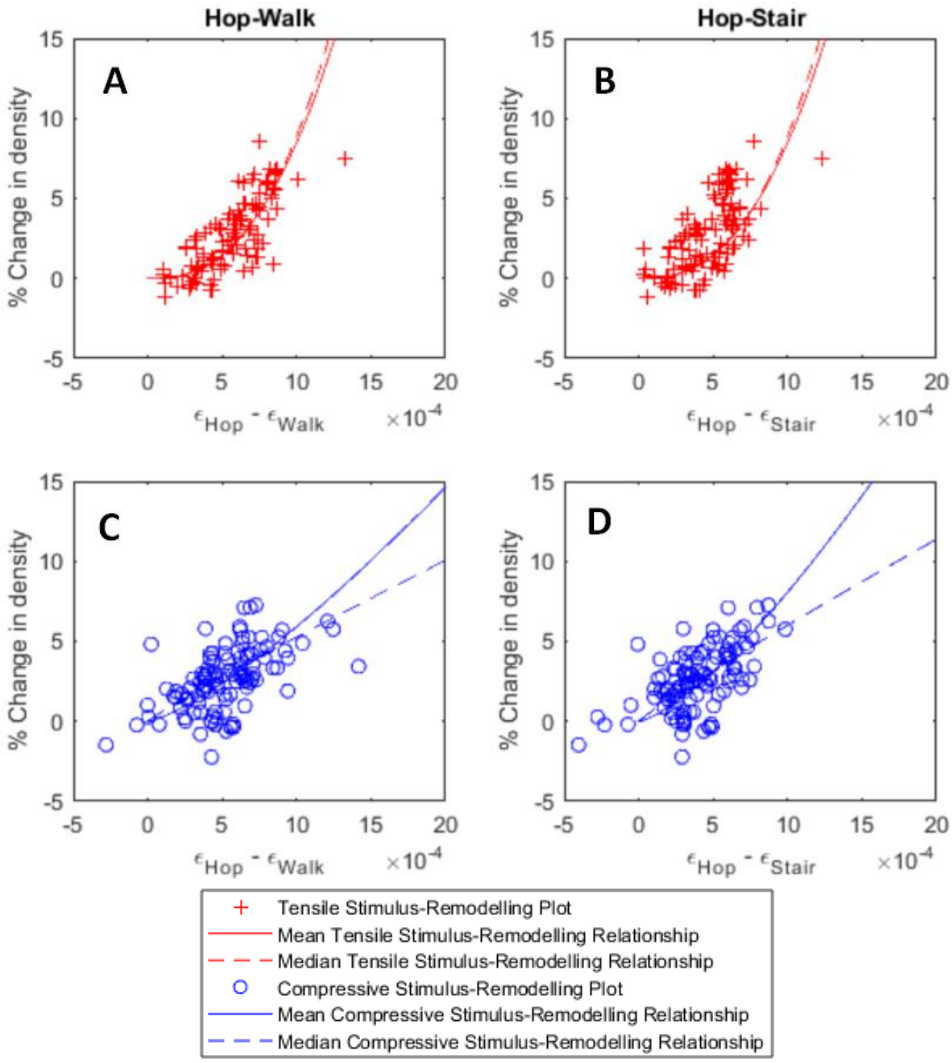

Figure 4-11: Data points from all 11 subjects for the tensile and compressive strain data sets, comparing the mean and median stimulus-remodelling relationships under tension for the Hop-Walk (A) and Hop-Stair (B) loading scenarios and comparing the mean and median stimulus-remodelling relationships under compression for the Hop-Walk (C) and Hop-Stair (D) loading scenarios, where the k value was calculated using equations 4-4 and 4-5.

4.4.2.2 Observed Typical and Atypical Stimulus-Remodelling Relationships

The stimulus-remodelling relationships observed in this study can be split into two categories of typical and atypical. In most cases, a typical stimulus-remodelling relationship was observed, which was defined as having a b value of 1 or more ($b \geq 1$) for the remodelling algorithm $\frac{\partial \rho}{\partial t} = k(\varepsilon - \varepsilon_o)^b$. However, 7 of the 11 subjects trialled in this study experienced what could be described as an atypical stimulus-remodelling relationship in one or more of the strain data sets; where an atypical stimulus-remodelling relationship can be defined as having a b value less than

one ($b < 1$). If the stimulus-remodelling relationships are split into typical and atypical, differences between those experienced under tension and compression are observed, as shown in Table 4-8 and Table 4-9.

Table 4-8: Mean and SD b values of the typical and atypical stimulus-remodelling relationships observed in this study for the Hop-Walk loading scenario, where n is the number of subjects who experienced each stimulus-remodelling relationship.

Stimulus-Remodelling Relationship		**b value**		
		General	**Tensile**	**Compressive**
Typical	n	9	9	5
	Mean	1.87	2.85	2.28
	SD	0.86	0.96	1.25
Atypical	n	2	2	6
	Mean	0.55	0.91	0.50
	SD	0.06	0.10	0.26

Table 4-9: Mean and SD b values of the typical and atypical stimulus-remodelling relationships observed in this study for the Hop-Stair loading scenario, where n is the number of subjects who experienced each stimulus-remodelling relationship.

Stimulus-Remodelling Relationship		**b value**		
		General	**Tensile**	**Compressive**
Typical	n	9	9	5
	Mean	1.89	3.04	2.54
	SD	1.17	1.47	1.46
Atypical	n	2	2	6
	Mean	0.61	0.87	0.40
	SD	0.01	0.06	0.29

It is clear that the atypical stimulus-remodelling relationship is more abundant under compression, where 6 of the 11 subjects experienced an atypical stimulus-remodelling relationship under compression. Alternatively, only 2 of the 11 subjects experienced an atypical stimulus-remodelling relationship under tension. Focusing on the atypical stimulus-remodelling relationship, the mean b value under tension is 0.91 and 0.87 (Hop-Walk and Hop-Stair loading scenarios) which is close to the typical-atypical threshold of $b = 1$. Alternatively, the mean b value under compression of the atypical stimulus-remodelling relationships was 0.50 and 0.40 (Hop-Walk and Hop-Stair loading scenarios), which is significantly further away from the typical-atypical threshold.

The atypical stimulus-remodelling relationship is however not a sign of abnormality; it is named "atypical" as the stimulus-remodelling relationship is typically associated with a b value of 1 or more. There are numerous factors which influence the cellular mechanisms involved in bone remodelling (Ruimerman, van Rietbergen et al. 2005, Robling and Turner 2009, van der Meulen and Hernandez 2013) resulting in no two bone remodelling processes being the same (Parfitt 2004). As a result Turner (1999) described how the stimulus-remodelling relationship can take any path, including an atypical one. This accounts for a wide range of stimulus-remodelling relationships observed throughout the 11 subjects used in this study.

In comparing the different b values observed in the different strain data sets, skewed normal distributions are observed, as shown in Figure 4-12. As such one can think of the range of b values as a normal distribution, or 'spectrum' of values, where different subjects will have different b values which are dependent on a variety of factors, as discussed in Chapter 2. Furthermore, it could also be considered that the b values of individual subjects can change over time. It was therefore decided to examine the subjects taking into account both the typical and atypical stimulus-remodelling relationships at the same time.

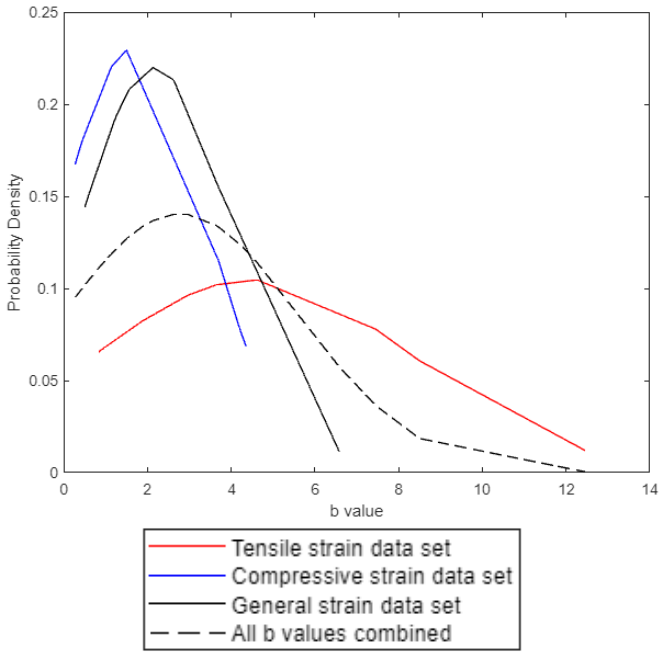

Figure 4-12: Comparison of the b values from the different strain data sets displaying skewed normal distributions.

4.4.2.3 Quantitative Difference in the Tensile and Compressive Stimulus-Remodelling Relationships

Differences between the tensile and compressive b values were observed, characterised by a smaller b value in the compressive strain data set (mean = 1.31 and 1.37 in the Hop-Walk and Hop-Stair loading scenarios) in comparison to the tensile strain data set (mean = 2.49 and 2.65 in the Hop-Walk and Hop-Stair loading scenarios), as shown in Table 4-3 and Table 4-4 as well as Figure 4-13. This observation was true for 10 of the 11 subjects, with only one subject being exempt from this observation; subject 9 for both the Hop-Walk and Hop-Stair loading scenarios. A potential factor in this apparent abnormality could be the age and BMI of the subject, where the b value was observed to decrease with the BMI and age under tension, whilst the correlation under compression is unclear, as discussed in 4.4.4 Correlation of Results with Physiological Variables. Subject 9 is the second oldest (73 years old) and has the second highest BMI (29.79 kg/m^2) suggesting that he would have a lower b value under tension than the rest of the subjects in this study.

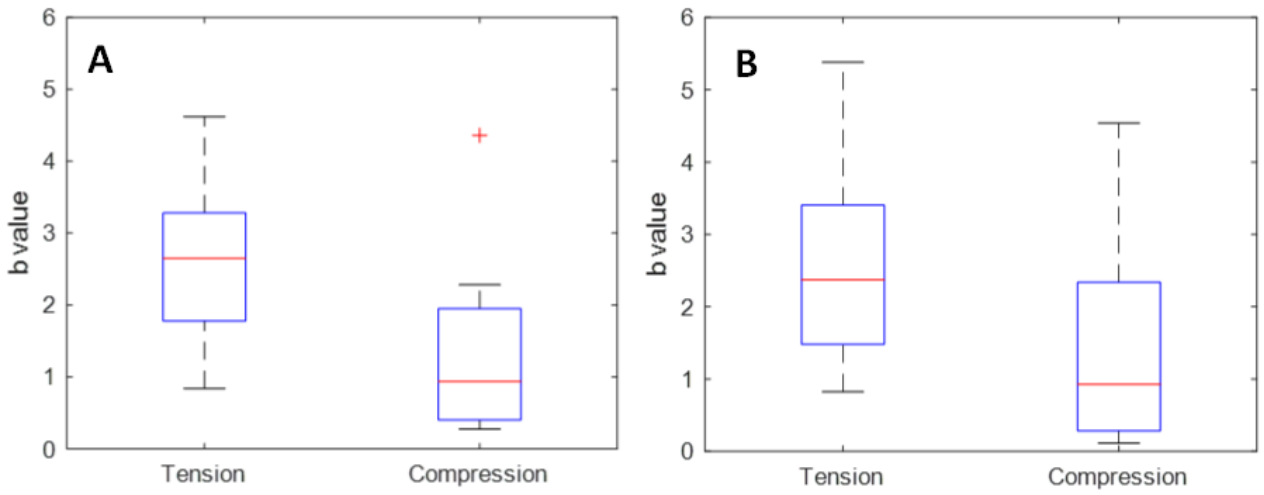

Figure 4-13: Boxplots of the stimulus-remodelling relationship b values experienced under the tensile and compressive strain data sets for the Hop-Walk (A) and Hop-Stair (B) loading scenarios, displaying the range (black), standard deviation (blue) and mean (red) values.

The difference in the b value is a significant observation, since it is one of the most important factors of the stimulus-remodelling relationship, as it is the primary indication of the relationship determining how the bone remodelling responds to the stimulus. No correlation between the tensile and compressive b values was observed for either the Hop-Walk or Hop-Stair loading scenarios,

as shown in Figure 4-14, which suggests that the stimulus-remodelling relationships under tension and compression could be independent of each other. With the exception of subject 9, all subjects had a higher tensile b value than compressive b value, as shown in Figure 4-14. This anomaly highlights how despite there being a distinctive pattern (tensile b value > compressive b value) there are numerous factors which influencing the bone remodelling behaviour, resulting in intersubjective differences.

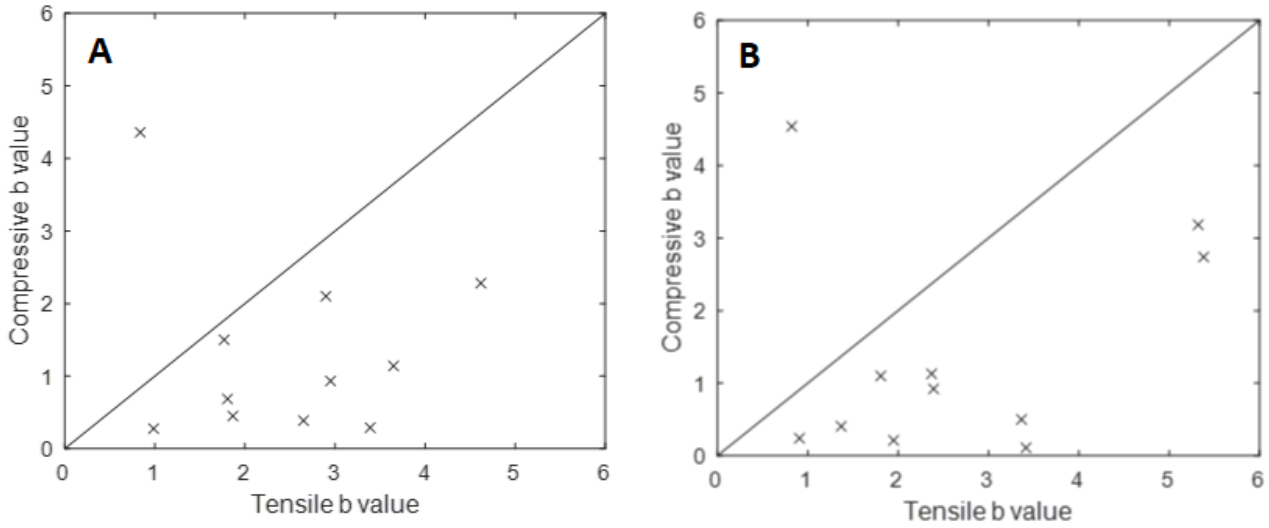

Figure 4-14: Comparison of the stimulus-remodelling relationship b values observed under tension and compression for the Hop-Walk (A) and Hop-Stair (B) loading scenarios displaying no correlation between the two values suggesting that they are independent of each other. NOTE: The black line in the graphs shows the centre, where the tensile b value equals the compressive b value. Below this line the tensile b value > compressive b value, and above this line the compressive b value > tensile b value.

Overall, a mean ± SD difference in the subject specific tensile and compressive b values of 1.18 ± 1.79 and 1.28 ± 1.88 was observed in the Hop-Walk and Hop-Stair loading scenarios, with the smallest difference being 0.27 which was observed under the Hop-Walk loading scenario. Using the Wilcoxon signed rank test in *IBM SPSS version 26* (as described in A.1.2 Wilcoxon Signed Rank Test) the difference in the compressive and tensile b values was found to be statistically significant to $p = 0.0537$ under both the Hop-Walk and Hop-Stair loading scenarios. This does not quite meet the $p < 0.05$ threshold held in statistics, however it is felt that more subjects may help improve the statistical significance.

4.4.2.3.1 Cross-Over Point

Figure 4-15 displays the mean and median tensile and compressive stimulus-remodelling relationships observed in this study when plotted on the same graph, which shows an increasing deviation between the two relationships beyond a cross-over point. This cross-over point is subject specific, however typically occurs at a stimulus of approximately 672 +/-254 με (mean ± S.D) for the Hop-Walk loading scenario and 522 ± 141 με (mean ± S.D) for the Hop-Stair loading scenario. Using the mean stimulus-remodelling relationships, shown in Figure 4-15, the cross-over point occurs at a stimulus of 736 με and 515 με for the Hop-Walk and Hop-Stair loading scenarios.

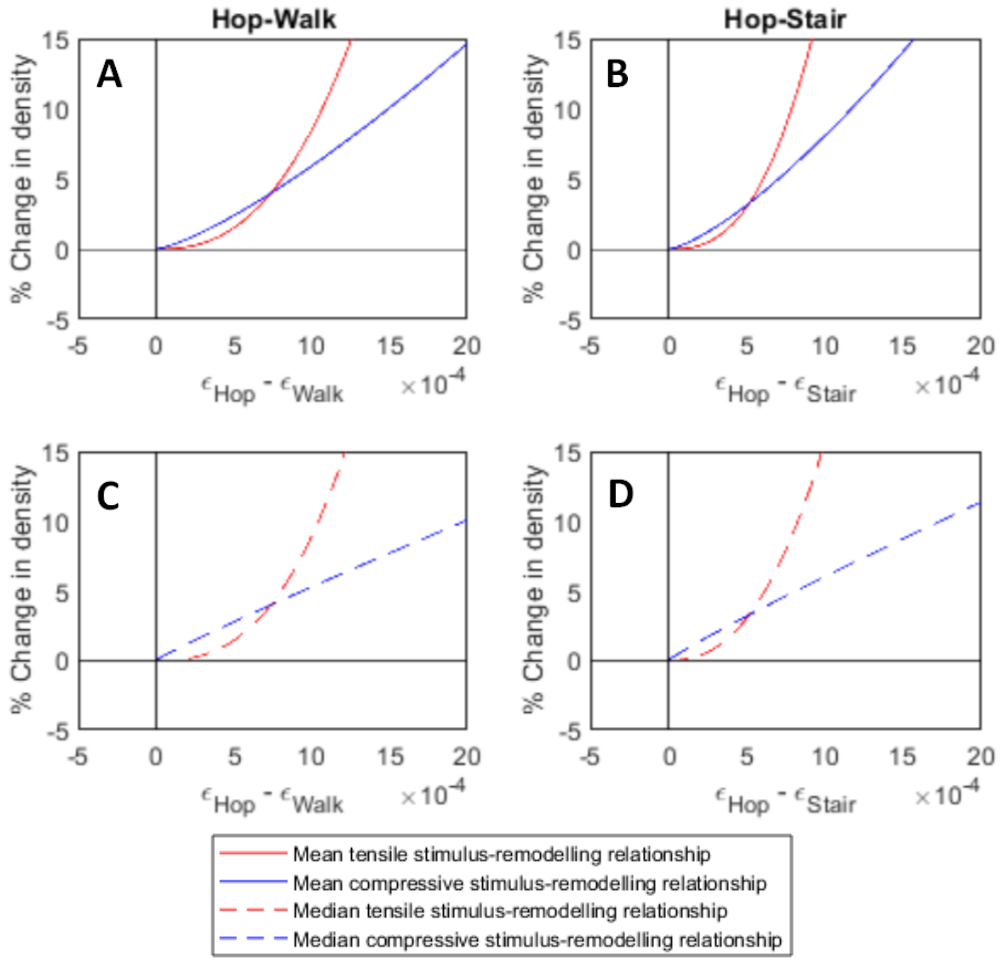

Figure 4-15: Figure displaying the mean tensile and compressive stimulus-remodelling remodelling relationships for the Hop-Walk (A) and the Hop-Stair (B) loading scenarios and the median tensile and compressive stimulus-remodelling remodelling relationships for the Hop-Walk (C) and the Hop-Stair (D) loading scenarios, where the k values for the stimulus-remodelling relationships were calculated using equation 4-4 and 4-5.

As demonstrated in Figure 4-15, due to how close the tensile and compressive stimulus-remodelling relationships are before this cross-over point; any difference between the average tensile and compressive stimulus-remodelling relationships before this point would be difficult to notice without differentiating between the tensile and compressive strain data sets. This indistinguishability is furthermore aided by the high RMSE and low R^2 value experienced under compression.

On average the cross-over point corresponds to a change in density of approximately 3 to 4% for both the Hop-Walk and Hop-Stair loading scenarios; with the mean stimulus-remodelling relationships predicting a cross-over point at approximately 4 and 3.25% change in density for the Hop-Walk and Hop-Stair loading scenarios. This is higher than the average change in density experienced by humans during exercise, which is approximately 2 to 3% (Kukuljan, Nowson et al. 2009, Kukuljan, Nowson et al. 2011, Allison, Folland et al. 2013). It is therefore likely that the differentiation of the tensile and compressive bone remodelling behaviours is not easily observed within studies which use physiological loading. It is also worth noting that this study could not differentiate between tensile and compressive remodelling behaviour, without purposefully separating them, as shown in 4.3 Preliminary Study. Assuming that mean and median tensile and compressive stimulus-remodelling relationships of this study can be applied to a wider population: The location of the cross-over point in comparison to other exercise studies and the stimulus-remodelling relationships observed in this study suggest that alternative bone remodelling behaviours become more prominent in very high impact loading scenarios which cause high stimuli.

4.4.2.3.2 Correlation with the R^2 and RMSE values

To determine if there was any correlation between the goodness of fit and the stimulus-remodelling relationships, the recorded R^2 and RMSE values were compared against the recorded b values for both tension and compression as shown in Figure 4-16. Using the Spearman's rank correlation coefficient test (described in A.1.1 Spearman's Rank Correlation Coefficient Test) in *IBM Statistical Package for the Social Sciences (SPSS) version 26*, the strength of the correlations shown in Figure 4-16 were determined, as shown in Table 4-10 and Table 4-11.

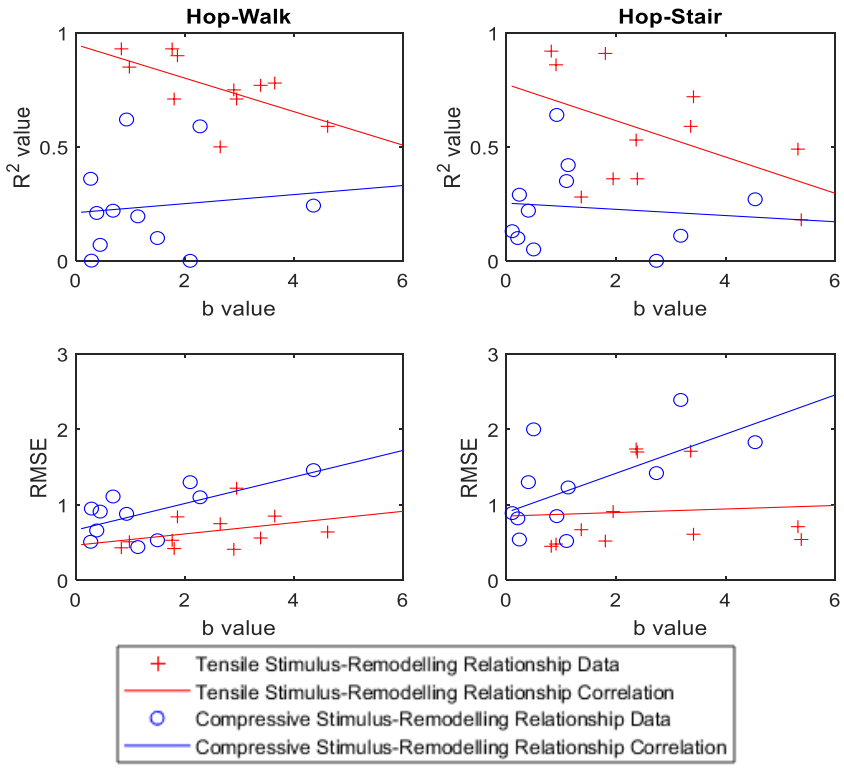

Figure 4-16: Observed relationships between the b value with the R^2 and RMSE, for the Hop-Walk and Hop-Stair loading scenarios

Table 4-10: Spearman's Rho Correlation Coefficients between the R^2 value of the stimulus-remodelling pattern and the power law constant (b)

Loading Scenario		Tensile	Compressive
H-W	Correlation	-0.584*	0.109
	Sig (2-tailed)	0.059	0.755
H-S	Correlation	-0.492	0.073
	Sig (2-tailed)	0.124	0.839

Table 4-11: Spearman's Rho Correlation Coefficients between the RMSE value of the stimulus-remodelling pattern and the power law constant (b)

Loading Scenario		Tensile	Compressive
H-W	Correlation	0.518*	0.481
	Sig (2-tailed)	0.107	0.137
H-S	Correlation	0.427	0.536*
	Sig (2-tailed)	0.193	0.094

** denotes correlation is significant at the $p < 0.05$ level (2-tailed) and **denotes that correlation is significant at the $p < 0.01$ level (2-tailed). A correlation of 0.1 is considered weak, a correlation of 0.3 is considered moderate and a correlation of 0.5 is considered strong (Field 2018).*

The tensile b value was strongly correlated with both the R^2 and RMSE values, whilst the compressive b value was only correlated with the RMSE values. Moderate to strong correlations, with Spearman's rhos of -0.584 and -0.492 were found between the R^2 value and the b value under tension for the Hop-Walk and Hop-Stair loading scenarios. Moderate to strong correlations with Spearman's rhos of 0.481 and 0.536 under compression and 0.518 and 0.427 under tension were found between the RMSE and the b value. The correlations indicate that as the b value increases, the R^2 decreases under tension and the RMSE increases under compression. A small increase in the RMSE was observed with the b value under tension, however this was slight. The correlations between the b and R^2 values under compression were disregarded because of the low Spearman's Rho correlation coefficients.

4.4.3 Regression Bias

Biases in the regression model can highlight if there are further variables which need to be taken into account (Field 2018). This is achieved by plotting the residuals of the regression analysis against the predicted value of the relationship. For this study the residual is the observed change in density minus the predicted change in density, as shown in equation 4-6.

$$Residual = \partial\rho_{observed} - \partial\rho_{predicted} \qquad 4\text{-}6$$

Where, $\partial\rho_{observed}$ is the measured (true) change in density, and $\partial\rho_{predicted}$ is the predicted change in density by the stimulus-remodelling relationship for that same stimulus. Using the equation y = mx + c, where x is the predicted change in density and y is the residual, the constants m (rate constant) and c (y-axis intercept) were used to describe the biases for the Hop-Walk loading scenario, with the results shown in Figure 4-17 and Table 4-12. The Hop-Walk loading scenario was chosen for the regression bias analysis because it was felt that it provided a better representation of the true stimulus-remodelling relationships than the Hop-Stair loading scenario, due to the higher R^2 and lower RMSE values obtained under the Hop-Walk loading scenario.

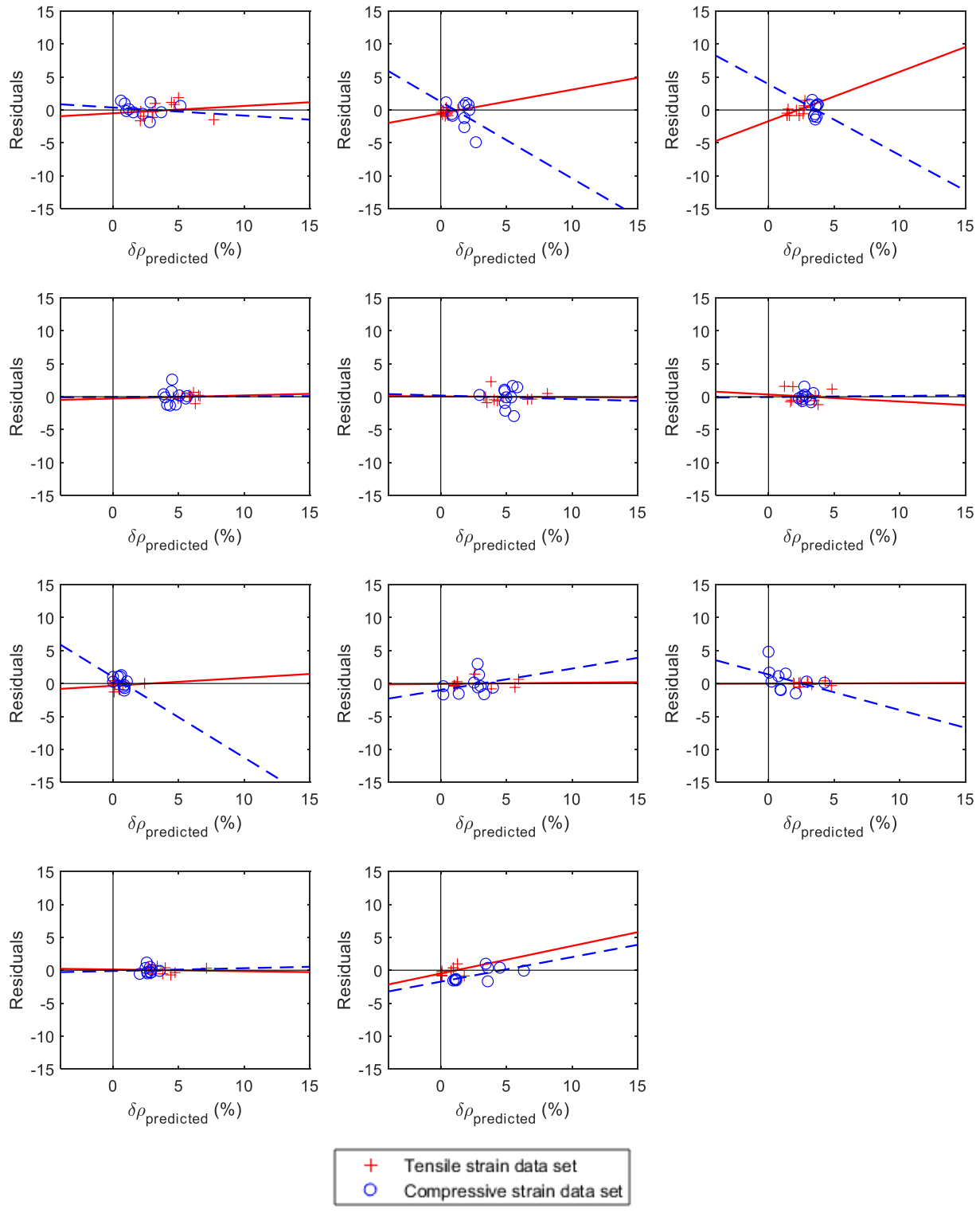

Figure 4-17: Regression biases for all subjects stimulus-remodelling relationships tension and compression in the Hop-Walk loading scenario, where subject 1 is top left, with incremental subjects going left to right. NOTE: The residuals and predicted change in density are plotted on the same scale to give perspective of the residual size.

Table 4-12: Observed biases in the tensile and compressive stimulus-remodelling relationships for the Hop-Walk loading scenario obtained using regression analysis.

	Tension		Compression	
Subject	**m**	**c**	**m**	**c**
1	0.11	-0.50	-0.12	0.37
2	0.36	-0.52	-1.17	1.26
3	0.75	-1.70	-1.08	3.92
4	0.05	-0.28	0.01	-0.04
5	-0.01	0.05	-0.05	0.19
6	-0.11	0.34	0.02	-0.05
7	0.12	-0.34	-1.23	0.99
8	0.02	-0.07	0.33	-1.00
9	0.01	-0.02	-0.54	1.36
10	-0.03	0.12	0.04	-0.12
11	0.42	-0.49	0.37	-1.74
Mean	0.15	-0.31	-0.31	0.47
SD	0.25	0.54	0.59	1.47

Large biases were observed in multiple compressive stimulus-remodelling relationship regressions. Alternatively, the tensile stimulus-remodelling relationship regressions experienced relatively small biases, with the exception of three subjects (2, 3 and 11). Using the Wilcoxon signed rank test in *IBM SPSS version 26* (as described in A.1.2 Wilcoxon Signed Rank Test), the difference in the biases observed under tension and compression were found to be different to a p-value of 0.141. This is not statistically strong, nonetheless, the observed biases suggest that the bone remodelling algorithm used to determine the stimulus-remodelling relationships in this study (equation 4-1) is better at determining the stimulus-remodelling relationship under tension, than it is under compression. The bone remodelling algorithm used in this study was chosen based on the fact it uses a well-accepted mechanical stimulus for bone remodelling, whilst removing other variables which may influence the results of this study. Remodelling algorithms and other studies which incorporate additional variables, apply these additional variables homogenously across areas of the bone under tension and compression (Burr, Martin et al. 1985, Qin, Kaplan et al. 2003, McNamara and Prendergast 2007, Vahdati and Rouhi 2009), which if applied to this study may have negatively influenced the results. Nonetheless, the biases observed in this study indicate that there is an omitted variable, or variables, that have a larger effect on the stimulus-remodelling relationship under compression, than tension.

4.4.4 Correlation of Results with Physiological Variables and Age

With this study using data from a clinical trial, it is important to take into account biological systemic factors, where systemic parameters are well known to influence bone remodelling (Eriksen 2010). The subjects of the Allison, Folland et al. (2013) clinical trial were all screened by a physician for orthopaedic and vascular pathological conditions along with any conditions which could influence bone remodelling. The result of this screening recorded all subjects to be healthy with no mental or physical conditions which can affect the undertaking of exercise or musculoskeletal growth and not to be taking any medication. The Allison, Folland et al. (2013) clinical trial also recorded several physiological parameters, with an overview of the parameters being shown in Table 2-5. Subject specific anthropometric data for the 11 subjects selected for this study is shown in Table 3-2, where detailed subject specific data for other parameters was not available.

For a valid analysis, any subject specific parameters used in a comparison against the observations made in this study needed to be intersubjectively comparable. Parameters such as height and mass alone are not considered intersubjective, as, particularly in the case of mass, there are numerous factors which could contribute to them. Two parameters from the subject specific data which were considered to be intersubjective were the BMI and age. BMI offers an insight into the subject's overall health (Bell, Carslake et al. 2018, NHS 2019), and is associated with bone remodelling (Cao 2011), where bone remodelling requires numerous cellular processes which are influenced by the subject's health (Kalervo Väänänen and Härkönen 1996, Schindeler, McDonald et al. 2008, Robling and Turner 2009, Eriksen 2010, Qin 2013). Similarly, many orthopaedic observations are associated with age, such as microdamage accumulation (Burr, Turner et al. 1998), reduction in density leading to osteoporosis and orthopaedic mechanical properties (Burstein, Reilly et al. 1976, McCalden, McGeough et al. 1993).

Focusing on the Hop-Walk loading scenario, the BMI and age of the subjects were compared against the results obtained in this study to determine if there are any correlations, with the results being shown in Figure 4-18. Similar to the regression bias study, the Hop-Walk loading scenario was focused on because it was felt that it provided a better representation of the true stimulus-remodelling relationships.

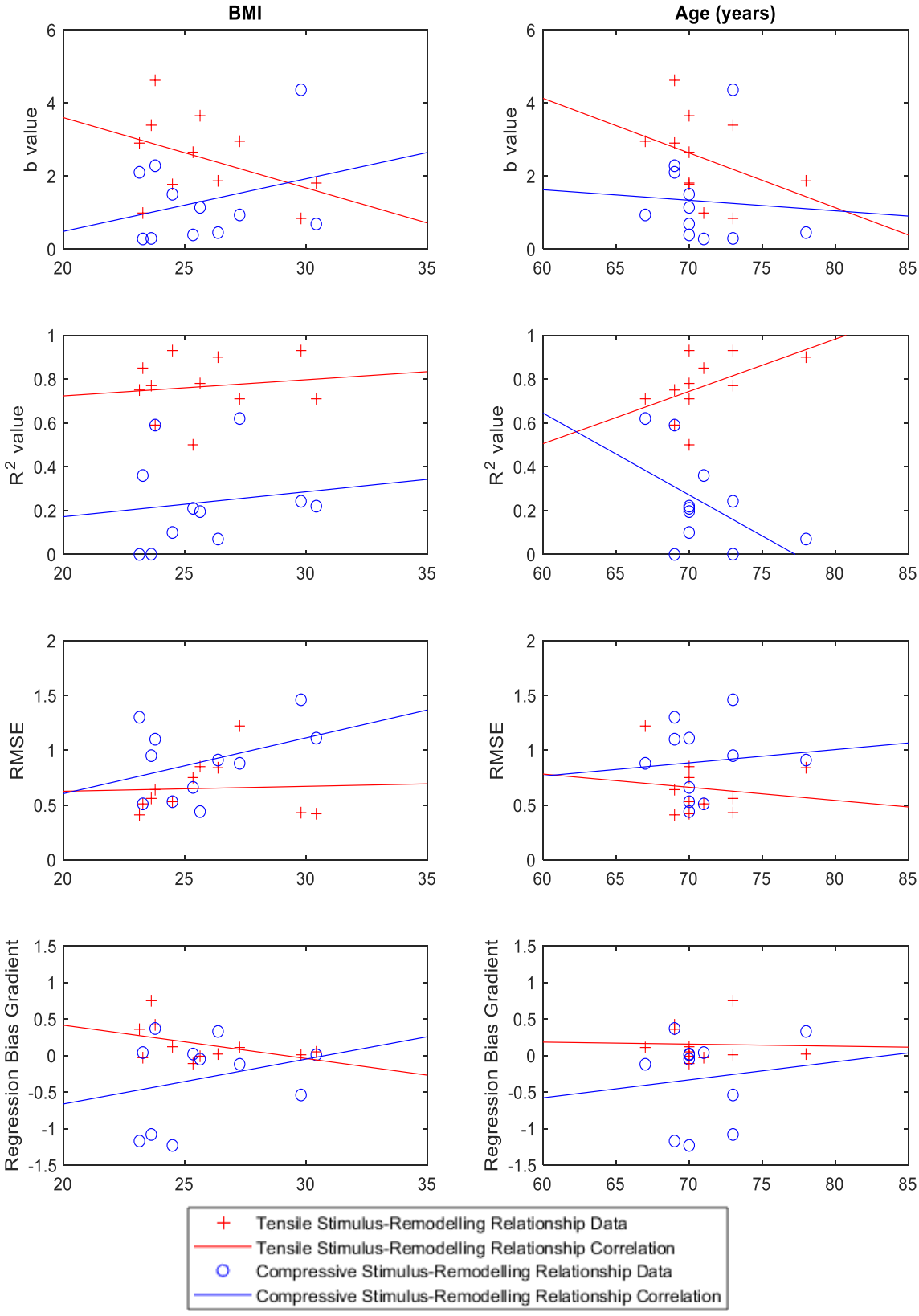

Figure 4-18: Correlations of the results from this study under the Hop-Walk loading scenario with the subjects' BMI and age(years)

Using the Spearman's rank correlation coefficient test (described in A.1.1 Spearman's Rank Correlation Coefficient Test) in *IBM Statistical Package for the Social Sciences (SPSS) version 26*, the strength of the correlations shown in Figure 4-18 were tested with the results shown in Table 4-13 and Figure 4-19.

Table 4-13: Spearman's Rho Correlation Coefficients between the BMI and the results observed in this study under the Hop-Walk loading scenario

Study Result		Tensile	Compressive
b value	Correlation	-0.246	0.173
	Sig (2-tailed)	0.468	0.614
R^2 value	Correlation	0.050	0.364
	Sig (2-tailed)	0.883	0.273
RMSE	Correlation	0.227	0.173
	Sig (2-tailed)	0.503	0.614
Regression Bias	Correlation	-0.309	-0.127
	Sig (2-tailed)	0.356	0.714

Table 4-14: Spearman's Rho Correlation Coefficients between the subjects' age (years) and the results observed in this study under the Hop-Walk loading scenario

Study Result		Tensile	Compressive
b value	Correlation	-0.472	-0.379
	Sig (2-tailed)	0.143	0.250
R^2 value	Correlation	0.618*	-0.341
	Sig (2-tailed)	0.043	0.304
RMSE	Correlation	-0.103	0.005
	Sig (2-tailed)	0.764	0.989
Regression Bias	Correlation	-0.271	0.103
	Sig (2-tailed)	0.420	0.763

** denotes correlation is significant at the p < 0.05 level (2-tailed) and **denotes that correlation is significant at the p < 0.01 level (2-tailed). A correlation of 0.1 is considered weak, a correlation of 0.3 is considered moderate and a correlation of 0.5 is considered strong (Field 2018).*

As determined by the Spearman's Rho Correlation, described in A.1.1 Spearman's Rank Correlation Coefficient Test, on average, for both BMI and age, stronger correlations were observed with the tensile bone remodelling behavioural characteristics than the characteristics observed under compression, with the exception of correlation of the R^2 value with the BMI. The b and R^2 values had weak correlations with the BMI and strong correlations with age under tension, where the b value decreased with the BMI and age and the R^2 value increased with age. An increase in the tensile R^2 value is observed with the BMI, however this is only slightly. The b and R^2 values had weak to moderate correlations with the BMI and age under compression. The most significant observed change under compression is with R^2 value decreasing with age, with all other changes being slight.

It needs to be considered that due to the small number of subjects, and all the subjects being white males aged 70.9 ± 2.78 years old (mean ± S.D) there isn't much of a variation in parameters being explored, therefore the correlations observed in this study may not be fully representative of a larger population, and further work is needed. Furthermore, the small population size means that the BMI and age cannot be separated and their influences on the alternative bone remodelling characteristics examined independently

4.4.5 Influence of Exercise Leg Allocation

Allison, Folland et al. (2013) randomly assigned the exercise leg to be used in the clinical exercise hopping trial. Of the 11 subjects used in this study, seven were assigned to use their right leg and four were assigned to use their left leg. The exercise leg assignment was compared against the results observed in this study under the Hop-Walk loading scenario to see if it had any influence, with the comparison shown in Figure 4-19.

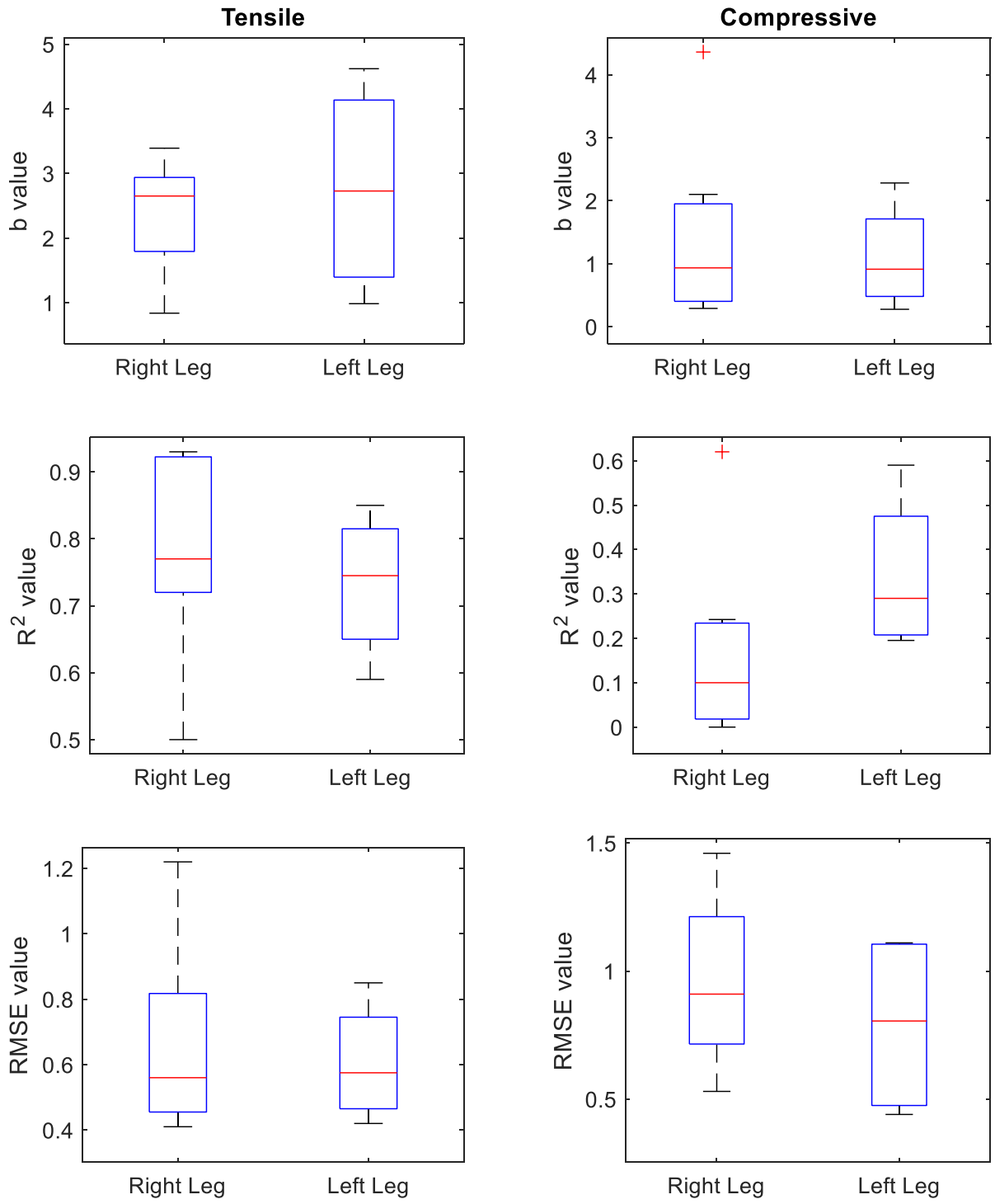

Figure 4-19: Comparison of the b, R^2 and RMSE values of the tensile and compression stimulus-remodelling relationships under the Hop-Walk loading scenario, against the exercise assignment leg, displaying the range (black), standard deviation (blue) and mean (red) values.

No difference in the change in density between the left and right exercise legs was reported by Allison, Folland et al. (2013). Figure 4-19 displays general consistency in bone remodelling observations between the leg allocation groups, with the exception of the R^2 value, where higher R^2 values are observed in the left leg under compression. The dominant leg of the subjects used in the study was not disclosed, however the right leg is typically the dominant leg, which could be a potential factor in this observation. It should be noted that no significant differences have been observed in the kinematics and kinetics between the dominant and contralateral leg (van der Harst, Gokeler et al. 2007) suggesting that this observation could be due to other unknown factors. Furthermore, it should also be considered that this could be the result of statistical chance. There are only four subjects in the left exercise leg assignment, and it is because of this low number that it was determined that no meaningful statistical tests could be carried out.

4.5 Linear Bone Remodelling Algorithms

Many bone remodelling algorithms like the Frost (1987) equation assume a linear stimulus-remodelling relationship. This study wondered what would be observed using a linear bone remodelling algorithm to determine the stimulus-remodelling relationships under tension and compression. Whilst there is clinical evidence that the lazy zone in-between the remodelling thresholds does not exist (Christen, Ito et al. 2014), the nature of a linear bone remodelling algorithms such as the Frost (1987) bone remodelling algorithm (equation 2-5) requires a lazy zone and bone remodelling thresholds to accommodate the stimulus-remodelling relationship. Still, the thresholds typically used in linear bone remodelling algorithms are fixed values, which do not account for the range in strain experienced by the bone. And so, in line with continual remodelling (van der Meulen and Hernandez 2013) a linear bone remodelling algorithm, with a lazy zone and location-specific reference strain in a stimulus was used. This required for the remodelling thresholds to be set by the study. This was achieved by defining the thresholds by using the stimulus-remodelling relationship of the plot results which had a change in density of > 0.5 %. A quantitative value for the remodelling thresholds, as a value of the strain difference ($\varepsilon - \varepsilon_o$) was then indicated by the x-intercept linear remodelling algorithm as demonstrated in Figure 4-20.

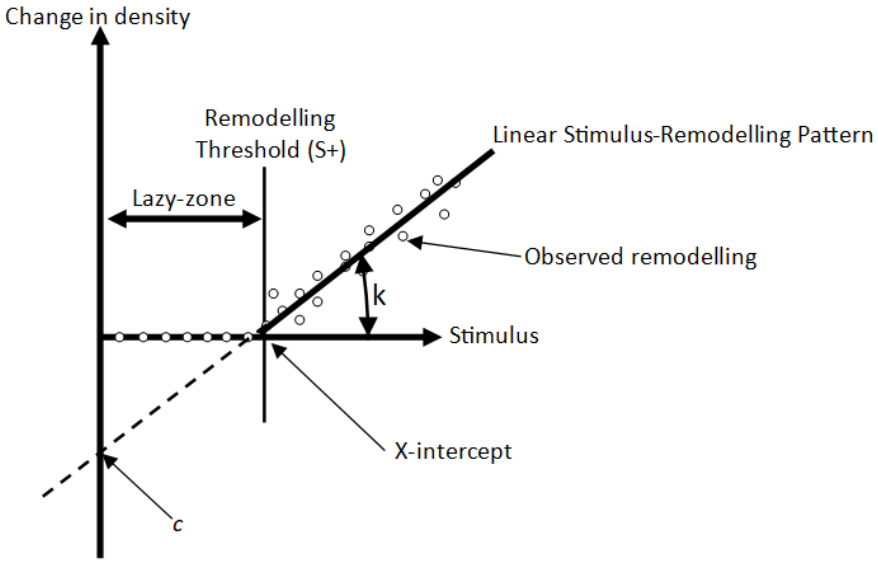

Figure 4-20: Bone remodelling positive threshold determination for linear bone remodelling algorithms.

Using this method, the linear bone remodelling algorithm used in this study is that shown in equation 4-7.

$$\frac{\partial \rho}{\partial t} = k(\varepsilon - \varepsilon_o) + c \qquad 4\text{-}7$$

Where $\frac{\partial \rho}{\partial t}$ is the percentage change in density over the year period, k is a rate constant, ε is the 'new' absolute peak principal strain ($|\varepsilon_{peak}|$) and ε_o is the 'reference' absolute peak principal strain ($|\varepsilon_{peak}|$) and c is a constant representing the y-axis intercept which allowed for a shift of stimulus-remodelling relationship to determine the bone remodelling threshold. The positive remodelling threshold was calculated as shown in equation 4-8.

$$S_+ = {}^{-c}/_{k} \qquad 4\text{-}8$$

where S_+ is the positive remodelling threshold. The two different loading scenarios, Hop-Walk and Hop-Stair, as described in 4.2 Methodology, were used to determine the stimulus. The individual stimulus-remodelling relationships for each of the 11 subjects are displayed in Figure 4-21 and Figure 4-22. The individual subject stimulus-remodelling relationship rate constants (k) and positive bone remodelling thresholds (S_+), for both the Hop-Walk and Hop-Stair loading scenarios are shown in Table 4-15 and Table 4-16.

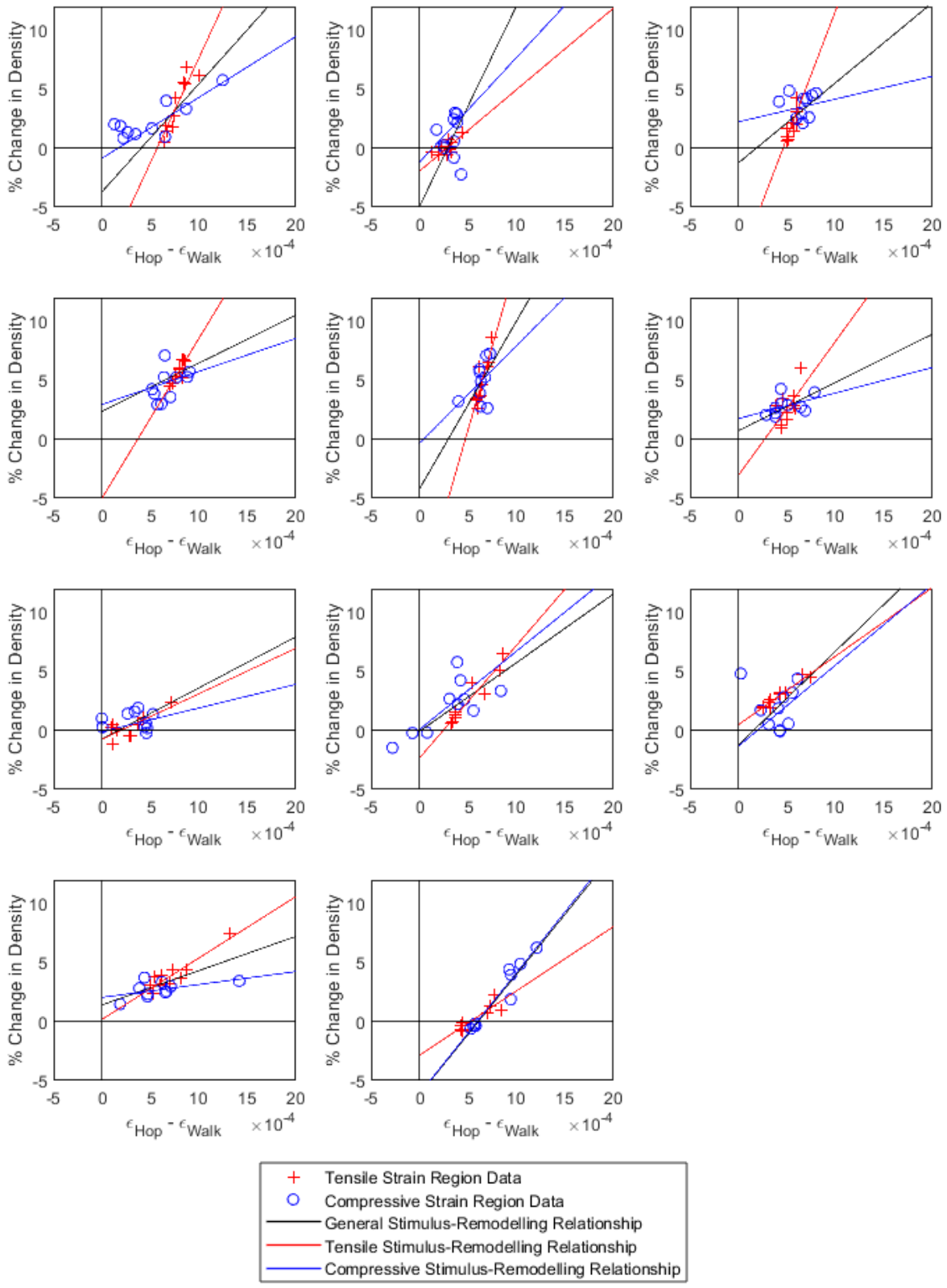

Figure 4-21: All subjects stimulus-remodelling plots in all three strain data sets in the Hop-Walk loading scenario when using the linear bone remodelling algorithm, where subject 1 is top left, with incremental subjects going left to right.

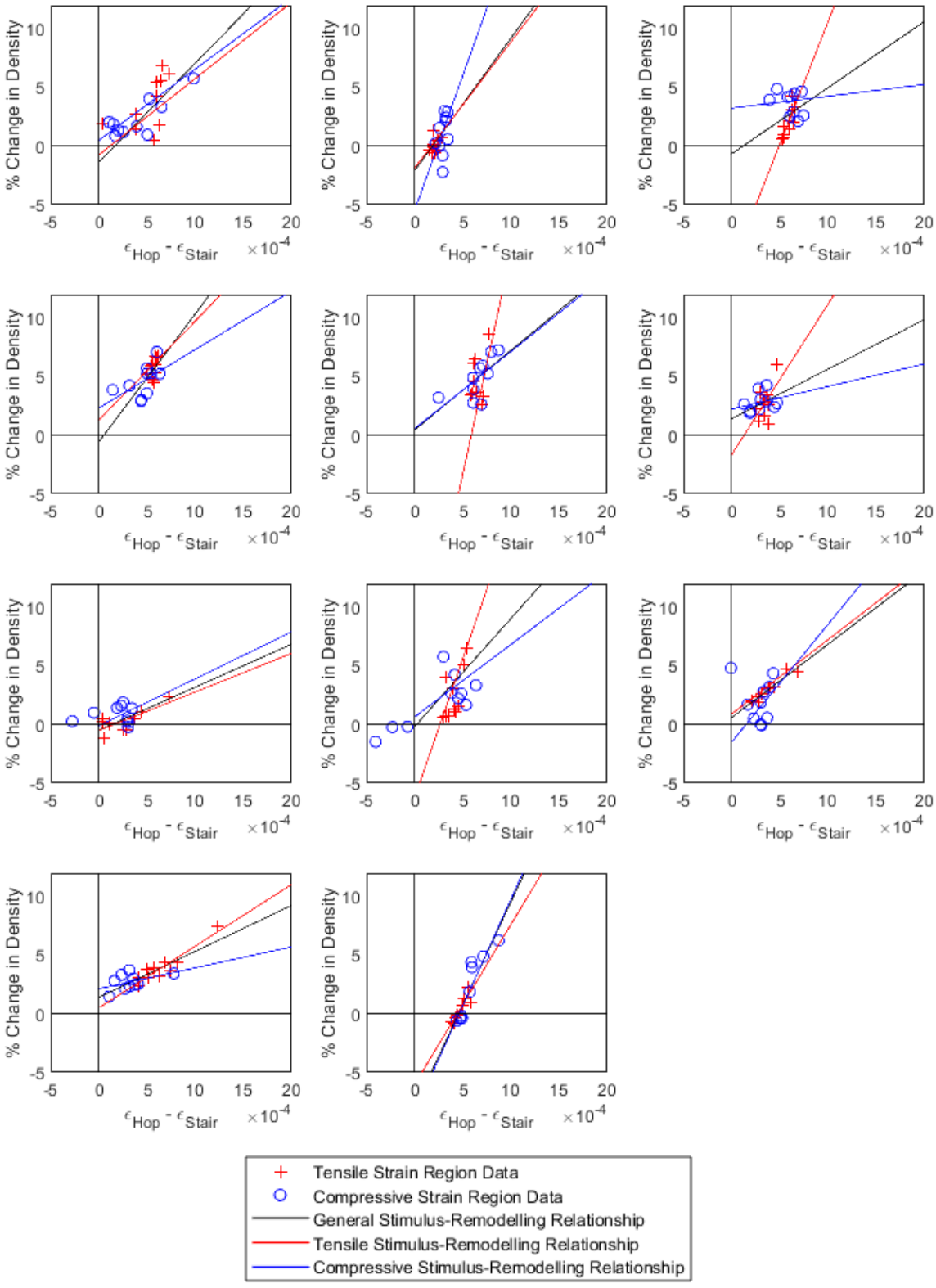

Figure 4-22: All subjects stimulus-remodelling plots in all three strain data sets in the Hop-Stair loading scenario when using the linear bone remodelling algorithm, where subject 1 is top left, with incremental subjects going left to right.

Table 4-15: Summary of all subjects' bone remodelling rate constants (k) and remodelling threshold (S_+) when using the Frost (1987) bone remodelling algorithm, for the Hop-Walk loading scenario

	General		Tension		Compression	
Subject	**k**	**S_+(με)**	**k**	**S_+(με)**	**k**	**S_+(με)**
1	9164	403	17800	569	5161	168
2	16990	290	6905	283	8870	133
3	6788	185	21500	459	1930	-1154
4	4083	-579	13500	368	2794	-1058
5	14210	294	28500	472	8279	42
6	4079	-182	11300	267	2164	-811
7	4330	168	3859	196	2000	50
8	5826	16	9540	243	6628	-12
9	7936	156	5810	-83	6861	195
10	2904	-486	5206	-34	1093	-1873
11	10170	605	5449	524	10300	594
Mean	7862	79	11761	297	5096	-339
±SD	4490	347	7891	204	3259	726

Table 4-16: Summary of all subjects' bone remodelling rate constants (k) and remodelling threshold (S_+) when using the Frost (1987) bone remodelling algorithm, for the Hop-Stair loading scenario

	General		Tension		Compression	
Subject	**k**	**S_+(με)**	**k**	**S_+(με)**	**k**	**S_+(με)**
1	8438	162	6510	117	6072	-80
2	11300	185	10770	175	23030	240
3	5645	121	20850	493	1007	-3210
4	10900	50	8438	-155	4984	-466
5	6785	-66	37730	589	6584	-84
6	4224	-336	12830	129	1923	-1165
7	3667	132	3292	155	4000	25
8	9229	19	23690	264	6186	-103
9	6260	-91	6335	-140	10040	149
10	3921	-357	5262	-95	1784	-1197
11	17580	457	13650	442	18200	463
Mean	7995	25	13578	179	7619	-493
±SD	4153	224	10250	241	7008	998

Mimicking the results from the nonlinear remodelling algorithm, distinctive differences were observed in the tensile and compressive stimulus-remodelling relationships. Overall, the difference in the stimulus-remodelling relationships was typically characterised by the tensile stimulus-remodelling relationship displaying a significantly higher remodelling rate constant and remodelling threshold than the compressive stimulus-remodelling relationship.

It was also observed in numerous subjects, that the general stimulus-remodelling relationship was not in-between the tensile and compressive stimulus-remodelling relationships. Furthermore, all three strain data sets experienced positive bone remodelling thresholds at a negative value ($S_+ < 0$), which would suggest that positive remodelling is occurring at stimuli below the reference stimuli. It was postulated that these observations were the result of the linear bone remodelling algorithms possible inability to account for the atypical stimulus-remodelling relationship. To test this postulation, the bone remodelling threshold (S_+) from the linear bone remodelling algorithm was plotted and compared against the b value of nonlinear bone remodelling algorithm, as shown in Figure 4-23.

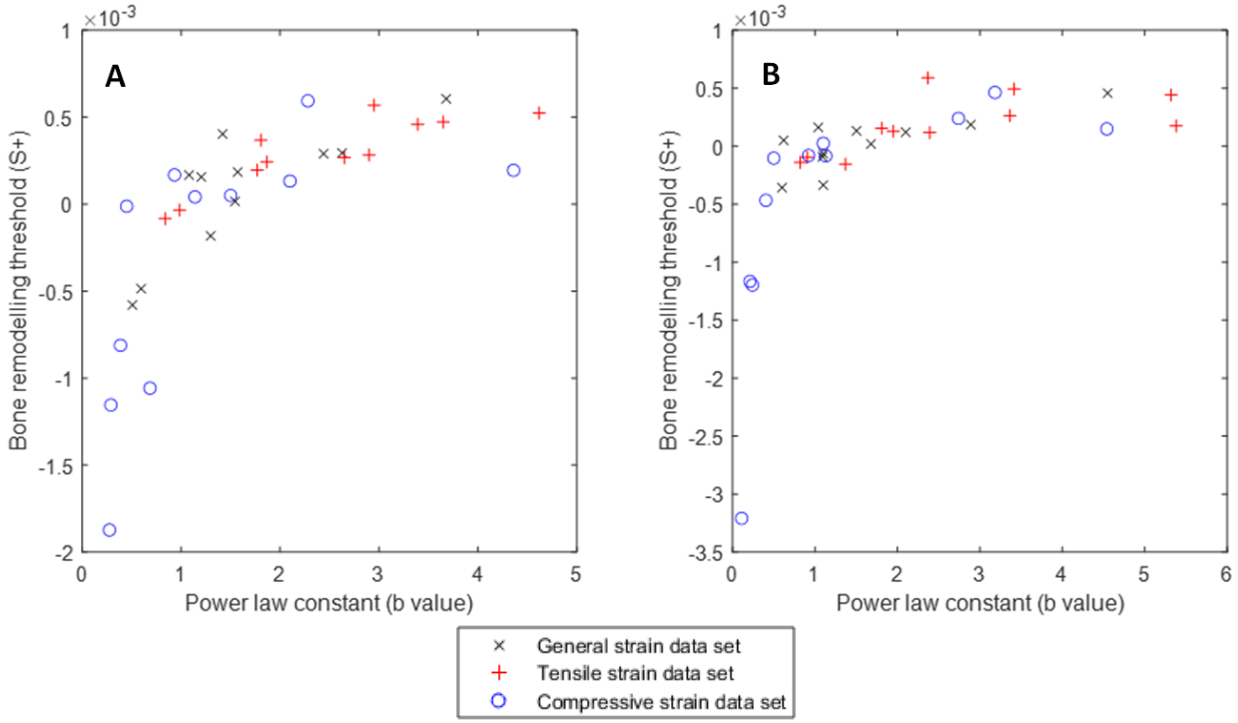

Figure 4-23: Relationship between the bone remodelling threshold (S_+) from the linear bone remodelling algorithm and the b value from the nonlinear bone remodelling algorithm for all three strain data sets under both the Hop-Walk (A) and Hop-Stair (B) loading scenarios

A relationship between the b value and bone remodelling threshold was observed for both the Hop-Walk and Hop-Stair loading scenarios, which confirmed that a stimulus-remodelling relationship with a b value of 1 or less (atypical stimulus-remodelling relationship) typically resulted in a negative value for the bone remodelling threshold. This supported the postulation that the linear

nature of the bone remodelling algorithm makes it unsuitable to properly account for the atypical stimulus-remodelling relationship nature which has been observed when using the nonlinear bone remodelling algorithm.

This study is not the first to notice that linear bone remodelling algorithms can struggle to accommodate the stimulus-remodelling relationships observed in clinical data. Turner (1999) stated that *"critical examination of the mechanostat theory indicates that it does not conform well with certain experimental observations."* Due to this, the decision was made to not use a linear bone remodelling algorithm when examining the tensile and compressive bone remodelling behaviour in this study.

4.6 Summary of Findings

Stimulus-remodelling data of the proximal femur of 11 male subjects (mean ± SD age: 70.9 ± 2.78 years) taking part in a year-long clinical hopping exercise trial was examined using regression analysis against a nonlinear bone remodelling algorithm (equation 4-1), by comparing the change in density, measured from qCT scans, against the mechanical stimulus determined using finite element simulation. Initial examination of the stimulus-remodelling data without differentiating between tensile and compressive principal strain regions revealed no obvious signs to indicate the presence of alternative bone remodelling behaviour. However, by differentiating between tension and compression, two significantly different stimulus-remodelling relationships were observed in cortical bone, which are demonstrated in Figure 4-24 and summarised in Table 4-17.

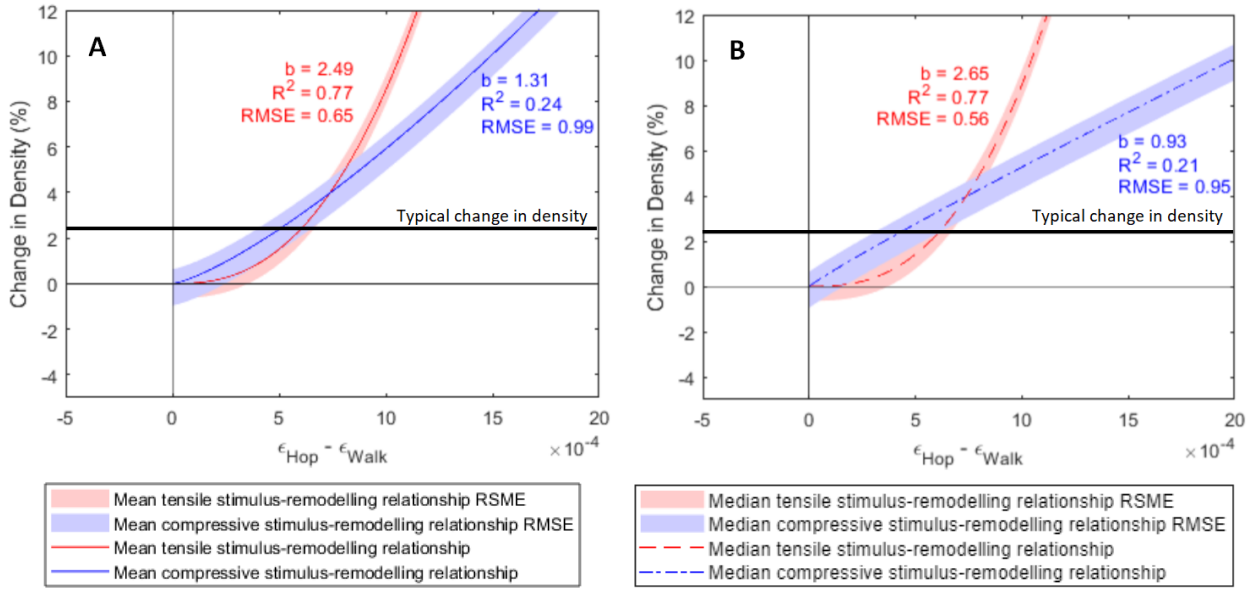

Figure 4-24: Mean (A) and median (B) tensile and compressive stimulus-remodelling relationships with the mean RMSE observed when using the nonlinear remodelling algorithm (equation 4-1) in the Hop-Walk loading scenario for the 11 subjects used in this study, where the k value was calculated using equation 4-4. Figure also shows the typical change in density experienced during exercise demonstrating the influence that alternative bone remodelling has on typical physiological loading conditions. NOTE: The Hop-Walk loading scenario was considered to be more representative of the actual stimulus-remodelling relationships due to it having an overall higher R^2 and lower RMSE value than the Hop-Stair loading scenario.

Table 4-17: Summary of findings in this study, detailing the observed differences in the bone remodelling observed under tensile and compressive loads, with the mean values and p-values of each observed difference from the Hop-Walk loading scenario

Characteristic	Description	Mean values		p-value
		Tens.	Comp.	
b value	The tensile b value is significantly higher than the compressive b value.	2.49	1.31	=0.054
R^2	The tensile R^2 value is significantly higher than the compressive R^2 value.	0.77	0.24	<0.01
RMSE	The tensile RMSE is on average lower than the compressive RMSE.	0.65	0.99	=0.164

The tensile and compressive stimulus-remodelling relationships are best described by remodelling algorithms which utilise a power law equation. Using a power law remodelling algorithm demonstrated that beyond a 'cross-over' point which is typically just above the average change in density experienced during exercise, the tensile and compressive stimulus-remodelling relationships separate, and deviate from each other increasing as the stimulus increases. This results in two different stimulus-remodelling relationships, where the tensile strain region experiences a higher change in density than the compressive strain region for the same stimulus. Below this 'cross-over' point, the compressive strain region typically has a marginally higher change in density for the same stimulus than the tensile strain region. However, below the 'cross-over' point the results from the tensile and compressive strain regions can overlap somewhat, particularly as the stimulus approaches zero and relationships converge, making them harder to distinguish and separate. The compressive stimulus-remodelling relationship also experiences a high variance in the change in density in relation to the stimulus in comparison to the tensile stimulus-remodelling relationship. This high variance in the change in density experienced by the compressive stimulus-remodelling relationship also contributes to the overlap of the two stimulus-remodelling relationships at low stimuli. However, in analysing these observations, and Figure 4-24, caution needs to be taken where uncertainty in the results, in particular due to the possibility of errors in the finite element model introduces the possibility of false results. Analysis of the results using what is available has indicated that the results of this study are accurate. Nonetheless, future studies into this phenomenon in similar or the same loading conditions, in the same location, would validate the results of this study.

Potentially one of the most important observations is the difference in the b value when using equation 4-1, which is considered to be the most indicative factor of the stimulus-remodelling relationship, where tension continuously had a higher b value than compression, with the k value being calculable from the b value. The bone under compression also experienced an abundance of atypical stimulus-remodelling relationships, which was defined by having a b value less than 1, where 6 of the 11 subjects experienced an atypical stimulus-remodelling relationship under compression. This study also observed that linear bone remodelling algorithms have an inherent inability to account for the atypical stimulus-remodelling relationships observed in this study.

The high RMSE and low R^2 experienced in the stimulus-remodelling relationship under compression make the differentiation between tension and compression difficult before this cross-over point. The cross-over point occurs at an average stimulus of 672 με and a change of density of approximately 3.5%. Other exercise studies typically do not reach a high enough change in density (or stimulus) to go beyond this cross-over point (Kukuljan, Nowson et al. 2009, Kukuljan, Nowson et al. 2011), with the typically achieved change in density of approximately 2.5% annotated on Figure 4-24. This suggests that alternative bone remodelling may not have such as drastic effect on the change in density on lower load physiological activities, and also offers a potential reason as to why alternative bone remodelling has not yet been observed outside of laboratory and pathological conditions.

In determining the goodness of fit of the regression analyses which dictated the stimulus-remodelling relationships, compression experienced high RMSE and low R^2 values in comparison to tension. It is believed that these high RMSE and low R^2 values are what caused high regression biases which deviated in direction almost unpredictably under compression. Alternatively, tension experienced relatively low regression biases.

With no statistical correlation observed between the tensile and compressive b values, the results of this study suggest that the b values of the stimulus-remodelling patterns under tension and compression are independent of each other. However, correlations of varying strength were observed between the b value with age, BMI, R^2 value and RMSE value. In most cases the correlation was significantly stronger under tension, with the exception of the RMSE value. Similarly, correlations of varying strength were observed with the R^2, RMSE and regression bias with the age and BMI, again stronger correlations were observed under tension. In determining these correlations the study acknowledged the small sample size and population demographic.

The combination of the characteristics observed in this study suggest that the bone remodelling under compression is more complicated that the bone remodelling under tension and introduces the possibility that either there are different bone remodelling mechanisms acting under tension and compression, or the same mechanism has different characteristics under tension and compression.

Chapter 5. Discussion

5.1 Introduction

Chapter 4 of this study has provided evidence towards differences in bone remodelling behaviour under tension and compression in the human proximal femur over one year of hopping with no pathological or remodelling abnormality. This thereby suggests that alternative bone remodelling behaviour does exist in physiological loading conditions and could have an impact on bone remodelling algorithms. However, Chapter 4 did not identify which bone remodelling mechanism is responsible for the observed alternative bone remodelling behaviour.

Until now, studies into alternative bone remodelling behaviour under tension and compression have only been conducted under laboratory conditions (Bentolila, Boyce et al. 1998, Stokes 2002, Stokes, Gwadera et al. 2005, Kuzyk and Schemitsch 2009, Herman, Cardoso et al. 2010), or in pathological conditions where abnormal remodelling has already been observed such as scoliosis (Stokes and Laible 1990, Lin 2010). These previous studies have an advantage over this study in that the pre-observed conditions (such as scoliosis) or the ability to remove the bone post loading (such as laboratory studies) allow the researchers to identify the mechanism causing the alternative bone remodelling behaviour. This study did not have this ability since there was neither a pre-observed condition nor could the researcher remove the subject's femur. Therefore, to investigate which bone remodelling mechanisms had a role in the alternative bone remodelling behaviour observed in Chapter 4, this study had to compare known characteristics of the different mechanisms against the observed results.

To make the observations detailed in Chapter 4, this study relied on the combinational use of finite element simulation and clinical data. As such, the aim of this chapter is threefold: 1) To compare the observations of this study to bone remodelling mechanisms known to cause alternative bone remodelling behaviour, as introduced in Chapter 2 (see 2.3 Alternative Bone Remodelling). 2) Explore how the finite element model used may have influenced the results. 3) Discuss the considerations and limitations of the study.

5.2 Potential Alternative Bone Remodelling Mechanisms Acting in This Study

As described in Chapter 4, distinct observations were made in this study in regard to alternative bone remodelling behaviour in tension and compression under physiological loading conditions, which are summarised in 4.6 Summary of Findings. Whilst the exact cellular mechanisms in response to mechanical loads are poorly understood, the observations of this study can be compared against known characteristics of identified alternative bone remodelling mechanisms, to suggest which mechanisms may have influenced the observed results in this study. This has been aided by the fact that the majority of previous studies into alternative bone remodelling have focused on single mechanisms, allowing for the unique characteristics of each mechanism to be easily identified, as described in 2.3 Alternative Bone Remodelling and summarised in Table 2-1.

5.2.1 Potential Influence of Microdamage

Microdamage production and the subsequent bone remodelling initiation as a result of linear microdamage is considered to be a strong candidate as one of the mechanisms causing the alternative bone remodelling observed in this study. As discussed in Chapter 2, there are two types of microdamage, linear microdamage and diffuse damage which are compartmentalised into compression and tension. Of the two types of microdamage, only linear microdamage initiates bone remodelling (Bentolila, Boyce et al. 1998, Herman, Cardoso et al. 2010, Seref-Ferlengez, Basta-Pljakic et al. 2014, Seref-Ferlengez, Kennedy et al. 2015). Both Burr and Martin (1993) and Taylor and Lee (2003) attempted to quantify and predict where linear microdamage would be produced and initiate bone remodelling. Both studies found it difficult to determine this due to the number of unmeasurable factors, such as crack growth halting due to cement lines and other microdamage being present. And so, linear microdamage production and bone remodelling initiation are considered almost random. Moreover, where linear microdamage initiates remodelling, the remodelling as a result is spread over a relatively large area, in comparison to the remodelling areas initiated by other processes, and is spaced apart by the presence of anti-apoptotic proteins (Jilka, Noble et al. 2013).

Linear microdamage only influences the initiation of bone remodelling, not the final output density. However, through the initiation of bone remodelling, linear microdamage does influence

the volume of the bone experiencing a change in density. Since the change in density measurement in a sample volume, is the proportion of sample volume which has experienced a change in density multiplied by the quantitative change in density experienced by that region: it was postulated that the random distribution of the linear microdamage, combined with the random initiation of bone remodelling would cause a high variance in the volume of the bone experiencing a change in density. This, therefore, would cause for random changes in the change in density measured in relation to the stimulus, as demonstrated in Figure 5-1. Both the R^2 and RMSE are based on the residuals of the dependent y-axis variables (change in density) in relation to the predicted value as a result of the independent x-axis variables (stimulus), as shown in Figure 5-2. Therefore, a high variance in the change in density in relation to the stimulus, as a result of linear microdamage would increase the RMSE and decrease the R^2, such as that observed in this study under compression in relation to tension. As such it was postulated that the high RMSE and low R^2 observed under compression in relation to tension is the result of linear microdamage only being produced under compression.

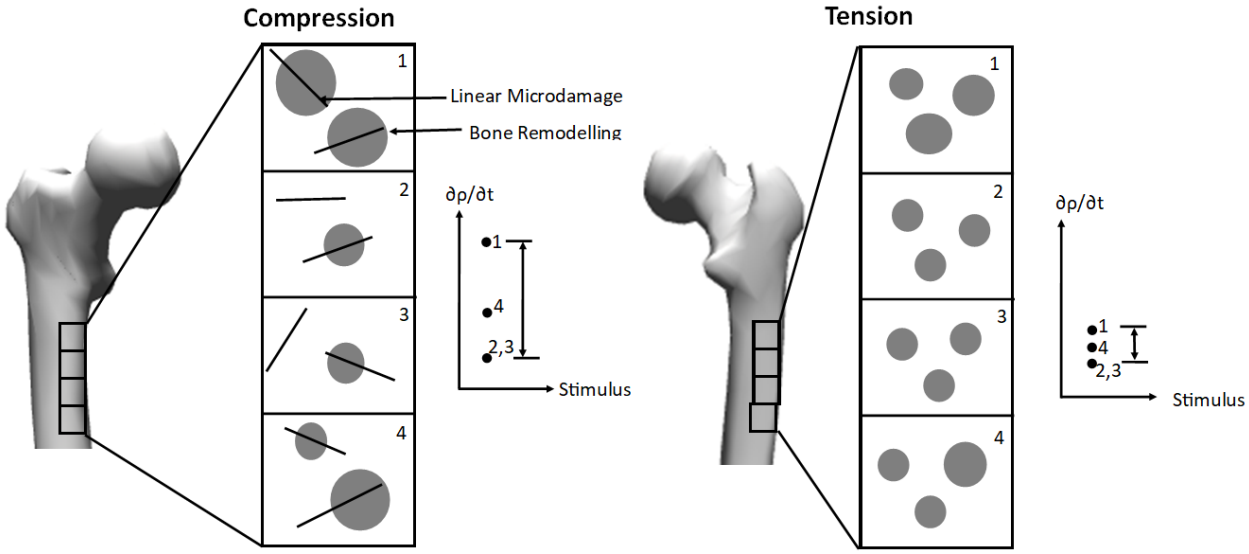

Figure 5-1: The difference in bone remodelling in compression and tension, demonstrating the effect of linear microdamage on the stimulus-remodelling relationship in the compressive strain data set, where both the production of linear microdamage and the initiation or bone remodelling is considered random. This figure assumes that all areas shown experience the same stimulus and all remodelling areas experience the same change in density: Here, different changes in density would be recorded due to the total area of the bone which has experienced a change in density. NOTE: In this figure the sample areas and the remodelling areas are larger than they are in reality, for visual effect.

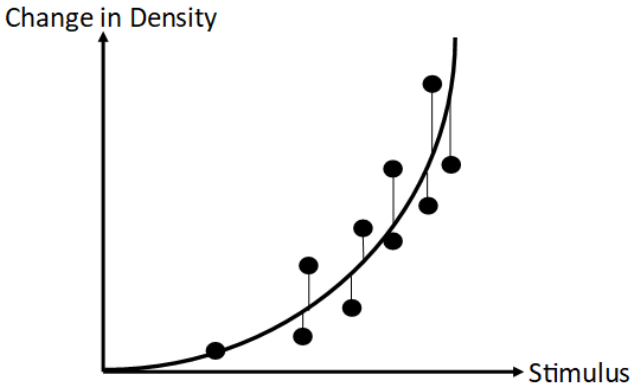

Figure 5-2: Evaluation of the residuals in the dependent variable (change in density) in relation to the predicted value, along with the independent variable (stimulus).

As shown in 4.4.3 Regression Bias, compression experienced numerous significant regression biases, which varied in direction and magnitude. It is thought that this variance in the change in density in relation to the stimulus, as a result of linear microdamage could also cause high residuals, resulting in high regression biases. The randomness of the linear microdamage production and initiation of bone remodelling, would in turn cause the residual to be random, therefore causing the regression bias to change unpredictably in direction and magnitude, as observed in this study.

5.2.1.1 Mathematical Representation

For a theoretical mathematical representation of how linear microdamage can influence the bone remodelling observations, the bone can be split into a mesh of different elements. The heterogeneity of bone remodelling results in some elements experiencing bone remodelling, whilst other elements do not. If an area of the bone with dimensions $D \times D$, made up of equal size elements with dimensions $l \times l$, was selected for investigation, as shown by Figure 5-3: The measured change in density for that area would be the proportional area of all the elements that did experience bone remodelling multiplied by the quantitative change in density experienced in those elements, against the elements which did not experience bone remodelling.

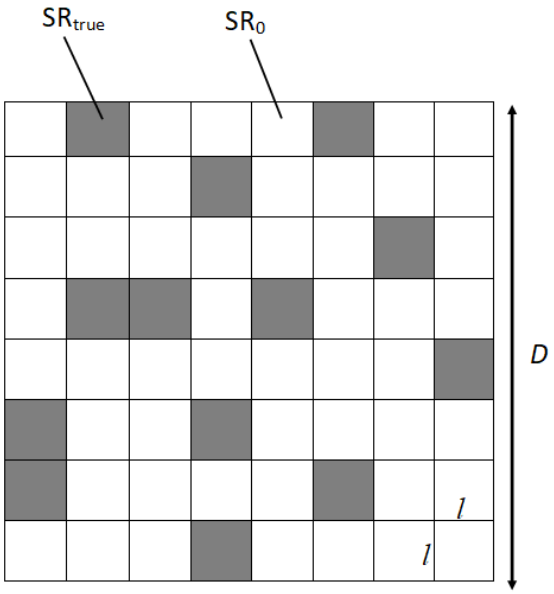

Figure 5-3: Mathematical representation of bone remodelling over a set area, showing the heterogeneity of bone remodelling, where SR_{true} is the stimulus-remodelling relationship of the bone experiencing bone remodelling, SR_0 is the stimulus-remodelling relationships of the bone not experiencing bone remodelling, D is the diameter/length of sample area and l is the diameter/length of the mesh element which the sample area has been split into.

Assuming that the change in density experienced by the elements undergoing bone remodelling is the result of the same stimulus-remodelling relationship, then the change in density experienced over time by these elements can be expressed as equation 5-1.

$$\frac{\partial \rho}{\partial t} = SR_{true} \qquad 5\text{-}1$$

Where SR_{true} is the stimulus-remodelling relationship experienced by the areas of the bone undergoing remodelling, $\partial\rho$ is the change in density and ∂t is a period of time. Alternatively, the elements of the sample area not experiencing bone remodelling, experience a zero change in density which is represented by SR_0, as shown in equation 5-2.

$$\frac{\partial \rho}{\partial t} = SR_0 = 0 \qquad 5\text{-}2$$

Taking into account both SR_{true} and SR_0, and assuming the same stimulus is applied over the area, the overall change in density, over time, in the sample area can be expressed as equation 5-3.

$$\frac{\partial \rho}{\partial t} = V \times SR_{true} \qquad 5\text{-}3$$

Where *V* is the proportion of the sample area experiencing remodelling. In this study, the stimulus-remodelling relationship was said to be the change in strain to the power of a constant, *b*. Assuming this can be applied to SR_{true}, one gets equation 5-4.

$$SR_{true} = k(\varepsilon - \varepsilon_o)^b \qquad 5\text{-}4$$

Where *k* and *b* are remodelling constants. Therefore, the equation used in this study to determine bone remodelling over a period of time, equation 5-4, can be updated to equation 5-5.

$$\frac{\partial \rho}{\partial t} = V \times k(\varepsilon - \varepsilon_o)^b \qquad 5\text{-}5$$

With the postulation that linear microdamage causes random initiations of bone remodelling in large areas, spaced out by anti-apoptotic proteins, this could cause a variation in the variable, *V*, which would cause a high variance in the change in density (y-axis) in relation to the stimulus (x-axis).

5.2.1.1.1 Influence of Sample Area

As discussed in Chapter 2, a too small sample area, in an observational-based study, may not provide an adequate representation of the bone remodelling, as shown in Figure 5-4. This study conducted a convergence-based study, as described in 4.2.1 Change in Density Measurement, to determine an optimal diameter/length, *D*, to allow for an adequate representation of the bone remodelling.

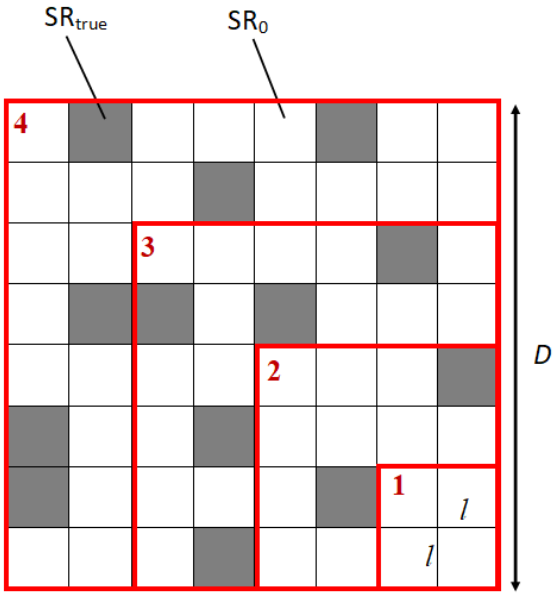

Figure 5-4: Image demonstrating the effect of different sample area sizes of 1 to 4 shown in red, where a too small sample area can result in an inadequate bone remodelling measurement.

Assuming that the diameter/length *D* used in this study was large enough to encapsulate the full variation of *V*, particularly under compression, and assuming that the stimulus-remodelling relationship for the elements/areas experiencing bone remodelling is the same in each individual sample area: Then if all points from a single bone were plotted on the same graph then the average change in density can be assumed to be equation 5-6, which is the same as the remodelling algorithm used in this study to determine the stimulus-remodelling relationships in tension and compression (equation 4-1).

$$\overline{\frac{\partial \rho}{\partial t}} = k(\varepsilon - \varepsilon_o)^b \qquad 5\text{-}6$$

5.2.1.1.2 Remodelling Initiation Probability

Some remodelling algorithms attempt to account for the heterogeneity of bone remodelling, such as the Huiskes, Ruimerman et al. (2000) remodelling algorithm, by stating that bone remodelling is spatially random. Huiskes, Ruimerman et al. (2000) gives a percentage probability, that bone remodelling will occur in each element, as shown in 2.5.8 Mechanistic Models. With the proportion of the bone not experiencing bone remodelling being significantly larger than the

proportion of the bone experiencing bone remodelling, Huiskes, Ruimerman et al. (2000) gave a relatively low probability of bone remodelling initiating of 10%. The Huiskes, Ruimerman et al. (2000) remodelling algorithm parameters can be applied to the remodelling algorithm used in this study, specifically equation 5-5. Here, the variable *V* can be seen as proportional to the percentage probability of bone remodelling initiation where in a sample area large enough to encapsulate the full variation of *V,* the mean *V* would equal the percentage probability. For example, using the probability of 10%, *V* would be 0.10, where on average 10% of the elements in the sample area would be experiencing bone remodelling as a result of the stimulus. Based on the observations of this study and the postulations made in this chapter: It is likely that those two different probability variations need to be applied in tension and compression, where *V* remains constant in tension, but is more complicated, with a varying value under compression as a result of linear microdamage.

5.2.1.2 Yield Strain and Microdamage Accumulation

As discussed in Chapter 2, linear microdamage production occurs at the compressive yield, which in cortical bone has been measured to be between 6000-11000 με (Biewener 1993, Niebur, Feldstein et al. 2000, Nyman, Ni et al. 2008, Zioupos, Hansen et al. 2008, Leng, Dong et al. 2009). This value remains constant and does not change with age (Kopperdahl and Keaveny 1998, Wang 2013) nor does it change to adapt to the typically experienced load. Furthermore, a single abnormally high load will not produce a significant amount of linear microdamage. In human cortical bone, Zioupos, Hansen et al. (2008) only found a relationship between strain and linear microdamage production, if the strain was kept above ~7500 με for numerous loading cycles. This is substantially higher than the strain measured during vigorous activities (Burr, Milgrom et al. 1996) and achieved under compression by the majority of subjects in this study, which had an average simulated strain of 3618 με across all anatomical faces during hopping, and with only three subjects reaching 7000-8000 με in one location on the posterior face. Whilst it is accepted that the strains in this study are based on a simulation, they are felt to reasonably represent the overall typical strain magnitudes and distribution.

There is however, contradictory evidence in the literature with some studies reporting that strains of approximately 3000 με (Milgrom, Finestone et al. 2002) and 4000 με (Frost 2003) are high enough to create linear microdamage to initiate bone remodelling. It should be noted that, these

studies are based on a combination of observations from animals (Frost 2003) and humans (Milgrom, Finestone et al. 2002) and are measured through temporarily implanted strain gauges, with neither study specifically removing the bone and observing microdamage in humans. Furthermore, these studies do not differentiate between tension and compression in the generation of linear microdamage and therefore make the inherited assumption that linear microdamage initiates remodelling throughout the bone. Although, there is evidence that a very limited amount of linear microdamage can be produced under the tensile dominant region (Karim and Vashishth 2013); there is overwhelming evidence that microdamage production is compartmentalised and therefore linear microdamage is almost exclusively formed under the compressive dominant region (Bentolila, Boyce et al. 1998, Boyce, Fyhrie et al. 1998, Herman, Cardoso et al. 2010, Karim and Vashishth 2013, Seref-Ferlengez, Basta-Pljakic et al. 2014). However, these studies produce an interesting debate, regarding the true strain required to produce linear microdamage.

There is an additional factor that should also be considered. As discussed in Chapter 2, linear microdamage initiates osteocytes apoptosis through damaging the osteocyte, removing the osteocyte from the extracellular matrix or damaging the extracellular matrix disrupting the essential fluid flow for osteocyte survival (Plotkin, Mathov et al. 2005, Jilka, Noble et al. 2013, Plotkin 2014). Linear microdamage does not always achieve this and therefore does not always initiate osteocyte apoptosis. There are no additional biological mechanisms to remove linear microdamage and therefore this results in a residual amount of linear microdamage building up in the bone. As a result, at any point in time, the human bone can contain thousands of linear microdamage cracks which have not initiated osteocytes apoptosis. It was therefore postulated that at any time, during the sudden onset of high loads, any of these residual fractures could randomly propagate and initiate bone remodelling. This could provide an explanation as to how linear microdamage could influence the observations of this study, even if the experienced strains were not typically high enough to produce a substantial amount of linear microdamage.

The amount of residual linear microdamage has been demonstrated to increase with age (Burr, Forwood et al. 1997), as shown in Figure 5-5. This therefore introduces the possibility that the age of the subjects in the Allison, Folland et al. (2013) clinical study could have contributed to the possible linear microdamage influence on the alternative bone remodelling observed in this study.

As a result, it is postulated that the influence that difference in microdamage experienced under tension and compression has on alternative bone remodelling, may increase with age, and may have contributed to the observations made in this study.

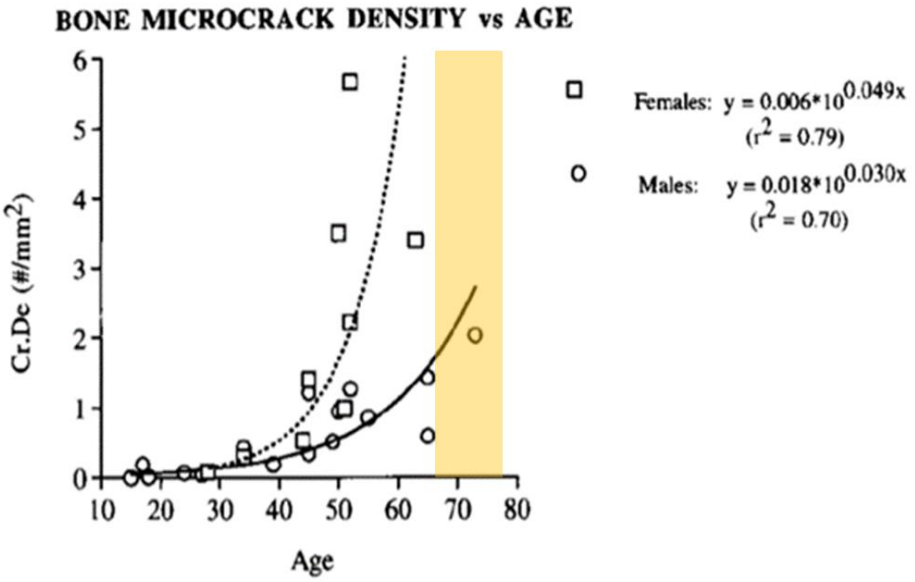

Figure 5-5: Exponential increase in linear microdamage in the femoral cortex under compression with age (Burr, Forwood et al. 1997), with the age of the subjects used in this study being highlighted, where Cr.Dc is the number of linear microcracks per mm².

As shown in Figure 4-18, this study observed a moderate correlation between the age of the subject and the R^2 value under compression (Spearman's Rho of 0.341, $p = 0.304$), where the R^2 reduced as the age of the subject increased. With the postulation that linear microdamage causes a decrease in the R^2 value through the residual linear microdamage which builds up over time causing random variations in the volume of the bone experiencing bone remodelling: It follows that the correlation observed in this study where the R^2 reduces with age could be a result of the build-up of linear microdamage with age. The moderate strength of the correlation could be due to the small population size and the small age distribution (11 years) between the subjects. Still, it should also be noted that a stronger correlation between the R^2 value and age was observed under tension, which cannot be explained by the linear microdamage remodelling mechanism. It is thought this observation could have something to do with the mechanoresponsiveness of the bone (Kotiya and Silva 2013), however it unclear exactly what.

5.2.1.3 Microdamage Detection

This study used non-invasive qCT scans to measure the change in density. Quantitative CT scans cannot verify the presence of microdamage since microdamage does not alter the density of the bone (Lee, Mohsin et al. 2003, Taylor and Lee 2003). The only method currently available to detect the presence of microdamage is to remove the bone from the host and stain the matrix (Lee, Mohsin et al. 2003). This is obviously not possible in human subjects; therefore, this study cannot confirm if microdamage was actually present. As a result, a new method of either detecting microdamage or measuring alternative bone remodelling behaviour in humans is required to continue research into whether microdamage has had an influence on alternative bone remodelling behaviour under physiological loading conditions.

5.2.2 Potential Influence of the Hueter-Volkmann Law

As shown in Chapter 4, compression consistently experienced a lower b value than tension and had an abundance of atypical stimulus-remodelling relationships (6 of the 11 subjects). A mechanism that could potentially contribute to the difference in the b and the abundance of atypical stimulus-remodelling relationships observed in the compressive strain data set is the Hueter-Volkmann law. This mechanism influences the resorption and formation stages of bone remodelling, where it has been demonstrated to retard bone formation under compression and not tension (Stokes 2002, Villemure, Aubin et al. 2004, Kim, Kim et al. 2010) which would cause a lower change in density in relation to the stimulus in compression in comparison to tension. The Hueter-Volkmann law has also been associated with a slight increase in bone growth rate under tension, but, the effects of this are significantly less than the bone growth retardation observed under compression (Stokes 2002).

It should be remembered that it is possible for more than one bone remodelling mechanism to act simultaneously in the same location (Cerrolaza, Duarte et al. 2017). However, since the Hueter-Volkmann law does not affect the initiation stage of bone remodelling, and linear microdamage does not affect the initiation and formation stages of bone remodelling, the two mechanisms act completely independent of each other and therefore neither impact on the remodelling influence of the other. The typical observation of this study is that compression experiences a higher change in density in relation to the stimulus in comparison to tension before the cross-over point, after this

compression experiences a lower change in density in relation to the stimulus in comparison to tension. Much like any other mechanism, the influence of the Hueter-Volkmann law has been demonstrated to increase as the strain magnitude increases (Stokes 2002, Stokes, Gwadera et al. 2005) which could explain the typical observation made in this study, where the mechanisms of the Hueter-Volkmann law increasingly retard bone formation under compression as the stimulus increases. It should be noted that the Hueter-Volkmann law is associated with a single strain, whilst the strain stimulus of this study is the difference between two strains. Nevertheless, a general positive correlation is observed between the strain stimulus of this study and the hopping strain magnitude, as shown by Figure 5-6. This would suggest that as the strain stimulus increases, so does the influence of the Hueter-Volkmann law.

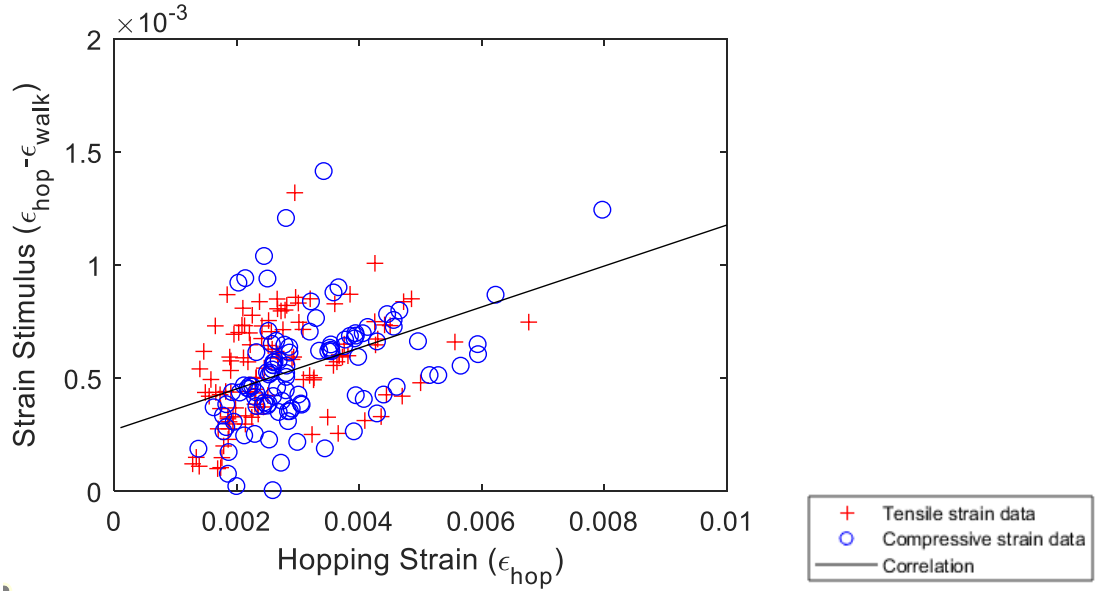

Figure 5-6: Comparison of the strain stimulus for the Hop-Walk loading scenario against the peak absolute hopping principal strain magnitude ($|\varepsilon_{peak}|_{hop}$) for tension and compression, demonstrating a positive correlation between the two.

The Hueter-Volkmann law is more associated with pathological conditions such as scoliosis of the spine and slipped capital femoral epiphysis in the femur, however it has been demonstrated to be present at lower strains with no pathological state (Stokes 2002). Therefore, it is possible that the Hueter-Volkmann law is continually present and occurring. Still, the Hueter-Volkmann law is associated with continual static loads (Stokes 2002, Villemure, Aubin et al. 2004, Kim, Kim et al. 2010) and the loads experienced by subjects in the Allison, Folland et al. (2013) clinical study

were dynamic. Nonetheless, the Hueter-Volkmann law has been described at idiopathic (Villemure, Aubin et al. 2004, Lin 2010) and the strain shift as described in Chapter 2 (see section 2.3.3 Hueter-Volkmann Law) provides a possible explanation for how it could be present under dynamic loading.

5.2.3 Potential Influence of the Piezoelectric Effect

Whilst there is evidence that the piezoelectric properties of the bone could influence bone remodelling (McDonald and Houston 1990, Navarro, Michiardi et al. 2008, Cerrolaza, Duarte et al. 2017, Tandon, Blaker et al. 2018, Orthofix Holdings 2019) there is little literature on the piezoelectric effect causing alternative bone remodelling behaviour; with the researcher only being able to find one study which suggests that the piezoelectric effect could cause alternative bone remodelling (Rubinacci, Black et al. 1988). Still, the literature that does exist suggests that the electronegative potentials under compression signal for formation and the electropositive signals produced under tension signal for bone resorption (Becker, Bassett et al. 1964, Kuzyk and Schemitsch 2009). The combination of these effects would likely result in a lower change in density under tension in comparison to compression for the same stimulus. This characteristic was observed particularly in subject 9, where this subject experienced an atypical stimulus-remodelling relationship under tension. This suggests the possible presence of this alternative bone remodelling mechanism in these subjects. However, the recorded characteristics of this mechanism go against the typical observations made in this study. It is felt that further studies are required into the specific nature and effects of the bone's piezoelectric properties on alternative bone remodelling, to determine the influence of this mechanism.

5.2.4 Additional Mechanisms

In addition to the postulation made by this study that the identified alternative bone remodelling mechanisms could be causing atypical stimulus-remodelling relationships in a higher abundance under compression in relation to tension: Both cellular accommodation (Turner 1999) and the maximum resorption rate of osteoclasts (Adachi, Kameo et al. 2010) have been attributed to cause atypical stimulus-remodelling relationships. Therefore, there is a possibility that either of these mechanisms could have a higher presence under compression than tension. Receptors for different

stages of mechanotransduction have been demonstrated to react differently under tension and compression (Zhong, Zeng et al. 2013) which could further assist either of these mechanisms in causing different stimulus-remodelling relationships in tension and compression. However, neither cellular accommodation nor the influence of the maximum respiration rate of osteoclasts have been attributed to alternative bone remodelling. Additionally, whilst both mechanisms have had high conformity to clinical data, the effect they have on the stimulus-remodelling relationship is theoretical. Therefore, the connection of these mechanisms to the observations of this study can only be speculative. Nonetheless, the idea that either of these mechanisms could be contributing to the alternative bone remodelling observed in this study demonstrates that there could be additional alternative bone remodelling mechanisms which are yet to be identified.

5.3 Potential Influences of Method Parameters on the Results

To conduct the investigation into alternative bone remodelling behaviour in the human proximal femur, this study relied upon the use of finite element simulation and previously collected clinical data. Whilst the combination of finite element simulation with clinical data is a well tried and tested method, which has been shown to provide good results (Stokes and Laible 1990, Turner, Anne et al. 1997, Stansfield, Nicol et al. 2003, Bitsakos, Kerner et al. 2005) this method introduced parameters into the study which could have potential influences on the results, which are explored here.

5.3.1 Bone Density Measurement

The change in bone density used by this study was determined using qCT images taken by the Allison, Folland et al. (2013) clinical trial where the bone density was reported to be measurable to the closest 0.001 g/cm^3. This was considered to be able to comfortably measure a 0.1 % change in density across every subject. It was accepted that this may introduce a small, but acceptable, amount of error in the stimulus-remodelling relationship.

5.3.2 Finite Element Simulation and Musculoskeletal Model

The idea that the finite element simulation could induce an error into the stimulus as a result of the finite element simulation itself or the musculoskeletal loads was considered. It was considered that

two basic types of error could be induced: 1) Strain magnitude error, causing a shift in the stimulus but maintaining the same basic result. 2) Strain distribution error, causing a different stimulus distribution, changing the overall results. The effect of both of these errors are demonstrated in Figure 5-7.

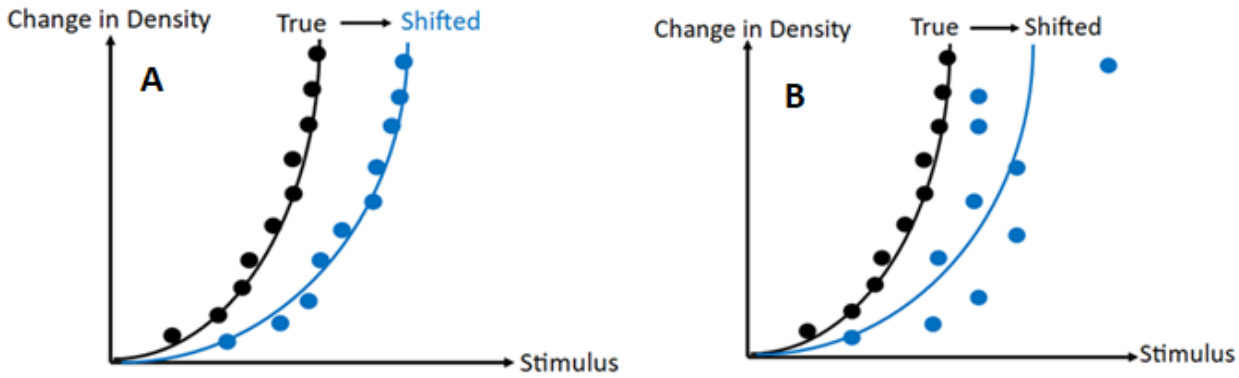

Figure 5-7: Theoretical influences of simulation errors, showing strain magnitude error (A) and strain distribution error (B).

Both error types are the result of incorrect stimulus magnitude calculations, resulting in a shift in the data point(s) along the x-axis. However, over the total region being examined, strain magnitude errors occur when the strain distribution of the entire data set is correct, but the strain magnitude is incorrect. Here, the entire data set is affected by the error equally, and as a result the influence of this error is a shift in the k value when using equation 4-1, whilst the b value, R^2 and RMSE all remain unaffected. Alternatively, a strain distribution error occurs when each data point in the data set is affected by the error unequally. This would result in changes in the R^2 and RMSE, and most likely result in changes in the b and k values.

Due to the complexity of the models, the precise origin of most errors cannot be pinpointed, however the origin of all errors in the finite element simulation and musculoskeletal model can be traced back to the setup of the individual subject specific models. These error origins can be split into two categories of the musculoskeletal loading and material properties. Regarding the musculoskeletal loading, although the models were made to be subject specific and accurate as possible, using what previous studies have demonstrated to be the most accurate methods, as described in Chapter 3; potential errors are introduced through the simplification of the

musculoskeletal system and the assumptions made in hip contact and muscle force calculations, both of which are necessary to enable a finite element simulation. However, as discussed in section 3.6.3 Critical Evaluation of the Finite Element Musculoskeletal loads, the impact of this simplification was reduced to a minimum, where studies have demonstrated that the standard femoral model produces an accurate strain distribution for the proximal femur (Speirs, Heller et al. 2007). Additionally, the introduction of more muscles, would also increase the risk of introducing strain distribution errors through the introduction of strain artefacts (Modenese, Phillips et al. 2011). Therefore, due to the bones linear elasticity, assuming the standard femoral model does not introduce any strain distribution errors, any errors in the musculoskeletal loads should result in strain magnitude errors. This was confirmed through deliberately inducing strain magnitude errors, where it was found that any simulation error of this type results in a change in the k value but does not change or affect the b, R^2 and RMSE values.

Errors in the material properties of the bone in this study have the potential to introduce strain distribution errors. Where some studies use a homogenous material distribution, to increase local strain accuracy this study utilised a heterogenous material property distribution based off subject specific qCT scans. This requires the use of a density-elasticity equation, which is described and evaluated in Chapter 3. Since the equation cannot be exact, there is the possibility for error introduction, which in a heterogenous material distribution could result in local areas with incorrect density assignment. This would result in local strain magnitude errors, which would cause an overall strain distribution error. The chance of this type of error is furthered by the application of the material properties (Helgason, Taddei et al. 2008) which can result in phenomenon such as the partial volume effect (Hangartner 2007). Furthermore, assumptions made about the material properties could further this error even more, where this study assumed the bone to be near elastic and isotropic, when in reality it is viscoelastic and orthotropic. As described and explored in Chapter 3, this was to best represent the bone behaviour under the loading conditions, however it is possible that under certain conditions these assumptions could be incorrect and thus add to the error. Nonetheless, it was felt that the risk of this error was relatively low and acceptable, where as described in chapter 3, the assumptions and modelling method in the material properties have a proven reliability.

In assessing the results of this study, the b, R^2 and RMSE values of the stimulus-remodelling relationships obtained between the Hop-Walk and Hop-Stair loading scenarios differ slightly; however, the same overall stimulus-remodelling relationships were observed. Nonetheless, the differences in the b, R^2 and RMSE values observed under the Hop-Walk and Hop-Stair loading scenarios demonstrate that a deviation in the musculoskeletal model from the true loads experienced by each subject can induce a potential strain distribution error. However, with this considered, the consistency in the stimulus-remodelling relationships observed in this study under the Hop-Walk and Hop-Stair loading scenarios, combined with the findings from Speirs, Heller et al. (2007) and the validation of the finite element simulation model by comparing the strain distribution and magnitude results of this study against other studies in Chapter 3, the researcher of this study was confident that any musculoskeletal loading errors did not contribute any significant error to the stimulus-remodelling relationships. As such, it was considered that the finite element simulation provided an accurate representation of the strain stimulus, suitable for use in a bone remodelling study and the b, R^2 and RMSE values observed in this study can be considered to be an accurate representation of the true stimulus-remodelling relationships experienced by the subjects used in this study.

5.4 Considerations & Limitations

5.4.1 Clinical Trial Methodology

The use of clinical trial data for this study allowed for the true bone remodelling behaviour to be observed, which in-turn allowed for the identification of alternative bone remodelling behaviour in physiological loading conditions. This study and its observations would not be possible, or at least would be much more difficult to demonstrate, using a self-design simulation. Similarly, observations of laboratory-based studies are not directly applicable to physiological loading conditions, and as such are also not applicable for this study and its aims. Yet, the method of using clinical trial data which allowed for the identification of alternative bone remodelling in physiological loading conditions is the very method which limited the determination of which bone remodelling mechanisms are contributing to the observed alternative bone remodelling in this study. The Allison, Folland et al. (2013) clinical trial used hopping exercise and qCT scans to induce and measure a change in bone density over a one-year period. The use of hopping exercise

produces loading conditions which are not specific to any single alternative bone remodelling mechanism and the qCT scans cannot directly observe or measure any bone remodelling mechanism. As a result, a direct comparison cannot be made between the observations made in this study and the known characteristics of a single bone remodelling mechanism.

5.4.2 Subjects

The subjects used in this study only represent a limited proportion of the total population demographic, where this study only examined the bone remodelling in the proximal femurs of subjects of one sex and one age group: males of the age of 70.9 ± 2.78 years (mean ± SD). The subjects all being male reduces the effect of hormonal differences influencing the results (Kalervo Väänänen and Härkönen 1996). However, the question is raised: Would different alternative bone remodelling behaviours be observed across different demographics and populations?

In addition to focusing on a limited population demographic, this study examined the bone remodelling in 11 subjects from a clinical exercise trial. From these 11 subjects, this study managed to derive statistical differences and correlations in the bone remodelling behaviour under tension and compression. Still, the limitations of using 11 subjects to derive statistical conclusions is acknowledged. This does not diminish the results of this study; where clear differences in bone remodelling behaviour were observed, but instead, highlights the fact that a larger study is required to develop a better understanding.

5.4.3 Inclusion Criteria

The second inclusion criteria of this study was that the subjects from the Allison, Folland et al. (2013) clinical trial is that subject must have experienced at least a 2% change in density, which eliminated 8 of the 19 subjects which had passed the initial criteria. The decision to use this inclusion criteria was to increase the chance of observing alternative bone remodelling, where it was considered that subjects who had less than 2% change in density would have not experienced enough bone remodelling to exhibit alternative bone remodelling behaviour. Although some alternative bone remodelling was observed at changes in density below 2%, this decision was supported by the results, where the main characteristics of alternative bone remodelling were observed in remodelling beyond the 2% change in density. Since a 2% change in density is

approximately the typical amount of bone remodelling experienced during an high impact loading exercise trial (Kukuljan, Nowson et al. 2009, Kukuljan, Nowson et al. 2011, Allison, Folland et al. 2013), this limits the findings that different subjects can provide in this study and others, where only those which experience a high amount of bone remodelling will provide good data for all the alternative bone remodelling characteristics.

5.4.4 Influence of Age

Age is usually associated with negative connotations, in both biomechanics and bone mechanoresponsiveness, regardless of if they are true or not. The average age of the subjects used in this study was 70.9 ± 2.78 years (mean ± SD), and consequently the influence of age on the results of this study was a major consideration. Fortunately, several studies have been conducted into the influence of age on biomechanics and bone mechanoresponsiveness prior to this study.

As explored in Chapter 2, Anderson and Madigan (2013) demonstrated that older subjects experienced similar muscle force and hip contact loads as younger subjects. Little research has been conducted into the influence of age on the density elasticity equation due to lack of available data. Nonetheless, the density-elasticity equation used in this study to determine the bone's mechanical properties was taken from Keller (1994), where the density-elasticity equation was developed using a similar sex and age subject demographic as the subjects used in this study.

Despite the research being conducted into bone mechanoresponsiveness due to conditions such as osteoporosis, little is known about the effect of age on the mechanoresponsiveness. However, older bones have been demonstrated to be mechanoresponsive if adequate stimuli is applied (Kotiya and Silva 2013). The stimuli experienced by the femur of the subjects in this study was already demonstrated to be adequate before this study began, by the Allison, Folland et al. (2013) clinical trial who observed an overall increase in bone density.

Therefore, the researcher of this study is confident that the subjects used in this study were suitable for the investigation into alternative bone remodelling behaviours. Though, with such a narrow population age used in this study, an interesting question for future studies is raised and warrants

further research: Are age and alternative bone remodelling behaviours linked? Does age influence one or more of the alternative bone remodelling mechanisms?

5.4.5 Positive vs Negative Remodelling

The current alternative remodelling theories are all concerned with positive remodelling environments, where the bone should or does experience an increase in density (Rubinacci, Black et al. 1988, Bentolila, Boyce et al. 1998, Stokes, Gwadera et al. 2005). This study was unable to provide evidence for or against the presence of alternative bone remodelling in negative remodelling as it only had the data available to examine positive remodelling. As a result, further research is required into alternative bone remodelling in negative remodelling situations.

5.4.6 Other Stimuli

This study utilised a nonlinear, strain-based stimulus, which used the experienced strain and a reference strain which was calculated using subject specific finite element simulation and previously determined musculoskeletal models. The use of this stimulus was based on: 1) The current literature and biological evidence that states this is the most accurate stimulus. 2) The aim of this study; where the aim of the study was to investigate a potential difference in bone remodelling between tension and compression. It was thought that additional factors would complicate the comparison and may introduce parameters which would have to be set on pre-set assumptions; for example a mechanism acting homogenously in compression and tension. The stimulus used in this study is one that is widely used and said to be accurate and hence was not considered to be too simple for the task. However, it needs to be considered that other stimuli may observe different results or improve on the observations of this study when examining the bone remodelling behaviour under tension and compression.

Chapter 6. Conclusion

This study set out to conduct an initial investigation into whether alternative bone remodelling behaviour under tension and compression which has been observed in laboratory and pathological conditions could be observed under physiological loading conditions. In the undertaking of this study, it was unclear what, if any, differences in the bone remodelling under tension and compression, would be observed. Yet, by comparing the change in density against the mechanical stimulus by using a remodelling algorithm (equation 4-1), this study has managed to identify differences in bone remodelling behaviour under tension in compression in the proximal femur of 11 subjects from the Allison, Folland et al. (2013) clinical exercise trial. The differences in bone remodelling observed in this study, as summarised in 4.6 Summary of Findings, were characterised by: 1. Differences in the b value of the bone remodelling algorithm, where tension has a higher b value (p = 0.054) with the k value being calculable by the b value (p < 0.01); 2. Differences in the RMSE and R^2 values, where tension has a lower RMSE (p = 0.164) and higher R^2 value (p < 0.01), and, 3. Differences in the observed regression biases, where tension has a significantly lower regression bias (p = 0.141).

An interesting observation made in this study was the increasing deviation in the change in density in response to the stimulus as a result of the alternative bone remodelling mechanisms. This deviation occurs beyond a cross-over point of the two stimulus-remodelling relationships, which whilst being subject specific occurred at a mean stimulus ($\varepsilon - \varepsilon_o$) of 672 με, which corresponds to a change in density of approximately 3.5% in both tension and compression. This is higher than the typical change in density experienced during exercise (Kukuljan, Nowson et al. 2009, Kukuljan, Nowson et al. 2011). Before this cross-over point, the difference in the change in density in response to the stimulus is less pronounced, suggesting that alternative bone remodelling only becomes a consideration in high loading conditions.

The study also found that bone under both tension and compression could experience typical and atypical stimulus-remodelling relationships, with there being an abundance of atypical stimulus-

remodelling relationships under compression, with it being experienced by 6 of the 11 subjects in this study under compression. Still, the atypical stimulus-remodelling relationship was not considered to be different to the typical stimulus-remodelling relationship, just a continuation of the b values which could be experienced by tension and compression as a result of bone remodelling mechanisms. Nonetheless, it was found that linear bone remodelling algorithms struggle to account for the observed atypical stimulus-remodelling relationships.

By comparing the observations of this study against the known characteristics of alternative bone remodelling mechanisms, this study has found evidence that the high RMSE, low R^2 and significant regression biases observed under compression in relation to tension could be influenced by linear microdamage. This form of microdamage, which only forms under compression and is the only type of microdamage to initiate bone remodelling, is thought to cause random variations in the volume of the bone experiencing remodelling, effecting the measured change in density. Furthermore, by comparing the results of this study against the known alternative bone remodelling mechanisms, it was thought that the difference in the b values, where compression had a continuously lower b value than tension could be influenced by the Hueter-Volkmann law, which retards bone growth under compression, but not tension.

6.1 Impact of Study

It is well accepted that different people will experience different bone remodelling behaviour due a variety of different factors (Parfitt 2004, Robling and Turner 2009), it is even accepted that different areas of the skeletal system (e.g. the skull and the femur) will experience different rates of bone remodelling (Parfitt 2002). However, it is generally assumed that bone will experience the same remodelling behaviour under tension and compression. Following evidence from laboratory studies and pathological conditions, this thesis provided evidence that the bone is continuously experiencing alternative bone remodelling behaviours under regions of tension and compression. As such it has highlighted an area which requires further research and as a result, this study could help further our understanding of how bone remodelling occurs and could have a potential impact on future bone remodelling simulations.

6.2 Future Work

This study was an initial investigation into if alternative bone remodelling between tension and compression could be observed in the cortical bone of the proximal femur under physiological loading conditions. However, despite the findings of this study, there are still numerous questions into alternative bone remodelling that need further investigation.

By examining the bone remodelling in the cortical bone of the proximal femur, of 11 men aged 70.9 ± 2.78 years (mean ± SD), taking part in a yearlong clinical hoping study, this study found evidence that alternative bone remodelling is present in tension and compression under physiological loading conditions. The next stage from this study would be to examine alternative bone remodelling in areas of the body that experience both tension and compression, and to examine alternative bone remodelling in the context of other bone remodelling algorithms, to see if any additional clarity to the alternative-bone remodelling phenomenon can be added. In particular, the author feels research into remodelling initiation probability in the context of alternative remodelling is of particular importance, as this would potentially allow for remodelling algorithms to incorporate alternative bone remodelling in smaller areas/volumes, which increases the resolution of the remodelling prediction. Following this, any findings, can implemented into self-design simulation studies, and the results to be compared against the traditional methods/algorithms which do not account for alternative bone remodelling, to determine if any improvement in predictive accuracy is made.

Furthermore, the results of this study, whilst indicative that alternative bone remodelling does occur under physiological loading conditions, cannot be applied unreservedly to all populations, lengths of time and areas of the skeletal system, and can only be used as a reference for the proximal femur. For this reason, further studies into the potential presence of alternative bone remodelling under physiological loading conditions is needed, allowing for a range of different populations, parameters, anatomical locations and periods of time to aid a better understanding of alternative bone remodelling, its factors, and its effects on the skeletal system in different people. Additionally, in this age of orthopaedic implants, and the rise of 3D printed implants, research is needed into if alternative bone remodelling is present around orthopaedic implants of all sizes, and into if it influences the implants clinical success rate. Therefore, in future studies, a particular focus

should be made on the spine and femur, as these are key locations for orthopaedic implants and conditions where alternative bone remodelling is known to exist.

Additionally, a better understanding of the biomechanical and cellular mechanics involved in alternative bone remodelling is needed since understanding the mechanisms which cause alternative bone remodelling behaviour is of importance as it could aid in preventative measures before pathological conditions occur. In comparing the results of this study to current alternative bone remodelling literature, this study managed to align known behaviours of different bone remodelling mechanisms with the observed bone remodelling behaviour: where this study identified microdamage production and the Hueter-Volkmann law as likely mechanisms to contribute to alternative bone remodelling behaviour in physiological loading conditions. However, this was simple postulation through the correlation of known and observed alternative bone remodelling behaviours. Furthermore, with this study's design, where any and all alternative bone remodelling mechanisms could be present, it is difficult to pinpoint exactly which mechanism is responsible for which observed behaviour. As such, further research using controlled studies where alternative bone remodelling mechanisms are encouraged or discouraged (e.g. using bisphosphonates to prevent linear microdamage induced alternative remodelling) would aid the understanding of which alternative bone remodelling mechanisms are responsible for which behaviours.

References

Aamodt, A., J. Lund-Larsen, J. Eine, E. Andersen, P. Benum and O. S. Husby (1997). "In vivo measurements show tensile axial strain in the proximal lateral aspect of the human femur." Journal of Orthopaedic Research **15**(6): 927-931.

Adachi, T., Y. Kameo and M. Hojo (2010). "Trabecular bone remodelling simulation considering osteocytic response to fluid-induced shear stress." Philosophical Transactions of the Royal Society A **368**: 2669-2682.

Albogha, M. H., T. Kitahara, M. Todo, H. Hyakutake and I. Takahashi (2015). "Maximum principal strain as a criterion for prediction of orthodontic mini-implants failure in subject-specific finite element models." The Angle Orthodontist **86**(1): 24-31.

Allison, S., J. Folland, Rennie, G. Summers, Brooke-Wavell and K (2013). "High impact exercise increased femoral neck bone mineral density in older men: A randomised unilateral intervention." Bone **53**: 321-328.

Allison, S., K. Poole, G. Treece, A. Gee, C. Tonkin, W. Rennie, J. Folland, G. Summers and K. Brooke-Wavell (2015). "The Influence of High-Impact Exercise on Cortical and Trabecular Bone Mineral Content and 3D Distribution Across the Proximal Femur in Older Men: A Randomized Controlled Unilateral Intervention." Journal of Bone and Mineral Research **30**(9): 1709-1716.

Anderson, D. E. and M. L. Madigan (2013). "Effects of age-related differences in femoral loading and bone mineral density on strains in the proximal femur during controlled walking." Journal of applied biomechanics **29**(5): 505-516.

Andrade-Campos, A., A. Ramos and J. Simoes (2012). "A model of bone adaptation as a topology optimization process with contact." Journal of Biomedical Science and Engineering **5**: 229-244.

Andreas Hölzera, Christian Schrödera, Matthias Woiczinskia, Patrick Sadoghib, Andreas Scharpfa, Bernhard Heimkesa, Volkmar Janssona (2013). "Subject Specific Finite Element Simulation of the Human Femur Considering Inhomogeneous Material Properties." Computer Methods and Programs in Biomedicine 82 - 88.

Andrew A. Marino, R. O. B., Sidney C. Soderholm (1971). "Origin of the piezoelectric effect in bone." Calcified Tissue Research **8**(1): 177-180.

Augustsson, J., R. Thomee, C. Lindon, M. Folkesson, R. Tranberg and J. Karlsson (2006). "Single-leg hop testing following fatiguing exercise: reliability and biomechanical analysis." Scandinavian Journal of Medicine & Science in Sports **16**: 111-120.

AZO. (2020). "Advancements in Micro-CT Technology." Retrieved 29 July, 2021, from https://www.azom.com/article.aspx?ArticleID=19548.

Baca, V., Z. Horak, P. Mikulenka and V. Dzupa (2008). "Comparison of an inhomogeneous orthotropic and isotropic material models used for FE analyses." Medical Engineering & Physics: 924 - 930.

Basu, B. (2017). Introduction to Biomechanics and Orthopedic Device Testing. Biomaterials for Musculoskeletal Regeneration: Concepts. B. Basu. Singapore, Springer Singapore**:** 385-407.

Beaupré, G. S., T. E. Orr and D. R. Carter (1990). "An approach for time-dependent bone modeling and remodeling—application: A preliminary remodeling simulation." Journal of Orthopaedic Research **8**(5): 662-670.

Becker, R. O., C. A. L. Bassett and C. H. Bachman (1964). Bioelectric factors controlling bone structure. Bone Biodynamics. H. Frost. Boston, Little, Brown and Company**:** 209-232.

Bell, J. A., D. Carslake, L. M. O'Keeffe, M. Frysz, L. D. Howe, M. Hamer, K. H. Wade, N. J. Timpson and G. Davey Smith (2018). "Associations of Body Mass and Fat Indexes With Cardiometabolic Traits." Journal of the American College of Cardiology **72**(24): 3142-3154.

Bentolila, A., T. Boyce, D. Fyhrie, R. Drumb, T. Skerry and M. Schaffler (1998). "Intracortical Remodeling in Adult Rat Long Bones After Fatigue Loading." Bone **23**(3): 275-281.

Bergmann, G., A. Bender, J. Dymke, G. N. Duda and P. Damm (2018). "Physical Activities That Cause High Friction Moments at the Cup in Hip Implants." JBJS **100**(19).

Bergmann, G., G. Deuretzbacher, M. Heller, F. Graicheb, A. Rohlmann, J. Strauss and G. Duda (2001). "Hip contact forces and gait patterns from routine activities." Journal of Biomechanics **34**: 859-871.

Bergmann, P., J. J. Body, S. Boonen, Y. Boutsen, J. P. Devogelaer, S. Goemaere, J. Kaufman, J. Y. Reginster and S. Rozenberg (2011). "Loading and Skeletal Development and Maintenance." Journal of Osteoporosis **2011**: 786752.

Biewener, A. A. (1993). "Safety factors in bone strength." Calcified Tissue International **53**(1): S68-S74.

BiologyOnline. (2001). "Lacuna | Anatomy and Physiology " Retrieved 01 March 2016, from https://www.biologyonline.com/.

Bitsakos, C., J. Kerner, I. Fisher and A. A. Amis (2005). "The effect of muscle loading on the simulation of bone remodelling in the proximal femur." Journal of Biomechanics **38**(1): 133-139.

BoneAndSpine.com. (2018). "Cortical Bone and Cancellous Bone." from http://boneandspine.com/cortical-bone-and-cancellous-bone/.

Bougherara, H., V. Klika, F. Marsik, I. Marik and L. Yahia (2010). "New predictive model for monitoring bone remodeling." Wiley Online Library.

Bouxsein, M. L., S. K. Boyd, B. A. Christiansen, R. E. Guldberg, K. J. Jepsen and R. Müller (2010). "Guidelines for assessment of bone microstructure in rodents using micro–computed tomography." Journal of Bone and Mineral Research **25**(7): 1468-1486.

Boyce, T., D. Fyhrie, M. Glotkowski, E. Radin and M. Schaffler (1998). "Damage Type and Strain Mode Associations in Human Compact Bone Bending Fatigue." J Orthop Res **16**: 322-329.

Buie, H. R., G. M. Campbell, R. J. Klinck, J. A. MacNeil and S. K. Boyd (2007). "Automatic segmentation of cortical and trabecular compartments based on a dual threshold technique for in vivo micro-CT bone analysis." Bone **41**(4): 505-515.

Burkhart, T., D. Andrews and C. Dunning (2013). "Finite element modeling mesh quality, energy balance and validation methods: A review with recommendations associated with the modeling of bone tissue." Journal of Biomechanics(46): 1477-1488.

Burr, D. (2002). "Targeted and nontargeted remodeling." Bone **30**(1): 2-4.

Burr, D. (2014). "Repair Mechanisms for Microdamage in Bone." Journal of Bone and Mineral Research.

Burr, D., M. Forwood, D. Fyhrie, R. Martin, M. Schaffler and C. Turner (1997). "Bone microdamage and skeletal fragility in osteoporotic and stress fractures." Journal of Bone Minearal Research **12**: 6-15.

Burr, D., R. Martin, M. Schaffler and E. Radin (1985). "Bone remodeling in response to in vivo fatigue microdamage " Journal of Biomechanics **18**: 189-200.

Burr, D., A. Robling and C. Turner (2002). "Effects of Biomechanical Stress on Bones in Animals." Bone **30**(5): 781-786.

Burr, D., C. Turner, P. Naick, M. Forwood and R. Pidaparti (1998). "Does microdamage accumulation affect the mechanical properties of bone?" Trans Orthop Res Soc **31**: 337-345.

Burr, D. B. and R. B. Martin (1993). "Calculating the probability that microcracks initiate resorption spaces." Journal of Biomechanics **26**: 613-616.

Burr, D. B., C. Milgrom, D. Fyhrie, M. Forwood, M. Nyska, A. Finestone, S. Hoshaw, E. Saiag and A. Simkin (1996). "In vivo measurement of human tibial strains during vigorous activity." Bone **18**(5): 405-410.

Burstein, A., H, D. T. Reilly and M. Martens (1976). "Aging of bone tissue: mechanical properties." (0021-9355 (Print)).

Canon. "Canon Medical Systems USA - Computed Tomography." Retrieved 29 July, 2021, from https://us.medical.canon/products/computed-tomography/.

Cao, J. J. (2011). "Effects of obesity on bone metabolism." Journal of orthopaedic surgery and research **6**: 30-30.

Carter, D. R. (1982). "The relationship between in vivo strains and cortical bone remodeling." Crit Rev Biomed Eng.(1): 1-28.

Cerrolaza, M., V. Duarte and D. Garzón-Alvarado (2017). "Analysis of Bone Remodeling Under Piezoelectricity Effects Using Boundary Elements." Journal of Bionic Engineering **14**(4): 659-671.

Cheung, A., L. Tile, Y. Lee, G. Tomlinson, G. Hawker, J. Scher, H. Hu, R. Vieth, L. Thompson and S. Jamal (2008). "Vitamin K Supplementation in Postmenopausal Women with Osteopenia (ECKO Trial): A Randomized Controlled Trial." PLoS medicine **5**: e196.

Christen, P., K. Ito, R. Ellouz, S. Boutroy, E. Sornay-Rendu, R. D. Chapurlat and B. van Rietbergen (2014). "Bone remodelling in humans is load-driven but not lazy." Nature Communications **5**(1): 4855.

Ciani, C., S. Doty and Fritton (2005). "Mapping bone interstitial fluid movement: Displacement of ferritin tracer during histological processing." Bone **37**(3): 379-387.

Cleather, D., J. Goodwin and A. Bull (2011). "An Optimization Approach to Inverse Dynamics Provides Insight as to the Function of the Biarticular Muscles During Vertical Jumping." Annals of Biomedical Engineerig **39**: 147-160.

Cleather, D., J. Goodwin and A. Bull (2013). "Hip and knee joint loading during vertical jumping and push jerking." Clinical Biomechanics **28**: 98-103.

Cleather, D. J. and A. M. J. Bull (2010). "Lower-extremity musculoskeletal geometry affects the calculation of patellofemoral forces in vertical jumping and weightlifting." Proceedings of the Institution of Mechanical Engineers, Part H: Journal of Engineering in Medicine **224**(9): 1073-1083.

Colloca, M. (2009). Bone Remodeling Process as an Optimal Structural Design. Ph.D, Universita Di Roma.

Correa, T. A., K. M. Crossley, H. J. Kim and M. G. Pandy (2010). "Contributions of individual muscles to hip joint contact force

in normal walking." Journal of Biomechanics **43**(8).

Cowin, S. and D. Hegedus (1976). "Bone remodeling I: theory of adaptive elasticity." Journal of Elasticity **6**.

Cristofolini, L., B. P. McNamara, A. Freddi and M. Viceconti (1997). "In vitro measured strains in the loaded femur: Quantification of experimental error." The Journal of Strain Analysis for Engineering Design **32**(3): 193-200.

Currey, J., K. Brear and P. Zioupous (1996). "The effects of againg and changes in minearl content in degrading the toughness of human femora." J Biomech **29**: 257.

Currey, J. D. (2004). "Tensile yield in compact bone is determined by strain, post-yield behaviour by mineral content." Journal of Biomechanics **37**(4): 549-556.

Delp, S. L. and J. P. Loan (1995). "A graphics-based software system to develop and analyze models of musculoskeletal structures." Computers in Biology and Medicine **25**(1): 21-34.

Depalle, B., R. Chapurlat, H. Walter-Le-Berre, B. Bou-Saïd and H. Follet (2013). "Finite element dependence of stress evaluation for human trabecular bone." Journal of the Mechanical Behavior of Biomedical Materials **18**: 200-212.

Dodd, J., J. Raleigh and T. Gross (1999). "Osteocyte hypoxia: a novel mechanotransduction pathway." Am Physiol Soc **277**: C598-C602.

Drake, M., B. Clarke and S. Khosla (2008). "Bisphosphonates: Mechanism of Action and Role in Clinical Practice." Mayo Clinic Proceedings **83**(9): 1032-1045.

Drevelle, O. and N. Faucheux (2013). "Biomimetic materials for controlling bone cell responses." Frontiers in Bioscience(5): 369-395.

Du, J., V. Silberschmidt, K. Brooke-Wavell, C. Hartley and S. Li (2018). A longitudinal HR-pQCT study of exercise on bone adaptation in postmenopausal women. World Congress of Biomechanics, Dublin.

Duda, G., D. Brand, S. Freitag, W. Lierse and E. Scheider (1996). "Variability of Femoral Muscle Attachments." Journal of Biomechanics **29**(9): 1185 - 1190.

Duda, G., M. Heller, J. Albinger, O. Schulz, E. Schneider and L. Claes (1998). "Influence of muscle forces on femoral strain distribution " Journal of Biomechanics **31**: 841-846.

Duda, G., E. Schneider and E. Chao (1997). "Internal forces and moment in the femur during walking." Journal of Biomechanics **30**: 933-941.

Eberle, S., M. Gottlinger and P. Augat (2013). "An investigation to determine if a single validated density-elasticity relationship can be used for subject specific finite element analyses of human long bones." Medical Engineering & Physics **35**: 875-883.

Edwards, W. B., R. H. Miller and T. R. Derrick (2016). "Femoral strain during walking predicted with muscle forces from static and dynamic optimization." Journal of Biomechanics **49**(7): 1206-1213.

Erdemir, A., S. McLean, W. Herzog and A. van den Bogert (2007). "Model-based estimation of muscle forces exerted during movement." Clinical Biomechanics **22**: 131-154.

Eriksen, E. (2010). "Cellular mechanisms of bone remodeling." Reviews in Endocrine and Metabolic Disorders **11**: 219-227.

Eriksen, E. F. (1986). "Normal and Pathological Remodeling of Human Trabecular Bone: Three Dimensional Reconstruction of the Remodeling Sequence in Normals and in Metabolic Bone Disease*." Endocrine Reviews **7**(4): 379-408.

Eriksson, C. (1974). "Streaming Potentials and Other Water-Dependent effects in Minearlized Tissues." Annals of the New York Academy of Sciences **238**(1): 321-338.

Fernández, J. R., J. M. García-Aznar and R. Martínez (2012). "Piezoelectricity could predict sites of formation/resorption in bone remodelling and modelling." Journal of Theoretical Biology **292**: 86-92.

Field, A. P. (2018). Discovering statistics using IBM SPSS statistics.

Frehill, B. (2010). Initial and Long Term Stability of Augmented Knee Arthroplasty using Finite Element Methods. PhD, University of Surrey.

Frehill, B., A. Crocombe, S. Cirovic, Y. Agarwal and N. Bradley (2009). "Initial stability of type-2 tibial defect treatments." Proceedings of the Institution of Mechanical Engineers, Part H: Journal of Engineering in Medicine **224**(1): 77-85.

Frost, H. M. (1983). "A determinant of bone architecture. The minimum effective strain." Clin Orthop Relat Res. (175): 286-292.

Frost, H. M. (1987). "Bone "mass" and the "mechanostat": a proposal." The Anatomical Record **219**: 1-9.

Frost, H. M. (2001). "From Wolff's law to the Utah paradigm: insights about bone physiology and its clinical applications." (0003-276X (Print)).

Frost, H. M. (2003). "Bone's Mechanostat: A 2003 Update." The Anatomical Record 1081 - 1101.

Fukada, E. and I. Yasuda (1957). "On the Piezoelectric Effect of Bone." Journal of the Physical Society of Japan **12**(10): 1158-1162.

Gaddini, G. W., R. T. Turner, K. A. Grant and U. T. Iwaniec (2016). "Alcohol: A Simple Nutrient with Complex Actions on Bone in the Adult Skeleton." Alcoholism, clinical and experimental research **40**(4): 657-671.

Galante, J., W. Rostoker and R. D. Ray (1970). "Physical properties of trabecular bone." Calcified Tissue Research **5**(1): 236-246.

Gere, J. and B. Goodno (2009). Mechanics of Materials. Stamford, Cengage Learning.

Gibson, L. J. (1985). "The mechanical behaviour of cancellous bone." Journal of Biomechanics **18**(5): 317-328.

Gong, H., L. Wang, M. Zhang and Y. Fan (2020). 10 - Computational modelling of bone and bone remodelling. Computational Modelling of Biomechanics and Biotribology in the Musculoskeletal System (Second Edition). Z. Jin, J. Li and Z. Chen, Woodhead Publishing**:** 227-249.

Goodship, A. E., T. J. Lawes and C. T. Rubin (2009). "Low-magnitude high-frequency mechanical signals accelerate and augment endochondral bone repair: preliminary evidence of efficacy." Journal of orthopaedic research : official publication of the Orthopaedic Research Society **27**(7): 922-930.

Gusmão, C. V. B. d. and W. D. Belangero (2015). "How do Bone Cells Sense Mechanical Loading." Revista brasileira de ortopedia **44**(4): 299-305.

Hadjidakis, D. and I. Androulakis (2006). "Bone Remodeling." Annals of the New York Academy of Sciences **1092**: 385-396.

Halldin, A., R. Jimbo, C. Johansson, A. Wennerberg, M. Jacobsson, T. Albrektsson and S. Hansson (2011). "The effect of static bone strain on implant stability and bone remodeling " Bone **49**(4): 783-789.

Hambli, R. (2014). "Connecting Mechanics and Bone Cell Activities in the Bone Remodeling Process: An Integrated Finite Element Modeling." Frontiers in Bioengineering and Biotechnology **2**: 6.

Hangartner, T. N. (2007). "Thresholding technique for accurate analysis of density and geometry in QCT, pQCT and microCT images." Journal of Musculoskeletal and Neuronal Interactions **7**(1): 9-16.

Hansen, U., P. Zioupos, R. Simpson, J. Currey and D. Hynd (2008). "The Effect of Strain Rate on the Mechanical Properties of Human Cortical Bone." J Biomed Eng **130**: 011011-011018.

Harrigan, T. and J. Hamilton (1994). "Bone remodeling and structural optimization." Journal of Biomechanics **27**(3): 323-328.

Hart, N. H., R. U. Newton, J. Tan, T. Rantalainen, P. Chivers, A. Siafarikas and S. Nimphius (2020). "Biological basis of bone strength: anatomy, physiology and measurement." Journal of musculoskeletal & neuronal interactions **20**(3): 347-371.

He, C., W. He, J. Hou, K. Chen, M. Huang, M. Yang, X. Luo and C. Li (2020). "Bone and Muscle Crosstalk in Aging." Frontiers in Cell and Developmental Biology **8**: 1450.

Hebert-Losier, K., L. Schelin, E. Tengman, A. Strong and C. Hager (2018). "Curve analyses reveal altered knee, hip, and trunk kinematics during drop–jumps long after anterior cruciate ligament rupture." the Knee **25**(2): 226-239.

Helgason, B., E. Perilli, E. Schileo, F. Taddei, S. Brynjolfsson and M. Viceconti (2008). "Mathematical relationships between bone density and mechanical properties: A literature review." Clinical Biomechanics **23**(2): 135-146.

Helgason, B., F. Taddei, H. Palsson, E. Schileo, L. Cristofolini, M. Viceconti and S. Brynjolfsson (2008). "A modified method for assigning material properties to FE models of bones." Medical Engineering & Physics: 444-453.

Heller, M. O., G. Bergmann, G. Deuretzbacher, L. Dürselen, M. Pohl, L. Claes, N. P. Haas and G. N. Duda (2001). "Musculo-skeletal loading conditions at the hip during walking and stair climbing." Journal of Biomechanics **34**(7): 883-893.

Heller, M. O., G. Bergmann, J. P. Kassi, L. Claes, N. P. Haas and G. N. Duda (2005). "Determination of muscle loading at the hip joint for use in pre-clinical testing." Journal of Biomechanics **38**(5): 1155-1163.

Helwig, P., U. Hindenlang, A. Hirschmüllera, L. Konstantinidisa, S. N and R. Schneiderc (2013). "A Femoral Model with All Relevant Muscles and Hip Capsule Ligaments." Computer Methods in Biomechanics and Biomedical Engineering **16**(6): 669 - 677.

Herman, B., L. Cardoso, R. Majeska, K. Jepsen and M. Schaffler (2010). "Activation of bone remodeling after fatigue: differential response to linear microcracks and diffuse damage." Bone(47): 766-722.

Hernandez, C., A. Gupta and T. Keaveny (2006). "A Biomechanical Analysis of the Effects of Resorption Cavities on Cancellous Bone Strength." J Bone Minear Res **21**(8): 1248-1255.

Hill, A. V. (1938). "The Heat of Shortening and the Dynamic Constants of Muscle." Proceedings of the Royal Society of London Series B **126**: 136-195.

Hill, P. A. (1998). "Bone Remodelling." British Journal of Orthodontics **25**(2): 101-107.

Holden, J. P., J. A. Orsini, K. L. Siegel, T. M. Kepple, L. H. Gerber and S. J. Stanhope (1997). "Surface movement errors in shank kinematics and knee kinetics during gait." Gait & Posture **5**(3): 217-227.

Hong, J., J. A. Hipp, R. V. Mulkern, D. Jaramillo and B. D. Snyder (1999). "Magnetic Resonance Imaging Measurments of Bone Density and Cross-Sectional Geometry " Calified Tissue International 74-78.

Horsman, K., H. Koopman, F. van der Helm, L. Poliacu Prose and H. Veeger (2007). "Morphological muscle and joint parameters for musculoskeletal modelling of the lower extremity." Clinical Biomechanics **22**: 239-247.

Hou, J., C. He, W. He, M. Yang, X. Luo and C. Li (2020). "Obesity and Bone Health: A Complex Link." Frontiers in Cell and Developmental Biology **8**: 1620.

Hsieh, Y.-F. and C. H. Turner (2001). "Effects of Loading Frequency on Mechanically Induced Bone Formation." Journal of Bone and Mineral Research **16**(5): 918-924.

Huiskes, R., R. Ruimerman, G. van Lenthe and J. Janssen (2000). "Effects of mechanical forces on maintenance and adaptation of form in trabecular bone." Nature **405**: 704-706.

Ingrid, E., H. Kjartan, W. Pär, F.-T. Li and R. Christer (1998). "Local Bone Deformation at Two Predominant Sites for Stress Fractures of the Tibia: An In Vivo Study." Foot & Ankle International **19**(7): 479-484.

Jang, I., I. Kim and B. Kwak (2009). "Analogy of Strain Energy Density Based Bone-Remodeling Algorithm and Structual Topology Optimization." Journal of Biomechanical Engineering **131**.

Jilka, R., B. Noble and R. Weinstein (2013). "Osteocyte apoptosis " Bone **54**: 264-271.

Jilka, R., R. Weinstein, T. Bellido, P. Roberson, A. Parfirr and S. Manolaga (1999). "Increased bone formation by prevention of osteoblast apoptosis with parathyroid hormone." Journal of Clinical Investigation **104**(4): 439-446.

Jowsey, J. (1966). "Studies of Haversian systems in man and some animals." Journal of Anatomy **100**(4): 859-864.

Juszczyk, M. M., L. Cristofolini and M. Viceconti (2011). "The human proximal femur behaves linearly elastic up to failure under physiological loading conditions." Journal of Biomechanics: 2259-2266.

Kalervo Väänänen, H. and P. L. Härkönen (1996). "Estrogen and bone metabolism." Maturitas **23**: S65-S69.

Karim, L. and D. Vashishth (2013). "Bone Microdamage and Its Contributions to Fracture." Studies in Mechanobiology, Tissue Engineering and Biomaterials **5**: 87-107.

Keller, T. S. (1994). "Predicting the compressive mechanical behavior of bone." Journal of Biomechanics **27**(9): 1159-1168.

Keyak, J. (2001). "Improved prediction of proximal femur fracture load using nonlinear finite element models." Journal of Medical Engineering Physics: 165 - 173.

Keyak, J. and Y. Falkinstein (2003). "Comparison of in situ and in vitro CT scan-based finite element model predictions of proximal femoral fracture load." Medical engineering & physics **25**: 781-787.

Keyak, J., I. Y. Lee and H. Skinner (1994). "Correlations between orthogonal mechanical properties and density of trabecular bone: use of different densitometric measures." Journal of biomedical materials research **28 11**: 1329-1336.

Kim, C. H., E. Takai, H. Zhou, D. Von Stechow, R. Müller, D. W. Dempster and X. E. Guo (2003). "Trabecular Bone Response to Mechanical and Parathyroid Hormone Stimulation: The Role of Mechanical Microenvironment." Journal of Bone and Mineral Research **18**(12): 2116-2125.

Kim, H., H.-S. Kim, E. Moon, C.-S. Yoon, T.-S. Chung, H.-T. Song, J.-s. Suh, Y. H. Lee and S. Kim (2010). "Scoliosis Imaging: What Radiologists Should Know—Erratum." Radiographics : a review publication of the Radiological Society of North America, Inc **30**: 1823-1842.

Knothe Tate, M. L. and U. Knothe (2000). "An ex vivo model to study transport processes and fluid flow in loaded bone." Journal of Biomechanics **33**(2): 247-254.

Koopman, H. and K. Horsman (2008). Hip compression force estimation with a comprehensive musculoskeletal model. 6th International Conference on Methods and Techniques in Behavioral Research. Wageningen.

Kopperdahl, D. and T. Keaveny (1998). "Yield strain behavior of trabecular bone." Journal of Biomechanics **31**: 601-608.

Kostka, J., M. Niwald, A. Guligowska, T. Kostka and E. Miller (2019). "Muscle power, contraction velocity and functional performance after stroke." Brain and behavior **9**(4): e01243-e01243.

Kotiya, A. and M. Silva (2013). "The Effect of Aging on Skeletal Mechanoresponsiveness: Animal Studies." Studies in Mechanobiology, Tissue Engineering and Biomaterials **5**: 191-216.

Kukuljan, S., C. A. Nowson, S. L. Bass, K. Sanders, G. C. Nicholson, M. J. Seibel, J. Salmon and R. M. Daly (2009). "Effects of a multi-component exercise program and calcium–vitamin-D3-fortified milk on bone mineral density in older men: a randomised controlled trial." Osteoporosis International **20**(7): 1241-1251.

Kukuljan, S., C. A. Nowson, K. M. Sanders, G. C. Nicholson, M. J. Seibel, J. Salmon and R. M. Daly (2011). "Independent and Combined Effects of Calcium-Vitamin D3 and Exercise on Bone Structure and Strength in Older Men: An 18-Month Factorial Design Randomized Controlled Trial." The Journal of Clinical Endocrinology & Metabolism **96**(4): 955-963.

Kuzyk, P. R. and E. H. Schemitsch (2009). "The science of electrical stimulation therapy for fracture healing." Indian journal of orthopaedics **43**(2): 127-131.

Lai, W. M., D. Rubin and E. Krempl (2009). Introduction to Continuum Mechanics. Oxford, Elsevier.

Langkamer, V. G., C. P. Case, P. Heap, A. Taylor, C. Collins, M. Pearse and L. Solomon (1992). "Systemic distribution of wear debris after hip replacement. A cause for concern?" The Journal of Bone and Joint Surgery. British volume **74-B**(6): 831-839.

Lanyon, L. and C. Rubin (1984). "Static vs dynamic loads as an influence on bone remodelling." Journal of Biomechanics(17): 897-905.

Lanyon, L. E., W. G. Hampson, A. E. Goodship and J. S. Shah (1975). "Bone deformation recorded in vivo from strain gauges attached to the human tibial shaft." (0001-6470 (Print)).

Lee, T. C., S. Mohsin, D. Taylor, R. Parkesh, T. Gunnlaugsson, F. J. O'Brien, M. Giehl and W. Gowin (2003). "Detecting microdamage in bone." Journal of Anatomy **203**(2): 161-172.

Lenaerts, G., F. De Groote, B. Demeulenaere, M. Mulier, Van Der Perre, A. Spaepen and L. Jonkers (2008). "Subject-specific hip geometry affects predicted hip joint contact forces during gait." Journal of Biomechanics **41**(6): 1243-1252.

Lencioni, T., I. Carpinella, M. Rabuffetti, A. Marzegan and M. Ferrarin (2019). "Human kinematic, kinetic and EMG data during different walking and stair ascending and descending tasks." Scientific Data **6**(1): 309.

Leng, H., X. N. Dong and X. Wang (2009). "Progressive post-yield behavior of human cortical bone in compression for middle-aged and elderly groups." Journal of biomechanics **42**(4): 491-497.

Lerebours, C., C. Thomas, D,L, J. Clement, G, P. Buenzli, R and P. Pivonka (2015). "The relationship between porosity and specific surface in human cortical bone is subject specific." Bone **75**: 109-117.

Li, Y., L. A. Jacox, S. H. Little and C.-C. Ko (2018). "Orthodontic tooth movement: The biology and clinical implications." The Kaohsiung Journal of Medical Sciences **34**(4): 207-214.

Lin, E. and A. Alessio (2009). "What are the basic concepts of temporal, contrast, and spatial resolution in cardiac CT?" Journal of cardiovascular computed tomography **3**(6): 403-408.

Lin, H. (2010). Biomechanical modeling of vertebral mechanobiological growth and of the deformation process in adolescent idiopathic scolosis. PhD, Ecole Polytechnique De Montreal.

Lindle, R. S., E. J. Metter, N. A. Lynch, J. L. Fleg, J. L. Fozard, J. Tobin, T. A. Roy and B. F. Hurley (1997). "Age and gender comparisons of muscle strength in 654 women and men aged 20–93 yr." Journal of Applied Physiology **83**(5): 1581-1587.

Lotz, J. C., T. N. Gerhart and W. C. Hayes (1990). "Mechanical properties of trabecular bone from the proximal femur: a quantitative CT study." (0363-8715 (Print)).

Lotz, J. C., T. N. Gerhart and W. C. Hayes (1991). "Mechanical properties of metaphyseal bone in the proximal femur." Journal of Biomechanics **24**(5): 317-329.

Mackin, D., X. Fave, L. Zhang, D. Fried, J. Yang, B. Taylor, E. Rodriguez-Rivera, C. Dodge, A. K. Jones and L. Court (2015). "Measuring Computed Tomography Scanner Variability of Radiomics Features." Investigative radiology **50**(11): 757-765.

Mak, A. and J. D. Zhang (2001). "Numerical Simulation of Streaming Potentials Due to Deformation-Induced Hierarchical Flows in Cortical Bone." Journal of biomechanical engineering **123**: 66-70.

Martin, R. (1984). "Porosity and specific surface of bone." Critical Reviews in Biomedical Engineering **10**: 179-222.

Martin, R. B. (1979). "Theoretical analysis of the piezoelectric effect in bone." Journal of Biomechanics **12**(1): 55-63.

Mashiba, J. and D. Burr (2001). "Bisphosphonate Treatment Suppresses Not Only Stochastic Remodelling but Also the Targeted Repair of Microdamage." Calified Tissue International **69**: 281-286.

Maurel, D. B., K. Jähn and N. Lara-Castillo (2017). "Muscle-Bone Crosstalk: Emerging Opportunities for Novel Therapeutic Approaches to Treat Musculoskeletal Pathologies." Biomedicines **5**(4): 62.

McCalden, R., J. McGeough, M. Barker and C. Court-Brown (1993). "Age-related changes in the tensile properties of cortical bone. The relative importance of changes in porosity, mineralization, and microstructure." Journal of Bone & Joint Surgery(75): 1193-1205.

McDonald, F. and W. J. Houston (1990). "An in vivo assessment of muscular activity and the importance of electrical phenomena in bone remodelling." Journal of anatomy **172**: 165-175.

McGarry, J. G., J. Klein-Nulend, M. G. Mullender and P. J. Prendergast (2005). "A comparison of strain and fluid shear stress in stimulating bone cell responses—a computational and experimental study." The FASEB Journal **19**(3): 1-22.

McNamara, L. M. and P. J. Prendergast (2007). "Bone remodelling algorithms incorporating both strain and microdamage stimuli." Journal of Biomechanics **40**: 1381-1391.

Milgrom, C., A. Finestone, Y. Levi, A. Simkin, I. Ekenman, S. Mendelson, M. Millgram, M. Nyska, N. Benjuya and D. Burr (2000). "Do high impact exercises produce higher tibial strains than running?" British Journal of Sports Medicine **34**(3): 195.

Milgrom, C., A. Finestone, N. Sharkey, A. Hamel, V. Mandes, D. Burr, A. Arndt and I. Ekenman (2002). "Metatarsal Strains Are Sufficient to Cause Fatigue Fracture During Cyclic Overloading." Foot & Ankle International **23**(3): 230-235.

Milgrom, C., M. Miligram, A. Simkin, D. Burr, I. Ekenman and A. Finestone (2001). "A Home Exercise Program for Tibial Bone Strengthening Based on In Vivo Strain Measurements." American Journal of Physical Medicine & Rehabilitation **80**(6).

Modenese, L., A. Phillips and A. Bull (2011). "An open source lower limb model: Hip joint validation." Journal of Biomechanics **44**: 2185 - 2193.

Morrison, R., K. N Kashlan, C. Flanagan, J. Wright, G. Green, S. Hollister and K. Weatherwax (2015). Regulatory Considerations in the Design and Manufacturing of Implantable 3D-Printed Medical Devices.

Morrison, T. M., P. Pathmanathan, M. Adwan and E. Margerrison (2018). "Advancing Regulatory Science With Computational Modeling for Medical Devices at the FDA's Office of Science and Engineering Laboratories." Frontiers in medicine **5**: 241-241.

Mosca, L. N., T. B. L. Goldberg, V. N. da Silva, C. S. Kurokawa, A. C. B. Rizzo, C. C. da Silva, A. dos Santos Teixeira and J. E. Corrente (2017). "The impact of excess body fat on bone remodeling in adolescents." Osteoporosis International **28**(3): 1053-1062.

Mullender, M. and R. Huiskes (1995). "Proposal for the regulatory mechanism of Wolff's law." Journal of Orthopaedic Research **13**(4): 503-512.

Murrills, R., L. Stein, C. Fey and D. Dempster (1990). "The effects of parathyroid hormone (PTH) and PTH-related peptide on osteoclast resorption of bone slices in vitro: an analysis of pit size and the resorption focus." Endocrinology **127**(6): 2648-2653.

Myer, G. D., N. A. Bates, C. A. DiCesare, K. D. Barber Foss, S. M. Thomas, S. C. Wordeman, D. Sugimoto, B. D. Roewer, J. M. Medina McKeon, S. L. Di Stasi, B. W. Noehren, M. McNally, K. R. Ford, A. W. Kiefer and T. E. Hewett (2015). "Reliability of 3-Dimensional Measures of Single-Leg Drop Landing Across 3 Institutions: Implications for Multicenter Research for Secondary ACL-Injury Prevention." Journal of sport rehabilitation **24**(2): 198-209.

Navarro, M., A. Michiardi, O. Castaño and J. A. Planell (2008). "Biomaterials in orthopaedics." Journal of the Royal Society, Interface **5**(27): 1137-1158.

NHS. (2019). "What is the body mass index (BMI)?" Retrieved 20 Aug, 2019, from https://www.nhs.uk/common-health-questions/lifestyle/what-is-the-body-mass-index-bmi/.

Niebur, G. L., M. J. Feldstein, J. C. Yuen, T. J. Chen and T. M. Keaveny (2000). "High-resolution finite element models with tissue strength asymmetry accurately predict failure of trabecular bone." Journal of Biomechanics **33**(12): 1575-1583.

NIH. (2000). "SEER Training Modules, Anatomical Terminology " Retrieved 19 June, 2020, from https://training.seer.cancer.gov/anatomy/body/terminology.html.

Niklas, A., P. Proff, M. Gosau and P. Römer (2013). "The role of hypoxia in orthodontic tooth movement." International Journal of Dentistry(1687-8728).

NJR (2018). 15th Annual Report 2018 National Joint Registry for England, Wales, Northern Ireland and the Isle of Man. M. Porter, National Joint Registry.

Nobel, B., N. Peet, H. Stevens, A. Brabbs, J. Mosley, G. Reilly, J. Reeve, T. Skerry and L. Lanyon (2003). "Mechanical loading: biphasic osteocyte survival and targeting of osteoclasts for bone destruction in rat cortical bone." Am J Physiol **284**: C934-C943.

Nyman, J., A. Roy, M. Reyes and X. Wang (2009). "Progressive mechanical behavior of human cortical bone in tension for two age groups." Journal of Biomedical Materials Research Part A **89**(2): 521-529.

Nyman, J. S., Q. Ni, D. P. Nicolella and X. Wang (2008). "Measurements of mobile and bound water by nuclear magnetic resonance correlate with mechanical properties of bone." Bone **42**(1): 193-199.

O'Brien, F., D. Taylor and T. Lee (2003). "Microcrack accumulation at different intervals during fatigue testing of compact bone." Journal of Biomechanics **36**: 973-980.

O'Connor, J., L. Laynon and J. MacFie (1982). "The influence of strain rate on adaptive bone remodelling." Journal of Biomechanics **15**: 767-781.

Oomens, C., M. Maenhout, C. van Oijen, M. Drost and F. Baaijens (2003). "Finite element modelling of contracting skeletal muscle." Philosophical transactions of the Royal Society of London B: 1453 - 1460.

Orthofix Holdings, I. (2019). "About Bone Growth Therapy." Retrieved 23 April 2019, 2019, from http://bonestimulation.com/how-it-works/.

Owan, I., D. Burr, C. Turner, J. Qiu, Y. Tu, E. Onyia and R. Duncan (1997). "Mechanotransduction in bone: Osteoblasts are more responsive to fluid forces than mechanical strain." The American journal of physiology **273**: C810-815.

Paker, N., D. Bugdayci, D. Tekdos, C. Dere and B. Kaya (2009). "Relationship between Bone Turnover and Bone Density at the Proximal Femur in Stroke Patients." Journal of Stroke and Cerebrovascular Diseases **18**(2): 139-143.

Papapoulos, S. (2008). "Bisphosphonates: how do they work?" Best Practice & Research Clinical Endocrinology & Metabolism **22**: 831-847.

Papathanasopoulou, V., D. Fotiadis and C. Massalas (2004). "A theoretical analysis of surface remodelling in long bones." International Joural of Engineering Science **3-4**(42): 395-409.

Parfitt, A. (2002). "Misconceptions (2): Turnover Is Always Higher in Cancellous Than in Coritcal Bone." Bone: 807 - 809.

Parfitt, A. (2004). "What is the normal rate of bone remodelling." Bone: 1-3.

Parsamian, G. and T. Norman (2001). "Diffuse damage accumulation in the fracture process zone of human cortical bone specimens and its influence on fracture toughness." J Mat Sci: Mat Med **12**: 779-783.

Plotkin, L. (2014). "Apoptotic osteocytes and the control of targeted bone resorption." Current Osteoporosis Reports **12**(1): 121-126.

Plotkin, L., I. Mathov, J. Aguirre, A. Parfitt, S. Manolagas and T. Bellido (2005). "Mechanical stimulation prevents osteocyte apoptosis: requirement of integrins, Src kinases, and ERKs." American Journal of Physiology - Cell Physiology **289**: C633-C643.

Pollack, S. R., E. Korostoff, M. E. Sternberg and J. Koh (1977). "Stress-generated potentials in bone: Effects of collagen modifications." Journal of Biomedical Materials Research **11**(5): 677-700.

Prendergast, P. and D. Taylor (1994). "Predction of bone adaption using damage accumulation." J Biomech **27**: 1047-1076.

Qin, Q.-H. (2013). Mechanics of Cellular Bone Remodeling Boca Raton CRC Press.

Qin, Y.-X., T. Kaplan, A. Saldanha and C. Rubin (2003). "Fluid pressure gradients, arising from oscillations in intramedullary pressure, is correlated with the formation of bone and inhibition of intracortical porosity." Journal of Biomechanics **36**(10): 1427-1437.

Ramos, A. and J. Simoes (2006). "Tetrahedral versus hexahedral finite elements in numerical modelling of the proximal femur." Medical Engineering & Physics **28**: 916-924.

Rhoa, J.-Y., L. Kuhn-Spearingb and P. Ziouposc (1998). "Mechanical Properties and the hierarchial structure of bone." Med Eng Phys: 92 - 102.

Robling, A. G. and C. H. Turner (2009). "Mechanical signaling for bone modeling and remodeling." Critical reviews in eukaryotic gene expression **19**(4): 319-338.

Romero, F. and F. Alonso (2016). "A comparison among different Hill-type contraction dynamics formulations for muscle force estimation." Mechanical Sciences **7**: 19-29.

Rubin, C. and L. Lanyon (1984). "Regulation of bone formation by applied dynamic loads " Journal of Bone & Joint Surgery **66-A**: 397-402.

Rubin, C. T. and L. E. Lanyon (1982). "Limb mechanics as a function of speed and gait: a study of functional strains in the radius and tibia of horse and dog." Journal of Experimental Biology **101**(1): 187.

Rubinacci, A., J. Black, C. T. Brighton and Z. B. Friedenberg (1988). "Changes in bioelectric potentials on bone associated with direct current stimulation of osteogenesis." Journal of Orthopaedic Research **6**(3): 335-345.

Rudman, K., R. Aspen and J. Meakin (2006). "Compression or tension? The stress distribution in the proximal femur." Biomed Eng Online **5**(12).

Rueckel, J., M. Stockmar, F. Pfeiffer and J. Herzen (2014). "Spatial resolution characterization of a X-ray microCT system." Applied Radiation and Isotopes **94**: 230-234.

Ruimerman, R., B. van Rietbergen, P. Hilbers and R. Huiskes (2005). "The Effects of Trabecular-Bone Loading Variables on the Surface Signaling Potential for Bone Remodeling and Adaptation." Annals of Biomedical Engineering **33**(1): 71-78.

Sangeux, M. (2019). Biomechanics of the Hip During Gait. The Pediatric and Adolescent Hip: Essentials and Evidence. S. Alshryda, J. J. Howard, J. S. Huntley and J. G. Schoenecker. Cham, Springer International Publishing**:** 53-71.

Sasaki, N. and A. Enyo (1995). "Viscoelastic properties of bone as a function of water content." Journal of Biomechanics **28**(7): 809-815.

Schaffler, M. B., W. C. Pitchford, K. Choi and J. M. Riddle (1994). "Examination of compact bone microdamage using back-scattered electron microscopy." Bone **15**(5): 483-488.

Scheerlinck, T. and P.-P. Casteleyn (2006). "The design features of cemented femoral hip implants." The Journal of Bone and Joint Surgery **88**(11): 1409-1418.

Schindeler, A., M. M. McDonald, P. Bokko and D. G. Little (2008). "Bone remodeling during fracture repair: The cellular picture." Seminars in Cell & Developmental Biology **19**(5): 459-466.

Schriefer, J., S. Warden, L. Saxon, A. Robling and C. Turner (2005). "Cellular accommodation and the response of bone to mechanical loading " J Biomech **38**: 1838-1845.

Scofield, K. and S. Hecht (2012). "Bone Health in Endurance Athletes: Runners, Cyclists, and Swimmers." Am Coll Sports Med **11**(6): 328-334.

Seeman, E. (2003). "Physiology of Aging, Invited Review: Pathogenesis of osteoporosis." Journal of Applied Physiology **95**: 2142-2151.

Seraphim, A., N. Al-Hadithy, S. Mordecai and S. Al-Nammari (2012). "Do bisphosphonates cause femoral insufficiency fractures?" Journal of Orthopaedics and Traumatology **13**(4): 171-177.

Seref-Ferlengez, Z., J. Basta-Pljakic, O. Kennedy, C. Philemon and M. Schaffler (2014). "Structural and Mechanical Repair of Diffuse Damage in Cortical Bone In Vivo." Journal of Bone and Mineral Research **29**(12): 2537-2544.

Seref-Ferlengez, Z., O. Kennedy and M. Schaffler (2015). "Bone microdamage, remodeling and bone fragility: how much damage is too much damage?" Internal Bone and Mineral Society(4).

Shahi, M., A. Peymani and M. Sahmani (2017). "Regulation of Bone Metabolism." Reports of biochemistry & molecular biology **5**(2): 73-82.

Sharp, D. J., K. E. Tanner and W. Bonfield (1990). "Measurement of the density of trabecular bone." Journal of Biomechanics **23**(8): 853-857.

Sinsurin, K., R. Vachalathit, W. Jalayondeja and W. Limroongreungrat (2013). "Different Sagittal Angles and Moments of Lowe Extremity Joints during Single-leg Jump Landing among Various Directions in Basketball and Volleyball Athletes." Journal of Physical Therapy Science **25**: 1109-1113.

Spägele, T., A. Kistner and A. Gollhofer (1999). "A multi-phase optimal control technique for the simulation of a human vertical jump." Journal of Biomechanics **32**(1): 87-91.

Speirs, A., M. Heller, G. Duda and W. Taylor (2007). "Physiologically based boundary conditions in finite element modelling." Journal of Biomechanics **40**: 2318-2323.

Stansfield, B., A. Nicol, J. Paul, I. Kelly, F. Graichen and G. Bergmann (2003). "Direct comparison of calculated hip joint contact forces with those measured using instrumented implants. An evaluation of three-dimensional mathematical model of the lower limb." Journal of Biomechanics **36**: 929-936.

Stokes, I. (2002). "Mechanical effects on skeletal growth." Journal of Musculoskeltal Neuron Interact **2**(3): 277-280.

Stokes, I. A., J. Gwadera, A. Dimock, C. E. Farnum and D. D. Aronsson (2005). "Modulation of vertebral and tibial growth by compression loading: Diurnal versus full-time loading." Journal of Orthopaedic Research **23**(1): 188-195.

Stokes, I. A. and J. Laible (1990). "Three-dimensional osso-ligamentud model of the thorax representing initiation of scoliosis by asymmetic growth." Journal of Biomechanics **23**(6): 589-595.

Stroe, M., J.-M. Crolet and M. Racila (2011). "Mechanotransduction in cortical bone and the role of piezoelectricity: A numerical approach." Computer methods in biomechanics and biomedical engineering **16**.

Su, K., L. Yuan, J. Yang and J. Du (2019). "Numerical Simulation of Mandible Bone Remodeling under Tooth Loading: A Parametric Study." Scientific Reports **9**(1): 14887.

Supervia, A., X. Nogues, A. Enjuanes, J. Vila, L. Mellibovskuy, S. Serrano, J. Aubia and A. Diex-Perez (2006). "Effect of smoking and smoking cessation on bone mass, bone remodeling, vitamin D, PTH and sex hormones." Journal of musculoskeletal & neuronal interactions **6**(3): 234-241.

Taddei, F., E. Schileo, B. Helgason, L. Cristofolini and M. Viceconti (2007). "The material mapping strategy influences the accuracy of CT-based finite element models of bones: An evaluation against experimental measurements " Medical Engineering & Physics: 971-979.

Tandon, B., J. J. Blaker and S. H. Cartmell (2018). "Piezoelectric materials as stimulatory biomedical materials and scaffolds for bone repair." Acta Biomaterialia **73**: 1-20.

Taylor, D. and T. Lee, C (2003). "Microdamage and mechanical behaviour: predicting failure and remodelling in compact bone." Journal of Anatomy **203**: 203-211.

Taylor, W., M. Heller, G. Bergmann and G. Duda (2004). "Tibio-femoral laoding during human gait and stair climbing." Journal of Orthopaedic Research **22**: 625-632.

Treece, G. M. and A. H. Gee (2015). "Independent measurement of femoral cortical thickness and cortical bone density using clinical CT." Medical Image Analysis **20**(1): 249-264.

Tria, A. J. (2020). "Instrumentation in Total Knee Arthroplasty." Retrieved 09 Feb 2020, from https://www.78stepshealth.us/knee-arthroplasty/instrumentation-in-total-knee-arthroplasty.html.

Troy, K. L., M. E. Mancuso, J. E. Johnson, Z. Wu, T. J. Schnitzer and T. A. Butler (2018). "Do mechanical strain magnitude and rate drive bone adaptation in adult women? A 12-month prospective study." bioRxiv: 421156.

Turner, A. W. L., R. M. Gillies, R. Sekel, P. Morris, W. Bruce and W. R. Walsh (2005). "Computational bone remodelling simulations and comparisons with DEXA results." Journal of Orthopaedic Research **23**(4): 705-712.

Turner, C. (1998). "Three Rules for Bone Adaptation to Mechanical Stimuli " Bone **23**: 399-407.

Turner, C. (1999). "Toward a Mathematical Description of Bone Biology: The Principle of Cellular Accommodation " Calcified Tissue International **65**: 466-471.

Turner, C. and M. Akhter (1999). The Mechanics of Bone Adaptation. Mechanical Loading of Bone and Joints. H. E. Takahashi. Japan, Springer Science & Buisness Medial.

Turner, C., M. Forwood and M. Otter (1994). "Mechanotransduction in bone: Do bone cells act as sensors to fluid flow " Federation of American Societies for Experimental Biology(8): 875-878.

Turner, C., I. Owan and Y. Takano (1995). "Mechanotransduction in bone: Role of strain rate." Americal Journal of Physiology **269**: E438-E442.

Turner, C. H., V. Anne and R. M. V. Pidaparti (1997). "A uniform strain criterion for trabecular bone adaptation: Do continuum-level strain gradients drive adaptation?" Journal of Biomechanics **30**(6): 555-563.

Umemura, Y., T. Ishiko, T. Yamauchi, M. Kuronon and S. Mashiko (1997). "Fiver jumps per day increase bone mass and breaking force in rats " Journal of Bone Mineral Research (45): 1480-1485.

Unlu, M. C., H. Kesmezacar, F. Kantarci, B. Unlu and H. Botanlioglu (2011). "Intraoperative estimation of femoral anteversion in cementless total hip arthroplasty using the lesser trochanter." Archives of Orthopaedic and Trauma Surgery **131**(9): 1317-1323.

Vahdati, A. and G. Rouhi (2009). "A model for mechanical adaption of trabecular bone incorporating cellular accommodation and effect of microdamage and disuse." Mech Res Commun **36**: 284-293.

van der Harst, J. J., A. Gokeler and A. L. Hof (2007). "Leg kinematics and kinetics in landing from a single-leg hop for distance. A comparison between dominant and non-dominant leg." Clinical Biomechanics **22**(6): 674-680.

van der Helm, F. C. T. and R. Veenbaas (1991). "Modelling the mechanical effect of muscles with large attachment sites: Application to the shoulder mechanism." Journal of Biomechanics **24**(12): 1151-1163.

van der Meulen, M. C. H. and C. J. Hernandez (2013). Chapter 21 - Adaptation of Skeletal Structure to Mechanical Loading. Osteoporosis (Fourth Edition). R. Marcus, D. Feldman, D. W. Dempster, M. Luckey and J. A. Cauley. San Diego, Academic Press**:** 477-495.

van Staa, T. P., E. M. Dennison, H. G. M. Leufkens and C. Cooper (2001). "Epidemiology of fractures in England and Wales." Bone **29**(6): 517-522.

Veilleux, L. N. and F. Rauch (2010). "Reproducibility of jumping mechanography in healthy children and adults." Journal of Musculoskeletal and Neuronal Interactions(1108-7161 (Print)).

Vert, G. and J. Chory (2011). "Crosstalk in cellular signaling: background noise or the real thing?" Developmental cell **21**(6): 985-991.

Villemure, I., C. E. Aubin, J. Dansereau and H. Labelle (2004). "Biomechanical simulations of the spine deformation process in adolescent idiopathic scoliosis from different pathogenesis hypotheses." European spine journal : official publication of the European Spine Society, the European Spinal Deformity Society, and the European Section of the Cervical Spine Research Society **13**(1): 83-90.

von Meyer, G. H. (2011). "The classic: The architecture of the trabecular bone (tenth contribution on the mechanics of the human skeletal framework)." Clinical orthopaedics and related research **469**(11): 3079-3084.

Wang, E., T. Nelson and R. Rauch (2004). Back to Element - Tetrahedra vs. Hexahedra. Munich, CAD-FEM GmbH.

Wang, X. (2013). "Cortical Bone Mechanics and Composition: Effects of Age and Gender." Studies in Mechanobiology, Tissue Engineering and Biomaterials **5**: 53-85.

Wang, X. and J. S. Nyman (2007). "A novel approach to assess post-yield energy dissipation of bone in tension." Journal of Biomechanics **40**(3): 674-677.

Warden, S. and C. Turner (2004). "Mechanotransduction in cortical bone is most efficient at loading frequencies of 5 - 10 Hz." Bone(34): 261-270.

Warrener, A. G. (2017). "Hominin Hip Biomechanics: Changing Perspectives." The Anatomical Record **300**(5): 932-945.

Webster, D., F. A. Schulte, F. M. Lambers, G. Kuhn and R. Müller (2015). "Strain energy density gradients in bone marrow predict osteoblast and osteoclast activity: A finite element study." Journal of Biomechanics **48**(5): 866-874.

Webster, D., A. Wirth, C. van Lenthe and R. Muller (2012). "Experimental and finite element analysis of the mouse caudal vertebrae loading model: prediction of cortical and trabecular bone adaption." Biomech Model Mechanobiol **11**(1): 221-230.

Wolff, J. (1896). Das Gesetz der Transformation der Knochen A. Hirschwald: Berlin, 1892. The Law of Bone Remodelling. P. Manquet and R. Furlong. Berlin, Springer.

Wong, K. C. (2016). "3D-printed patient-specific applications in orthopedics." Orthopedic research and reviews **8**: 57-66.

Wu, G., S. Siegler, P. Allard, C. Kirtley, A. Leardini, D. Rosenbaum, M. Whittle, D. D. D'Lima, L. Cristofolini, H. Witte, O. Schmid and I. Stokes (2002). "ISB recommendation on definitions of joint coordinate system of various joints for the reporting of human joint motion—part I: ankle, hip, and spine." Journal of Biomechanics **35**(4): 543-548.

Yanashita, J., X. Li, B. Furman, R. Rawls, X. Wang and M. Agrawal (2002). "Collagen and Bone Viscoelasticity: A Dynamic Mechanical Analysis." Journal of Biomedical Materials Research **63**: 31-36.

Zannoni, C., R. Mantovani and M. Viceconti (1998). "Material properties assignment to finite element models of bone structures: a new method." Medical Engineering & Physics: 740.

Zehnder, Y., S. Risi, D. Michel, H. Knecht, R. Perrelet, M. Kraenzlin, G. A. Zäch and K. Lippuner (2004). "Prevention of Bone Loss in Paraplegics Over 2 Years With Alendronate." Journal of Bone and Mineral Research **19**(7): 1067-1074.

Zhong, Z., X.-L. Zeng, J.-H. Ni and X.-F. Huang (2013). "Comparison of the biological response of osteoblasts after tension and compression." European Journal of Orthodontics **35**(1): 59-65.

Zioupos, P., U. Hansen and J. D. Currey (2008). "Microcracking damage and the fracture process in relation to strain rate in human cortical bone tensile failure." Journal of Biomechanics **41**(14): 2932-2939.

Appendix A. Statistical Tests

A.1 Non Parametric Statistical Tests

The dataset used in this study, consisted of two or more measurements being carried out in different locations in the same femur, which are then compared. The data was not large enough to be meet parametric assumptions, namely to be normally distributed, therefore non-parametric tests were chosen. Non parametric tests use some method of ranking the measurement and testing for skewness and kurtosis of the distribution, and therefore were considered able to accommodate the dataset used in this study. Whilst non-parametric tests provide a lesser statistical power, they still provide a powerful statistical tool (Field 2018).

A.1.1 Spearman's Rank Correlation Coefficient Test

The first non-parametric test chosen was the Spearman's rank correlation coefficient test, which is used to assess the relationship between two variables. A 2-tailed correlation test was chosen, as it accepts that the user is unaware of the direction of the correlation (e.g. positive or negative) before the test is used. From this two outputs are provided, the strength and direction of the relationship (Correlation Coefficient, otherwise known as effect size) and the statistical percentage likelihood that the observed correlation is due to chance which is otherwise known as the p-value (Field 2018). The correlation coefficient ranges between |0| and |1|, where 1 denotes a perfect correlation and 0 denotes no correlation at all. Within these values, a correlation of |0.1| is considered weak, a correlation of |0.3| is considered moderate and a correlation of |0.5| is considered strong (Field 2018). A positive value indicates a positive correlation (y increases as x increase) and a negative value indicates a negative correlation (y decreases as x increase). In Chapter 4, the results of the Spearman's rank correlation coefficient test are presented in a table, like that shown in Appendix A-1.

		Variable 2
Variable 1	Correlation Coefficient	-0.682
	p-value	0.021

Appendix A-1: Typical presentation of the Spearman's rank correlation coefficient test

Here, variable 1 and variable 2 have a negative correlation with a strong correlation coefficient of -0.682, to a p-value of $p = 0.021$, meaning that the correlation is 2.1 % likely due to chance.

A.1.2 Wilcoxon Signed Rank Test

The Wilcoxon signed rank test is a non-parametric statistical test used to determine the statistical difference between repeated measures in a single population (e.g. two measurements within the same person). This was considered appropriate for this study and its aim, in comparison to other statistical tests such as the Mann-Whitney U test, which examines single measurements in multiple populations (Field 2018). In Chapter 4, the Wilcoxon signed rank test was used to determine the statistical difference between the characteristics observed under tension and compression, where the output of the statistical test is a single value determining the statistical percentage likelihood that the observed difference was due to chance (p-value).

A.2 Goodness of Fit Analysis

The goodness of fit of the stimulus-remodelling relationships was assessed using two statistical tools, being: 1) The root mean square error (RMSE), and 2) The coefficient of determination, known as the R-squared (R^2) value. The RMSE is used to demonstrate the difference between observed and predicted values, whilst the coefficient of determination determines the percentage of variance of the dependent variable (y-axis, change in density) which can be explained by the independent variable (x-axis, stimulus). The R^2 ranges between 0 and 1, where a value of 0.7 represents a correlation where 70% of the dependent variables align with the relationship. A negative R^2 value indicates that the fit is worse than using a horizontal line, where a horizontal line would be a better representation of the x-y relationship (Field 2018).

Appendix B. Material Transfer Agreement

UNIVERSITY OF SURREY

POSTGRADUATE STUDENT UNDERTAKING: CONFIDENTIALITY AND IPR

To: University of Surrey ("the University"),
Guildford,
Surrey
GU2 5XH, UK

By: **Matthew Taylor** ("the PG Student") who is registered as a postgraduate student in the Faculty of Engineering and Physical Sciences of the University of Surrey for the purpose of studying for a degree of PhD in Biomedical Engineering and who, in connection with such studies, proposes to undertake work involving data owned by the University of Loughborough and the University of Leicester Hospital NHS trust ("the Data Providers") in connection with the analysis of bone strength and performance of finite element simulations with the aim to determine a bone remodelling theorem ("Agreed Purpose").

THE PG STUDENT AGREES AND UNDERTAKES AS FOLLOWS:

1. IP Code

I accept that the University's Code of Practice in relation to the Protection and Exploitation of Intellectual Property Rights in force from time to time ("the IP Code") is applicable to me as a postgraduate student of the University.

2. Conduct of Agreed Purpose

2.1 If working in a laboratory (at the University's premises or elsewhere) I will keep a laboratory notebook in accordance with the requirements of the IP Code and as directed by my assigned university supervisor.

2.2 I will comply with all requirements of the University in relation to the Agreed Purpose.

3. Confidentiality

3.1 I will treat as confidential, and (except as instructed by the University) will **not** disclose to any third party, whether orally or in writing:

3.1.1 any business, technical or other information relating to the Agreed Purpose, received by me from the University or the Data Providers; or

3.1.2 any results arising from the Agreed Purpose.

3.2 Save as permitted by the University and the Data Providers I will **not**:

3.2.1 publish any thesis, dissertation or other paper containing; or

3.2.2 use for any purpose other than for the Agreed Purpose any information, material or findings derived from the Agreed Purpose or any confidential information received from the Data Providers, provided however that nothing in this Undertaking prevents or hinders me from:

3.2.2.1 submitting my thesis to the University for a degree from the University (with the thesis being based on results generated within the scope of the Agreed Purpose); or

3.2.2.2 from following the University's procedures for examination and for admission to postgraduate degree status (such

procedures to include provisions to place the thesis on restricted access within the University's library).

4. Assignment of Intellectual Property Rights ("IPR")

4.1 I assign to the University all copyright, database right, design right, and rights of a similar nature, which exist now or may at any time in the future exist, in any work created by me (alone or jointly with others) in the course of the Agreed Purpose, other than the copyright in any thesis or dissertation submitted to the University for any degree or other academic award of the University.

4.2 I agree to assign and (on written instructions from the University) to execute any further document required for the assignment to the University or its nominated subsidiary company, or for the assignment or licence to the Data Providers or their nominees, of any invention that I make (alone or jointly with others) in the course of my work on the Agreed Purpose, and to do all things necessary to enable the University or such other assignee to seek (at its own expense) patent or any similar protection for any such work or invention.

4.3 I irrevocably appoint the University and any nominated official or employee of the University, jointly and severally, as my Attorney to execute any document and do anything as may be required by this clause or in accordance with the IP Code and I authorise such Attorney and any duly appointed employee or agent of such Attorney to act as required by the terms of the University's contract with the Sponsor in relation to such work or invention.

5. Registered IPR

5.1 I accept that neither the University nor the Data Providers shall be obliged to file, prosecute or maintain any application for patent or similar protection for any work or invention referred to in clause 4 above.

5.2 I will not make any claim against the University or the Data Providers based on acts or omissions connected with the filing, prosecution or maintenance of any such application for patent or other similar protection.

6. Revenue sharing

Unless otherwise agreed, I accept that the provisions of the IP Code shall apply to revenue derived by the University from the exploitation of any intellectual property rights assigned by me to the University by or pursuant to clause 4 hereof.

7. Law, jurisdiction, disputes

7.1 This undertaking shall be governed by and construed in accordance with English law.

7.2 Any dispute under this undertaking or the IP Code shall in the first instance be referred to the Vice-Chancellor or his nominee for resolution. If such dispute is not so resolved the parties will attempt to settle it by mediation in accordance with the CEDR Model Mediation Procedure as specified in the IP Code.

7.3 I hereby accept the jurisdiction of the English courts.

Signed as a deed by the PG Student

Signature: Matt Taylor	In the presence of: (Witness' signature)
Date: 23 SEP 2016	Witness' name: P. Deniz TOSUN Address: 35 School Meadow GU2 8GY Occupation: PhD Student

models\studentundertaking Revised EB2016 UNCLE 11599
11599 - Postgraduate IP undertaking2016 - cln.doc